College of Engineering & Technology
Derby

Doctorate of Philosophy in Renewable Energy Technology

COMPUTER AIDED DESIGN OF A 3D RENEWABLE ENERGY PLATFORM FOR TOGO'S SMART GRID POWER SYSTEM INFRASTRUCTURE

MOGLO KOMLANVI

2018

UNIVERSITY OF DERBY

COLLEGE OF ENGINNERING & TECHNOLOGY

The undersigned herby certify that they have read and recommend to the college of Engineering and Technology exams and Assessment board for acceptance of the Thesis entitled "COMPUTER AIDED DESIGN OF a 3D RENEWABLE ENERGY PLATFORM FOR TOGO'S POWER SYSTEM INFRASTRUCTURE" by MOGLO KOMLANVI in partial fulfilment of the requirements for the Degree of Doctor of Philosophy

Dated: JANUARY 2018

External Examiner: Dr MOHAMED DARWISH

First supervisor: Dr MAHMOUD SHAFIK

Second Supervisor: Dr JOSE ARTURO GARZA REYES

Examining chair: Dr HEIDI SOWTER

UNIVERSITY OF DERBY

COLLEGE OF ENGINNERING & TECHNOLOGY

Date: JANUARY 2018

Author: MOGLO KOMLANVI

Faculty: College of Engineering & Technology

Degree: Ph.D. Convocation: January Year: 2018

Permission is hereby granted to the University of Derby to circulate and to have copies for non-commercial purpose at its discretion, for the above title upon the request of individuals or institutions.

Signature of Author

ABSTRACT

Keywords: 3Dimentional, Smart Grid, Renewable Energy Systems

The global requirement for sustainable energy provision will become increasingly important over the next fifty years as the environmental effects of fossil fuel use become apparent. Therefore, the issues surrounding integration of renewable energy supplies need to be considered carefully. The focus of this work was the development of an innovative computer aided design of a 3 Dimensional renewable energy platform for Togo's smart grid power system infrastructure. It demonstrates its validation for industrial, commercial and domestic applications.

The Wind, Hydro, and PV system forming our 3 Dimensional renewable energy power generation systems introduces a new path for hybrid systems which extends the system capacities to include, a stable and constant clean energy supply, a reduced harmonic distortion, and an improved power system efficiency. Issues requiring consideration in high percentage renewable energy systems therefore includes the reliability of the supply when intermittent sources of electricity are being used, and the subsequent necessity for storage and back-up generation

The adoption of Genetic algorithms in this case was much suited in minimizing the THD as the adoption of the CHB-MLI was ideal for connecting renewable energy sources with an AC grid. Cascaded inverters have also been proposed for use as the main traction drive in electric vehicles, where several batteries or ultra-capacitors are well suited to serve as separate DC sources.

The simulation done in various nonlinear load conditions showed the proportionality of an integral control based compensating cascaded passive filter thereby balancing the system even in nonlinear load conditions. The measured total harmonic distortion of the source currents was found to be 2.36% thereby in compliance with IEEE 5191992 and IEC 61000-3 standards for harmonics

This work has succeeded in developing a more complete tool for analysing the feasibility of integrated renewable energy systems. This will allow informed decisions to be made about the

technical feasibility of supply mix and control strategies, plant type, sizing and storage sizing, for any given area and range of supply options.

The developed 3D renewable energy platform was examined and evaluated using CAD software analysis and a laboratory base mini test. The initial results showed improvements compared to other hybrid systems and their existing control systems.

There was a notable improvement in the dynamic load demand and response, stability of the system with a reduced harmonic distortion. The derivatives of this research therefore proposes an innovative solution and a path for Togo and its intention of switching to renewable energy especially for its smart grid power system infrastructure. It demonstrates its validation for industrial, commercial and domestic applications

ACKNOWLEDGMENTS

It is my pleasure to have this opportunity to present my deepest thanks and my sincere appreciation to my supervisor Mahmoud Shafik, Senior Lecturer and University reader in Intelligent Mechatronics system for giving me the opportunity to conduct research in such interesting area and for his professional supervision, constructive discussions and guidance throughout the progress of this research work.

All my thanks go to Jose Arturo Garza Reyes, Professor of operations Management and head of the Centre for supply chain improvement for his guidance, support, help and constructive discussion throughout this research work.

I would like to express particular thanks for M. Riyad Elsaadi, Mr. Elvis M Ashu, Dr Basem Rashid Alamri for their help during the time of my research and their valuable support, constructive discussions and encouragement throughout preparing the material of this thesis.
Finally, I would like to present particular wishes and sincere appreciation for my parents, whom have instilled in me the value of education, self-discipline, hard work and the importance of faith. My sincere appreciations also goes to my siblings and my partner for supporting me spiritually throughout the course of this thesis.

Finally I thank my God, my good Father, for his everlasting blessing, grace and favor upon my life and his guidance and protection throughout the challenges and success I have experienced through my Academic life. I will keep on trusting you for my future.

Thank you, El SHADDAI.

CONTENTS

List of figures

NOMENCLATURE

AC	Alternating Current
AFD	Agence Francaise de Developpement- *France Development Agency*
AfDB	African Development Bank
ANN	Artificial Neural Network
APF	Active Power Filter
ARREC	ECOWAS Regional Electricity Regulatory Commission
ARSE	Electricity Sub-Sector Regulatory Authority
BOAD-	Banque Ouest Africaine de développement
CEB	Communauté Electrique du Benin
CEET	Compagnie d'Energie Electrique du Togo
CHB-MLI	Cascaded H-Bridge Multilevel Inverter
CSI	Current Source Inverter
DC	Direct Current
DSP	Digital Signal Processing
EA	Evolution Algorithm
ECOWAS	Economic Community of West Africa
EMI	Electro-Magnetic Interference
ESW	Economic Sector Work
EU	European Union
FACTS	Flexible AC Transmission System
FC-MLI	Flying Capacitor Multilevel Inverter
GA	Genetic Algorithm
GDP	Gross Domestic Product
GOT	Government of Togo
GTO	Gate Turn-Off Thyristors

HDI	Human Development Index
HP	High Pass
HV	High Voltage
HVDC	High Voltage Direct Current
IDA	International Development Association
IEA	International Energy Agency
IEEE	Institute of Electrical and Electronics Engineers
IEEE-519	IEEE *Recommended Practice and Requirements for Harmonic Control in Electrical Power Systems*
IFC	International Finance Corporation
IGBT	Insulated Gate Bipolar Transistor
IPP	Independent Power Producer
ISN	Interim Strategy Note
LPG	Liquefied Petroleum Gas
LV	Low voltage
ML-VSI	Multilevel Voltage Source Inverter
MME	Ministère des Mines et de l'Energie
MV	Medium Voltage
NPC-MLI	Neutral-Point Clamped Multilevel Inverter
NR	Newton Raphson
OPIC	Overseas Private Investment Corporation
PPF	Passive Power Filter
PPP	Public Private Partnership
PSO	Particle Swarm Optimisation
PV	Photo Voltaic
PV	Photovoltaic
PWM	Pulse Width Modulation
PWM-CSI	Pulse width modulation – Current Source Inverter

SBEE	Société Béninoise d'Energie Electrique
SHE	Selective Harmonic Elimination
SIE	Energy Information System (*Système d'Information Energétique*)
SPWM	Sinusoidal Pulse Width Modulation
STATCOM	Static Synchronous Compensator
TEP	Ton Equivalent Pétrole
WAEMU	West African Economic and Monetary Union
WAPP	West Africa Power Pool

Engineering Nomenclatures

$\vec{c}$ = absolute velocity, m/s

C_D = drag coefficient, related to the mean velocity, dimensionless

C_L = lift coefficient, dimensionless

C_{psmin} = minimum suction pressure coefficient, dimensionless

C_p = pressure coefficient, dimensionless

C_b = camber coefficient, dimensionless

c_r = radial velocity component, m/s

c_m = meridian velocity, m/s

D = runner diameter, m

E = specific energy, J/kg

H = head, m

l = chord of profile, m

l/s = solidity of profile, dimensionless

n = rotational speed, rpm

n_q = specific speed, dimensionless

P = power, W

p = static pressure on the blade profile, Pa

P_h = hydraulic power, W

P_u = shift power, W

p_o = reference pressure, Pa

Q = flow rate, m^3/s

R = radius, m

s = distance between the airfoil cascade, m

T = torque, Nm

$\vec{u}$ = rotation velocity, m/s

$\vec{w}$ = relative velocity, m/s

$\vec{w}_¥$ = mean relative velocity, m/s

E =Young's modulus of elasticity, [N/m2]

g =Acceleration due to gravity, [m/s2]

Hf =Head losses due to friction effects in the conduit,[m]

id =Current flowing in the d-axis armature coil, [pu]

iq =Current flowing in the q axis armature coil, [pu]

y =Turbine wicket gate position, []

z =Elevation of the pipe centreline, [m]

α =Slope of the pipe axis, [°]

∂ =Power angle with respect to an infinite busbar

ε =Internal pipe roughness, [m]

λ =Eigen value

Greek Symbols

D p_o = loss stagnation pressure, Pa

D c_u = difference between the tangential velocity components, m/s

a = angle of attack in relation to $\vec{w}_{¥}$, degree

b = stagger angle, degree

$b_{3\text{-}4}$ = inlet flow angle, degree

b_{μ} = mean angle of flow velocity, degree

D b = cascade deflection angle, degree

D W_u = difference between the tangential velocity components, m/s

d_u = cascade deflection coefficient, dimensionless

z_v = loss coefficient, dimensionless

h = efficiency, dimensionless

j = flow number, dimensionless

l = hydraulic power number, dimensionless

n = velocity coefficient, dimensionless

r = fluid density, kg/m^3

s = cascade solidity, dimensionless

t = torque number, dimensionless

J = specific diameter, dimensionless

w = angular velocity, rad/s

y = pressure coefficient number, dimensionless

Subscripts

e = relative to the external region of the turbine

i = relative to the internal region of the turbine

m = relative to the meridian direction

u = relative to the tangential direction

¥ = relative to the mean direction of the flow

CHAPTER 1

CHAPTER 1 INTRODUCTION

1.1. GENERAL INTRODUCTION

The republic of (Togo) is one of the smallest and low-income West African states (USDS, 2015). It is geographically situated on the Gulf of Guinea and has a population of 6.6 Million (USDS, 2015). The year 1960 saw the country gain its independence which was followed by a very long social, economic and political crisis that led into the deterioration and closure of many of its infrastructures (USDS, 2012). In 2006 alongside its neighbouring countries (Ghana and the Benin Republic), the country faced a serious energy crisis as energy demands grew and supply inadequate. This was also in effect due to hydro energy being the main country source of power generation declining due to climate change effects (PPIAF, 2015 report). In 2008 a plan to invigorate various sectors crumbling the economy was engaged by the Government and this included the energy sector. In the invigoration of various Government sectors, an emphasis was also placed in the telecommunication and transport sectors which are vital sectors of the economy.

Energy has always been an issue for Togo since the sharing of Togoland (the loss of German colonies, Britannica, 2011). Togo depends on its fossil fuel reserves, mainly natural gas and diesel for its electricity generation (UNFCCC, 2003a). Currently there are four main diesel power utilities and a number of hydro power stations spread around the country that generates about 130 MW of electricity, of which 30 MW is of Hydro power (DGE, 2001). The Togolese energy sector has a heavy reliance on imported fuel oil and electricity, an increasing gap between demand and supply, a lack of reliability of the grid and poor performance of equipment and appliances used by consumers. The peak load is currently at 100 MW, while the base-load is between 50 and 60 MW. By comparison, power availability in the dry season in 2007 was roughly 40 MW, leading to a high level of unsatisfied demand. Imports accounted for 84% of the total electricity supply in 2008, with nearly a quarter of domestic generation capacity relying on fuel oil imports. Transmission and distribution losses in 2008 were 19.1% (REEP, 2016). This rise in demand is envisaged to continue due to accelerated growth in the republic of Togo industrial sector (IEPF, 2015). Current statistics shows that electricity generation of

fossil fuel is estimated at 78% and Hydro power of 22% and it's been argued that such figures could lead to a projection of CO2 emission for the year 2020 to be approximately 2000t of CO2 generated per year. It is therefore eminent that there is a strategical need to: utilise the available renewable energy resources, meet growing demand, replace the aforementioned technology and reduce CO2 emission. This PhD research project is to conduct the necessary theoretical and practical investigation, into barriers to implement the technology for the benefits of Togo's Energy industry, environmental sustainability and economic sector.

The country geographical position is an advantage as the country is expected to have more rains in the years to come which means levels of rivers would automatically rise. Considering the country's aim to attain full electrification in the long run, it is important to consider cleaner sources of energy generation. It is in that light that this research aims to provide a system of which its preamble indicates the possibility of a computer aided design of a 3D renewable energy platform for Togo's smart grid power system infrastructure that will efficiently help the country in attaining its long term vision being the full electrification of the country by the year 2030. The computer aided design of a 3D renewable energy platform for Togo's smart grid power system infrastructure will go a long way to help any other country, government, organization that will feel the derivatives of this research will help them in one way or the other in generating cleaner energies and meeting up demands of a particular city, country or community.

Energy generation methods and its supply is one of the most discussed and worrying issues in current world press (M. Komlanvi et al, 2015). The supply of clean energy and its security is becoming an issue for most developing countries considering new policies on limitations of fossil fuels usage for energy generations, and also the high dependency on imported fuels and their ever climbing prices.

Problems in the energy sector do not only abstain to the safe supply of clean Energy, but also in terms of environmental degradation due to carbon emissions for which the energy sector is the main contributor. It is believed that the development of sustainable energy infrastructures would be efficient contribution to defining solutions to successfully reduce on global carbon emissions and promote the usage and development of Green technology for Green power generation and distribution through smart grids. The research covered by this PhD program being a computer aided design of a 3D renewable energy platform for Togo's smart grid power system infrastructure is also presented as business model.

1.2. AIM & OBJECTIVES OF THIS INVESTIGATION

The main aim of this research programme is to conduct the necessary investigation, into the barriers to implement renewable energy technology generation in the Republic of Togo's and develop an efficient renewable energy platform that would suit the energy sector smart grids industrial applications.

Objectives

The objectives of the research are:

- Conducting a primary research and assessing information's from the Togolese Ministry of Mines & Energy.
- assessing the current energy generation methods and business models in Togo and their impact on the current environmental and economic sectors,
- examining the possible available renewable energy resources and their impact on the current energy generation method with an evaluation of the impact on Togo environmental and economic sectors,
- investigating the current barriers to the successful implementation of renewable energy technologies,
- conduct a forecast analysis into the energy demand for the country in the next 5 to 10 years considering population growth rate and industry expansion/power demand,
- investigate the current challenges facing the renewable energy resources technology and investigate the possible technological advancement to improve the efficiency at a low cost,
- Conduct the necessary computer simulation using MATLAB /Simulink software to the proposed 3D renewable energy platform. This will entail simulation of two of the three renewable energy sources (Wind-Hydro). The objectives of the simulation will then be used to evaluate power generation abilities of these system's and efficiency of the sustainable renewable power station
- Design and build an actual mini 3D practical platform,
- adapting the business model in Togo's and other neighbourhood countries

1.3. RESEARCH METHODOLOGY

Research methodology describes the overall approach to a research process. According to (Saunders, Lewis, & Thornhill, 2007) Research methodology can be described as consecutive steps taken by a researcher in analysing a problem with project objectives and goals in mind. The research method adopted for this research will be a deductive, Exploratory, Constructive and Empirical in nature. The three methods will allow the researcher to investigate the needs, identify the application design specifications, develop system architecture, define the system main hardware & software units, develop a solution by obtaining an outline design, and then test the feasibility of the design using empirical evidence. A prototype will be developed and will be tested based on design specifications and needs to verify the potential of the technology from an economic, social and policy point of view.

1.4. ORGANISATION OF THE THESIS

The remainder of this thesis is divided into eight chapters (see Figure 1-2).

Chapter 2. Presents a critical literature survey of the key database, governmental reports, publications, technical reports and case studies, related areas to the current research programme. This is to conclude with the possible recommended business model and renewable energy platform.

Chapter 3. Introduces the possible business model and recommended renewable energy platform that could suit Togo's smart grid power systems infrastructure and industrial applications.

Chapter 4. Provides Computer Aided Design and Analysis of the front End renewable energy resources of the proposed platform. This is mainly aiming to investigate the possible factors of improving the efficiency of the front end units. The computer aided design and analysis has been carried to Hydropower units (water wheels, Kaplan turbine, dual feed arrangement for both water wheel and Kaplan turbine …etc.), Wind turbine units, 2D arrangements i.e. wind and hydropower …etc.

Chapter 5. Presents the Computer Aided Design, simulation and Modelling of the Backend of System (BoS) of the proposed renewable energy platform i.e. control system, multi-level converted and relevant filtration system. The chapter concluded with the possible

recommendation of multi-level converter, relevant filtration system based on possible load nature and applications.

Chapter 6. Introduces system integration of the proposed renewable energy platform into the smart grid. The chapter gives a good introduction about the smart grids, relevant technology development, the steps that can be taken to integrate the proposed renewable energy platform into the grids …etc. The Chapter concluded with a computer simulation and analysis model of the system that shows the dynamic behaviour of the proposed model which is examined under different operating conditions.

Chapter 7. Presents the laboratory validation and evaluation of the proposed renewable energy platform. It demonstrates a series of experimental evaluation into the dynamic response of the system, stability of the system and its output and control capability.

Chapter 8. Sets out the general conclusion and discussion for this research. It also provides an overview of the innovation, contributions and limitations of the developed system.

Chapter 9. Presents the recommendations and future work. This is followed by a list of references, appendices and list of publications.

- **Appendix (A)** Simulink Models
- **Appendix (B)** MATLAB Scripts
- **Appendix (C)** Overview of the system architecture
- **Appendix (D)** Laboratory validation key components
- **Appendix (E)** Author Publication

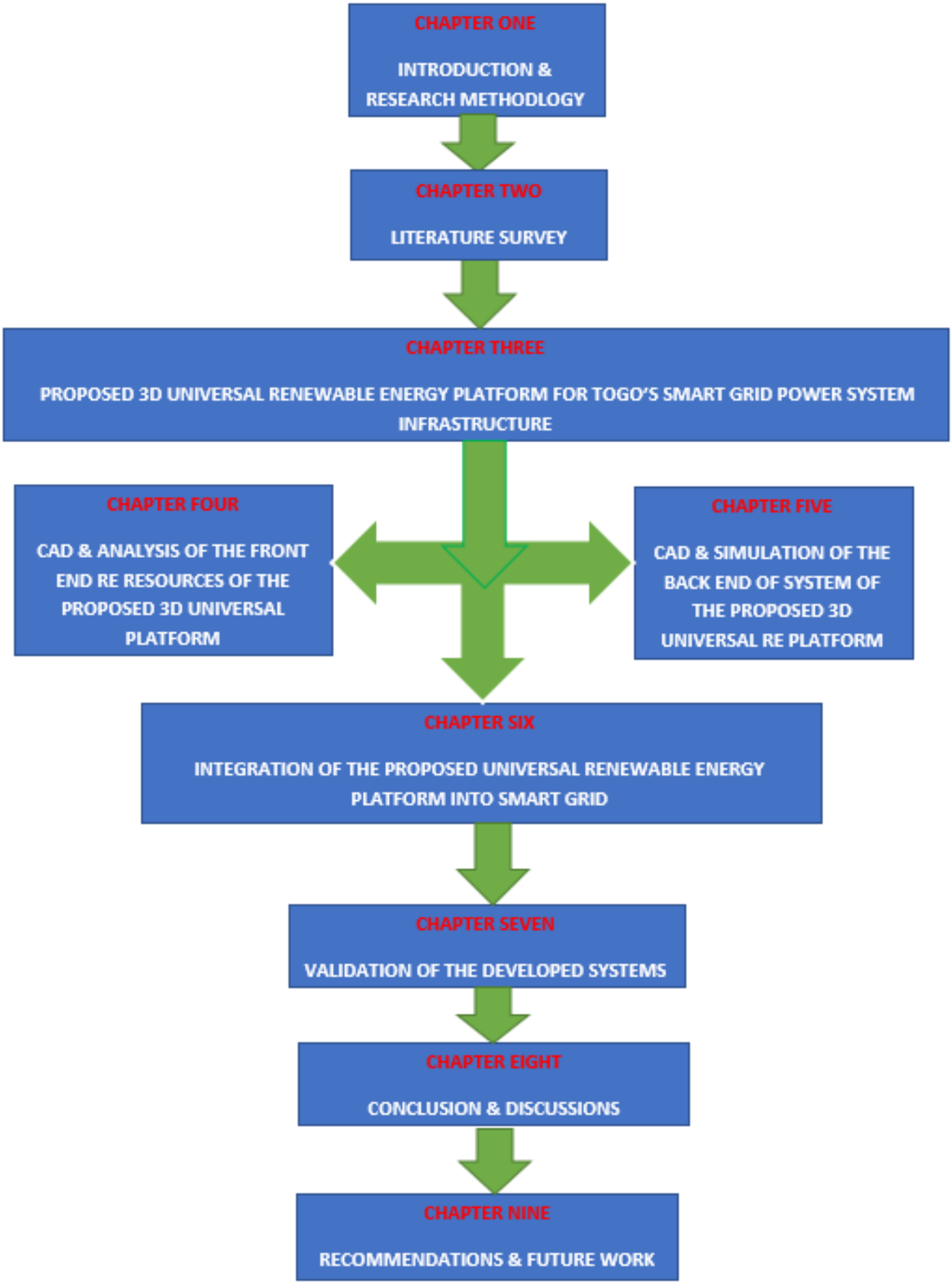

Figure 1-1 Structure and organisation of Thesis

CHAPTER 2

CHAPTER 2: LITTERATURE SURVEY

2.1. INTRODUCTION

This chapter presents a comprehensive literature survey into current and previous work related to the theme of this work. It covers the components of the design and development of a Computer aided design of an efficient renewable energy platform for Togo's smart grid infrastructure able to provide clean energy on a micro scale, medium, and industrial scale

2.1.1. TOGO'S ENERGY SECTOR

Total energy consumption in Togo in 2012, was estimated at 976 million Kwh, of which 67% was biomass. Oil accounted for 29%, electricity 4% of annual energy consumption. The national electrification rate is approximately of which 13.5% was for urban areas and 5% in rural areas. The Government of Togo expects to achieve a rate of 50% of national electrification by 2024 (SCAPE, 2017). Final energy consumption is mainly distributed between households (64%), transport (24%), market and public services (9%), and industry accounts for 3% (CEET, 2015).

ENERGY SUB SECTOR

The energy sector is represented by two main companies "CEB" Benin Electricity company whose primary mission is to Generate and transmit electricity through the power grid whilst "CEET"- Togo's energy and Electricity Company distribute low and medium voltages whilst also in charge of maintaining the power distribution network

The total power delivered to Togo's network was 1042GWh in 2012, of which 886 GWh delivered to CEET by CEB. CEET own production based on thermal power plants in 2012 amounted to 14.3 GWh. Given a total guaranteed power of 40 MW from CEB plants, 100 MW from independent producer plants and 10 MW from CEET's own available plants, the total implemented power capacity of Togo raises to 150 MW, 20 of which (13%) is from renewable hydroelectric source. The peak power of the network was 140 MW in 2012 and 163 MW in 2013. Production facilities and distribution are old and are causing frequent power outages. CEB has installed 105 MW of which 65 MW is hydropower and 2×20 MW thermal gases. One of the turbines of the thermal power plant is currently broken, and the hydroelectric power plant Nangbéto (2 x 32.5 MW) requires rehabilitation; as a result, they cannot produce full

power. Therefore, most of Togo's electricity consumption is imported (65-70 %) from Transmission Company of Nigeria (TCN), Nigeria, the Volta River Authority (VRA) of Ghana and Compagnie Ivorienne d'Electricité (CIE) in Côte d'Ivoire. Since October 2010, an independent producer, "CONTOURGLOBAL" built a 100 MW thermal power plant that can run on heavy fuel oil, the DDO or natural gas service. The plant currently operates on heavy fuel oil (HFO), which has the effect of significantly raising the cost of production (from 40 F/kWh with gas to 80 F/kWh with fuel oil), but discussions are underway with Nigeria's potential gas suppliers to feed the West Africa Pipeline. For an average growth of 8% per year, the demands for electricity will eventually increase over the next 10 years, therefore an additional need for 200 MW to meet the country's demand would be needed. Taking into account the fact that Nigeria and Ghana are the main electricity providers through CEB, they could reduce their electricity exports due to an increase of the demand in their own countries. The projected hydroelectric dam of Adjarala (147 MW of implemented capacity) will provide an average power supply of 42 MW for both countries (Benin and Togo). Togo should then construct 180 MW over the next 10 years to fill the gap. Providing modern, reliable, cheap and clean energy to consumers still remains a challenge.

2.1.2. INSTITUTIONAL FRAMEWORK IN TOGO

The Ministry of Mines and Energy (MME) is responsible for the energy sector, including the subsector of electricity through the General Directorate of Energy (DGE), which has the task to : (i) develop and implement the energy policy , (ii) monitor the implementation of the investment program , (iii) preserve state assets , (iv) carry out studies when necessary to ensure the reliability of energy and equipment safety, (v) identify and propose measures of energy efficiency and energy technology proven , and (vi) act as energy advisor to the Government, the local communities and investors. Other institutions in the energy sub-sector are: The Regulatory Authority for Electricity Sector (ARSE), established in July 2000 to regulate the sub-sector of electricity : (i) defining and enforcement of the sub-sector (ii) reviewing and overseeing procurement mechanisms (iii) advising on proposals and decisions regarding tariff , (iv) providing advice on the development of energy infrastructure , (v) providing advice on issuances of expropriation for public utility (vi) monitoring and certifying electrical installations , and (vii) managing potential conflicts between distributors and consumers. It should be noted that CEB, is not regulated by the ARSE yet.

The Compagnie d'Energie Electrique du Togo (CEET): public entity created in 1963, is responsible for the distribution of electricity in the country. CEET operates some thermal

power plants in areas where the CEB network is absent, but buys most of its electricity from CEB and ContourGlobal (a private producer). Most of the network is interconnected, but several provinces of the country are not yet connected to the national network. These communities are powered by diesel generators power plants with an installed capacity ranges from 32kW to 750 kW. In 2012, there were 37 localities supplied with insulated electrical system, with a total installed capacity of 9.6 MW.

The Communauté Electrique du Benin (CEB): was created in 1968 by Benin and Togo through the Benino-Togolais electricity code to import, produce and transmit electricity for the benefit of the two countries. This code Benino- Togolais was revised in December2003 to open the sector to independent producers. However, CEB remains the sole buyer of the power system (both countries) and delivers electricity to Benin Electric Power Corporation (SBEE) in Benin, and CEET in Togo and some large industrial customers. Exceptionally, the energy produced by ContourGlobal is sold directly to CEET.

The independent producer Contour-Global Togo: is an independent power producer (IPP), operating since 2010 in Lomé, with a thermal power plant with a capacity of 100 MW operable with natural gas, heavy fuel or DDO. The power plant is equipped with six (06) production groups, working with heavy fuel oil (HFO) due to the lack of natural gaz. The government has initiated discussions with potential gas suppliers in Nigeria to get the necessary volume of gas delivered through the West Africa Pipeline to operate the plant. Contour-Global does not work full time; it is requested in case of shortage of power supplied from CEB.

2.1.3. REGULATORY FRAMEWORK

The adoption of Law No. 2000-012 of 18 July 2000 on electricity and its implementing Decree No. 2000-089/PR 08 November 2000 defines the conditions to exercise certain regulated activities, as decided by Law n° 2000 regulating the electricity sector. This was an important step forward to ensure the development of sub-electricity sector. However, this legislation has a number of shortcomings related to the absence of provisions on:

- The electrification of rural areas;
- the use of renewable energy;
- the need for technology transfer in the energy field;
- the fate that should be reserved for production surpluses made by private companies, particularly in the context of industrial operation;

- The obligation to ensure price transparency through the development, publication and wide dissemination of tariff policy;

The Code Benino- Togolais of electricity revised in 2003 opened the segment of power generation to the private sector and dedicated CEB as the sole buyer. This code should be revised to adapt itself to the new regional ECOWAS recommendations.

2.1.4. ENERGY POLICY

Togo's energy policy as adopted in 2014 (REEEP, 2015). The draft energy policy has a lot of provisions such as, to: (i) the development and adoption of an investment code or law which includes tax and incentives for the promotion of renewables energies; (ii) development and adoption of rules defining the conditions for the production of renewable energy and connection to the national network at a discounted price; (iii) development and adoption of a law to define energy efficiency policy by promoting equipment using low energy; (iv) develop and adopt specific legislation to promote the electrification of rural and economically disadvantaged areas, specifically setting up a national rural electrification agency and a Rural Electrification Fund. (v) Implement the program for the liberalization of the electricity market to promote the inclusion of Togo in the Regional Market ECOWAS. (vi) develop an institutional framework to establish a public-private partnership: • Definition of a favourable tax and customs arrangements for electrification projects in rural areas; • Establishment of a funding mechanism with the participation of external donors and the national financial system; (vii) Encourage the production and off-grid energy supply in remote or isolated areas and provide appropriate incentives to businesses to ensure a reasonable return on investment. (viii) Facilitate the creation of industrial facilities for the local manufacture of electrical equipment; (ix) Explore sedimentary basin for petroleum products and gas.

2.1.5. RESILIENCE TO CLIMATE CHANGE

Togo, in its draft energy policy aims to promote alternative energy sources to reduce pressure on wood resources, develop appropriate technologies for the use of these alternative energy sources (ARSE, 2015). The country also intends to develop and promote the use of efficient wood stoves and raise awareness about the problems of desertification and soil erosion from deforestation, as well as alternative technologies for fuel wood and charcoal wood

2.1.6. TARRIF POLICY

Togo does not have a formal tariff policy. The practice is that CEET and CEB formulate their requests for revision of tariffs to the ministry of Energy. For CEET, the regulator (ARSE)

examines the merits and issues professional advice to Government authorities. The Ministry of Mines and Energy (MME) is responsible for the tariff policy for electricity and is responsible for proposing revisions to the Government after review. The last rate increase was adopted in November 2010 and implemented in January 2011. Rates revised were below the level expected by CEET. An operating subsidy of CFAF 3 billion, £4M approx... Is paid annually by the Government to CEET to supply fuel to the power plant Contour-Global. Energy is bought by CEET at the average of 58 FCFA, (£0.77)/KWh form CEB and 121 FCFA / kWh from Contour-Global. Average tariffs (tax free) for distribution are 100 FCFA, (£1.60) /kWh for medium voltage customers and 98 FCFA / kWh for low voltage customers. When tariff policy is defined, implemented and sustained by an independent regulatory, it gives more visibility and confidence to private businesses willing to invest in the sector. The sector reform will aim to reinforce the independence of the regulator and make it decide for tariffs.

2.1.7. ELECTRICITY SUB SECTOR REGULATION

The regulator of the electricity sector (ARSE), although under the Ministry of Mines and Energy, has a relative independence. ARSE is following the implementation of the performance contract between CEET and the Government. ARSE does not have the responsibility to regulate tariff, but advises the Government. The ARSE is not associated with the negotiation of power purchase agreements for electricity production. In the context of sector reform agenda, the authority of ARSE should be strengthened.

2.1.8. ECONOMIC PERFORMANCE OF THE SECTOR

a) CEET ECONOMIC PERFORMANCE

- The rate of energy billing recovery is 84 %, a rate of technical and non-technical losses by 16%, which is respectable result, compared to several countries in the sub-region.
- The recovery rate of private bills costumers is 95 %, while the administrative costumers are only 35- 50 %. They represent 32 % of consumption and seriously affect the results of CEET. - The time of interventions to achieve small scale work and connections are still very high (30 to 40 days) due to the difficulties to address supply and connection materiel.

Net operating income of CEET revolves around balance (WB, 2015). In 2009, it was positive to 0.1 billion FCFA, before falling to - 3.8 billion FCFA in 2010,and then rose to 2.4 billion in 2011 and 3.24 billion FCFA in 2012. The financial situation of CEET has improved due to: (i)

impact of tariff increase in January 2011, (ii) the change in the power purchase contract of Contour Global by CEB (decrease of about 10 billion FCFA francs in the expenses of CEET) (iii), an annual operating subsidy of about 3 billion FCFA. However, the financial results of CEET the past three years remain fragile. The electricity from the CEB and Contour Global purchase represent 70 % of the expense of CEET. The financial situation of CEET is therefore strongly influenced by the prices of electricity imported from Nigeria and Ghana, and by fluctuations in fossil fuel prices on international markets. The financial flexibility is limited; CEET is limited to self-finance the investment needed for its development.

b) CEB ECONOMIC PERFORMANCE

The benefits of CEB were positive from 2008 to 2010 but then deteriorated in 2011 and 2012 with respective losses of 3.67 billion FCFA and 7.45 billion FCFA despite the increase of 10% of the tariff effective in July 2009 (the rate increased from 50 to 55 FCFA / kWh) (CEET, 2015). CEB is highly dependent on its purchases in Ghana and Nigeria. Like CEET, it is essential that CEB has a clear tariff policy and an adjustment mechanism to pass on increases in the cost of imports of electricity (WAPP, 2014).

2.1.9. INSTITUTIONAL AND TECHNICAL CAPACITY

A) INSTITUTIONAL CAPACITY

Procurement is regulated by the Law 2009-013 of 30/06/2009 relating to public procurement and delegation of publics services. There is a procurement control institution (Direction Nationale du Contrôle des Marchés Publics -DNCMP) and a regulator of public procurement (Regulatory Authority for Public Procurement -AGP). All public institutions have a person responsible for public procurement and a procurement board which is controlled by the National Board. This is to ensure transparency in procurement process. The procurement law is consistent with the sub-regional organization West African Economic and Monetary Union (WAEMU) directives that require tenders to be open to the economic space of the WAEMU. However, after a certain threshold, bids are open internationally. In case of dispute in the acquisition process, bidders may appeal to the ARMP for arbitration.

B) TECHNICAL CAPACITY

Togo has already experienced the production and use of renewable energy for productive purposes.

Solar: experiences of using the solar energy were made in the 80's and 90's for the electrification of social infrastructure such as schools, health centres, drinking water pumping in rural areas. In 2003, UNDP supported the project «Solar energy for domestic needs of women in Regions of Central and Kara" in Program Improvement Livelihoods Populations (PAMEP). In 2009, UNDP has also funded under the program mentioned above, the municipalities of Kountoiré and Naki-East. This program has helped to promote this form of energy through the use of solar cookers, solar dryers and solar equipment but hasn't been scaled up (UNDP, 2013).

Wind: The use of wind power is marginal or almost non-existent. Installed capacity is estimated at about 5.7 kW. It is used for various purposes in rural areas, particularly in Atalote (Prefecture Keran) and Gapé - Kpédji (Zio Prefecture) for water pumping (WBG, 2012).

Hydroelectricity: the country capitalizes a long experience with hydroelectric power plant; Nangbéto (65 MW) for the CEB and a mini hydropower system of Kpimé (1.6 MW) for CEET. The Ministry of Energy will strengthen its staff capacity through various programs. The Government is identifying capacity building needs in the context of the administration's modernization. More staff will be recruited to reinforce the capacity at the Ministry. Furthermore, ECREEE organization (one of ECOWAS organization in charge of renewable energy) regularly trains staff of the Ministry and the CEET each year (WBG, 2014).

It is to be noted also that CEB has undertaken a study of pre-feasibility in order to conduct a pilot plant from solar photovoltaic system power 5 MW with a private developer. Similarly, a project of 13,000 solar street lights is being implemented with funding from China Exim Bank. This project was preceded by a pilot phase and enters its implementation phase. The contract has been awarded and work is scheduled to start in June 2014. Another project called Program of development of renewable energy and energy efficiency (PRODERE) is funded by WAEMU and aims to power 22 rural community infrastructures (schools, health centres); nearly 1340 households and 19 boreholes for water drainage are programmed to be equipped. This program is now in its implementation phase after contract award to selected contractors.

AFDB and the World Bank have agreed to participate in the financing of the construction of the hydroelectric dam Adjarala; the project is at the stage of evaluation.

2.2. OUTLOOK FOR RENEWABLE CAPACITY IN TOGO

Figure 3-1-1 shows a trend of renewable capacity in Togo showing an installed capacity of 67MW since 1992 clearly pointing out a staganation of the renewable market till date. The main renewable energy contributor in Togo is Hydro power and no other renewable sectors are currently forecasted to have operational installed capacity any time soon (Energi-ci, 2016).

	Initial	Added	Installed	1yr % change	% Total
1992	67 MW	0 MW	67 MW	0.00%	69.07%
1993	67 MW	0 MW	67 MW	0.00%	69.07%
1994	67 MW	0 MW	67 MW	0.00%	69.07%
1995	67 MW	0 MW	67 MW	0.00%	69.07%
1996	67 MW	0 MW	67 MW	0.00%	69.07%
1997	67 MW	0 MW	67 MW	0.00%	69.07%
1998	67 MW	0 MW	67 MW	0.00%	69.07%
1999	67 MW	0 MW	67 MW	0.00%	72.83%
2000	67 MW	0 MW	67 MW	0.00%	72.83%
2001	67 MW	0 MW	67 MW	0.00%	72.83%
2002	67 MW	-37 MW	30 MW	-55.22%	62.50%
2003	30 MW	0 MW	30 MW	0.00%	62.50%
2004	30 MW	10 MW	40 MW	33.33%	68.97%
2005	40 MW	10 MW	50 MW	25.00%	73.53%
2006	50 MW	10 MW	60 MW	20.00%	76.92%
2007	60 MW	6 MW	66 MW	10.00%	78.57%
2008	66 MW	1 MW	67 MW	1.52%	78.82%
2009	67 MW	0 MW	67 MW	0.00%	78.82%
2010	67 MW	0 MW	67 MW	0.00%	78.82%
2011	67 MW	0 MW	67 MW	0.00%	78.82%
2012	67 MW	0 MW	67 MW	0.00%	78.82%
2013	67 MW	0 MW	67 MW	0.00%	78.82%
2014	67 MW	0 MW	67 MW	0.00%	78.82%
2015	67 MW	0 MW	67 MW	0.00%	78.82%
2016	67 MW	0 MW	67 MW	0.00%	78.82%
2017	67 MW	0 MW	67 MW	0.00%	78.82%

Initial = capacity at beginning of year, megawatts
Added = capacity added during year, megawatts
Installed = Initial + Added, megawatts

Capacity figures are for aggregated renewable energy capacity including biomass and waste power, geothermal power, hydroelectric power, solar power and wind power.

1yr % change = Percent change over prior year
% Total = Percent of total capacity (all conventional and renewable power sources)

Figure 2-1 renewable Capacity Data sheet 1992-2017 (World Bank data, 2015)

2.2.1. ENERGY POTENTIAL

Togo is not a producer of neither oil nor petroleum products (World Bank, 2015). The country relies on imports to meet its needs for petroleum products. It has, however, resources in renewable energy untapped.

2.2.2. SOLAR POTENTIAL

Togo is located in an area of strong sunlight where solar radiation is fairly well distributed throughout the country. its geographical position makes it quite ideal for solar power harnessing as the country benefits from at least 10-12 hours of sun rays with an average temperature of 33 (°C) degree Celsius daily (Sunspec, 2015) . With unstable electricity supply, the application of single PV systems will enable the delivery of approximately 79KW over a 12hours period depending on panel's size and ideal weather conditions. The average home consumption per capita in the country is rated at 103 KWh daily (W-underground, 2015) making two (02) solar panels enough for a single home. The global solar energy irradiation on a horizontal plane is estimated at 4.4 kWh/m²/day for Atakpamé (Plateaux Region) and 4.5 kWh/m2 /day in Mango in savanna Region. The use of solar energy for thermal or electrical purposes began in the 80's with: (i) the installation of solar water heaters in some health services and hotels by NGO's, (ii) power telecommunications relays (iii) illuminated billboards and (IV), the installation of solar pumps in rural areas.

Togo average weather conditions (2012-2013)

Weather Underground. 2015. Lomé, Togo History | Weather Underground. [ONLINE] Available at: https://www.wunderground.com/history/daily/DXXX/date/2013-12-27. [Accessed 11 October 2015].

CONTENT REMOVED FOR COPYRIGHT REASONS

Figure 2-2 Togo average weather conditions May 2012-May 2013 (W-underground, 2015) (a) the map and geographical location of Togo's & (b) weather forecast

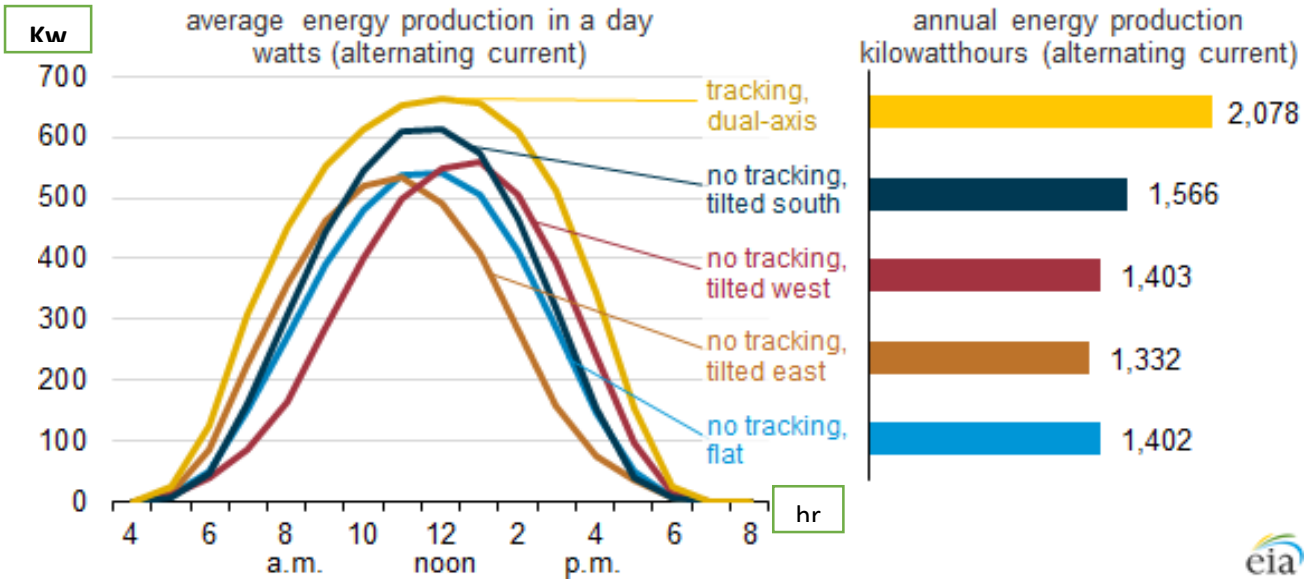

Figure 2-3 Average daily solar power generation (power (kW) versus time Period, (EIA, 2013)

2.2.3. WIND POTENTIAL

Togo is ranked among the quiet areas although transient spikes wind can reach high values up to 4m/s in some areas especially in the northern part of the country during the dry season period. Only the coastal area of the country has favourable evidence with wind speeds of 7m/s on average. The development of wind power can be considered as a viable alternative. The main project, currently being considered by the country is the proposed construction and operation of a 25.2 MW plant by Delta Wind Togo who has signed a concession agreement with the Government for its implementation. The wind in Togo is quite an advantage to this proposed technological model as the country's geographic location on the gulf of guinea benefits from the wind coming from the Atlantic Ocean which is located at the south side of the country (Weather-spark, 2015).

Mean Annual Wind speed in Togo

Average Weather in Togo, Year Round - Weather Spark. 2015. [ONLINE] Available at: https://weatherspark.com/y/45795/Average-Weather-in-Lom%C3%A9-Togo-Year-Round. [Accessed 07 October 2015].

CONTENT REMOVED FOR COPYRIGHT REASONS

Figure 2-4 Mean annual wind speed in Togo's around one year (Weather-spark, 2015)

2.2.4. HYDROPOWER POTENTIAL

Studies conducted in 1984 identified nearly forty sites on different streams of which nearly half (23) has potentials greater than 2 MW of energy production. The expected energy production of all sites is estimated to be around 850 GWh for an installed capacity of about 224 MW. The most important project is Adjarala located on the Mono River whose watershed is shared with Bénin. Some rivers are almost dry now, that's why updating the studies is needed. Adjarala dam one's potential estimated at 100 MW is now 147 MW after new studies were done recently (World Bank, 2015). Togo imports at least 85% of its electricity (Tititudorancea, 2013) while there are great possibilities of using its hydro sites for power generation. The country equally has a wonderful coastline that extends to about 55 Km on the Atlantic sea, River Oti and Mono of which water flow strength could be great for hydro and tidal power generation.

2.2.5. BIOMASS AND BIOGAS POTENTIAL

BIOMASS MAP OF TOGO

BIOMASS MAP Togo. 2018. Togo. [ONLINE] Available at: https://www.worldenergy.org/data/resources/country/togo/biomass/. [Accessed 05 September 2014].

CONTENT REMOVED FOR COPYRIGHT REASONS

Figure 2-5 Togo Biomass carbon on the wider land scale& (b) Soil carbon (Carbon bio-diversity, 2013)

Figure 2-5 shows the country biomass carbon on a wider scale with a closer view on the soil carbon potential available in Togo. The analysis reveals that the terrestrial carbon stocks is estimated at 680Mt made up of 362 Mt of carbon in above and below ground biomass shown in part (a), 317 Mt of soil carbon is then obtained in the soil figure (b) (Carbon bio-diversity, 2013). Soil biomass potential and carbon biomass are spread around the country as shown in figure 3-5; the highest area having a 15% of carbon density hence covers only a mere 5% (2800 km^2) of the country land area (Carbon bio-diversity, 2013). These data's means that the country generally has a low biomass potential and most of the considered part are formed of high soil carbon. Its importance however shouldn't be overlooked as considerable development strategies could see the light if these biomass potentials are efficiently used in the production of energy.

2.2.6. RENEWABLE ENERGY POLICY AND ITS APPLICATION

The development of alternative energy in Togo is a real necessity in a context of scarcity of natural resources, the fight against climate change and desertification and reducing greenhouse gas emissions. Togo has so resolutely committed to the promotion of renewable energies to overcome its energy deficit and ultimately contribute to the reduction of poverty. At Government level, the activities related to renewable energy are governed by the General Directorate of Energy, housing a division of renewables. It should be noted that the Government of Togo in its development strategy SCAPE 2013-2017, is committed to (i) improve the regulatory and institutional framework for the promotion of renewable energy, (ii) exempt taxes on imported equipment in the context of renewable energy and (iii) promote the construction of solar power plant (5 MW) and wind turbines (12 MW) in order to generate electricity. In the context of energy policy being finalized, it is envisaged the establishment of a Rural Electrification Agency whose missions will also be to cover the development of renewable energy and energy efficiency. The revision of the law 2000 - 012 - (on the electricity sector) is in project and includes provisions to promote renewable energies.

2.2.7. ENERGY POLICY

The demand for electricity in Togo continues to increase at an average rate of 8% per year and could double in the coming next 10 years. The country's electricity supply is heavily dependent on oil and its derivative products (including natural gas), which are subject to international price volatility. Diversification of energy supplies will achieve a broader energy mix and will ensure greater energy security to the nation. The Togolese Government intends to

develop renewable energy. This orientation was included in the axis 2 of the Accelerated Growth Strategy and Promotion of Employment (SCAPE), adopted in 2013.

2.2.8. BARRIERS TO THE IMPLEMENTATION OF RENEWABLE ENERGY

Although the option of promoting renewable energy has been acknowledged by the Government in its strategy to accelerate economic growth and employment (SCAPE 2013-2017), there were obvious some barriers to overcome so as to enable potential investors to invest considering energy state at the time. Indeed, at the regulatory level, besides the code Benino- Togolais of electricity which legislated a joint venture for energy sharing and infrastructure support, there were no laws or directives that regulated the promotion of renewable energy in the country. In addition, the lack of studies on the potential of renewable energy sources and specific policies encouraging the private sectors contribution to the energy mix are obstacles to the development of these renewables energies. Moreover, CEET, the country's energy management institution should conduct a study on the capacity of its distribution network to integrate alternative power generation from renewable energy including the use of smart grid and green systems that private producers may have the opportunity to also inject in the network.

To meet the key challenges of ensure an adequate and reliable supply of electricity over the next 10 years, it is detrimental that an increasing access to electricity services in a context of future demand increase be considered through the implementation of an energy mix approach thereby reducing reliability from neighbouring countries. Togo needs to be focused and proactive. Substantial private and public financing will also need to be mobilized over the next 10 years and the sub-sector financial equilibrium will need to be secured through adequate tariffing.

The key challenges and recommendations facing Togo's electricity sub-sector and the Ministry responsible for Electricity can therefore be regrouped in four broad categories: (i) implementing investment in generation, transmission and distribution and in personnel; (ii) increasing access to electricity services; (iii) ensuring the financial equilibrium of the sub-sector, CEET and CEB, and reviewing the tariffs; (iv) adjusting the regulatory framework to account for internal and regional requirements. This is discussed in the proposed business model in chapter (5)

2.2.9. CURRENT BUSINESS MODEL

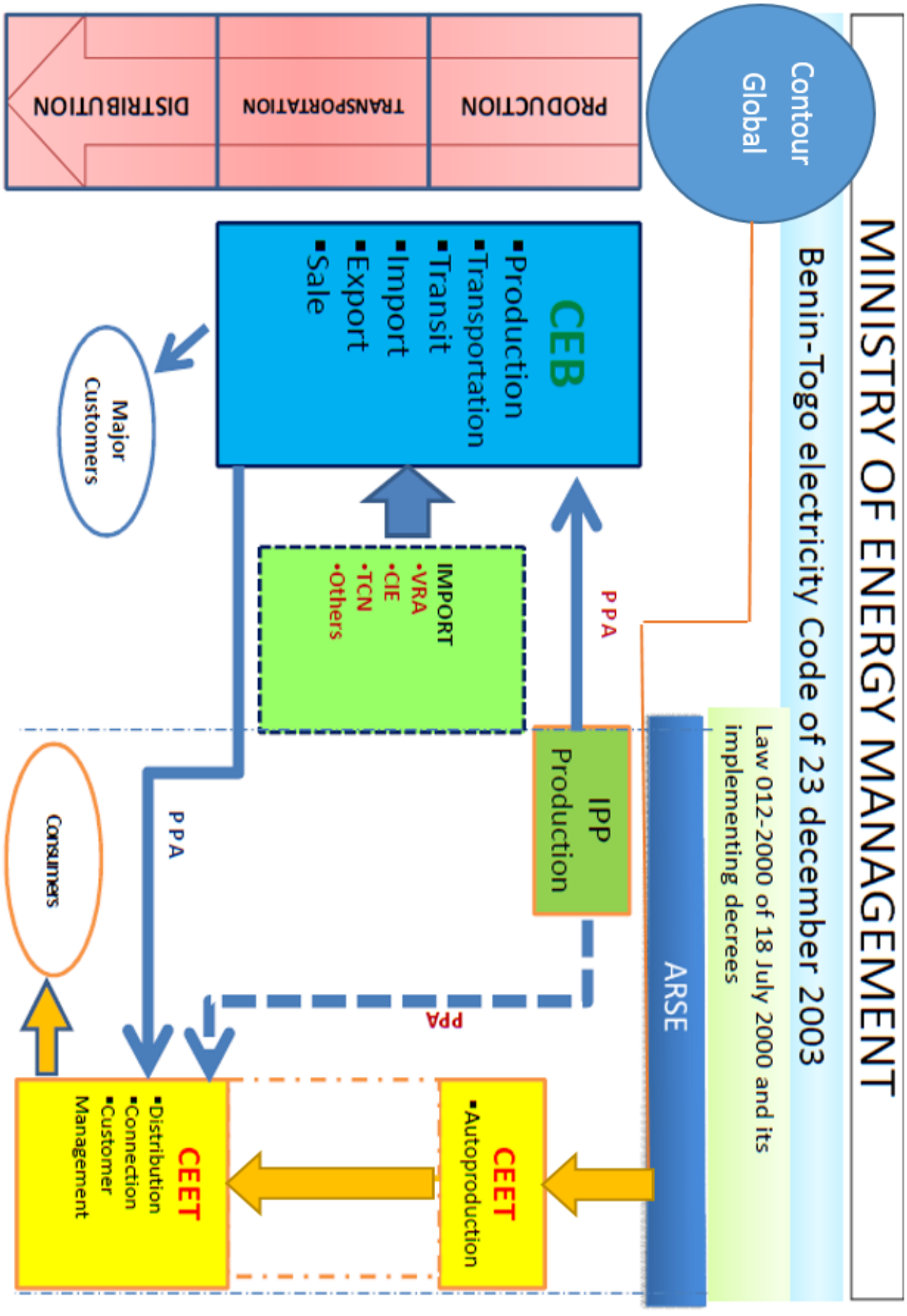

Figure 2-6 Current Energy Business model &Energy management operations in Togo

Figure 2-6 depicts the current business model in Togo. The business model as one can see agrees with some of the findings from the literature review in the earlier chapter. The business model has three parts, the production, the transportation and the distribution of electricity. From 2003, Electricity production / transportation, its transit, import from Ghana, export to Togo and sales were conducted by CEB - Republic of Benin under the agreement of the joint electricity scheme between CEET & CEEB (World Bank report, 2010, no 52831-TG).

The business model currently adopted in Togo satisfies current Energy demand but does not take into account future challenges, demand growth and grid expansion. The criticism of this business model would also take into account on cost incurred by the import of Diesel from Nigeria via the West African power pool pipeline for the 6 Tri fuel diesel engines plant for contour global even though potential for renewable energy sources would have been the most sustainable investment

Efforts therefore, needs to be conjugated to meet future energy demands hence the full optimisation and implementation of renewable energy systems for sustainable energy production and supply must be sought (MOE, 2014). The possibilities of this however becomes a reality if Political, Economic, Social, Technological, legal and environmental factors in the country are favourable for the implementation of a new business model that will ensure the production of clean energy and would ensure sustainability over a long period. A PESTLE analysis was then carried out to this effect.

Political Factors

- Stable political environment
- Taxes are regulated by the Government
- Marketing ethics are set by Unions, and regulated by Government
- Good economic policy planned and regulated by Government
- Government isn't involved in any company's culture and religion unless necessary
- High Government involvement in trading agreement

Economic factors

- High interest rates are realisable but depending of management

- There is a low inflation employment per capita
- A good and long term prospect for the economy GDP due to good governing policies put in place
- Encouraging reforms by the Government through support funds into entrepreneurship/ business ideas/ and opening of a company within 24 hours of request approval

Sociocultural factors

- Foreign products and ideas are well embraced
- The dominant religion is Christianism followed by Islam
- Speaking the local language isn't considered a barrier as a bunch of people do speak English due to the sharing border with Ghana and French which is the national language
- There is a high level of Nepotism as a culture at CEET almost at all management levels

Technological Factors

- There is a low technical knowledge at CEET and in the country in general as new technologies are not quickly introduce at higher education and technological institutions
- At CEET, when a new technology is introduce, the machines are being bought and installed, and set to work by manufacturers but no proper training is given to CEET staff for them to carry out maintenance of those machines or equipment's when damaged
- As the country isn't involved in manufacturing of any parts either electrical or mechanical of any kind, getting new electrical parts becomes very expensive as they have to be imported
- There is a bad and poor internet reception in the country generally hence this affects communication
- License to operate walky-talky systems are expensive and the only available way to communicate which is mobile phones is equally costly.

- There is no proper effort on the government side to improve communications hence industries and companies such as CEET found it hard to create a proper Customer relationship Management

Legal factors

- CEET has recently in the interest of improving their image offered legal compensations to any customers complaining of bad installation or connection fault done by their staff

- Accident insurance and public liability insurance has recently been introduced and offered to clientele

- The government also reserve the right to anyone in terms of fairness to take CEET to court if an agreement cannot be reached upon discussion of both parties.

Environmental Factors

- Both companies never had any recycling policies

- Presence of bad and archaic ways of connections to the power grid which left cable criss-crossing and hanging in the air

- High rate of pollution due to diesel engines being used

- No planning of generating carbon neutral electricity (CEET, 2016)

The PESTLE analysis carried out above shows that both companies had issues towards dealing with customers and meeting their needs. The analysis shows that politically, the Government had too much involvement in the trading agreement act which could lead to the government implementing a tax law on any foreign company which might consider investment in this sector, on the other hand having a stable political environment is really an advantage for any business hence this could lead to the encouragement of any foreign companies or industries with a good aim of contributing to the country economy to assist in matter such as meeting energy demand in the country. The technological laxness however is a discouraging factor to any foreign investment that would want to implant its operation in the country, hence any new business model should be one that requires less maintenance and a dedicated personnel that will be in charge ensure system maintenance, function and efficiency. Looking at the new call for energy companies and industries to emit less CO2 and switch to a zero carbon culture, it is believed that the derivative of this research could form basis of a new business venture that will solely operate on close to or a zero carbon energy generation.

Like other renewable energy technologies, the problem of high upfront costs has always been a huge challenge for energy mix implementation. This problem is particularly pronounced in emerging economies where limited purchasing power and a lack of suitable financial products constitute additional obstacles for a broader dissemination of RE technology. The present is a collection of case studies of business models and financing mechanisms which show possible ways how such obstacles can be addressed and overcome in innovative ways.

Three case studies of innovative business models and financing mechanisms are presented, ranging from pico-sized systems to large-scale PV plants including grid-connected as well as off-grid PV systems: 1) A pay-as-you-go business model, developed by Azuri Technologies, UK, shows how thousands of low-income households in Africa can get access to affordable lighting and phone charging systems. 2) A business model developed by Mosaic, United States, shows how crowdfunding can be used to offer individual people investment opportunities in PV installations. 3) Gham Power, Nepal, has developed a business model for urban hybrid micro-grids as an answer to unreliable electricity supplies from the public grid. The case studies illustrate that the generation of successful business models is not an easy task that can be done in just a couple of days. The specific regulatory, economic, social and cultural situation in a region has to be well understood and addressed in business models. Successful business models usually include a financing component. This is particularly important for the mass market in rural areas of emerging regions where most people do not have access to commercial financing, or are overwhelmed in dealing with loan applications. Furthermore, to be attractive for potential customers, business models must appear to be clear and simple, even if sophisticated processes run below the surface.

2.2.10. CASE STUDY ENERGY SECTOR, ETHIOPIA

Though producing 82% electricity from renewables, electricity access in Ethiopia is rated at a mere 16%(EEPC, 2006). The power sector development program (PASDEP) of the country hence was mandated to increase this to 50 % by (2009/10) which will mean an increament of energy generation from 791MW to 2218MW (EEPC, 2007) hence a grid expansion to 13,054 Km. This new development will mean an improvement of the energy efficiency and energy reduction from 19.5% to the agreed international standard 13.5%. This daring project partly funded by the Ethionpian and Chinese government; the world bank was estimated at $ 5.3 billion USD (World bank, 2006) and completion estimated in the next five years. At the completion of the project in 2011, 86% of the country generated electricity comes from

hydropower, 13% from diesel and 1% from gethermal and an increase of available power from 30 MW in 2006 to 3000MW in 2012 (EEPCO, 2011).

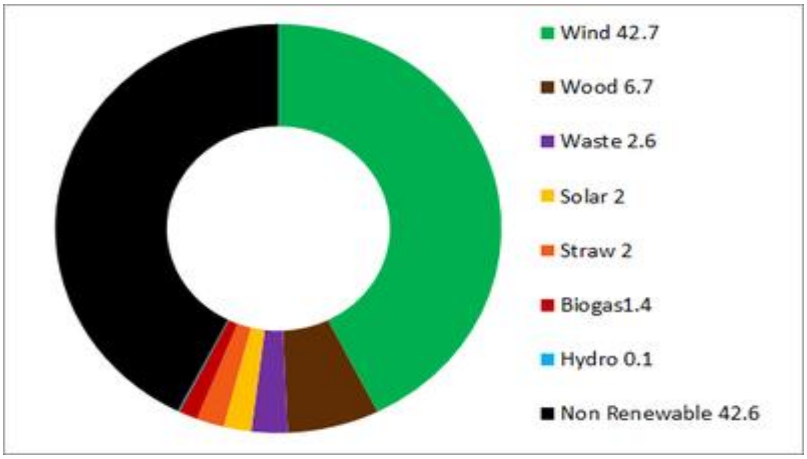

Figure 2-7 Ethiopia Energy production proportion (EEPCO, 2011)

The analysis reveals that the Ethipopian government is fully involved in the energy sector and have the sole responsibility of providing energy for its country in order to promote long term development and imporve the country's economy through industrialization. For such system to be possible the Ethiopian government has set energy policies in conjunction with the Ethiopian electricity power cooperation (EEPCO) in order to promote the use of renewable enrgy sources, and prepare and integrate a plan in order to highlight the power sector development by 2018 to a further 7850 MW of power considering the envisaged industrial growth and household demands due to grid expansion (EEPCO, 2010) . The policies drafted by the EEPCO and the Ethiopian government has also voted an enactment to promote independent power producers to invest in the energy sector so as to encourage economic devellopment and the usage of renewable energy in the country. (EEPCO, 2007)

Considering all of the above, The energy business strategy put in place by the Ethiopian government is an initiative that can very well work in Togo if energy policies are drafted for that purpose hence an energy booard or electricity survey board could be put in place to assess with certainty the country's current energy policies and current business model in order to draft policies that will enable energy production and its sustainability in the long run.

Independent power producers will definetely bring about a new business model in the country that could be adopted in order to promote the use of renewable energy sources and at the same time act as a strong tool for economic development as this doesnt exist currently.

Several studies have shown that global energy demand, currently estimated at 12.5 TW is due to increase to 17 TW in 2030, and can be met with just 2.5% of accessible wind and solar resources, using current technologies (L. Brown, 2010). Delucci and Jacobson (2010) picked one mix of eight renewable generation technologies, increased transmission, and storage in grid integrated vehicles (GIV), and shows without equivocation that a single mix is sufficient to provide world electricity and fuels. However, these global studies do not assess the ability of variable generation to meet real hourly demand within a single transmission region, nor do they calculate the lowest cost mix of technologies.

O.Ekren and Ekren (2010) analysed a small-scale system with batteries, PV, wind turbines, and auxiliary power. The study assumes near-constant load (for communications), calculates only an energy capacity for the batteries and not power limits, and optimizes the configuration for minimum capital cost, not minimum total cost. Unfortunately, Ekren and Ekren only report their optimized system cost and area of solar and wind rotor as well as battery size so it is difficult to analyse these results. In a real grid, we must satisfy varying load, and with high-penetration renewables, charging and discharging storage will at times be limited by power limits not just by stored energy. More typical studies combining wind and solar do not seek any economic analysis and/or do not look at hourly match of generation to load (e.g. Markvart, 1996).

A critical literature research also shows that Hart and Jacobson (2012) determined the least cost mix for California of wind, solar, geothermal and hydro generation (E.K. Hart et al, 2012). Because their mix includes dispatchable hydro, pumped hydro, geothermal, and solar thermal with storage, their variable generation (wind and photovoltaic solar) never goes above 60% of generation. Because of these existing dispatchable resources, California poses a less challenging problem than most areas as practical renewable energy sources are variable generation, and dedicated storage must be purchased for levelling power output. We cannot draw general conclusions from the California case's results; for example, one might plausibly infer from this study that it is possible to have a power system with 60% variable generation, but not a higher fraction; or, we might conclude that a grid based exclusively on variable generation would require prohibitively expensive amounts of storage.

For developing countries, a large number of studies exist and a detailed review of this literature is beyond the scope of this paper. Instead we focus on a selected set for our purpose. Givler and Lilienthal (2010) conducted a case study of Sri Lanka where they identified when

a PV/ diesel hybrid becomes cost effective compared to a stand-alone small solar home systems (50 W PV with battery). This study considers an individual household base load of 5W with a peak of 40 W, leading to a daily load average of 305 watt-hours. Through a large number of simulations, the study found that the PV-diesel hybrid becomes cost effective as the demand increases. However, this study focuses on the basic needs as such and does not include productive use of energy.

Munuswamy et al (2011) compared the cost of electricity from fuel cell-based electricity generation against the cost of supply from the grid for a rural health centre in India, applying HOMER simulations. The results showed beyond a distance of 44km from the grid, the cost of supply from an off-grid source is cheaper. This work just considered the demand of a rural health centre and was not part of any traditional rural electrification programme.

Hafez and Bhattacharya (2012) analysed the optimal design and planning of renewable energy-based micro-grid system for a hypothetical rural community where the base load is 600 kW and the peak load is 1183 kW, with a daily energy requirement of 5000 kWh/day. The study considers solar, wind, hydro and diesel resources for electricity generation. Although the study considers electricity demand over 24 hours, the purely hypothetical nature of the assumptions make the work unrealistic for many off-grid areas of developing countries.

Lau et al (2010) analysed the case of a remote residential area in Malaysia and used HOMER to analyse the economic viability of a hybrid system. The study uses a hypothetical case of 40 households with a peak demand of 2 kW. The peak demand is 80kW and the base demand of around 30 kW is considered in the analysis. Although such high rural demand can be typical for Malaysian conditions, it is certainly not true for others. The study also does not consider any productive use of electricity.

Similar case studies are presented in other studies as well. For example, Himri et al (2009) present a study of an Algerian village; Nandi and Ghosh (2013) discuss the case of a Bangladeshi village, while Nfah et al (2014) and Bekele and Palm (2010) provide case studies of Cameroon and Ethiopia respectively. The table below summarises the technology choices, demand focus and country of application of these studies

Table 2-1 Literature review derivatives

Reference	Technology application	Country of application	Supply duration/ type
Givler and Lilienthal (2005)	PV-battery – diesel	Sri Lanka	Domestic Application
Hafez and Bhattacharya (2012)	PV, Wind, Hydro, Diesel, Battery	Hypothetical	24 hour service but unrealistic demand profile for a rural area of developing countries.
Lau et al (2010)	PV-diesel hybrid	Malaysia	24 hour service but uses a high demand profile for a rural area
Himri et al (2008)	Wind-diesel hybrid	Algeria	Adding wind turbine to an existing diesel-based supply; Limited technology options.
Bekele and Palm (2010)	PV-wind hybrid	Ethiopia	Randomised load profile from hypothetical load data.
Nfah et al (2012)	PV, Micro-hydro, LPG generator, battery	Cameroon	Diesel as main generator supplemented by PV and micro-hydro, load based on grid

It can be seen that the hybrid options have often considered a limited set of technologies. Moreover, most studies concentrate on supplying electricity merely for domestic purposes and

do not take into account the electricity demand for industrial activities and for small-scale business units for the socio-economic developments. The load profiles are also not carefully considered in many cases. These issues are considered in the present study, thereby bridging the knowledge gap.

2.3. STATE OF THE ART OF EXISTING RENEWABLE ENERGY TECHNOLOGY

2.3.1. EXISTING WATER WHEELS

There are three main categories of hydro wheels, overshoot, undershoot and Breastshoot or Zuppinger wheel (Muller et al, 2002). Secondary research data shows that the most efficient of the wheels is the overshoot wheel with an average output of 80% guarantying a good output power due to its distinctive geometry of cells and design inflow details (Muller et al, 2002).Considering the aim of this research to provide an improved efficiency than the 80% average for the overshoot at an affordable cost, an evaluation of the wheels is conducted to analyze which will best fit the renewable energy platform for Togo's smart grid infrastructure model guarantying a high efficiency machined at a low cost. The design specification of all the wheels presented will help in evaluating and considering a better design which will offer a more improved efficiency

2.3.2. OVERSHOT WATER WHEEL

ARCHITECTURE OF OVERSHOOT WATER WHEEL

TES Teach with Blend space. 2017. *Hydro Electricity-Overshoot Water Wheel.* [ONLINE] Available at: https://www.tes.com/lessons/kMBZdxfPAvDZCQ/hydro-electric-water-wheel. [Accessed 03 February 2017].

CONTENT REMOVED FOR COPYRIGHT REASONS

Figure 2-8 Schematic of the overshot water wheel (Wedner et al, 2002)

The principle of operation of this wheel is to capture the water in its bucket or cells where its weight permits a constant rotation of the wheel turning mechanical energy into electrical energy. The buckets or cells shape play a significant role in obtaining a good efficiency hence they are shape in such a way that air can escape allowing the water jet from the inflow to enter each cell at its natural angle (Shire P, 2001). Capturing the water makes the wheels effective almost immediately and in order to avoid loss of water the design should consider a perpendicular shape of the buckets allowing it to be filled up to 30-50% of its total volume (Muller et al, 2009). The efficiency of the overshot wheel for a given application is dependent of the head difference, the diameter and flow volume with the considerations of a free or regulated inflow which impacts the head hence the speed (Stephen et al, 2009).

EFFICIENCY OF OVERSHOOT WATER WHEEL

TES Teach with Blend space. 2017. *Hydro Electricity-Overshoot Water Wheel.* [ONLINE] Available at: https://www.tes.com/lessons/kMBZdxfPAvDZCQ/hydro-electric-water-wheel. [Accessed 03 February 2017].

CONTENT REMOVED FOR COPYRIGHT REASONS

Figure 2-9 Efficiency Kauppert, 2003 (a) Efficiency flow rate of any turbine & (b) Efficiency against speed of overshot wheel (Muller et al, 2002).

Figure 2-9 shows Test carried out on the overshot water wheel and efficiency flow rate measurements of turbines generally. Figure 2-8(b) shows a typical efficiency curve of the overshot water wheel with the efficiency reaching above 80% allowing a ratio of Q / Qmax of ≈ 0.3 and maintain an almost constant curve so as to allow the water wheel when well design to be efficient and have a wide performance ratio.

2.3.3. UNDERHSOT WATHER WHEEL

ARCHITECTURE OF AN UNDERSHOOT WATER WHEEL

Alternative Energy Tutorials. 2016. *Waterwheel Design and the Different Types of Waterwheel*. [ONLINE] Available at: http://www.alternative-energy-tutorials.com/hydro-energy/waterwheel-design.html. [Accessed 15 April 2016].

CONTENT REMOVED FOR COPYRIGHT REASONS

Figure 2-10 Schematic of the undershot (Zuppinger) water wheel (Green Museum, 2012)

The undershot water wheels operates exactly as the overshot water wheel however differs in the direction of water inflow as the Zuppinger wheel has a side elevation with a backward inclined blade with a dam type inflow. The potential energy (mgh) is used as the driving force and the size of the blades and weight offers a rotation allowing the buckets to be filled rapidly (Culture P., 2012). The cells are designed in such a way to accommodate about 25 to 40% of the water at entry point, which is comparably less than the overshot but less water is loss due to blade head of each cell which is gradually reduce where water is discharge as wheel rotates with again minimum loss of water (UOS, 2012) . It is apparent that Geometry requirements and measurements of the space between the blades with diameter considerations as shown in Figure 2-9 should be the key to getting a good output and efficiency hence should be considered before any design is carried out (Informers, 2013)

EFFICIENCY OF AN UNDERSHOOT WATER WHEEL

Alternative Energy Tutorials. 2016. *Waterwheel Design and the Different Types of Waterwheel*. [ONLINE] Available at: http://www.alternative-energy-tutorials.com/hydro-energy/waterwheel-design.html. [Accessed 15 April 2016].

CONTENT REMOVED FOR COPYRIGHT REASONS

Figure 2-11 Efficiency as a function of flow rate (Q) max for the Zuppinger water wheel (UOS, 2012)

Figure 2-10 shows the expected efficiency curve measurements of a Zuppinger wheel designed with a head difference of 1.35 m; diameter of 6.0 m; width of ≈ 2.5m and available max flow rate of 4.0 m^3/s. Measurements were then taken with a speed of 4.87 rpm over two flow rates thus 1.53 and 3.3 m^3/s which showed an efficiency of 77% when Q /Qmax = 0.5 and 71% for when Q /Qmax = 1. Secondary research data reveals that most efficiency for the undershoot wheel are within the range of 60 -75% making the overshot much efficient than the undershot

2.3.4. BREASTSHOT WHEEL

ARCHITECTURE OF AN BREASTSHOOT WATER WHEEL

Breastshoot Design ideas final - 2015. [ONLINE] Available at: http://www.powerinthelandscape.co.uk/water/water_wheels.html. [Accessed 10 May 2015].

CONTENT REMOVED FOR COPYRIGHT REASONS

Figure 2-12 Schematic of the Breastshoot water wheel, (a) breast shoot wheel & (b) Principle of operation of Breastshoot wheel

The Breast shot water wheel is one that is used mainly considering location and where it application could best fit (British Hydro, 2015). The design is done in such a way that the water enters the bucket at a rather steep angle which allows the bucket to be filled quicker hence these cells are designed to respond to the resultant force acting in the rotation direction of the wheel (Muller et al, 2002); making water to be reduced at a downstream of 90° angle (Muller et al, 2002). Similarly, like the undershot the potential energy is used as the driving force where the water pushes the paddles to allow a rotation. The buckets or paddles are aired in order to allow air to escape during inflow and captivated when the paddles rise above lowermost point. The simple mechanism hence reflects the working principle of the undershot where the rotation of the wheel is created with the constant or high speed inflowing water (Muller et al, 2010).

EFFICIENCY OF A BREASTSHOOT WATER WHEEL

Breastshoot Design ideas final - 2016. [ONLINE] Available at: http://www.powerinthelandscape.co.uk/water/water_wheels.html. [Accessed 10 May 2016].

CONTENT REMOVED FOR COPYRIGHT REASONS

Figure 2-13 Efficiency of Breast shot as a function of flow rate (Muller et al, 2010).

The test for the breast shoot of which its efficiency characteristics is shown in figure 2-13 was carried out under a model test on a 1m Diameter and 1:4s scale model for the breast wheel (Weidner, 2003). Practically it was noticed that the wheel of the breast shoot could only absorb 10% of its design flow rate making the rotation of the wheel very slow. The maximum efficiency obtained was estimated at approx. 79% (Weidner, 2003) making it the closest to the overshot efficiency obtained shown in fig.2-10. It is therefore eminent to say that the efficiency could be improved in case there is a further increase in both inflow and outflow rate hence the design of the buckets and the availability of high flow of water could lead to an improved efficiency overall. Considering design specifications and accurate measurements assumptions, water wheels can generate greater power even with low flow volumes without using complex control systems, the experiments carried out revealed that the power / speed curves were quite smooth, indicating that speed control of the wheels isn't the focus to obtain good efficiencies but rather design speed due to good design specifications (Muller et al, 2010).. Slow flow of water means that small gear transmissions ratios needs to be employed making energy loss within the range of 2-3% but undoubtedly haver significant effect on project cost thus ≈ 30% for undershot wheels and ≈45% for overshot. The experiments results carried out for the 3 wheels shows that the most efficient is the Overshot water wheel with over 80% efficiency obtained

2.3.5. PV PANELS TECHNOLOGY

Energy from sun can be considered the main source of all types of energies. It can be used by various techniques such as making full use of sunlight to directly generate electricity or by using heat from the sun as a thermal energy. In this section, a comparison survey is included which investigates the three generations of PV cells with the latest characteristics.

First-Generation: Crystalline Silicon

Crystalline Silicon is a semiconductor material suitable for PV applications, with energy band gap of 1.1 eV. Crystalline silicon is the material commonly used in the PV industry, wafer-based C-Si PV cells which also dominate current market (A Farghly, 2012). Crystalline silicon cells are classified into three types as:

• Mono-crystalline (Mono c-Si).

• Poly-crystalline (Poly c-Si), or multi-crystalline (mc-Si).

• Ribbon silicon

Commercial production of C-Si modules began in 1963 when sharp Corporation of Japan started producing commercial PV modules and installed a 242 W PV module on a light house, the world's largest commercial PV installation at that time (Green M, 2015). Crystalline silicon technologies accounted for about 87% of global PV sales in 2010(S Shoot, 2014). The efficiency of crystalline silicon modules ranges from 14% to 19%. While a mature technology continued cost reductions through improvements in materials and manufacturing processes. Similar efficiency improvements were also noted for Ribbon and crystalline silicon

Second Generation: Thin film

Thin - film solar cells are beginning to be deployed in significant quantities. Thin - film solar cells could potentially provide lower cost electricity than c-Si wafer based solar cells (K.I. Chopra, 2010). Thin - film solar cells are comprised of successive thin layers, just 1 to 4 μm thick, of solar cells deposited into a large inexpensive substrate such as glass, polymer, or metal and Cadmium is a by-product of zinc. A potential problem is that tellurium is produced in far lower quantities than cadmium and availability in the long term may depend on whether the copper industry can optimize extraction, refining and recycling yields (E, Sachs, 2015). Cadmium also has issues around its toxicity that may limit its use. As a consequence, they require a less semiconductor material to manufacture in order to absorb the same amount of sunlight (up to 99% less material than crystalline solar cells). In addition, thin films can be packaged into flexible and light weight structures, which can be easily integrated into building Components building integrated Photovoltaic (BIPV). The three primary types of thin-film solar cells that have been commercially developed are: Amorphous silicon (A-Si and A-Si/μc-

Si), Cadmium -Telluride (CdTe), Copper-Indium-Selenide (CIS) and Copper-Indium-Gallium Diselenide (CIGS).

Third Generation: PV Technology

PV technologies are at the pre-commercial stage and vary from technologies under Demonstration (Multi - junction concentrating PV) to novel concepts still in need of (quantum-structured PV cells). Some third - generation PV technologies are beginning to be commercialized, but it remains to be seen how successful they will be in taking market share from existing technologies. There are four types of third-generation PV technologies: Concentrating PV (CPV), cooling of concentrating PV system, Organic solar cells and Dye-sensitized solar cells (DSSC).Responsible for the charge separation (photocurrent)

Reviewing the three generations, we can say that the First-generation solar cells dominate the market with their low costs and the best commercially available efficiency. They are a relatively mature PV technology, with a wide range of well-established manufacturers. Although very significant cost reductions occurred in recent years, the costs of the basic materials are relatively high. It is not clear whether further cost reductions will be sufficient to achieve full economic competitiveness in the wholesale power generation market in areas with modest solar resources. Second-generation Thin-film PV technologies are attractive because of their low material and manufacturing costs, but this has to be balanced by lower efficiencies than those obtained from first-generation technologies. Thin-film technologies are less mature than first generation PV and still have a modest market share, except for utility-scale systems. They are struggling to compete with very low c-Si module prices and also face issues of durability, materials availability and materials toxicity (in the case of Cadmium). Third-generation technologies are yet to be commercialized at any scale. Concentrating PV has the potential to have the highest efficiency of any PV module, Other organic or hybrid organic/conventional (DSSC) PV They offer low efficiency, but also low cost and weight, and free-form shaping. Therefore, they could fill niche markets

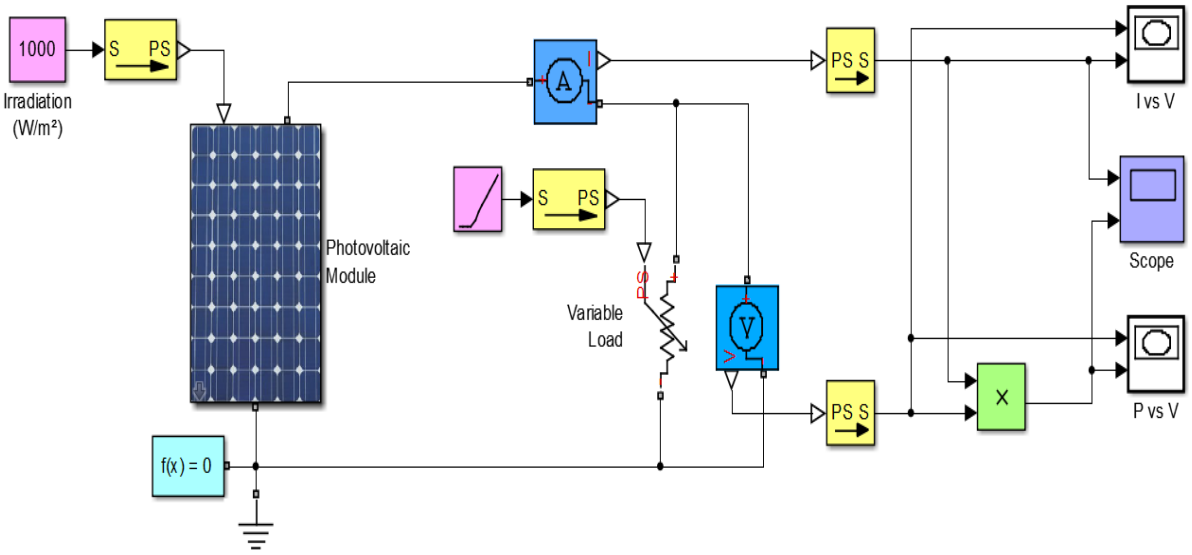

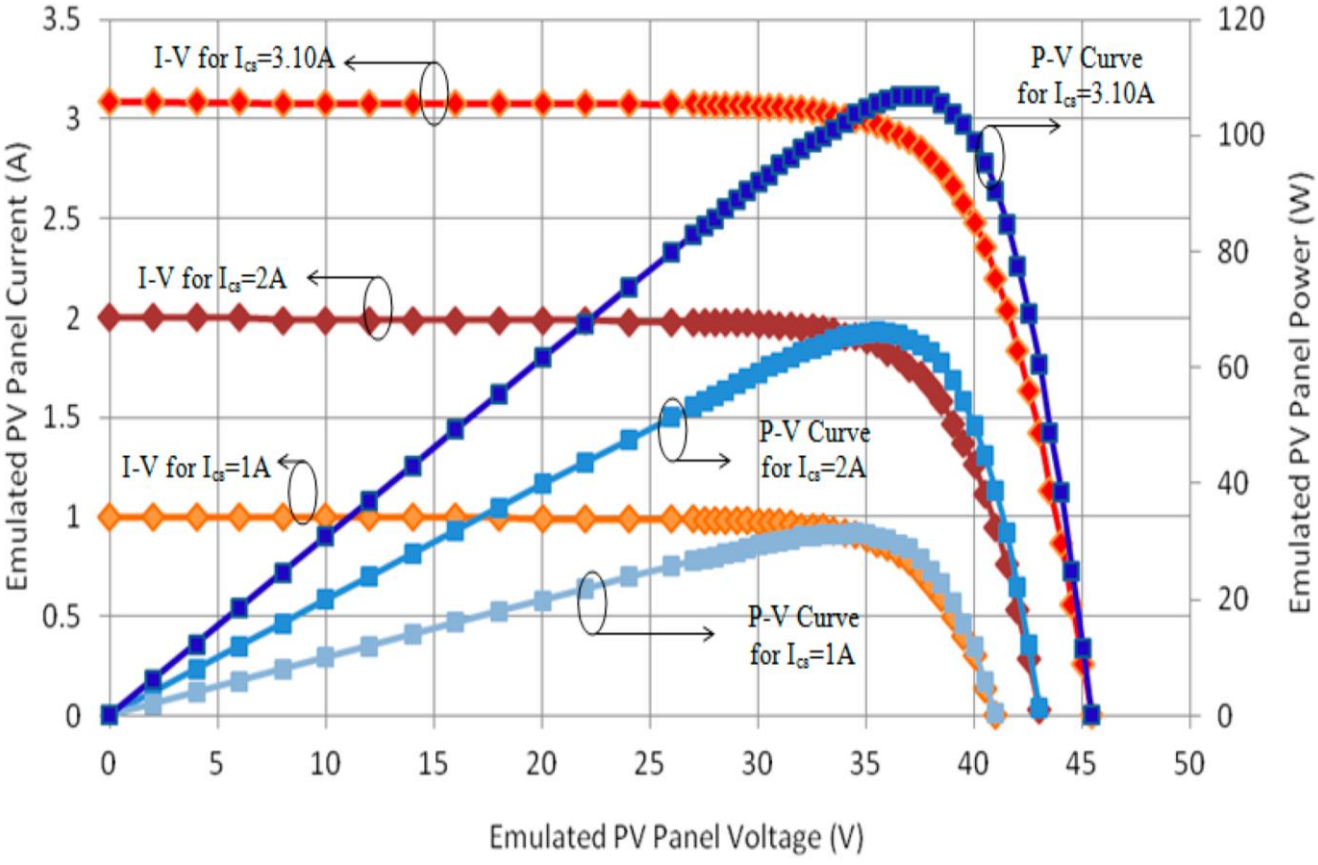

Figure 2-14 PV system Architecture & simulation output

Since the field tests can be expensive and depend primarily on weather conditions it is very convenient to have simulation models to enable work at any time. For this reason the research investigates a simple one-diode solar cell mathematical model, which was implemented applying MATLAB script. The model can be considered as an easy, simple, and fast tool for characterization of different types of solar cells, as well as, determines the environmental conditions effect on the operation of the proposed system. It can conclude that the changes in irradiation mainly affect the output current, while the changes in temperature mainly influence the output voltage. The characteristics of PV system have been developed. The simulation helps in understanding the PV characteristics, whilst the simulation model shows the curve between P-V & V-I relationship for varying temperature & varying irradiance. The results obtained from the model show close correspondence to manufacturer's curve. The results as it can be seen provides a clear and concise understanding of the I-V and P-V characteristics of the PV module which may be a suitable model for our renewable energy platform.

2.3.6. WIND TURBINE TECHNOLOGY

A wind turbine, like all forms of power generating technologies, is a device that converts one type of energy into electrical energy (BBC, 2016): in this case, the kinetic energy of the wind. The turbine does this by slowing down the stream of air flowing past it and the resulting change in momentum is converted to electrical output via a generator. In order for the turbine to be 100% efficient, all the kinetic energy would need to be removed from the air stream (Ra Eng., 2015). But this would mean that the air behind the turbine blades would be stationary and no air could flow. In the early part of the 20th century, Frederick Lanchester, Albert Betz and Nikolay Zhukovsky independently determined that the theoretical maximum efficiency of any turbine, irrespective of design, is 59.3%(F Lanchester, 2012). This is similar to the theoretical efficiency of heat engines that are limited by Carnot's theorem and, as is the case in heat engines, in the real world; this theoretical maximum is never reached. Additional losses occur as the result of a variety of factors such as wake rotation, tip-loss and turbulence (Green E, 2013). In practice, the highest attainable power coefficient is around 0.47 or about 80% of the theoretical limit (F Beltz, 2010). It is often said that wind power is 'inefficient', but 'efficiency' can be confused with 'load factor' which is the measure of how much electricity is actually generated relative to its theoretical potential. Turbines achieve overall efficiencies of almost 50% compared to approaching 60% for a modern combined cycle gas turbine or a maximum of around 30% for an internal combustion engine. In practice, a wind turbine will produce its maximum power output over a range of wind speeds and will be designed in such a way as to

maximise the energy output for the wind speed distribution at the location where it is to be installed. In general, a turbine will not produce any output for wind speeds below around 3m/s (7mph); it will attain maximum output at around 12m/s (27mph) and will cut out at about 25m/s (56mph). Cut-out at high wind speed can create problems for the grid system as it occurs more abruptly than cutting in from low wind speeds but current turbines are being designed to cut out in a more gradual and controlled fashion.

Technical Appraisal of wind systems

Wind turbines come with different topologies, architectures and design features. The schematic of a wind turbine generation system is shown in Fig. 5. Some options wind turbine topologies are as follows

- Rotor axis orientation: horizontal or vertical;
- Rotor position: upwind or downwind of tower;
- Rotor speed: fixed or variable; Rigidity: still or flexible;
- Hub: rigid, teetering, gimbaled or hinged blades; Yaw control: active or free
- Number of blades: one, two, three or even more;
- Power control: stall, pitch, yaw or aerodynamic surfaces;

Reviewing most literature's, horizontal-axis wind turbines (HAWTs), are the prevailing type of wind turbine topology, as is confirmed in the design below

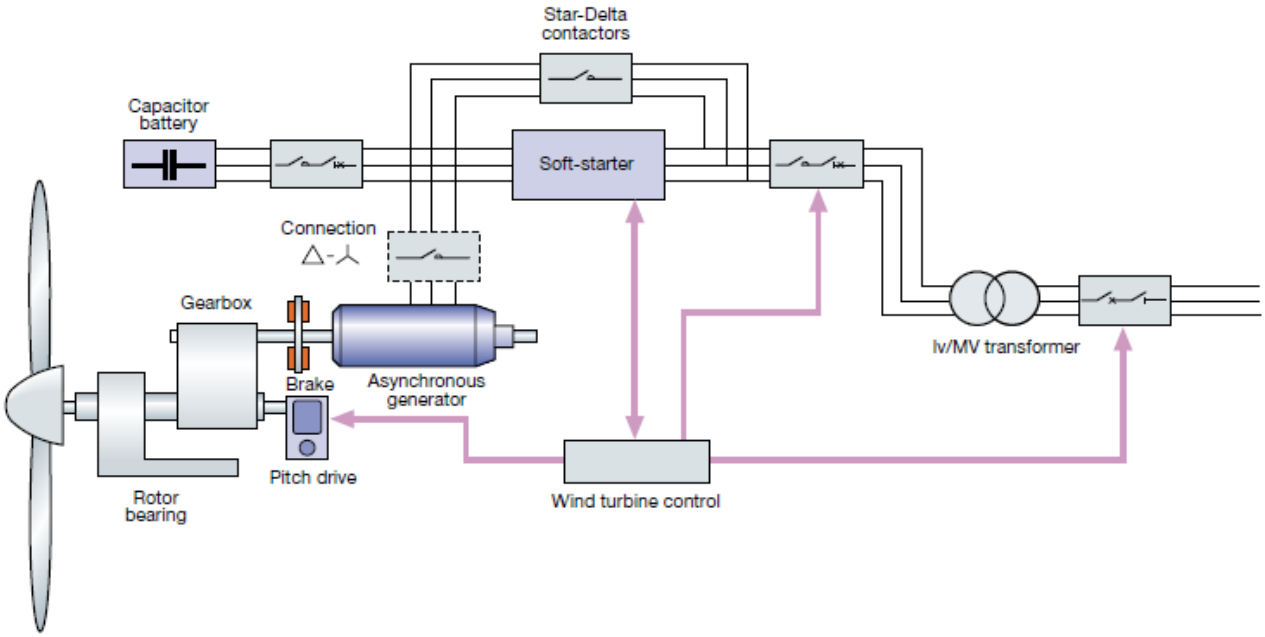

Figure 2-15 Wind turbine generation systems

Wind turbines include critical mechanical components such as turbine blades and rotors, drive train and generators. They cost more than 30% of total capital expenditure for offshore wind project (Jamieson, 2015). In general, wind turbines are intended for relatively inaccessible sites placing some constraints on the designs in a number of ways. For offshore environments, the site may be realistically accessed for maintenance once per year. As a result, fault tolerance of the wind turbine is of importance for wind farm development.

One of key components in the wind turbine is its drive train, which links aerodynamic rotor and electrical output terminals. Optimization of wind turbine generators cannot be realized without considering mechanical, structural, hydraulic and magnetic performance of the drive train. An overview of the drive train technologies is illustrated in Fig. 2-15 for comparison. Generally, they can be broken down into four types according to their structures (Jamieson, 2015):

- Conventional: gearbox and high speed generator with few pole pairs.
- Direct drive: any drive train without a gearbox and low speed generator with many pole pairs.
- Hybrid: any drive train with a gearbox and the generator speed between the above two types.

Multiple generators: any drive train with more than one generator. Drive train topologies may raise the issues such as the integration of the rotor and gearbox/ bearings, the isolation of gear and generator shafts from mechanical bending loads, the integrity and load paths. Although it may be easier to service separate wind turbine components such as gearboxes, bearings and generators, the industry is increasingly in favour of system design of the integrated drive train components.

Wind energy has attracted much attention from research and industrial communities. One of growth areas is thought to be in the offshore wind turbine market. The ongoing effort to develop advanced wind turbine generator technologies has already led to increased production, reliability, maintainability and cost-effectiveness. At this stage, the doubly-fed induction generator technology (equipped with fault-ride-through capacity) will continue to be prevalent in medium and large wind turbines while permanent magnet generators may be competitive in small wind turbines (Liserre, 2016). Other types of wind turbine generators have started to penetrate into the wind markets to a differing degree. The analysis suggests a trend moving from fixed-speed, geared and brushed generators towards variable-speed, gearless and

brushless generator technologies while still reducing system weight, cost and failure rates (Ma, H, Chen, 2015)

In summary, there may not exist the best wind turbine generator technology to tick all the boxes. The choice of complex wind turbine systems is largely dictated by the capital and operational costs because the wind market is fundamentally cost-sensitive. In essence, the decision is always down to a comparison of the material costs between rare-earth permanent magnets, superconductors, copper, steel or other active materials, which may vary remarkably from time to time, location and amount of energy that is to be produced.

2.3.7. CONTROL TECHNIQUES

Control technique plays a very important role in enhancing system efficiency and desired output of a combined RE system such as ours. The availability of power from a hybrid system can be economically maximized by choosing proper control technique in the system design process. Jonathan et al (2014) presented a control technology for HRES that track and make control decisions based on the definite battery state of charge offering significant advantages over other methods. Ottoson et al (2012) used a data logger and gave exhaustive analysis of the energy production and performance of a remote hybrid power plant having solar, wind and diesel plant. Nogaret et al (2012) developed a new expert system based control system tool for HRES and used an advanced control system for the optimal operation and supervision of Photovoltaic and wind based medium size power system. CAD (Computer aided design) tool is used by Chedid et al (2010) for optimal design and control of a hybrid wind solar power systems considering all ecological factor. Linear programming techniques are used to reduce the production cost while meeting the load requirement. Pitrone and Pitrone (2011) used an expert system, fuzzy logic theory, neural network and programmable logical controller for on line supervision and control of distributed hybrid renewable energy power plant. A real time analysis of the control structure and management functions of a solar wind hybrid micro-grid system is reported by Gaztanaga et al (2011) which works perfectly in both operation and transition mode. Based on the power transfer utility concept Jinhong and Seulki (2014) developed several power control module in service modes such as normal operation, power dispatching and power averaging according and effectively controls the inverter. The control module has environmental and utility friendly operation policy such that power injection into network is less fluctuating. Based on supervisory controller, Abdulwahid and Manwell (2014) developed a dynamic central communication system for hybrid power system. Capacitor voltage equilibrium control scheme is used to control hybrid cascaded H bridge inverter with

single direct current (DC) source to get rid of higher order harmonics for an integrated energy system by Hui et al (2010). Research also shows that Vechu et al (2011) developed digital control over analogue control with a 3 phase four leg inverter for HRES. This system compensates unbalance voltage conditions and the addition of a fourth leg provides an extra degree of freedom, making it possible to handle the natural current caused by unbalance load. In this technological amalgamation , we also found out that Zhang et al (2011) used PSO based statistical dynamic control system to manage Wind-PV hybrid system operation giving a new concept control design using a Petri-net regulator which calculates the operating mode of the multisource renewable energy system to optimize the energy transfer and the load irregularity for Hybrid RES. Arulampalam et al (2009) also developed micro-grid control of PV-wind-diesel hybrid system with island and grid linked function suing an MPPT control scheme to track the global power of the wind–solar hybrid generating system according to the basic standard of the variable step perturbation tracking maximum power point algorithm. On the other hand, Prabhakar et al (2015) proposed a control system for accomplishing consistent harmonization of wind–solar energy adaptation system in remote locations. The control technique is formulated to utilize the available energy source in an efficacious manner to render power at nearly constant voltage and frequency to the isolated load. This was compensated by Croci et al (2011) whom developed obedience based control method which handles the energy exchange directly for PV-Wind HRES. The review of control methodologies used for the combined renewable energy technologies for clean energy generation shows that various methods have been adopted by various researchers and engineers for various projects and although research is on-going in this field to define the most appropriate control methodologies for combined renewable energy systems, control methodologies differs with each project as they are particularly designed to suit a the demand of each project. It is therefore clear that one of these methodologies mentioned above would be considered and possibly modified so as to ensure its suitability for our intended renewable energy platform.

2.4. TOGO'S SOCIO-ECONOMIC, ENVIRONMENTAL, AND FUTURE DEVELOPMENT OF THE ENERGY SECTOR IN TOGO

2.4.1. SOCIO ECONOMIC CONTEXT

Togo's 2010 population was 6,191,155 (4th Census, 2010), with an average annual growth rate of 2.84% (WB, 2010). On that basis, the country can expect to reach 7,121,673 inhabitants in 2018, 60% of whom under the age of 25. As a result, Togo will need to meet the challenge of providing decent jobs to that population, once it hits the labour market. Gross domestic product

(GDP) rose from FCFA 1,581.3 billion in 2010 (baseline year) to FCFA 2,076.6 billion in 2015, or a per capita GDP of FCFA 255,419 and FCFA 291,583 respectively (WB, 2013). Despite the progress made (0.459 in 2012 (HDI Report, 2013), or a 0.007 improvement over 2010), Togo's Human Development Index (HDI) remains low (ranked 159th out of the 187 countries evaluated). Poverty is still very high in Togo, affecting 58.7% of the population in 2011 (SCAPE, 2013), compared with 61.7% in 2006. The household lighting penetration rate stands at 23%, according to the National Energy Efficiency Action Plan (NEEAP, 2015). The 2011 QUIBB well-being indicator questionnaire showed that the main social indicators had generally improved, although their levels are still worrying: net primary schooling rate (87.8%), adult literacy rate (60.3%, with a clear disparity between the sexes: 74.0% for men and 47.9% for women), and unemployment rate (24.3%) (World Bank, 2014).

2.4.2. COMMITMENT TO SUSTAINABLE DEVELOPMENT

For several years now, Togo has been engaged in a proactive strategy for sustainable development and against global warming (AFD, 2013). Its efforts focus mainly on: bad production practices in the economic sectors; lack of institutional control; and the high poverty rate, which is exacerbated by the negative impacts of climate change, further reinforcing the vulnerability of the production sectors and the pressure on natural resources. This political will can be seen, amongst others, in the National Environmental Action Plan (NEAP), the National Environmental Management Programme (NEMP), the National Sustainable Development Strategy (December 2011), the National Environmental Management Capacity-building Strategy (October 2008), the National Programme for Reducing Greenhouse Gas Emissions from Deforestation and Forest Degradation (REDD+) 2010-2050, the National Strategy for Reducing the Risk of Catastrophes in Togo (December 2009), the National Medium Term Priority Framework (NMTPF) for Togo (2010-2015), and the National Action Plan for Marine and Coastal Environmental Resources Management. Further, Togo's membership in the Climate & Clean Air Coalition (CCAC) means it could raise funds to finance its short term GHG and climate pollutant mitigation actions.

2.4.3. ENVIRONMENTAL AND GHG EMISSIONS IN TOGO

Togo plans to adopt an approach based on contributions founded on both measures to be introduced and targeted results in order to better identify any opportunities for co-benefits in terms of reducing GHG emissions that might potentially be derived from synergies between adaptation and mitigation. Togo's contributions to global mitigation work can be characterized as follows:

Commitments: Togo confirms its commitment to contributing to the achievement of the UNFCCC's objectives to limit temperature rises to 2°C by 2030 (UNDP, 2015). Togo has already implemented activities to reduce greenhouse gas emissions, especially in the energy, agriculture and LULUCF (land use, land-use change and forestry) sectors. Subject to being in possession of the necessary resources, Togo has confirmed that it is aiming for a more ambitious reduction target.

- ***Main data sources:*** national climate strategies, policies and actions plans; prior UNFCCC submissions; declarations at the United Nations Climate Summit; Nationally Appropriate Mitigation Actions (NAMA); national communications; and a new analysis performed for the purpose of producing the INDC.
- ***Cover:*** Entire economy.

- Main sectors: Energy, agriculture and LULUCF.
- Gases: CO2, CH4 and N2O.

- ***Scenario trajectories:*** Togo aims to reduce its emissions as shown in the graph in Figure 2-15 below, which provides information on both unconditional and conditional options.

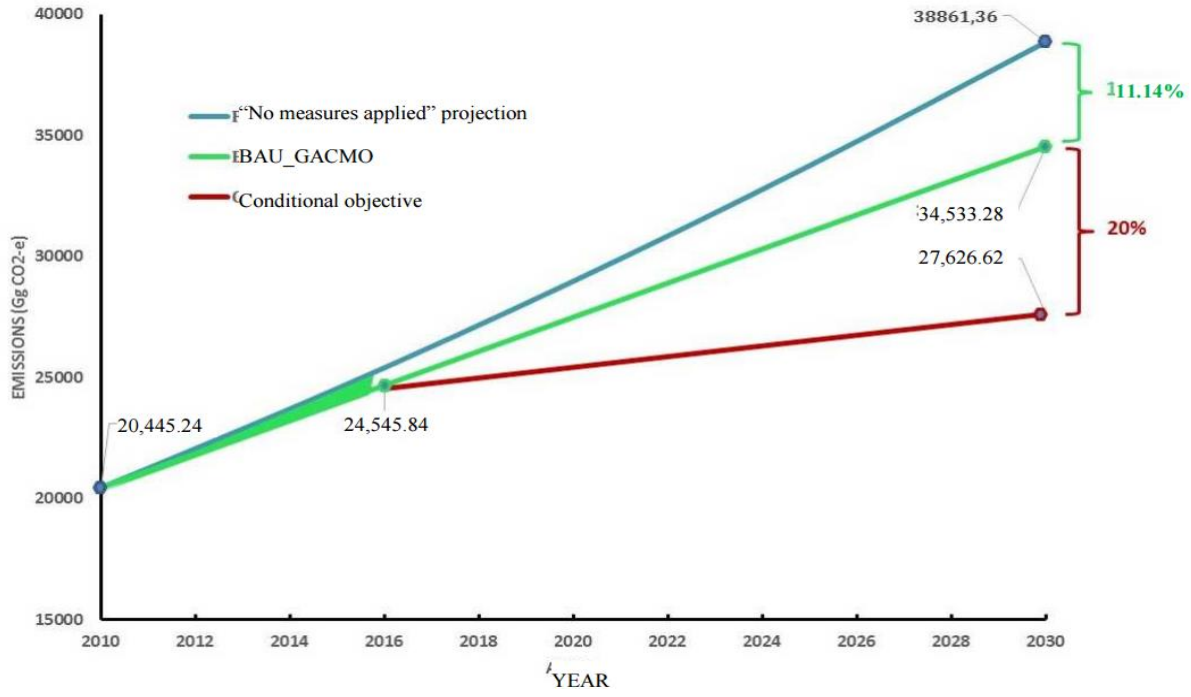

Figure 2-16 Togo aims to reduce its emissions (MOE, 2016)

Togo's GHG mitigation measures in its three priority sectors (energy, agriculture, and land use, land use change and forestry) and the associated costs (totalling US$1.1 billion) are described below.

I. In the energy sector, they pertain to the promotion of household using Renewable Energies plus solar electricity for road transport. As concerns with RES, this will entail the implementation of a proactive policy (with incentives, support and training for craftsmen, appropriate distribution channels, etc.) that can promote the roll-out of energy-efficient stoves, which can yield 50-60% savings in wood and charcoal. Emphasis will also be placed on the introduction of solar equipment in households and on capacity-building for the various actors concerned. In terms of road transport, the planned actions aim to reduce the consumption of fossil fuels in Togo by 20% over the course of the period under review, by improving the road system, promoting the use of public transport, reducing the average age of imported vehicles (to 5-7 years) and promoting active modes of transport (bicycles, walking, bike paths)

II. For the agricultural sector, mitigation options have been identified in the fields of livestock farming, rice growing, farmland and the burning of the savannahs. Concerning livestock, the actions will involve the introduction of fodder to improve animal digestion, support in the promotion of local breeds, and extensive livestock farming. In terms of the rice industry, the actions will target the identification and promotion of varieties of rain-fed rice, and support and guidance in the better use of organic matter (for faster decomposition) in the paddy fields. For farmland, a study will be conducted to characterize it into agro-ecological zones, as well as a research and support programme on organic and synthetic enriching agents that release less GHG, the study and promotion of optimal waste management for livestock and harvest remnants, and the promotion of land use planning practices that boost carbon's binding to farmland and agroforestry. In respect of the burning of the savannahs, the planned actions target a participatory fight against bush fires (World Bank, 2016)

III. In the land use, land-use change and forestry sector, the priority actions relate to: (i) the promotion of private, community and State reforestation through the creation of plantations and the promotion of agroforestry on cultivated land; (ii) sustainable forest planning and protection (by managing brush fires, regenerating degraded sites, and demarcating and developing protected areas and tourist sites); and (iii) the cartographic study of geographic areas with a strong potential for the development of biofuels in conjunction with food security issues (World Bank, 2016).

2.4.4. FUTURE DEVELOPMENT PF THE ENERGY SECTOR

The commendable efforts Togo has made these past years have helped to raise the electricity access rate from 20% in 2010 to 28% in 2014 (CEET, 2015). However, this rate remains lower than the 40% average for ECOWAS countries and 35% for Sub- Sahara Africa. The current situation falls short of the minimum standard access rate set by ECOWAS at 50 %(ECOWAS, 2012). The objective set by the national Accelerated, Inclusive Growth and Employment Promotion Strategy Paper (SCAPE 2013-2017) was set to increase electricity generation capacity from 161 MW in 2010 to at least 300 MW in 2015, which is today far from achieved. Since 2010, the only probable investment is the current on-going construction of a 147-MW hydropower dam at the Adjarala site (Mono River) to be shared by Togo and Benin. This outlook points to an aggravation of the energy deficit in the short to medium term which can only be remedied by opening up the generation segment to the private sector

Also, SCAPE (2013-2017) indicates that until July 2009, the average price of low voltage electricity in Togo was CFAF 100/kWh, compared to the average of CFAF 56/kWh in Sub Saharan Africa, CFAF 30/kWh in Latin American and CFAF 17/kWh in Southern Asia (World Bank data, 2013). These price proportions have not changed significantly from that time. Togo operates with highly administered electricity prices which are not sufficiently influenced by market forces and competition (UNDP, 2012). Applying a price that is lower than the generation cost and at the same time relatively higher than the price applied in the rest of the world is among the major constraints of Togo.

Furthermore, electricity generation, transmission and distribution activities are not sufficiently segmented to achieve economies of scale. They are rather managed as a single package. In some situations, no distinction is made at the accounting and fiduciary levels between distinct activities of the electricity value chain. Togo can draw lessons from reforms already undertaken in Ghana and Côte-d'Ivoire to successfully adapt its electricity sector to the vagaries of market forces. The Togolese authorities are aware that strong State presence and monopolies in the electricity value chain have been partly responsible for the structural financial deficits of national electricity companies for several decades (K Moglo, 2012). These deficits are reflected in over 70% electricity imports and weak institutional capacity to meet an aggressive demand which resulted in the informal acquisition of «cobwed» electricity. They, in a nutshell, are weak electricity generations with comparatively high electricity prices thereby reducing the level of competitiveness of Togolese enterprises and the influx of investments (TVT, 2014). The current challenge is no longer the fiscal consolidation of State owned enterprises in the

electricity value chain but the need for their in-depth reform (AFDB, 2015). An in-depth structural reform of electricity generation, transmission, distribution and supply activities, embracing private sector participation, will allow for a better visibility of the profitability of the different electricity segments. These restructuring efforts will culminate in other appropriate measures the large-scale generation of electricity and lower costs in order to increase the level of access. The short and medium-term challenge of the Togolese State is to define appropriate terms and conditions for competition among electricity producers using Renewable energy preferably. They will have to sell to competing wholesale dealers, through transmission and distribution networks that are only partially subjected to market forces (AFBD, 2015).

2.5. SUMMARY OF CONTRIBUTIONS

The litterature review covered three main sections

- Togo's energy sector, Togo's energy regulatory framework and its renewable energy potential
- Togo's curent energy business model
- State of the Art of existing renewable energy technology

Technical feasability of the energy renewable energy platform for Togo's smart grid infrastructure

The outcome of this chapter focusing on Togo's energy potential has shown that the country has enough renewable energy potential for the exploitation of these resources to be included as part of the energy and economic sector development and also offer an opportunities for green businesses implementation and for Independent energy producers to successfully implement a solid business model allowing the expansion of already existing industries and new ones to come. Fine-tuning a business model can easily take several months or even years. To be attractive for potential customers, business models must appear to be clear and simple, even if sophisticated processes run below the surface. This is particularly important for the mass market in rural areas of developing countries where most people do not have access to commercial financing, or are overwhelmed in dealing with loan applications.

The technical feasability of the computer aided design of a 3D renewable energy platform for Togo smart grid power system infrastructure shows that the amalgamation of these three sources represents the advanced stage in hybrid power generation systems with litteratures

showing easy integration into smart grid enabling this innovative 3D renewable energy platform to come as a sustinable methodlogy to developing solutions to Togo's energy issues. The current business model also shows significant encouragement from the government for IPP's to be integrated and for the promotion of renewable energy power generation

The case study presented and discussed has shown that the generation of a successful business model is not an easy task. The specific regulatory, economic, social and cultural situation in a region has to be well understood and addressed when generating new business models. Fine-tuning a business model can easily take several months or even years. To be attractive for potential customers, business models must appear to be clear and simple, even if sophisticated processes run below the surface. Of course, customers should be given a guarantee that the systems function properly. Successful business models usually include a financing component. This is particularly important for the mass market in rural areas of developing countries where most people do not have access to commercial financing, or are overwhelmed in dealing with loan applications. Traditional trading companies seem to have trouble with this fact. In contrast, younger firms with a concern for economic and sustainable development seem to be able to manage this. The importance of a simple financing component for business models is also reflected in the success of third party ownership models in the residential PV sector in western countries. Such lease models may not be the most attractive option in financial terms, but they are definitely the most comfortable option for the customer in administrative terms.

The outcome of this chapter focusing on Togo's energy potential has shown that the country has enough renewable energy potential for the exploitation of these resources to be included as part of the energy and economic sector development and also offer an opportunities for green businesses implementation and for Independent energy producers to successfully implement a solid business model allowing the expansion of already existing industries and new ones to come. Fine-tuning a business model can easily take several months or even years. To be attractive for potential customers, business models must appear to be clear and simple, even if sophisticated processes run below the surface. This is particularly important for the mass market in rural areas of developing countries where most people do not have access to commercial financing, or are overwhelmed in dealing with loan applications.

CHAPTER 3

CHAPTER 3- PROPOSED RENEWABLE ENERGY PLATFORM FOR TOGO'S SMART GRID POWER SYSTEMS INFRASTRUCTURE

3.1. INTRODUCTION

This chapters introduces the possible business model and recommended 3D renewable energy platform that could suit Togo's smart grid power systems infrastructure and industrial applications.

- A proposed business model is thereby presented and explained due to earlier findings in chapter 2 of this thesis.
- The possible 3-Dimentional (3D) renewable energy platform and its relevant Architectures and system of operations is critically analysed with simulation results presented as a validation process prior to field testing and further evaluation's.
- Economic and Environmental impact on Togo is also evaluated and discussed thoroughly

3.2. POTENTIAL ENERGY BUSINESS MODEL THAT COULD BE IMPLEMENTED IN TOGO

Electricity systems across Africa and Togo in particular face significant challenges in the transition to low-carbon energy. While the transition provides plenty of opportunities for investors, businesses, and consumers alike, the current business and regulatory models of investor owned utilities (IOUs) and independent power producers (IPPs), which have mainly developed around competitive markets for fossil fuel generation, are particularly ill-suited to take advantage of these new opportunities.

Innovations in business models across all subsectors of the industry are crucial to scaling-up renewable energy deployment. The businesses that have played the largest role to date –IOU and IPPs– are facing significant challenges. In both the Africa and Togo in particular, many of the most important players have been hard hit by slower demand growth, partly a result of a slowing economy, along with adverse trends that are emerging as a transition to a low-carbon system accelerates.

To create a clean, secure, and low-cost electricity system at scale, each of the main business segments of the existing electricity industry will need to evolve:

1) Generation – New business models are needed to reduce renewable financing costs and focus conventional generation on providing grid flexibility. New financing models should match the investment characteristics of renewable generation with investors, like institutional investors, that are looking for investments with the profile of renewable energy.
2) Transmission – Transmission systems must improve integration of renewable energy. Transmission grids should continue to consolidate to balance renewable resources across a greater area.
3) System balancing and market operation – Markets and business models need to adapt to promote investment in flexibility resources for a low carbon grid. Markets will need to be adjusted to value the differences between the flexibility services provided by fossil fuel generators and energy supply provided by renewables.
4) Distribution – Models for financing and operating distribution systems will need to adapt to changing demand patterns and new distributed energy and flexibility resources. Distribution grids will need to adapt to the greater levels of distributed generation, reducing load on local systems.
5) Customer Management – Customers will play an increasingly active role in the electricity sector. Customer management must bring in new models to finance and integrate the demand response, energy efficiency and electrification of the system, including, especially, integrating the electrification of energy services such as the charging of electric vehicles into the system in ways which reduce system costs.

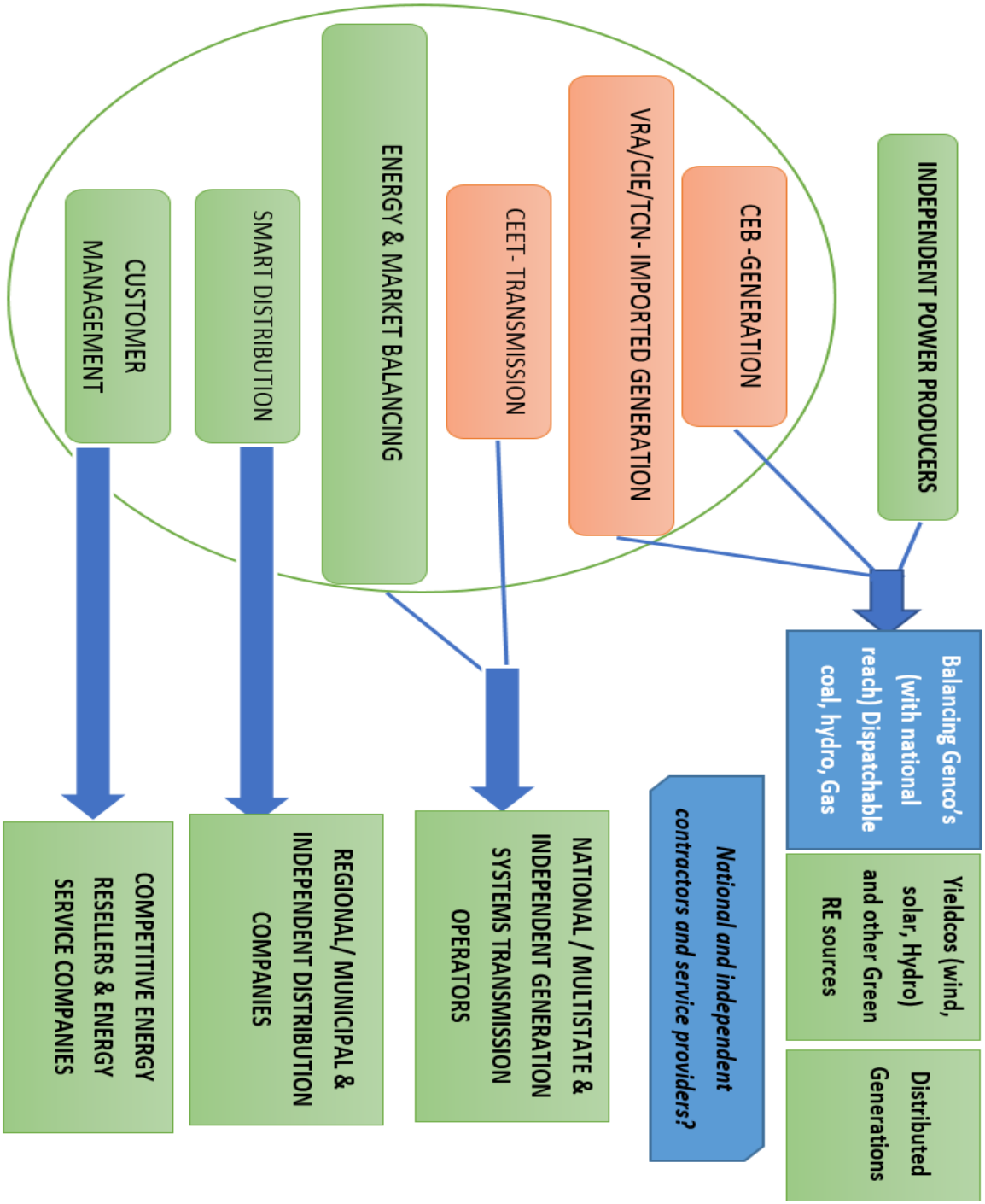

Figure 3-1 Possible future energy business model (investigators own design)

Moving away from existing models will involve major changes in the way of doing business. However, the first steps are already happening. As an example, financing models for renewable energy are emerging that can substantially lower costs and catalyse changes across the industry. These models, such as Yield-Cos, can be built to provide investors secure cash flows from renewable energy projects and other benefits such as the liquidity and diversification potential of exchange-traded stocks and bonds. While these models are already

emerging, they are not yet in a form that will realize the full potential cost advantage available and still require adjustments and fine tuning to optimize their value to the system. The industry needs creative thinking, careful design, and a regulatory, financial, and structural push to reduce the cost and improve the value and reliability of the electricity system. Policymakers can help accelerate this transition by working with investors, electricity companies, financial regulators, and consumers to enable the development of new financing vehicles, redefine markets, and build new institutional structures for a 21st century low carbon electricity system. With these changes, the costs of renewable electricity can be lowered by up to 20%, customers can benefit from the value they can lend to the system, and new markets can reduce the cost of integrating new energy sources, and uses, all while improving reliability and accelerating innovation.

Recommendations following this new business plan could be

- ***Implementing investment in generation, transmission and distribution and in personnel.***

This would include

a) improving the quality of supply (imports and distribution) by rehabilitating, strengthening and extending CEET's distribution networks;
b) developing a generation and transmission master plan, to firm up priorities, including reassessing the technical, economic and financial viability of Togo's medium size hydro plants, and adopting a short-term supply management plan
c) For the Adjarala hydro project (147MW), accelerating the completion of the technical, economic, environmental and social and financial studies, the definition of the implementation arrangements and the mobilization of financing;
d) Mobilizing the Governments and ECOWAS to secure and speed-up the delivery of natural gas from Nigeria through the WAGP pipeline, as this is one of the cheapest supply options, and would also diversify the energy matrix; and
e) Defining and mobilizing financing for capacity building and technical assistance in the Ministry of Energy and CEET.

- ***Increasing access to electricity services, in the urban/Peri-urban and rural areas***

a) CEET, of an access and quality strengthening program for the main cities; and

b) The Government, of a rural electrification program promoting innovative approaches based on decentralized and small scale operations. To significantly increase access to electricity services in rural areas, many countries have decided to: (i) set-up new institutions such as a Rural Electrification Agency focusing solely on rural electrification and delivering the services using a mix of service providers (small private enterprises, NGOs, communities, etc.), proposing various levels of services and of tariffs, supporting productive activities and financing of the up-front investment; and to (ii) let the main power utility concentrate on urban/Peri-urban areas with different tools. Togo should benefit from the experiences of emerging economies and design a RE strategy and an implementation plan that meets its objectives and traditions, and ensure sustainability

- ***Ensuring the financial equilibrium of the sub-sector, CEET and CEB, and reviewing the tariffs.***
  a) A thorough analysis of the investment programs (including of CEET and of CEB);
  b) a detailed financial and tariff analysis together of CEET and CEB, building up on the financial modelling tools now available to CEET; and
  c) a transparent and open framework for all the stakeholders to participate in the initial design and in the development of solutions

- ***Adjusting the regulatory framework to account for internal and regional requirements***
  a) Deciding and adjusting if necessary the regulatory framework including amendments to the Benin-Togo Electricity Code ("Code Benino-Togolais de l'Electricité") applicable to CEB to align it with Togo's commitments with ECOWAS and WAEMU;
  b) Increasing the autonomy and capacities and reviewing the modus-operandi regarding the regulator, ARSE;
  c) Strengthening and adopting a new PPP framework and key implementing regulations, covering also renewable energies and rural electrification

- **Another approach would be**

To Delineate an energy efficiency and demand management program through first a feasibility study covering the priorities areas, assessing the benefits and costs, the financing requirements, the sustainability of such program and the implementation arrangements.

3.3. ENERGY CURRENT TARRIF

Customer Category	Tariff Level	Comment
Average tariff (including taxes)	FCFA106.5/kWh USc21.3/kWH (2009)	
CEET Low Voltage (LV) customer	FCFA111.6/kWh USc22.3/kWh	Varying with consumption level. Latest adjustment in November 2010, effective January 1, 2011
CEET Medium Voltage (MV) customer	FCFA99/KWh USc19.8/KWh	Varying if Free Economic Zone or not. Tariff varies with-time-of-day: Peak: 6pm-11pm; Off-PeaK:11pm-6am
CEB Tariff to the Distributing Companies: CEET (Togo) and SBEE (Benin)	FCFA 55KkWh USc11/KWh	

1 US$=500 FCFA

Figure 3-2 Electricity tariffs levels (2011-2016) (World Bank data, 2016)

Generating Plant	Available Capacity and Energy	Togo's Share	Type of Fuel	Fuel Cost	Total Cost (FCFA/kWh and USc/Wh)	Variable Cost (FCFA/kWh and USc/KWh)
Nangbeto Hydro	63MW 170GWh (220 in 2009)	32MW 85GWh			FCFA25 USc5	
Contour Global	95MW 750GWh	95MW 750GWh	Trifuels (Natural Gaz, HFO, DDO)	Gaz 9$/mmbtu HFO: FCFA 400/ton		HFO: FCFA80 (USc16) Gas: FCFA36 (USc7.2)
TAG CEB Lome	20MW 36GWh	20MW 36GWh	JetA1, Natural Gaz	Jet: FCA400/KWh Natural Gaz: 9$/mmbtu		Jet: FCFA150 (USc30/KWh) Natural Gas: FCFA65(USc13)
Diesel CEET	10MW	10-15GWH	DDO	FCFA500/liter		FCA160/kWh (USc32/KWh)

Figure 3-3 Generating companies Electricity tariffs levels (2011-2016) (World Bank data, 2016)

Figure 3-2 and 3-3 shows the various generating companies and their electricity tariffs. In Togo, the energy prices are estimated at 21.3 c/Kwh for domestic usage and 35.3 c/Kwh for Industrial purposes. These Prices are predicted to rise due to increasing diesel prices used for the 100MW power plant, making an increment by 25% for industries and 10% for households. In a country where 58.7% of the population live below the poverty line (World Bank data,

2013), there is a social and moral need to subsidies the energy sector, opt for renewables energy power generation in order to alleviate energy cost on the population and promote development.

As indicated earlier, CEET current tariff levels are too low on average as the utility can barely cover its costs, and cannot contribute adequately to the mobilization of the financing required for executing any investment program. Private sector investors (such as IPPs) must therefore seek additional comfort and guarantees from the Government. Furthermore, the tariff challenge will get more acute over time as CEET's generation and import costs are expected to increase over time and are not geared to quickly reflect changes in the prices of fossil fuels.

Therefore, the delineation of a clear tariff policy accompanied by a comprehensive financial and tariff study should be carried out as soon as possible covering CEET's services (and may be other services such as rural electrification) together with potential investment studies. Such policy formulation and financial analysis should also be coordinated with CEB's own review and modelling of its financial outlook including in particular the impacts of likely tariff adjustments to be expected from Nigeria and Ghana, and the incorporation of Adjarala's in-service costs.

3.3. PROPOSED 3D RENEWABLE ENERGY PLATFORM

The proposed 3D renewable platform presents a new approach of implementing the renewable energy technology in Togo's smart grid system. This proposed innovative system can be implemented using Solar, Wind and Hydropower technology. It also can be implemented as a 1D, 2D or 3D depending on the geographical location and the availability of the renewable energy resources. Design and development of such system and its relevant back of system i.e. control and power electronics in modular forms would make it easy for any energy sector to adopt such platform with high flexibility. However, there are many other consideration that should be taken into account such as the type of load, power demand and cost of maintenances.

3.3.1. PROPOSED 3D RENEWABLE ENERGY PLATFORM DESIGN AND STRUCTURE

Figure 3-4 shows the platform structure and it consists of a wind turbine, a dual overshoot wheel and Kaplan turbine together with a PV system. The platform structure is therefore made up of three section representing the Back end of the entire system thus (wind, hydro, solar generation systems unit). With the purpose of having an efficient and eco-friendly system, the platform structure been created with a high level of modularity and flexibility. They should be sustainable and are supposed to show stable parameters of produced energy (according to the relevant standards). Figure 3-4 shows the general structure of a renewable energy system

platform. This proposed 3D renewable energy platform will be ideal for smart grids where distributed generation is made possible using this renewable platform technology.

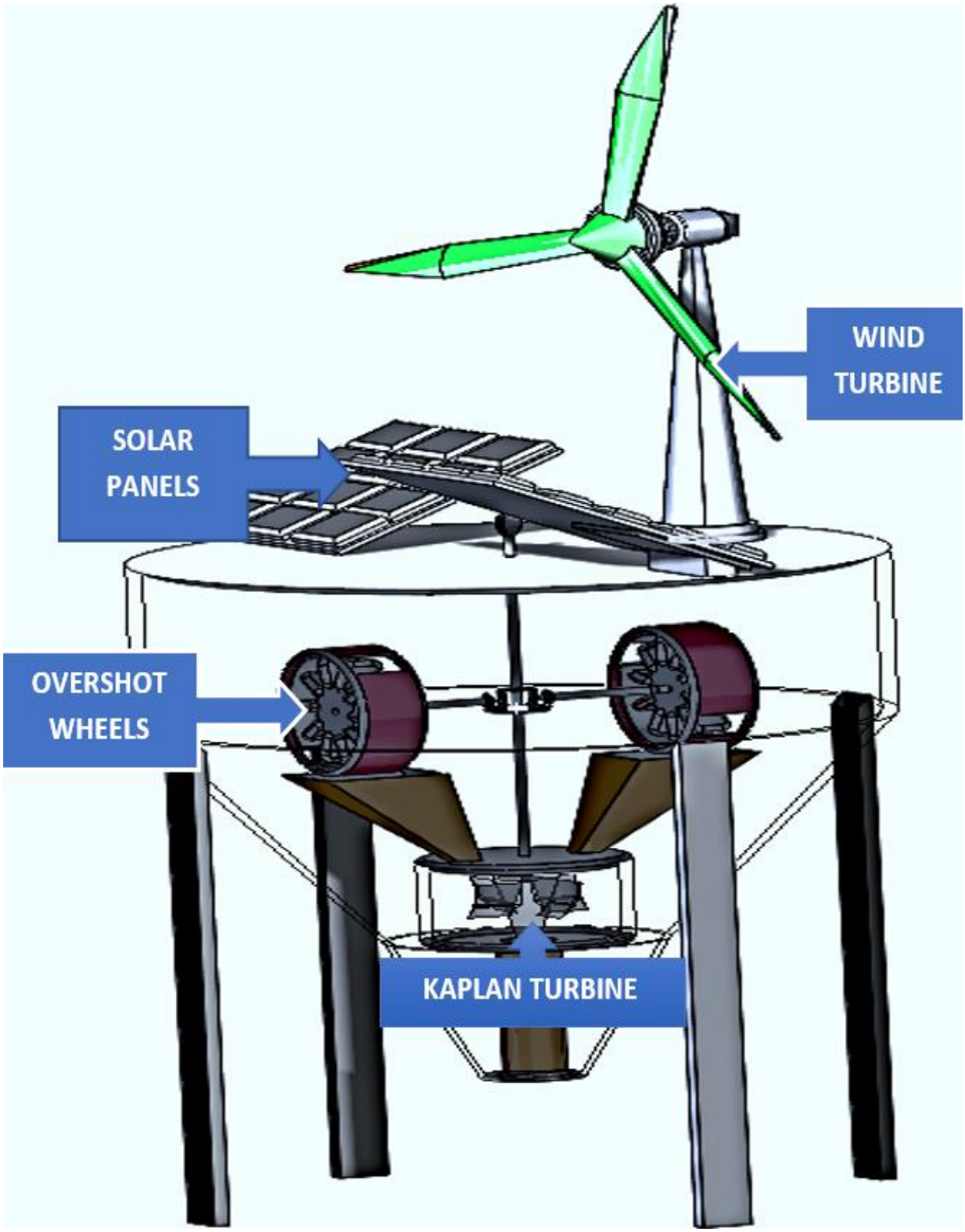

Figure 3-4 Designed Assembled unit

Figure 3-4 shows the assembled unit of the 3D renewable energy platform. The 3D renewable energy platform architecture presented initial results showing the importance of the approach used in the design and its smart grid application possibilities. It also demonstrated challenges that should be considered prior to building the system for reel field test. To typify this feature, the investigation considered studies for the suitability of using solar, wind and hydro resources available in Simulink tools allowing the development of the simulation model referred to steady, transient systems, with the possibility of active and reactive power flowing evolution. It is worth noting the importance of the presented model considering its usefulness tool in energy management system domain and its technological advantages for future sustainable, hybrid, and smart applications developments.

The assembled unit presented the preliminary research undertaken to develop the 3D renewable energy platform for smart grid applications. It introduced a solution to challenges in the energy generation sector which do not only refrain only to the safe supply of clean Energy but the reduction of carbon emissions. A major importance for the theoretical study of hybrid systems, based on renewable energy (photovoltaic, wind, hydro system) is the availability of the models that can be utilized to study the behaviour of hybrid systems and most important, computer aided design simulation tools. As the available tools are quite limited, the outcome of this research presented the most current and up to date model which was designed using SOLIDWORKS and each segments of the design, studied with simulation showing safety margins and purposes of the 3D renewable energy platform for smart grid applications as well as for educational purposes.

3.3.2. PROPOSED 3D RENEWABLE ENERGY PLATFORM ARCHITECTURE

Figure 3-5 show the 3D renewable energy system architecture. It shows also the possible back up system using storage battery or fossil fuel generation arrangement. The architecture presented shows a probable assembled version of the 3D renewable platform architecture. The intent of the design is therefore for the 3D renewable platform generation to be directly fed into the storage “battery” where load power is driven from. This also is ideal for meeting losses in power network where the surplus power generated could be directly injected into LPN (local public network). Active power shows approximately $3 \times 104\ W$ generated for both active and reactive power which shows that power compensation within the network is efficiently managed with the capacitive bank within the network. It can therefore be concluded from the simulation analysis that the presence of reactive power is a result of the nonlinear elements used within the simulation model thus the power transformers, converters based on electronic

switching elements and the highly nonlinear nature of the consumer loads. This then introduce the question about optimizing the 3D system so as to exercise control over the power generation and its output. The proposed control model for the 3D renewable platform and its control strategy offers a proper tool for optimizing 3D renewable platform power system performance, such that it may be used in smart-grid applications. Circuit models are developed; using "MATLAB" simulations software to highlight the characteristics of the control circuitry and output power characteristics. The control system therefore focuses on the development and use of an efficient multilevel inverter capable of synthesizing a near sinusoidal voltage from several levels of DC/AC voltages whilst generating output voltages with very low distortion, whilst reducing the dv/dt stresses; thereby reducing on electromagnetic compatibility (EMC) problems. The advantages of using these type of inverters as well reside in their abilities to operate at both fundamental switching frequency and high switching frequency PWM. It should be noted that lower switching frequency usually means lower switching loss and higher efficiency.

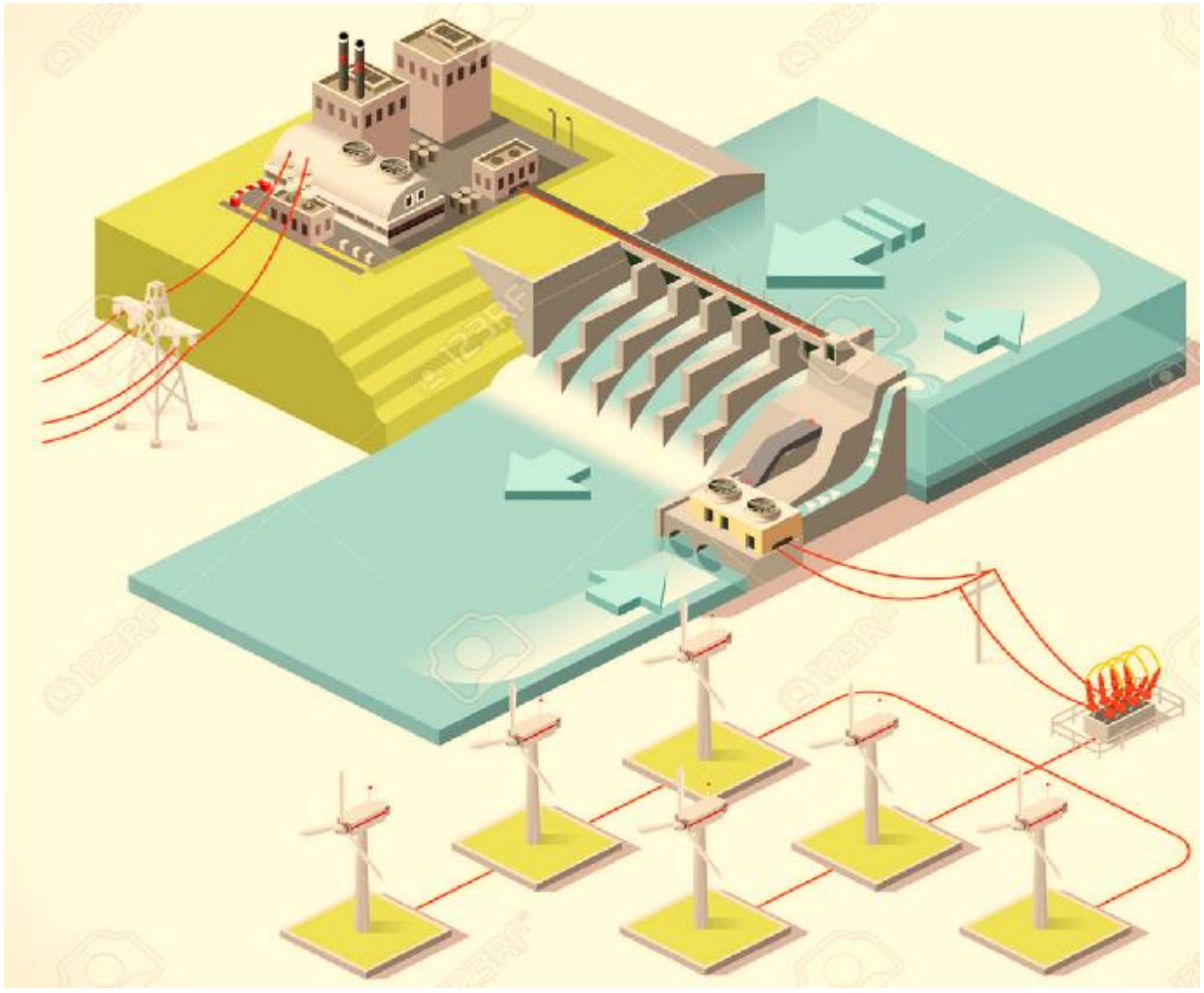

Figure 3-5 2D renewable energy platform system architecture

3.3.3. PROPOSED SYSTEM OPERATIONS PRINCIPLS AND IMPLEMENTATIONS

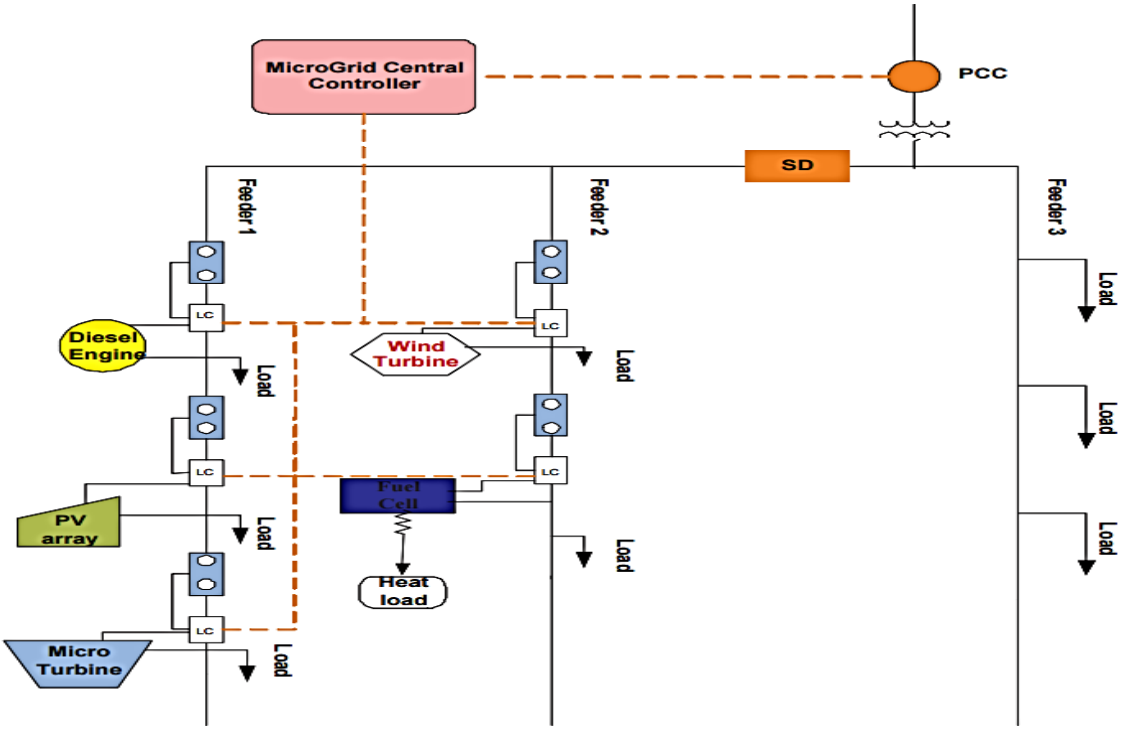

Figure 3-6 Integrated renewable energy Micro Grid system simulation

Figure 3-6 shows the design of the 3D renewable energy micro grid system simulation with a photovoltaic generator (PV), Dual wind turbines (wind1 and wind2), a diesel generator (diesel representing the Hydro system) and a battery as an accumulator. This mode of operation is characterized by both generation subsystems set to operate at their maximum energy conversion points. Moreover the battery bank in the system is able to revert its energy flow, acting as a power supplier instead as a recipient of energy. This has been introduced as an effective way of meeting power fluctuations and shortcomings of the renewable energy sources. Operation in state Wind, Battery (hydro) is maintained as long as the energy available in the battery bank is about a fixed percentage (said 24%) of maximum stored energy, otherwise the diesel generator is connected to fulfill the load demand. Three loads (load1, load2 and load3) representing houses were connected to a multi-plug system made up of a DC/AC converter used to determine the power output. Figure 3-6 shows the sustainable renewable micro grid with source intensities i_{s1}; i_{s2}; i_{s3} and load intensities i_{l1}; i_{l2}; i_{l3} representing current generated by the 3D renewable energy platform and load output current. Figure 3-7 shows the system dynamic model simulation which controls feedbacks from the output voltage (V). The modelling of the turbines drive (hydro/wind) considers the aerodynamic torque principles of the turbine which in theoretical terms is a non-linear function of the turbines rotation with respect to the tip speed ratio and the pitch angle. As the intended design of the turbines and the

application, stability is of high essence, the linear relation of the tip speed ratio, the pitch angle and the rotational speed could be analysed using the non-linear torque function taking into account the Taylor series theory.

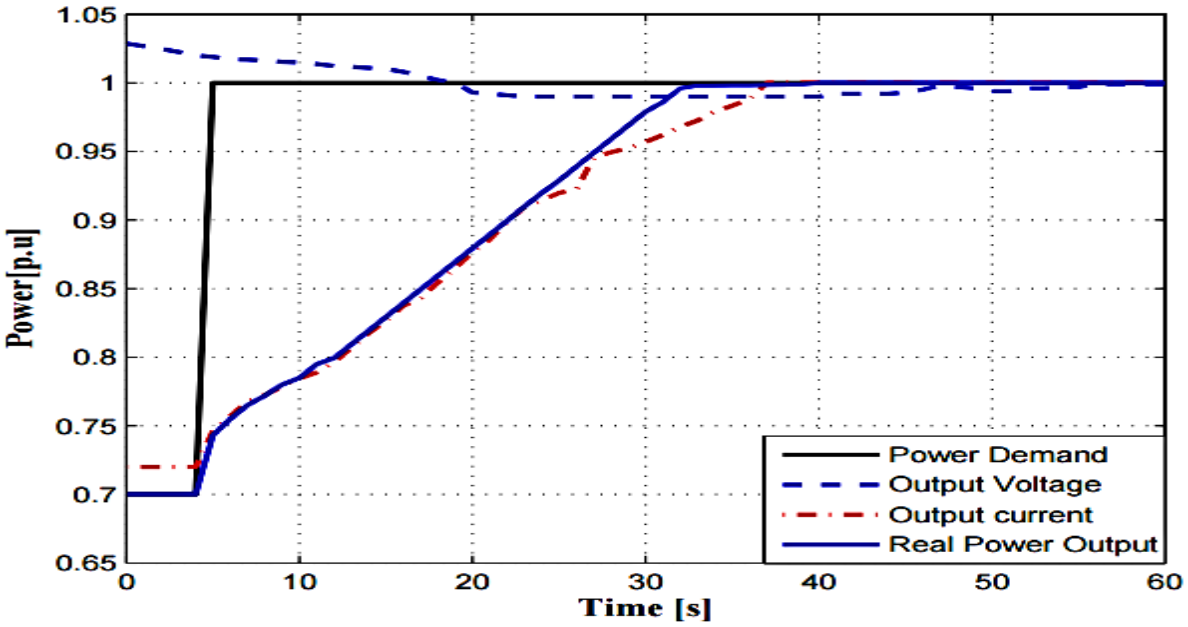

Figure 3-7 3D renewable energy platform Micro grid simulation [output voltage, output current, and real power]

3.3.4. ECONOMIC AND ENVIRONMENTAL IMPACT ON TOGO

- ***Environmental impact***

LOW CARBON ENERGY STRATEGY

What Is Community Energy | Community Energy - E. ON. 2018. [ONLINE] Available at: https://www.eonenergy.com/for-your-business/community-energy/what-is-community-energy. [Accessed 10 July 2016].

CONTENT REMOVED FOR COPYRIGHT REASONS

Figure 3-8 Environmental Assessment (Eon, 2017)

The implementation of the 3D renewable energy platform would significantly impact Emissions resulting to power plant emissions being lower than what would have occurred had

the prevalent fossil fuel technology been used. (ii) Emission reductions are expected to be real, measurable and long term. (iii) Establishment of emissions additionally (reduction in emissions) is a prerequisite under the implementation of the 3D renewable Energy platform and new energy business models in Togo. (iv)Baselines can be plant-specific or standardized. (v) The 3D platform would contribute to sustainable development in Togo and other developing countries. (vi)On a global scale the plant brings ‘‘clean’’ electricity to end-user, thus reducing even neglecting fossil fuel import dependence. Another important function of the 3D platform would be to improve the quality of power supply in the remote locations, through improvement in voltage, reduction in system losses and a reduction in the interruption of power supply. Our proposed system is one that could be applied as a 1D, 2D or 3D system and could be used for power generation as a decentralised system thereby reducing on transmission losses and lowers carbon emissions. Security of supply is increased nationally as customers don’t have to share a supply or rely on relatively few, large and remote power stations.

Economic Impact

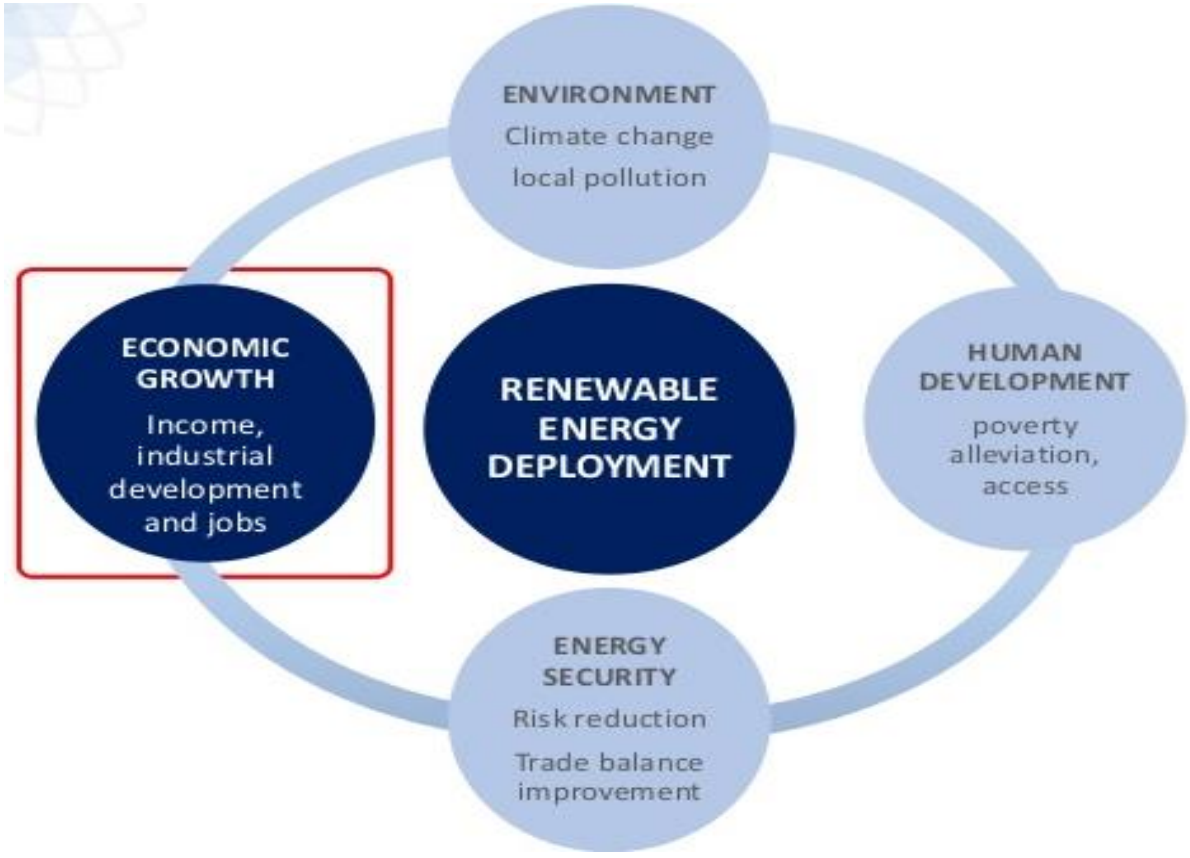

Figure 3-9 Impacts of Renewable Energy (IRENA, 2016)

Togo has worked hard since 2007 to boost its economy and build the foundation for a solid growth which has been among the most significant seen in the region (AU, 2016). This relaunch of the economy has helped to reposition Togo as a dynamic player in the region and seen it achieve some significant initial economic success, thereby earning the confidence of international investors (BBC, 2015). The country has seen flourishing growth (of 4% on average over the last five years) with a very stable Political environment allowing new investment code with many advantages for investors to be legislated and implemented (AU, 2016). Although there is continuous improvements being brought to the business environment (up 15 places in the 2015 Doing Business rankings), the country energy sector is one that needs a major transformation through which it is believed that the implementation of the proposed 3D renewable energy platform would be ideal in impacting the economy positively. Economic growth in countries is often a result as local technologies and resources increase their independence in supplying the energy needs of citizens (SF gate, 2015). The international Organisation for Economic Co-operation and Development explains that sustainability within a country's energy sector increases efficiency and security, encouraging prosperity and growth through energy access, industry development, job creation and competitive technological innovation (IOCD, 2015).

Predicted changes in Togo economy considering the implementation of our proposed system would therefore remain in the affordable access to energy in the form of electricity which is important not only for individual citizens, but also for the industries that drive the country's economy. As the development of renewable energy proceeds in increasing system capacity and efficiency, the costs of energy production will eventually drop (IRENA, 2015). These trends will increase the availability of clean electricity over time, eventually benefiting the country's manufacturing sector through lowered costs, and lowered pollution or energy taxes which will positively impact the economy

3.4. SUMMARY

The outcome of this chapter introduced the possible business model and recommended 3D renewable energy platform that could be adopted for Togo's smart grid power systems infrastructure and industrial applications. The proposed business model based on a critical literature review shows that the implementation of renewable energy businesses in Togo is highly encouraged as demonstrated by Government newly legislated policies. Togo's plan to expand its power infrastructure makes the business a viable one that could positively impact Togo's energy, environment and economic sector. We were able to expatiate on the possible

3-Dimentional (3D) renewable energy platform and its relevant Architectures and system of operations with possible back up system using storage battery or fossil fuel generation arrangement. The simulations showed that the 3D renewable energy platform mode of operation is characterized by both generation subsystems set to operate at their maximum energy conversion points with a battery bank in the system able to revert its energy flow, acting as a power supplier instead as a recipient of energy which makes the 3D renewable energy platform mode of operation an effective way of meeting power fluctuations and shortcomings of the renewable energy sources.

Economic and Environmental impact on Togo is also evaluated and discussed thoroughly. By supporting technologies such as renewable energy, Togo can remain ahead of the curve in worldwide industry development; by investing in renewable energy, Innovative technologies, adequate skills that could yield to competiveness in the international market. The OECD has found countries that embrace innovation more likely to strengthen their economies and rebound from recessions (OECD, 2015). By depending less on energy resources from other countries and more on local technological development, the economic growth of Togo can be regulated and encouraged from within.

CHAPTER 4

CHAPTER 4- COMPUTER AIDED DESIGN AND ANALYSIS OF THE FRONT END RENEWABLE ENERGY RESOURCES OF THE PROPOSED 3D RENEWABLE ENERGY PLATFORM

4.1. INTRODUCTION

This chapter provides Computer Aided Design and Analysis of the front End renewable energy resources of the proposed platform. This is mainly aiming at investigating the possible factors of improving the efficiency of the front end units. The computer aided design and analysis has been carried for Hydropower units (water wheels, Kaplan turbine; dual feed arrangement for both water wheel and Kaplan turbine), Wind turbine units, 2D arrangements i.e. wind and hydropower, wind and PV systems, PV and Hydro systems.

The work presented in this chapter also looked at the various relevant mathematical and control model of power conversion showing the dynamic behaviour of the proposed model which is examined under different operating conditions. Real-time measured parameters are used as inputs for the developed system. The proposed model and its control strategy offers a proper tool for optimizing hybrid power system performance, such that it may be used in smart-house applications, commercial and industrial applications as well. Solidworks models are developed; using simulations software to highlight the characteristics of the output power characteristics.

4.1.1. HYDRO WHEEL SYSTEM COMPUTER SIMULATION AND ANALYSIS

Hydropower generation of which production figures is widely encouraging is predicted by the International Energy Association, UN to rise up to 6000 Terrawatt-hours by 2050 (IEA, 2012), hence the technology innovation of hydrowheels/ turbines and their designs must be a self reliant and provide above the average 80% efficiency that is being currently marketed to be able to meet the set world hydro energy generation target by 2050 (EPRI, 2006). Various types of hydrowheels and turbines with the probability of reaching 80% efficiency are evaluated using secondary research data and suggestions on how this could be improved is clearly established. The research undertaken to design and develop a 3D platform to fully utilize Togo's renewable energy resources into their smart grid power system infrastructure couldn't possibly be complete without a critical review of the potentialities of hydro power and its generation. Studies reveal that hydro wheels are not as efficient as turbines but could offer

efficiency in excess of 80% for overshoot & undershoot water wheels, with 75% for Breast-shoot water wheels. The technical issues that limit the hydro wheel efficiency have been studied and a new design is presented. The simulation of the new design is hereby presented with the experimental measurements of efficiency and power generated. Designs will be carried out using Solidworks, and simulations carried out to study flow analysis patterns with possible calculations that will amount to efficiency improvement of the turbine offered at an affordable cost making the design cost effective.

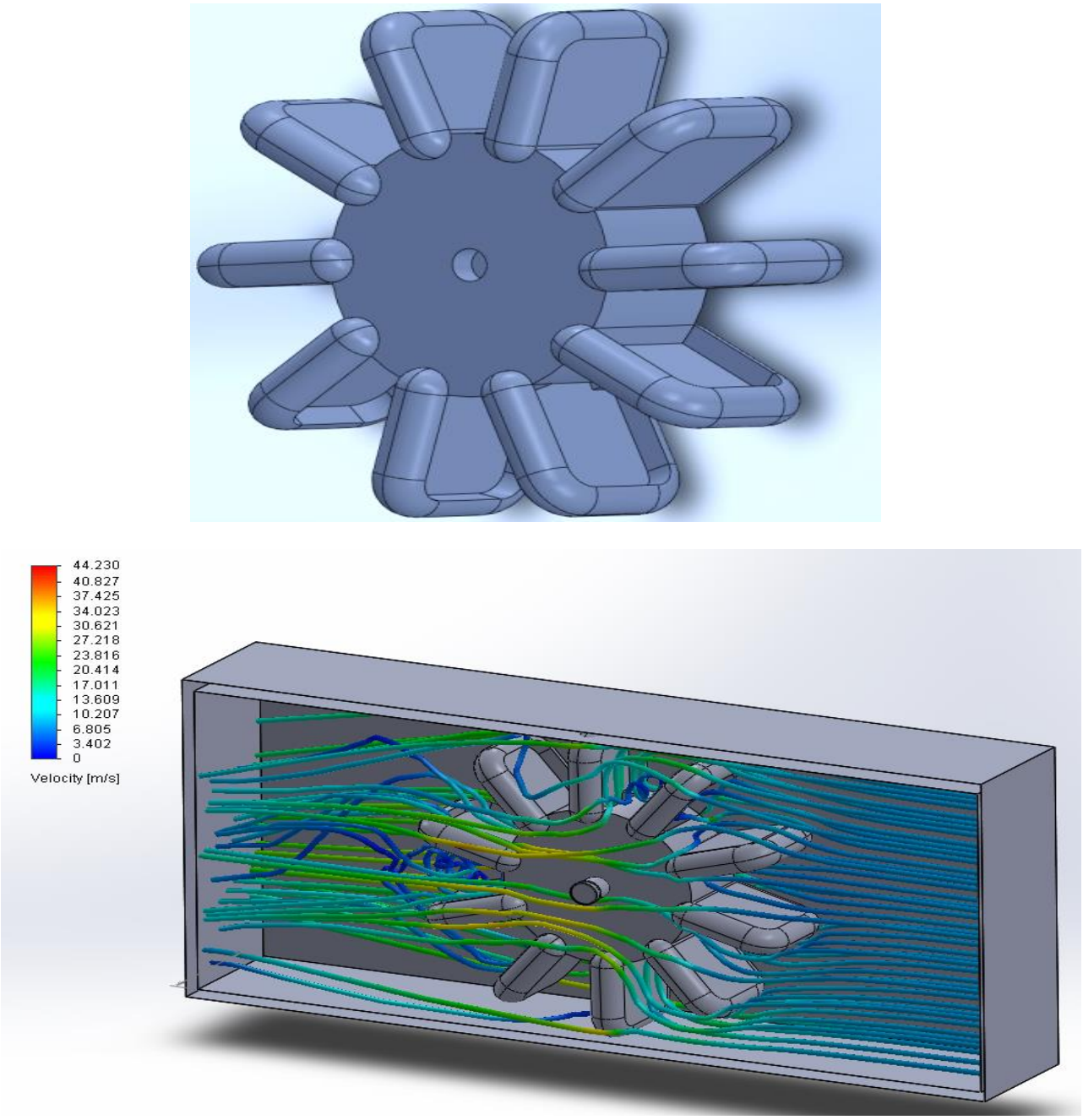

Figure 4-1 New Eco-wheel Design with Flow simulation (a) overview of wheel, (b) flow simulation of wheel (k Moglo et al, 2015)

The design of the Eco-wheel was conducted by first of all considering measurements of the hydro wheel test canal and implementations of the measurements was introduce in the mechanical CAD design software "Solidworks". Solidworks is a mechanical software used for design of 3D CAD (computer aided Design) able to transform ideas into product with aided tools such as 3D CAD solutions, simulations, product data management, life cycle assessment (Mathworks, 2013). The aim of the Eco-wheel design was to offer a wheel that will use Green products for its manufacturing and offer a better efficiency for the overshot wheel technology. As expressed earlier in this research and in reference to fig 2-7 the estimated overshot waterwheel output efficiency is ≈ 80% on average. Considering the design however, a flow simulation analysis of the wheel was conducted using the same software where we obtained a maximum velocity of 44.23 m/s as seen in the flow simulation enabling us to apply various theoretical models conducted. The efficiency was obtained by considering power derived from gravitaional potential energy with buckets tipped out at an angle θ. It was also assumed that the reaction force acting on the buckets is equal to the main force applied in the first instance by the water on the buckets but in different direction, in so doing the derivative of resultant force gave a clear understanding of the role of gravity on the wheels hence we applied Newton's second law of motion to determine the force and input power. The efficiency was then obtained to be higher than the expected overshot water wheel efficiency as it was obtained to be 85.3%. The design was done in such a way that it does allow buckets on the Eco-wheel to be filled ≥ 50% making weight a factor of faster rotation for the wheels. The experimental results obtained from the Eco-wheel; hence the 1D hydro optimisation system proves that the technology is efficient and would be very useful to the 3D renewable sustainable power station. It is however important to mention that there is a possibility of implementing a 2D system as well thus juxtaposing solar PV systems technology with Hydroelectric for example, the advantages of this would then be a higher total delivered output power as energy will be generated from two renewable sources. The disadvantages however of having a 1D, 2D as compared to a 3D system is that the geographical conditions and locations are not always ideal for a 1D or 2D system hence the necessity for a 3D system where if energy produced by the hydro could be used to feed the wind turbine, causing a rotation that will generate energy at all time.

4.1.2. MICRO-HYDROPOWER SYSTEM DATA ANALYSIS

Considering results obtained with the overshot, undershot and breastshoot wheels, it was apparent to consider efficiency improvement of the Overshot water wheel. Offering an average

of 80% already (PDMHS, 2013) this could be scaled up by taking a step by step approach of the designs with careful measurements and calculations. The aims of this design is hence to offer a much efficient overshoot water wheel that could offer a higher efficiency than what is already being obtained currently with careful material selection making the overall design a very affordable one by all standard. This will then be preferred than other designs considering efficiency improvement and affordability. A wide range of theoretical calculations will be done to determine the efficiency and flow simulation carried out using Solid works will equally be conducted to further explain how the efficiency of the overshot wheel could be obtained. The unit will then be practically done and used for a 3D Renewable sustainable Power station with Low cost and high efficiency.

4.1.3. KAPLAN TURBINE

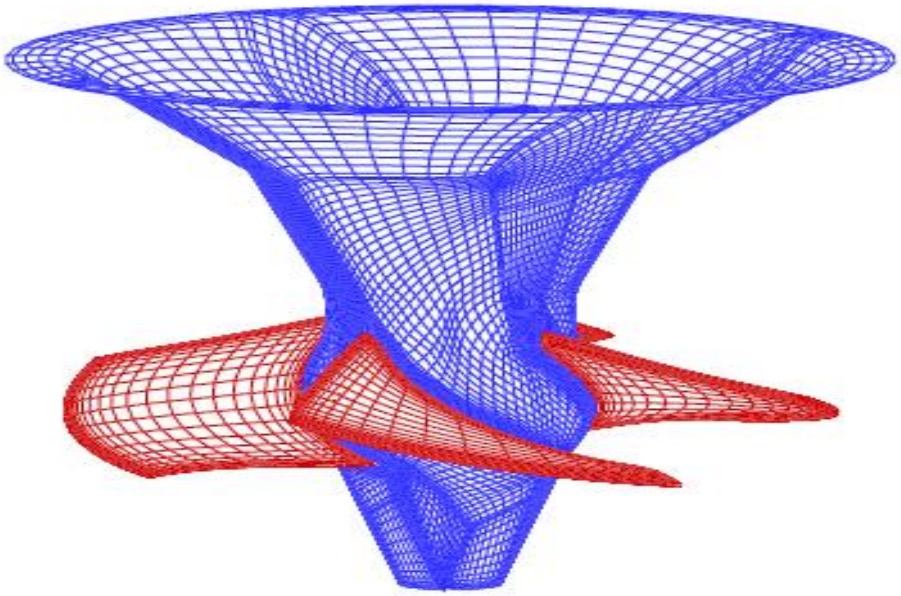

Figure 4-2 Schematic of Kaplan Turbine rate (K Moglo et al, 2015)

The ideal practical importance of a kaplan turbine adresses the technology behind its design, condition assessment, maintenance operations, with the sole objective of improving performance and its reliability in the hydro power production sector. The aim of this Kaplan turbine is to act as a prime mover directly producing horsepower to the generator. Secondary research shows that Kaplan turbine is the most significant and most reliable system in hydropower turbines as its design, operation and maintenance factors all aim to provide the most of impact on the overall efficiency, reliability and general performance. The performance however of the Kaplan turbine is dependent on the reliability of the related components used

such as the axial flow runner with adjustable wicket gates and control mechanism, draft tube, spiral case etc…. Kaplan turbines are mostly used in a low head and high flow application with adjustable blade types as earlier mentioned leading to a higher efficiency and power output range (EM, 2003). Figure 4-3, shows a typical efficiency performance curve of the Kaplan turbine is shown. The kaplan trurbine wicket gate control shows a very narrow range of high efficiency as a fixed blade unit, this shows that an accurate and optimal adjustament with careful considerations of flow analysis must be conducted in order to obtained an optimised performance of the blade. In contrast, the double regulated kaplan turbine reveals a much improved efficiency range which is due to its absolute peak setting and individual blade tilt enabling a gate blade relationship to be be established in order to obtained an optimised performance (EM, 2003).

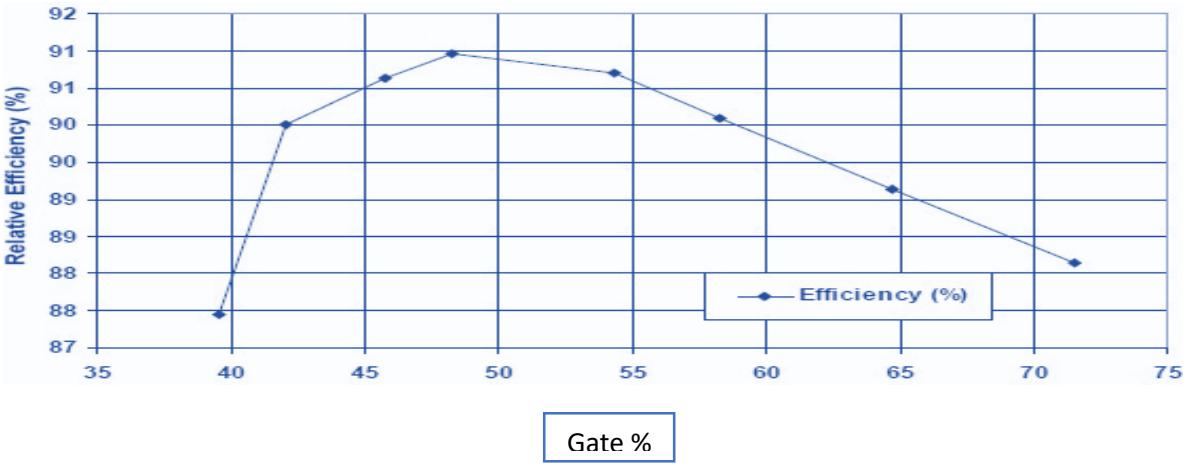

Figure 4-3 Kaplan Turbine efficiency evaluation

4.1.4. NEW MICRO HYDRO POWER GENERATOR

Considering the efficiency obtained during the practical test for the Eco wheel micro hydro generator, a better concept of the 1D hydropower system have been introduced with a blade pitch control system for the Kaplan turbine and a bevel gear directly connected to it and the generator. The DMGES (Dual Micro Generator Eco wheel system) consists of two overshot wheel positioned horizontally opposite each other and directly connected to the piston driving the Kaplan turbine and feeding the generator. Both positioned at an angle of 90 degrees receives water at the top of the wheels at the water inflow which with its forces a rotation. A minimised compact penstock is then used to collect the water at the outflow stage so as to build a strong pressure which will force a rotation of the Kaplan turbine. This pressure is then increased by water flowing from both angles and enclosed leading to a much stronger rotation experienced by the Kaplan blades.

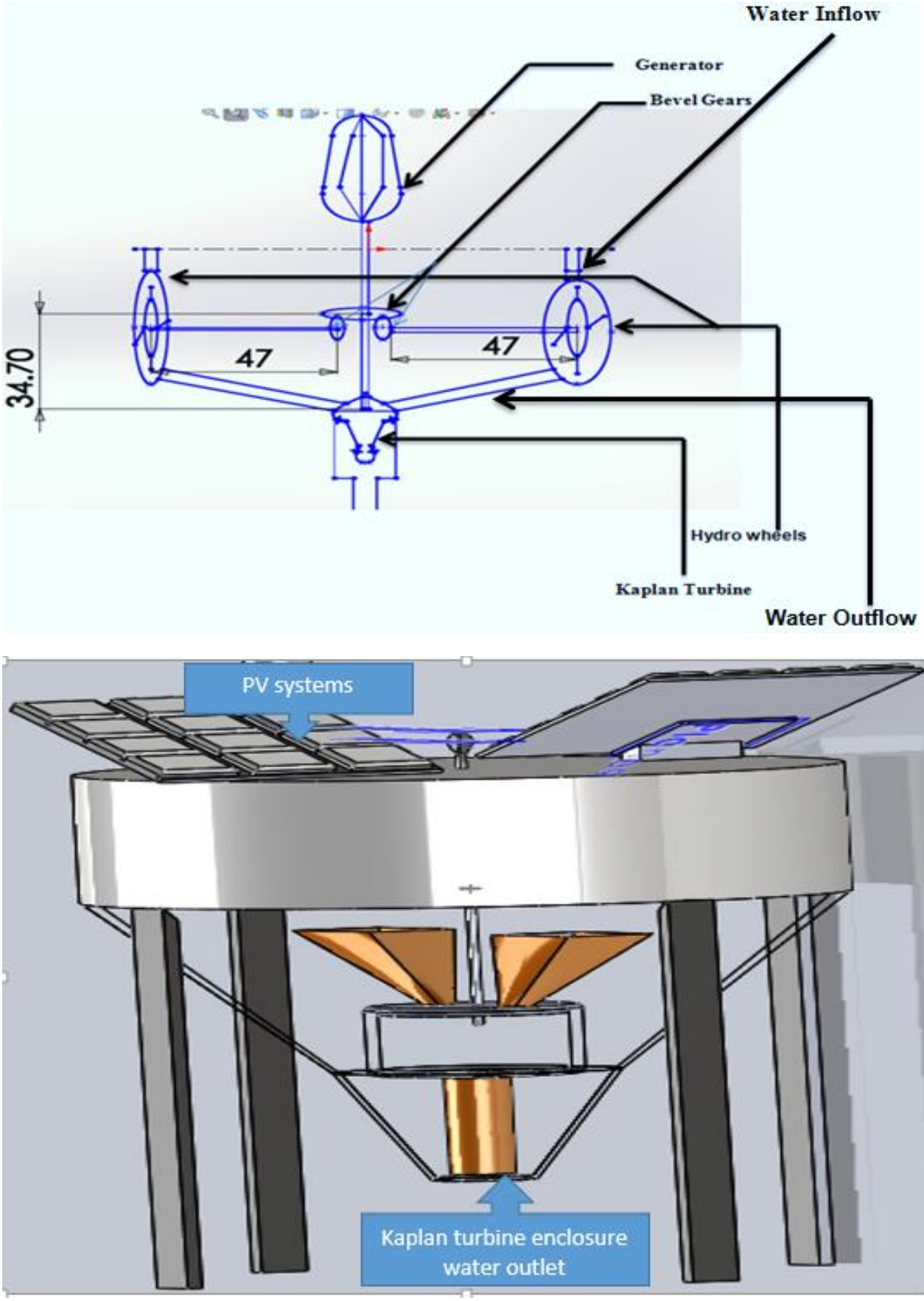

Figure 4-4 Dual micro-generator Eco-wheel system & the Kaplan Turbine

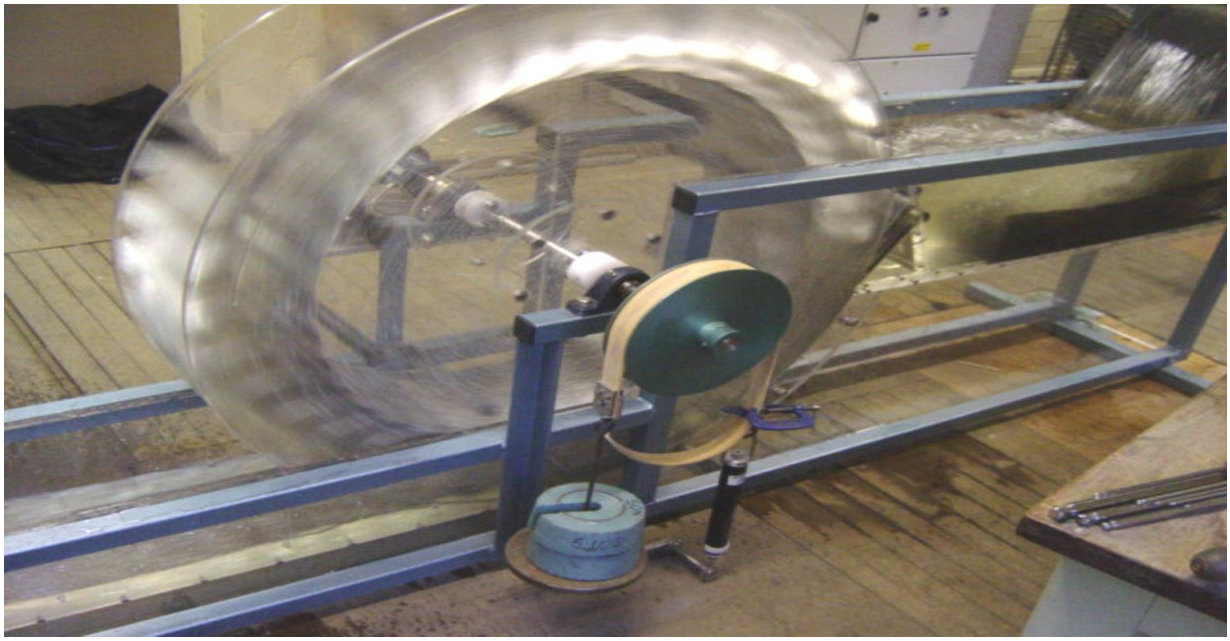

Figure 4-5 Hydro wheels test canal

$$Test\ Bed\ Lenght = 5\ m$$

$$Test\ Bed\ width = 7.2\ cm$$

$$Test\ bed\ Height = 24.5\ cm$$

$$Test\ Bed\ Diameter = 24\ cm$$

In order to determine the water flow Speed, a timed volume of water 0-30 Liters was allowed to flow

$$Looking\ for\ water\ flow\ speed = \frac{Volume\ of\ Water}{Time} = \frac{30}{35.95\ sec}$$
$$= 0.8344\ m/s \ldots\ldots\ldots\ldots\ldots\ldots (1)$$

$$Looking\ for\ Area\ of\ Canal\ tube = Width\ \times Height = 24.5\ \times 7.2 = A = 176.4\ cm^2 \ldots\ldots (1)$$

$$Looking\ for\ Volumetric\ Flow\ rate$$

$$= Area\ \times Water\ Flow\ speed = 0.1764\ x\ 0.8344 = 0.141\ m^{3/s} \ldots\ldots (2)$$

$$Looking\ for\ Mass = Density\ of\ Water\ \times Volume = 1000\ \text{Kg}\ /\ m^3\ \times 0.072 = 72\ \text{Kg} \ldots\ldots (3)$$

$$Looking\ for\ pressure = mgh = 72\ \times 9.81 \times 7.2 = 5085.504\ Pa\ or\ 5.08 Kpa \ldots\ldots (4)$$

$$Looking\ for\ Power = Pressure\ \times Volumetric\ Flow\ rate \ldots\ldots\ldots\ldots (5)$$

$$Therefore\ Max\ Output\ power = 5085.504\ \times 0.141 = 721.4\ Watt$$

$$Looking\ for\ Mass\ Flow\ rate = \rho\ \times V\ \times A = 1000\ \times 0.141 \times 0.176 \ldots\ldots (6)$$

$$Mass\ Flow\ rate = 24.82\ Kg/s$$

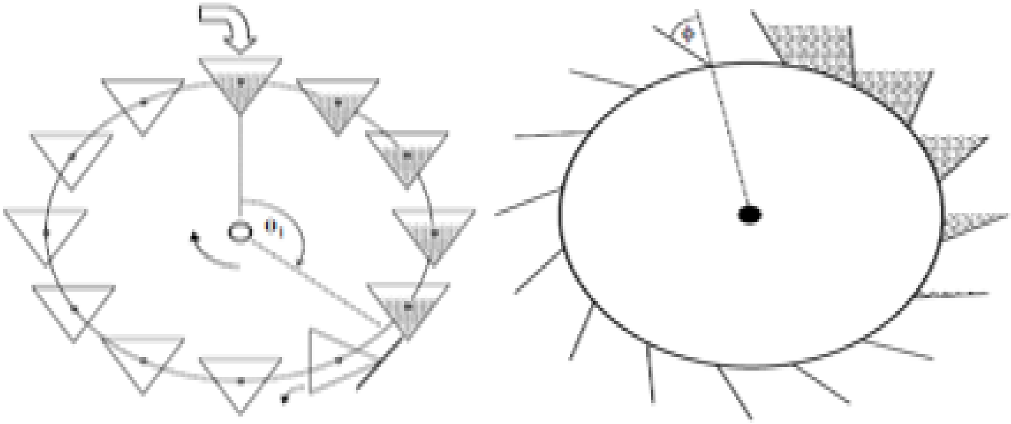

Figure 4-6 Overshot waterwheel powered by gravitational potential energy, with buckets tips out at angle ϑ (Denny et al, 2000)

The considerations to getting the overall efficiency value of the wheel will have to incorporate unavoidable realities such as the water momentum, probable spillage of the water and friction. We can then assume that the buckets in fig 4-6 are at angle of θ where $0< \theta \leq \theta_1$ are filled with water and the other buckets are empty. There are about 10 buckets on the designed wheels but other wheels could take more depending on the design. The buckets are at an angle of Δθ around the wheel so one could say that Δθ= 2π.

Considering that the mass of the water in each of the buckets is

$$\Delta m = \rho f \times \Delta t \ldots\ldots\ldots\ldots\ldots\ldots\ldots\ldots\ldots\ldots.. (7)$$

Where ρ represents the density, f is the flow rate and Δt the time interval taken to fill the next bucket on the rim. This is obtainable by equating equations $\omega\Delta t = \Delta\theta$ with ω representing the waterwheel angular speed hence the equation will be

$$\Delta m = \frac{\rho f}{\omega} \Delta\theta \ldots\ldots\ldots\ldots\ldots\ldots\ldots\ldots\ldots\ldots\ldots.. (8)$$

Considering that the mass of the water in each of the buckets is $\Delta m = \rho f \times \Delta t$ where ρ represents the density, f is the flow rate and Δt the time interval taken to fill the next bucket on the rim.

In order to obtain the efficiency, one needs to understand that the theorem of force applied on a body is obtained by the controlled volume of fluid excreted, which is similar to the rate of change of momentum, the theorem can be conveyed as

$$F = Mout.Vout - Min.Vin \ldots\ldots\ldots\ldots\ldots (9)$$

Where M represent the mass flow rate earlier obtained, F the force exerted by the water on a solid body, the total force exerted in the procedure could be expressed as

$$F = F1 + F2 + F3 = Mout.Vout - Min.Vin \ldots\ldots\ldots\ldots. (10)$$

F1 stands for the force of the fluid on the buckets, F2 the returning force of the buckets on the fluid and F3 the force of the fluid exerted outside the control volume. These different forces need to be in the analysis as the equation can be simplified by the simple understanding that the reaction force is equal to the main force applied in the first instance by the water on the bucket but in different direction hence it could be neglected due to gravity and the assumption made that the pressure of the water is maintain at a constant which will make F2 &F3 equal to zero. This now gives the clear understanding of the role of gravity and the two direction in which the waterwheel rotates in; hence considering for

$$Direction\ (x) Rx = m.(Vin - Vout) \ldots\ldots\ldots\ldots\ldots\ldots\ldots\ldots\ldots\ldots. (11)$$

$$while\ in\ Direction\ (y) Ry = m.(vin - Vout)y \ldots\ldots\ldots\ldots\ldots\ldots\ldots\ldots\ldots\ldots (12)$$

The resultant for Direction x and y can be expressed as

$$R = \sqrt{R_x^2} + \sqrt{R_y^2} \ldots\ldots\ldots\ldots\ldots\ldots\ldots\ldots\ldots\ldots\ldots\ldots\ldots\ldots. (13)$$

$$According\ to\ Newton's\ Second\ Law\ of\ Motion$$

$$F = m(vt - Vi) \ldots\ldots\ldots\ldots\ldots\ldots\ldots\ldots\ldots\ldots. (14)$$

Where m is the mass flow rate earlier obtained, vt is the velocity of the wheel and vi is the velocity of the water.

Using the above equation, Mass flow rate= 24.816 m^3/s, Vi= 0.8344 m/s, Vt= 44.23 m/s

$$F = 24.816(44.23 - 0.8344) = 1076.9N$$

$$F = RduetoF2\ \&F3 = 0\ andtheresultantforcebeingequaltothereactionforce = 1076.9\ N$$

The total input power will then be considered as the total sum of the input force on each bucket and the water flow rate applied on the buckets enabling a constant rotation, this could be found by applying

$$Pi = \sum \int_{\theta_i}^{\theta_f} R\, d\theta \ldots\ldots\ldots\ldots\ldots\ldots\ldots\ldots\ldots (15)$$

Where Pi= Input power; θ_f is the final angular displacement; θ_i is the initial angular displacement and $d\theta$ represents the change in angular displacement

$$Pi = \sum \int_{\theta_i}^{\theta_f} R\, d\theta = 1076.9 \times \frac{\pi}{4} = therefore\ Pi = 845.79\ watts$$

The mechanical efficiency of the wheel could then be determined by applying the formulae

$$Efficiency = \frac{Output\ Power}{Input\ power} \times 100\%\ ; Therefore\ E = \frac{721.36}{845.79} \times 100\%$$

$$Efficiency = 85.3\ \%$$

One of the research objectives was to design a 3D renewable energy platform to fully utilize Togo's renewable energy resources into their smart grid power system infrastructure. A computer simulation and modelling of a Micro-Hydro power generator using Kaplan turbine for domestic and industrial Applications has been done and presented. Studies reveal that water wheels are not as efficient as turbines although they contribute to an improved efficiency and offer efficiency in excess of 80% for overshoot and efficiency above 90% for Kaplan turbines. The technical issues that limit the water wheel efficiency and the Kaplan turbine have been studied and a new design is presented. The simulation to the new design is hereby presented with some modeling control.

4.1.5. DESEIGN APPROACH

- **Penstock**

A penstock is an intake structure that control water flow. The penstock is use to direct the flow to the turbine blades within the turbine enclosure in this design. The penstock in this design is not only used to direct the flow but also to increase the velocity of the flow which will in turn increase the rotational speed of the turbine resulting to a higher hydropower generation. Figure 3-23 below is an example of the type of penstock that will be used to direct water to the Kaplan turbine blade. The water inlet of this penstock is design to collect water at a very streamline form.

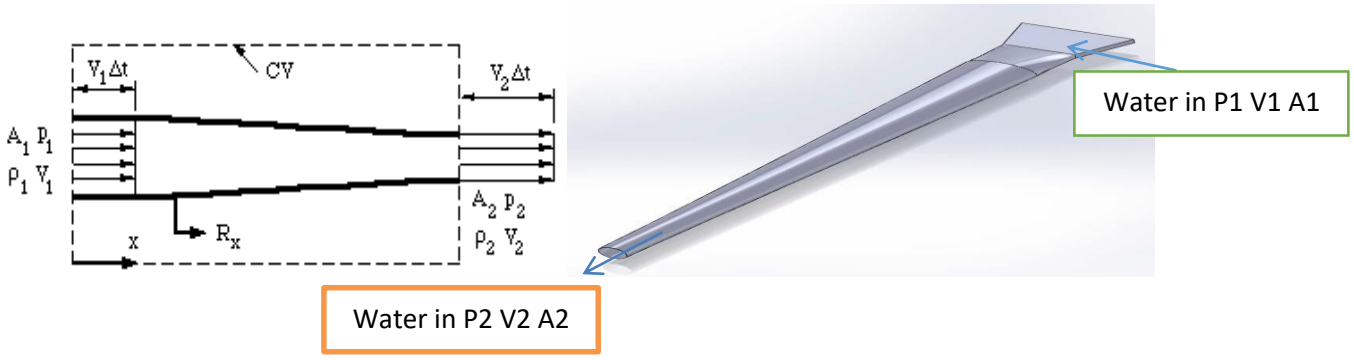

Figure 4-7 Dual micro-generator Eco-wheel system –Penstock design

- **Kaplan turbine**

The FEA analysis of the turbine is very important, as it provides an analysed detail of the design safety factor and how strong the turbine is with possible displacement of the blades. A factor of safety of 1.7 is obtained which is quite good for the design as shown in figure 4-8. Figure 4-8 shows the flow simulation of the Kaplan turbine using a single penstock to stimulate the turbine. The flow simulation reveals that with a reduced housing, a better focus of the penstock tube to the blades is achieved with an improved rotation per munities of the turbine, leading to a much better and more efficient result. It therefore means that, the reaction of the water to the turbine blades causes rotation and the circular motion of the flow also influences the rotation of the turbine. We then reduced the RPM of the blade to 500rpm, which is the expected amount of revolution per minutes for turbine at the flow head of 5m and obtained a much higher velocity of up to 33.75m/s.as demonstrated in figure 4-8 below.

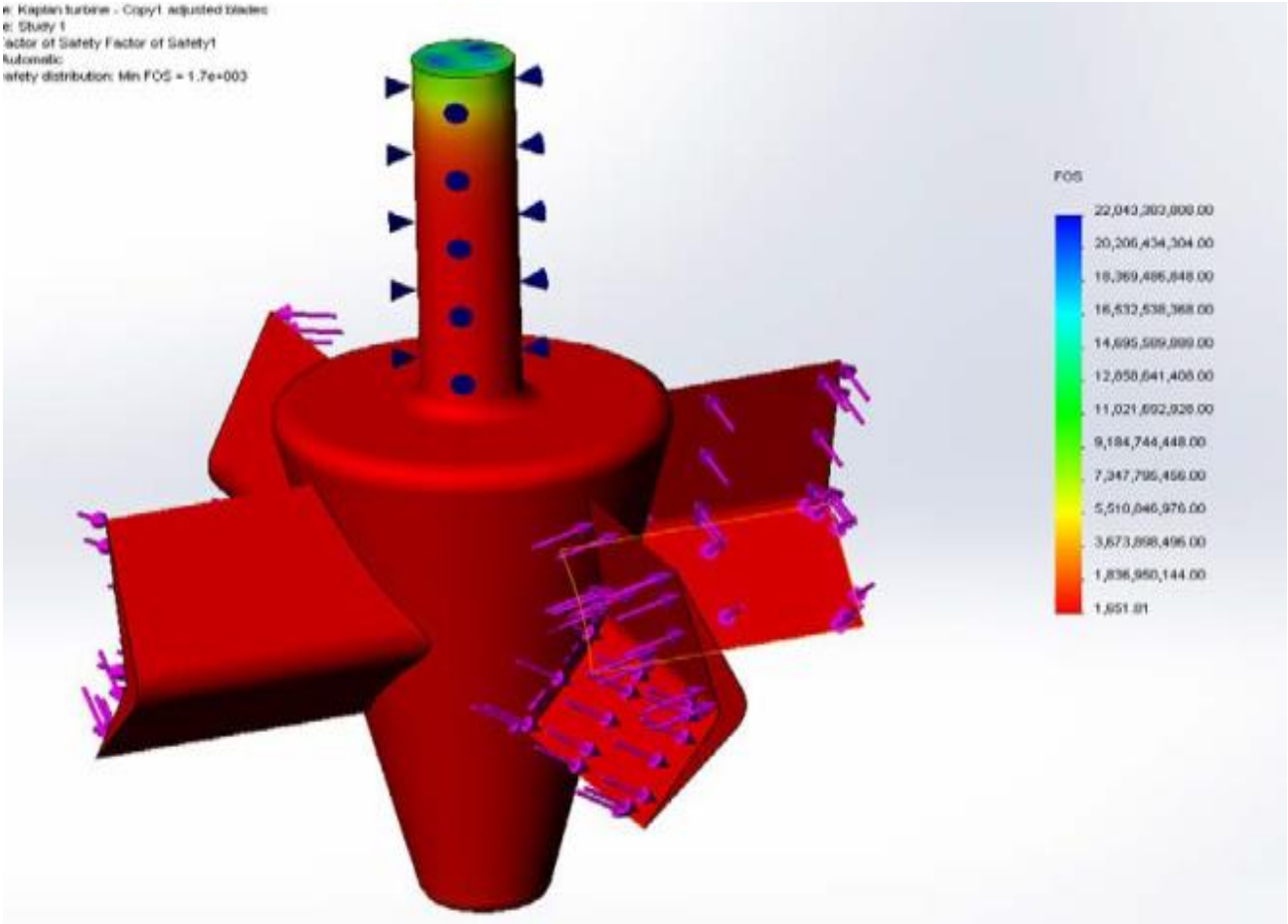

Figure 4-8 Kaplan turbine Design & Finite element analysis flow simulation

4.1.6. BEVEL GEARS

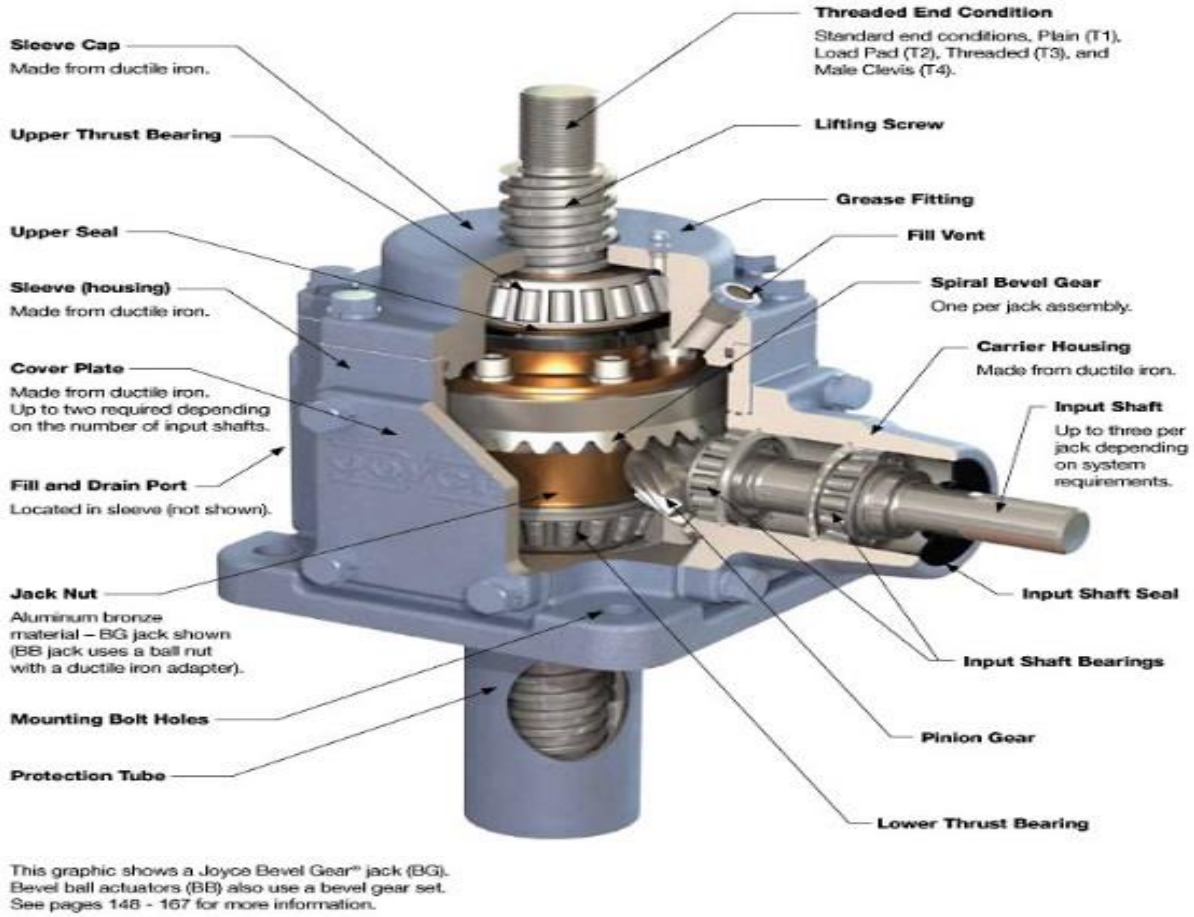

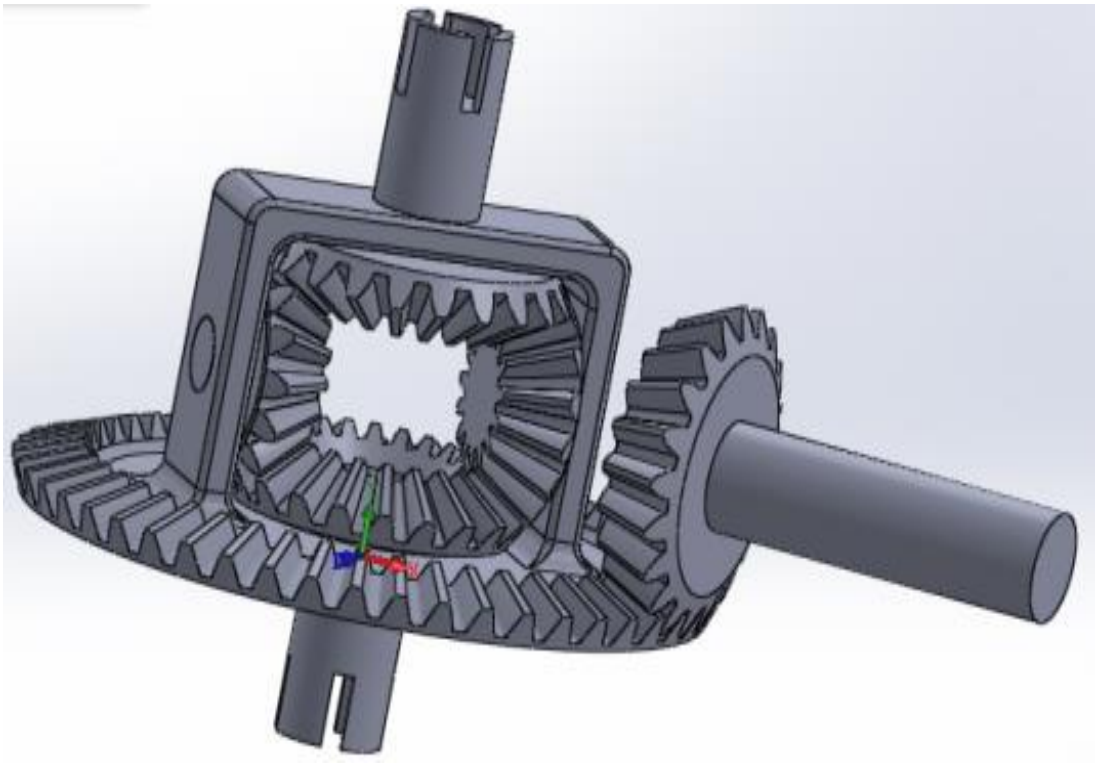

Figure 4--9 Bevel Gear design for the Generator (a) Overall gearing system

A bevel gear design for the overall system have been presented in Fig 4-9 (b) Bevel gearing system are gears where the axes of the two shafts intersect and the tooth-bearing faces of the gears themselves are conically shaped. This will permit the individual rotation of both standalone Eco wheel and that of the Kaplan hydro turbine to individually rotate and direct horsepower generated to the generator. A careful analysis of the gears was done in SOLIDWORKS in order to allow a close comfortable seat and fit of the Eco wheels on the gear system. The use of the bevel gears was perfect as it allows a joint system of the 3D to be possible whilst offering a high efficiency (can be 98% or higher), and can transfer power across nonintersecting shafts. This type of spiral bevel gears transmits loads evenly and are quieter than straight bevels.

4.1.7. DUAL MICRO GENERATOR ECO WHEEL SYSTEM & THE KAPLAN TURBINE DESIGN

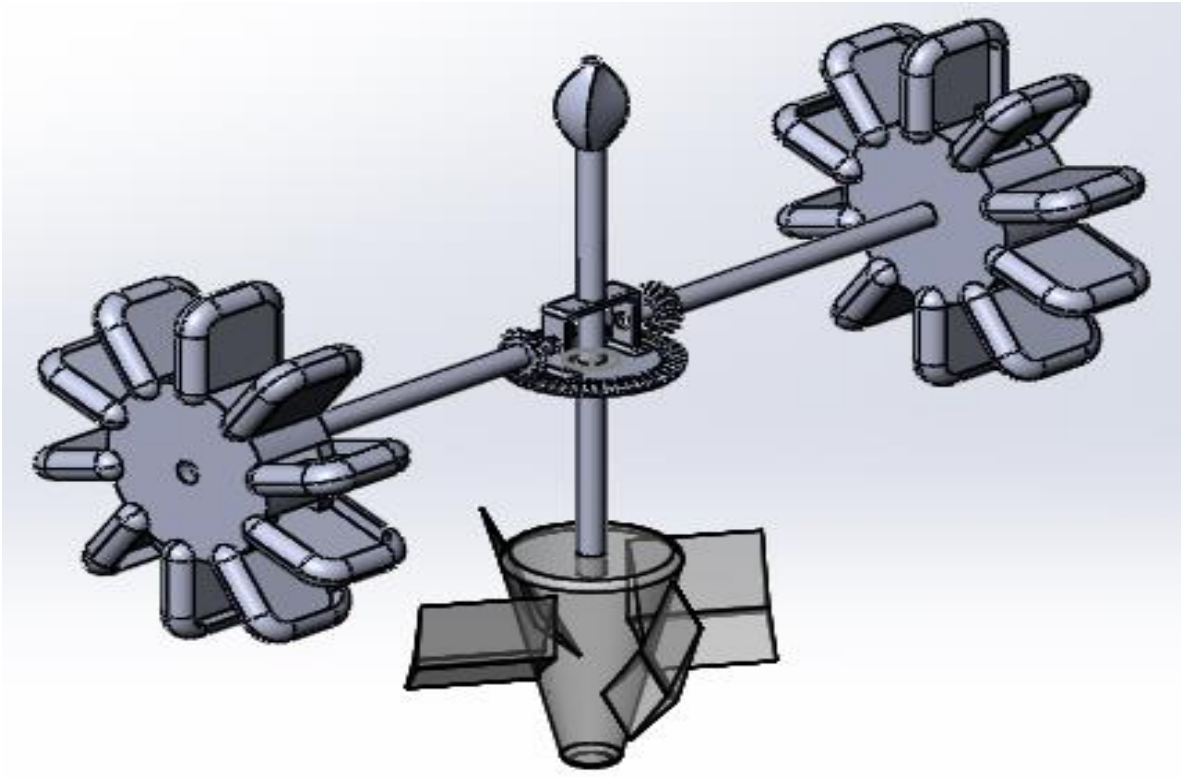

Figure 4-10 Dual micro-generator Eco-wheel system & the Kaplan Turbine design

The dual micro generator Eco wheel system and the Kaplan turbine design presented in figure 4-10, consists of two different overshot water wheel of improved efficiency for which test were carried out on. Aiming for a complete system to deliver a high output power and improved efficiency, a Kaplan turbine was added to the system for which test strength were equally carried on. The Importance of micro hydro generator design comes as a solution to provide

sustainability in energy supplies. The presented design offers a much more interesting approach to hydropower generation and the design approach expressed aren't limited to a small scale power production as the topology used could be applied on an industrial scale. The design will indeed affect how energy is consumed in homes or in industries as this does provide a much improved efficiency, a solid reliance on the system and another renewable energy system that is independent and comes at no cost except for the manufacturing and installation of the designed system

4.2. 2D WIND TURBINE AND HYDRO SYSTEM

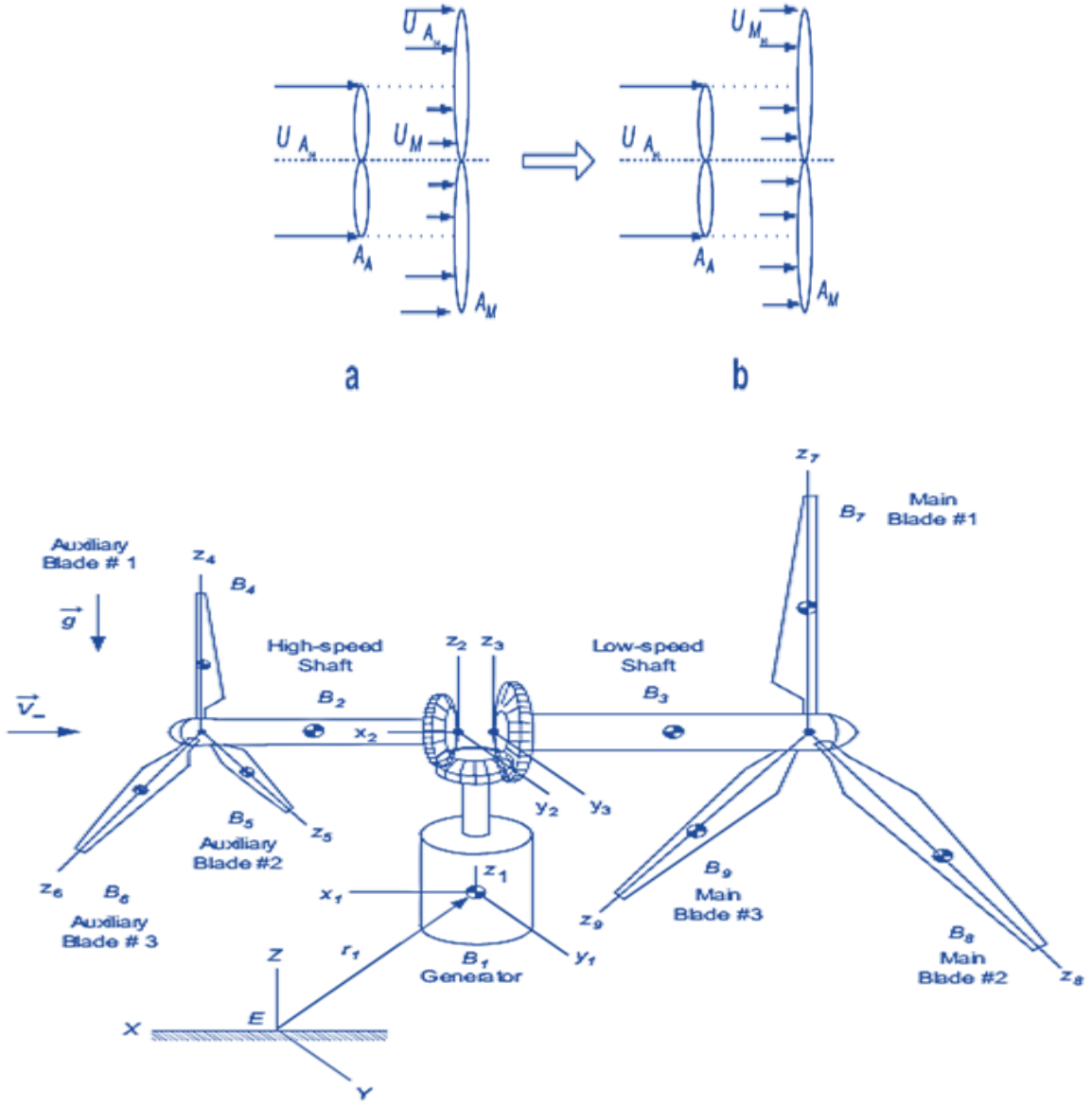

Figure 4-11 Double rotation Wind turbine system (k Moglo et al, 2016)

A double rotation wind turbine system will be used and nonlinear simulation software for the performance prediction will be presented. The notable feature of the double rotation wind

turbine system is that it consists of two rotor systems positioned horizontally at upwind and downwind, and a generator installed vertically inside the tower. The double rotation wind turbine system has a constrained multi-body system, and the equations of motion are obtained by using the multi-body dynamics approach. Aerodynamic forces and torques generated from each rotor blades are calculated using the blade element theory. A relatively simple model for the load torque will be obtained by using the test data of the doubly fed induction generator adopted in the double rotation wind turbine system. Finally, a MATLAB / Simulink-based hybrid simulation software will be used to predict and analyse the performance of the double rotation wind turbine system. The combination of the Hydro system and that of the wind trubine will form the 2 Dimensional system.

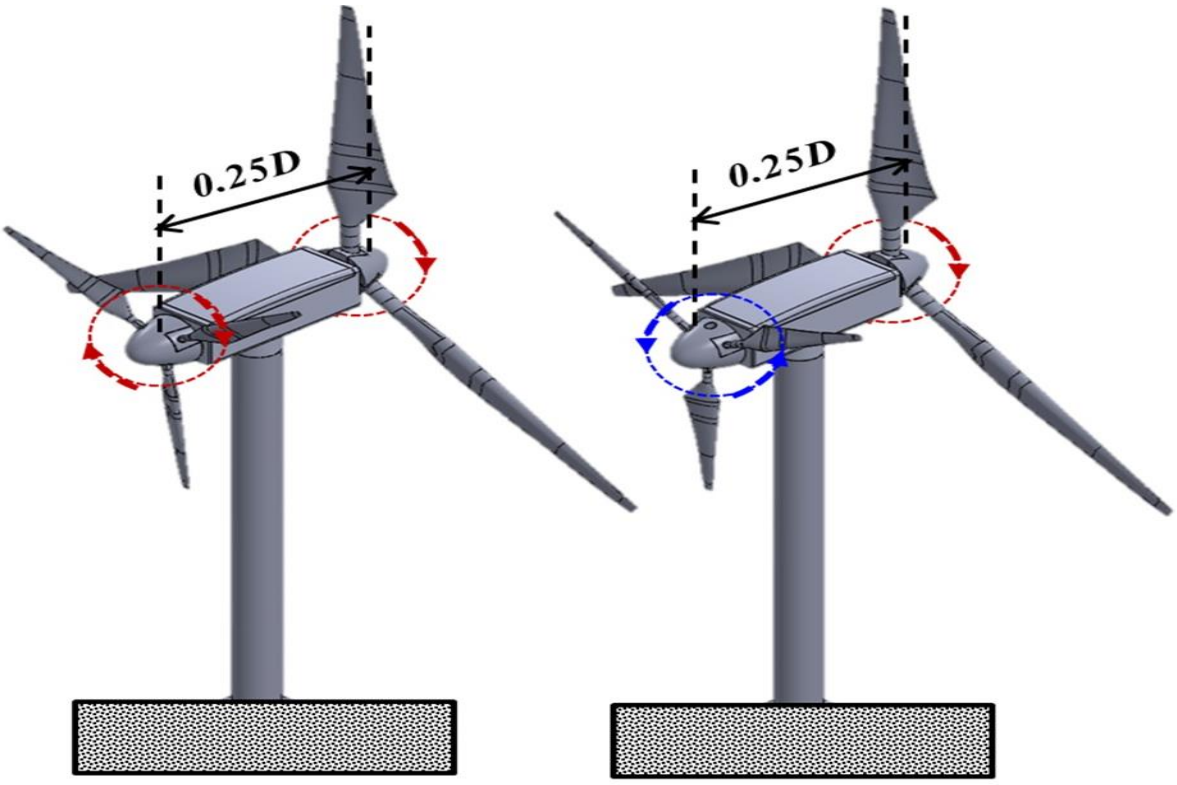

Figure 4-12 Double rotor wind turbine

Modern, utility-scale horizontal axis wind turbine rotor blades are aerodynamically optimized in outboard region, whereas blade sections near turbine hub (i.e., root of blades) are designed primarily to withstand structural loads (i.e., bending and torsional). Therefore, very high thickness-to-chord ratio aerofoils, which are aerodynamically poor, are used near turbine root to provide structural integrity. Such configuration results in a “dead” wind zone near rotor axis where virtually no energy is extracted from the wind which is why a distance of 0.25m is allowed between the two blades. Up to 5% loss in wind energy extraction

capability is estimated to occur per turbine due to this compromise (Sharma, 2010). These "root losses" occur even in turbines that operate in isolation, i.e., with no other turbine nearby. Array interference (wake) losses resulting from aerodynamic interaction between turbines in wind farms have been measured to range between 8 - 40% (Barthelmie et al., 2007) depending on wind farm location (e.g., onshore versus offshore), farm layout, and atmospheric stability condition. While there is abundant literature documenting root losses and wake losses in wind farms, researches on concepts that can mitigate these losses are still very inadequate.

As shown in Figure 4-13, the double rotor wind turbine system will employ a secondary, smaller, co-axial rotor with two objectives: (1) mitigate losses incurred in the root region of the main rotor by using an aerodynamically optimized secondary rotor, and (2) mitigate wake losses in the double rotor wind turbine system through rapid mixing of turbine wake. Mixing rate of the double rotor wind turbine wake can be enhanced by (a) increasing radial shear in wind velocity in wakes, and (b) using dynamic interaction between primary and secondary rotor tip vortices. Velocity shear in turbine wake can be tailored (by varying secondary rotor loading) to amplify mixing during conditions when wake/array losses are dominant. The increased power capacity due to the secondary rotor can also be availed to extract energy at wind speeds below the current cut-in speeds of conventional single rotor wind turbine. Given the substantial efficiency improvement potential, success of the proposed concept will be added innovative advantage to the 3D renewable energy platform.

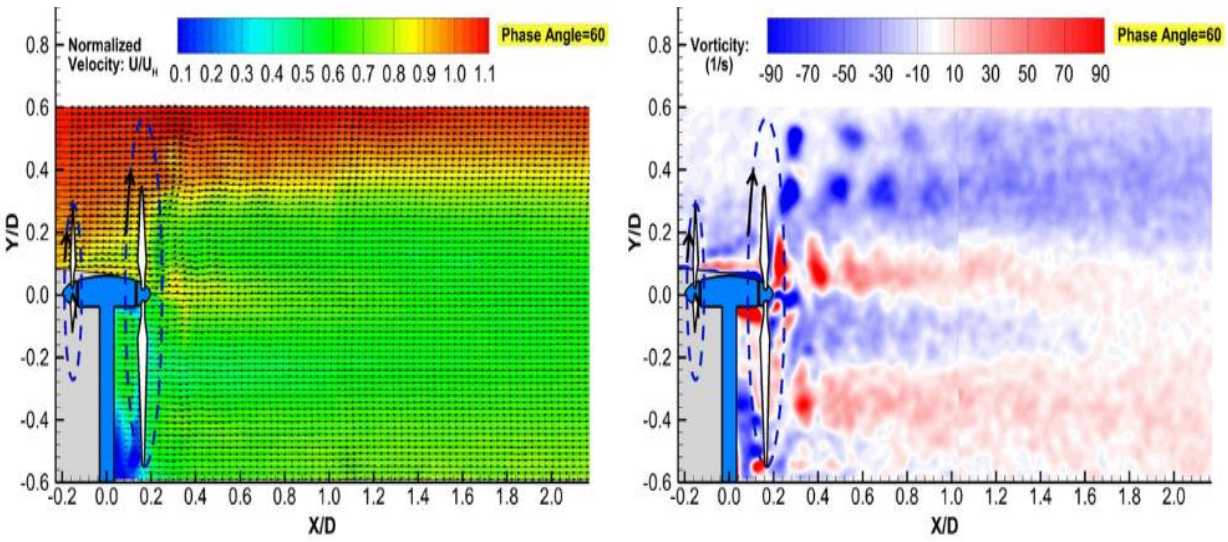

The wake vortices and turbulent flow structures behind a Co-rotating Dual-Rotor Wind Turbine (Co-DRWT)

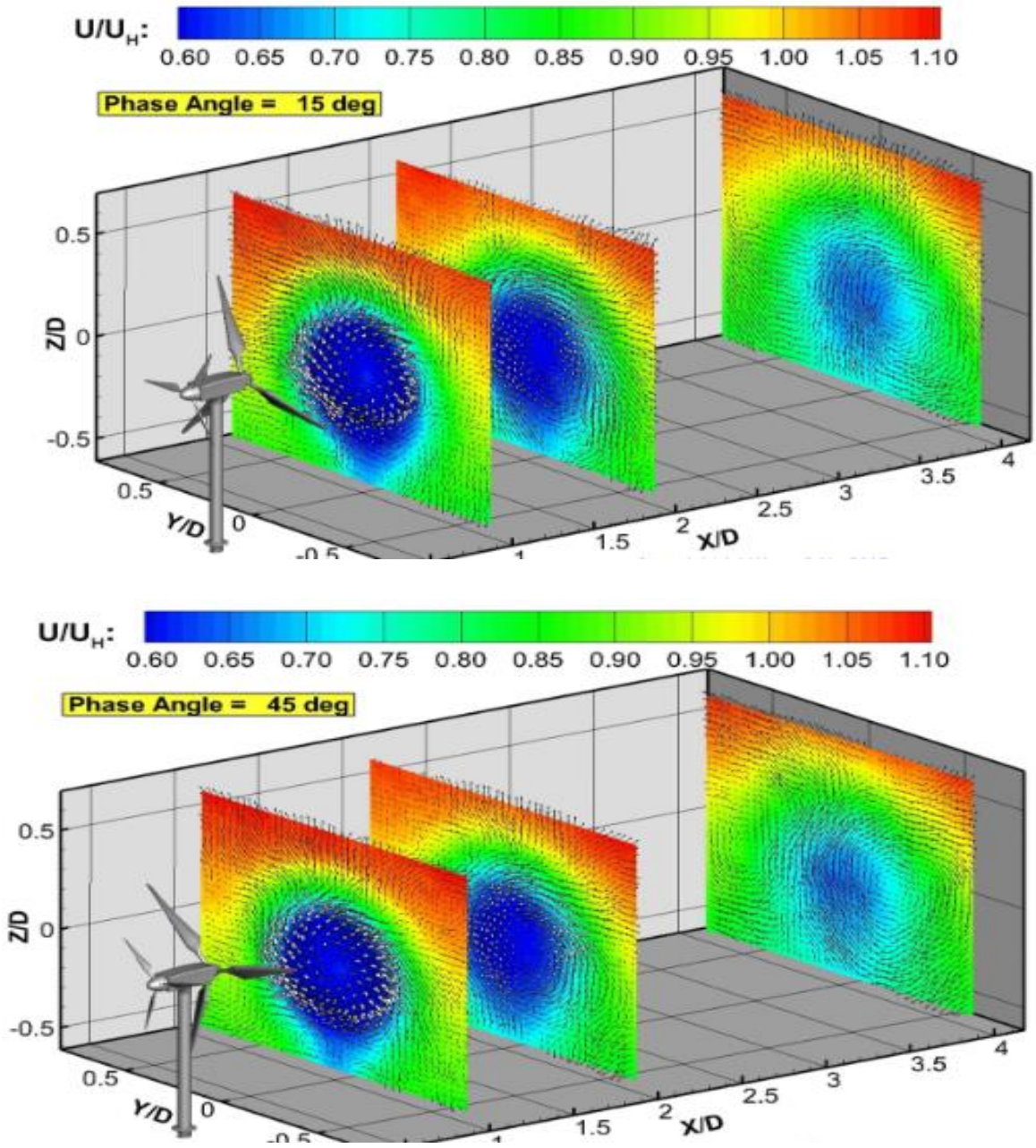

Figure 4-13 Double rotor wind turbine simulation

Figure 4-13 shows the simulation of the double wind rotor wind generator considering various angles so as to ascertain its ability to capture the most wind and ensure efficiency. Tests were carried out using a 15 and 45 degree angle and we noticed that the aerodynamics of the wind turbine is still revealing many challenges, like understanding and predicting the unsteady rotor blades performance, dynamic stress and aero-elastic response of the blades. Moreover, the wind turbines often subjected to complicated environmental conditions, such as atmospheric turbulent flow, ground effects, spatial and directional variation in wind shear. Hence, the understanding of these environmental phenomena and their impact on the wind energy

conversion process are essential for efficient exploitation of wind-energy. Recent developments have shown that the easiest way to increase power coefficient is to increase the rotor size, and develop an efficient pitch control system that could offer extended tracking of the rotation enabling efficient power generation.

4.2.1. PITCH CONTROL

In the strategy to be investigated, the turbine is controlled to operate near maximum efficiency (energy capture) in low and moderate wind speeds. At high wind speeds, the turbine is controlled to limit its rotational speed and output power. This is accomplished by forcing the rotor into an aerodynamically stalled condition. Referred to as the "soft-stall" approach, because it allows the introduction of rather benign stall characteristics for purposes of controlling maximum power. Thus, in contrast to a constant-speed wind turbine, the variable-speed wind turbine has the capability of shaping the RPM-power curve. This concept is explored in terms of its technical feasibility, rather than cost and reliability, which are the subject of future work. Figure 4-14 shows the system under consideration, with the dashed lines indicating the main control loop. The wind turbine rotor is connected to a variable-speed generator through a speed-increasing gearbox. The generator output is controlled by the power converter to follow the commanded RPM-power schedule. The generator responds to the torque command almost instantaneously.

FIXED BLADE PITCH DIAGRAM

J. F. Manwell, J. G. McGowan, and A. L. Rogers, Wind Energy Explained: Theory, Design and Application. Wiley, 2009 [Accessed 10 June 2014].

CONTENT REMOVED FOR COPYRIGHT REASONS

Figure 4-14 Physical diagram of the system

In general, a variable speed wind turbine has 3 main different operating regions: below, intermediate and above wind speed as illustrated in Figure 4-15. In a fixed pitch, variable speed, stall-regulated wind turbine, maximum power regulation below rated wind speed is regulated by changing the rotor/generator speed at large frequency range. In such a turbine, capturing the

power at a maximum value is obtained by keeping the power coefficient (Cp) at maximum peak point by maintaining the tip speed ratio (λ) at its optimum value.

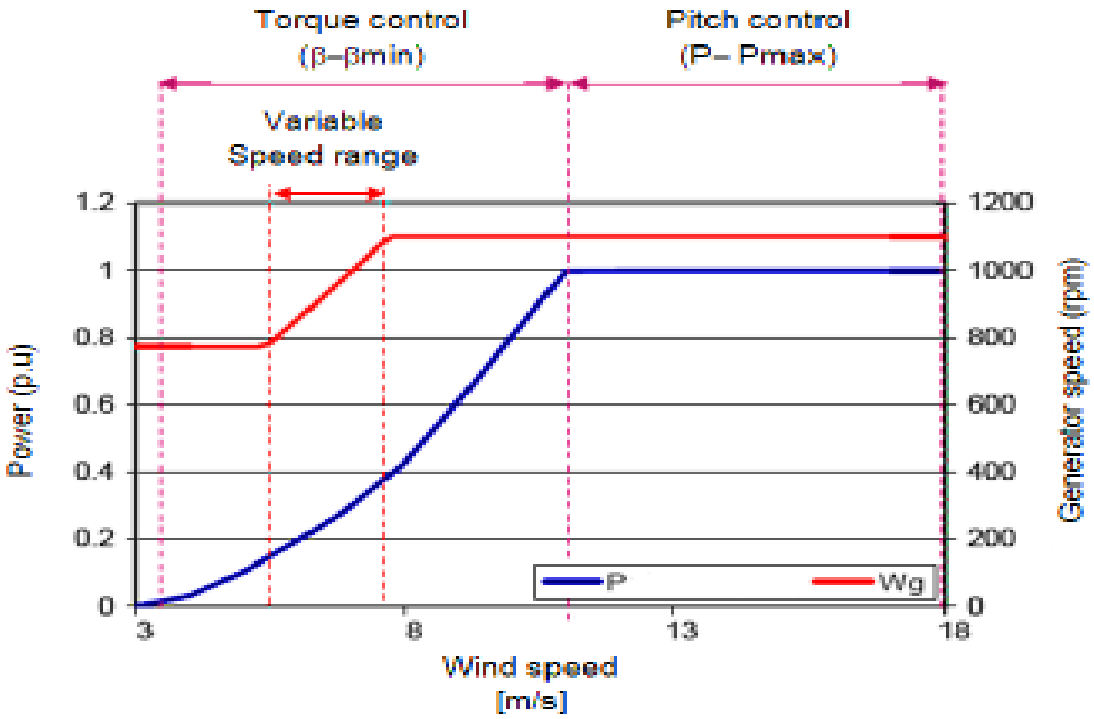

Figure 4-15 Operating regions vs. control strategies

The power (P) converted by a wind turbine is related to the wind speed as shown in Equation 16. In the present context, the equation represents net electrical power after considering the aerodynamic efficiency of the rotor blades and the mechanical and electrical system losses.

$$P = 0.5\rho ACpV3 \quad \text{..... (16)}$$

Where: ρ = mass density of air

A = area swept by the rotor blades

V = wind speed Cp = non- dimensional power coefficient

For a variable-speed turbine, the objective is to operate near maximum efficiency, where the resulting target power can be expressed as shown in Equation 2.

$$P_{Target} = 0.5\rho AC_{pTarget}\,(R/TSR_{Target})^3\omega^3 \quad \text{..... (17)}$$

Where: R = rotor radius measured at the blade tip

ω = rotational speed of the blade

The tip-speed-ratio (TSR), which is a non-dimensional tip speed, is defined as the ratio between the rectilinear speed of the blade tip and the wind speed, as shown in Equation 18.

$$TSR = \omega R/V \quad \text{..... (18)}$$

4.2.2. MODEL OF VARIABLE SPEED FIXED PICTH FOR WIND ENERGY CONVERSION SYSTEMS

A wind speed generally varies with elevation of the blades (i.e., every single spot on the turbines may not have the same speed). Modelling of both turbines speed takes into account all Different positions on the blades which could therefore be very difficult. For this reason, a single value of wind or hydro speed is normally applied to the entire turbines. Modelling the rotor blade characteristic requires the tip speed ratio (TSR) and the relationship of torque and power coefficient versus tip speed ratio. The tip speed ratio (TSR) is obtained from

$$\lambda = \lambda(v_t, \omega_t) = {}^{\omega_t R}/_{v_t} \text{ ... ...(19)}$$

where λ = tip speed ratio [rad^{-s}]
v_t = wind speed [m^{-s}]
ω_t = rotational speed [rad^{-s}]
R = blade radius [m]

The power captured by the blades, P_{turb} can be calculated by applying

$$P_{aero} = \frac{\rho}{2}\pi R^2 v_t^3 C_p(v_t, \omega_t, \beta) \text{ ... ...(20)}$$

The aerodynamic torque acting on the blades, T_a is obtained by

$$T_a = \frac{\rho}{2}\pi R^2 v_t^3 C_T(v_t, \omega_t, \beta) \text{ ... ... (21)}$$

Where ρ = Air density $\left[\text{Kg}^{-\text{m}^3}\right]$

C_p = Power coefficient [–]
C_T = Torque coefficient[−]
β = Pitch angle [degree]

Considering the following, C_p the aerodynamic torque can also be obtained from

$$T_a = \frac{\rho}{2}\pi R^2 v_t^3 C_T \ (v_t, \omega_t, \beta)/_{\omega_t} \text{ ... ...(22)}$$

Considering the above equations, C_p & C_T are functions of λ &β where β would be kept at a constant; namely the pitch angle would equally be fixed and this is generally true for small and medium sized turbines. Therefore C_p & C_T depend only on the tip speed ratio(λ)

Aerodynamic model represents the interaction between turbine and the wind stream. The performance of useful mechanical power in the wind is greatly depended on the blade profile. The efficiency of power extracted from the wind or also called as power coefficient, C_p of this kind of studied turbine has maximum power coefficient, $C_{p\ max}$ value of 0.4781 at tip speed ratio of 5.781. Tip speed ratio is the ratio between the peripheral blade speed, $\omega_r R$ and the wind speed, U. The value of power coefficient C_p is calculated by using Equation (2), whereas the tip speed ratio λ is computed by using Equation (18). Equation (19) and (20) then are used to calculate the aerodynamic torque, T_{aero} and aerodynamic power, P_{aero}.

4.2.3. MATHEMATICAL MODEL OF THE DRIVE TRAIN

The modelling of the turbines drive trains considers the aerodynamic torque principles of the turbine which in theoretical terms is a non-linear function of the turbines rotation with respect to the tip speed ratio and the pitch angle. Considering the intended design of the wind turbines and the application of a double fed wind turbine system, stability is of high essence, hence the linear relation of the tip speed ratio, the pitch angle and the rotational speed could be analysed using the non-linear torque function taking into account the Taylor series theory

$$Taylor\ series\ theory\ =\ \Delta T_a = \theta \Delta v_t + \gamma \Delta w_t + k\Delta\beta \dots\dots\dots\dots\dots (23)$$

Considering the linearization of the tip speed ratio, the pitch angle and the rotational speed, the linearization around the operating point is literally the product of the derivative of the aerodynamic torque and that of the wind speed as the wind speed is considered the disturbing factor. The application of the pitch control allows the linearization and the control of the turbine using the linear coefficient k and the tip speed ratio λ and the pitch angleβ. The aerodynamic control torque can then be written as

$$\Delta T_a = \theta \Delta v_t + \gamma \Delta w_t \dots\dots\dots\dots\dots\dots\dots\dots (24)$$

The modelling of the drive train can be considered as a single weight with the assumptions that there is little or no interaction between the drive train itself, the tower dynamics of the turbine and gravitational force has no impact on the turbine blades leading to further excitation. The aerodynamic torque of the drive train henceforth could be define as

$$T_a = [J_t.\omega_t] + [B_t.\omega_t] + T_g \ldots\ldots\ldots\ldots\ldots\ldots\ldots\ldots (25)$$

Where J_t is the Inertia of the turbine [kg / m^2]

B_t Is the Frictional coefficient of turbine [N.s / m^2]

T_g Is the Generator Torque [N. m]

The rotational speed $\omega_t = \frac{1}{J_t}\left(T_{aux} - T_g\right);\ T_{aux} = T_a - [B_t.\omega_t] \ldots\ldots\ldots (26)$

Figure 3-33 represents the drive train model of wind turbine system. In the drive train model, the difference between low speed shaft and the high speed shaft is shown by the gearbox ratio.

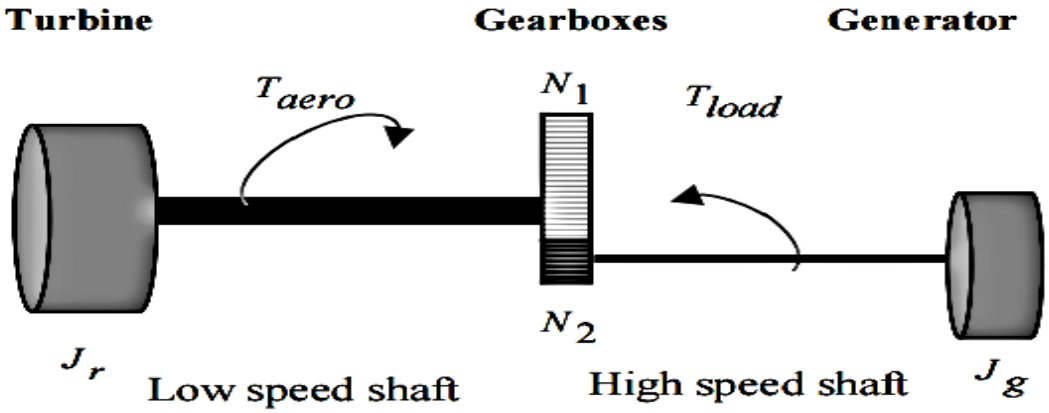

Figure 4-16 Drive Train Model

The drive train model is developed by using the simplest equation of motion to avoid the complex analysis where only rotational inertia is considered. The effects of damping and twisting angle of the shaft are ignored. In wind turbine system, unbalance torque occurs when turbine torque is dissimilar with the generator torque. As a result, shaft is accelerating or decelerating. The equation of motion for this rotation can be described as in the equation below

$$j\frac{d\omega_m}{dt} = T_{acc} = T_{aero} - T_{load} \ldots\ldots\ldots\ldots\ldots (27)$$

Where

J = moment of inertia of turbine and generator, kgm2 m

ω = Angular velocity of the rotor, rad/s

t = Time, s acc

T = Accelerating or decelerating torque, N.m

T_{aero}= Aerodynamic torque, N.m

T_{load} = Load torque or generator torque, N.m

Jr = rotor inertia

Jg = generator inertia

G = gearbox ratio

4.2.4. CLOSED LOOP SCALAR CONTROL

The main objective of this paper is to keep the power at the rated value,P_{rated} .It is where the tip speed ratio operated between the optimum value, λopt at 5.781 and λmin at 2.408, when wind speed reaches 12m/s up until 20 m/s. Then, from Equation (8) to (11), we can obtain the maximum power available in the wind by applying the foolowing

$$P = \frac{1}{2}\rho\pi R^5 C_{pmax}\frac{\omega r^3}{\lambda_{opt}^3} \ldots\ldots\ldots\ldots (28)$$

An effective way to change the generator speed for squirrel cage induction generator wind turbine with fixed number of poles, is to change the frequency of the applied voltage. With this adjustable frequency drive, the fixed frequency supply voltage is able to convert to a continuous variable frequency, thereby allowing a proportional change in synchronous speed and rotor speed. Equation (14) shows the relationship between flux, applied voltage and frequency of the machine. $\boldsymbol{E_1 = 4.44\emptyset \int N\,1}$

A closed-loop scalar control that was used to achieve this goal as shown in Figure 3-34. From the figure, it shows that the generator speed, ωm which is measured by a tachometer will be compared with the demanded generator speed, ωm*. The demanded generator speed is obtained from the demanded (optimum) rotor speed, ωr_dem which is calculated by using Equation (18), when λ vary between 2.408 or power coefficient vary from max Cp at 0.4781 to min C p at 0.1032. Then, the error of these speeds is entered into a PI controller. The result of PI control is the reference value of slip speed, ωsl* where this reference slip speed can be limited in the constant value even though the frequency and the voltage of the stator are varied. For the purpose of stability, it is necessary to ensure that the reference slip speed must be smaller than the critical slip speed. This is important because if the slip speed is larger than the critical slip speed, the current will become too large and hence will lead to overheat of the generator.

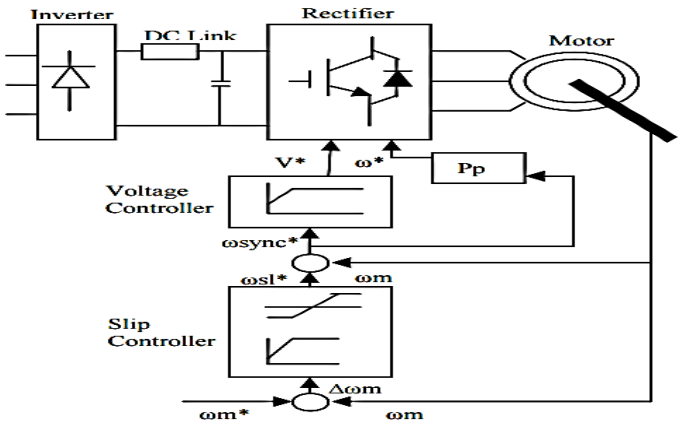

Figure 4-17 Scalar controlled drive system with slip speed controller

Then, the estimated reference slip speed, ωsl* is added with the current value of the generator speed to calculate the new reference of synchronous speed, ωsynch*. With new ωsynch*, the stator's reference voltage and the stator's reference frequency can be estimated. All mentioned speeds are in the unit of rad/s. These two variables are then fed into the generator side converter or also known as inverter. For variable speed drive, there are two types of inverter which is called as voltage source inverter (VSI) or current source inverter (CSI). VSI is more common used in the industry than the CSI. By using VSI, the six-step or pulse width modulation (pwm) inverter can be used. However, the detail modeling of the inverter is not covered since this part concerns mostly in the grid interface side.

4.2.5. PITCH CONTROL IMPLEMENTATION

$$\text{It is given: } \lambda = \frac{\omega_t}{v_t} R \text{ and } T_a = \frac{\frac{\rho}{2}\pi R^2 v_t^3 C_p}{\omega_t} \dots\dots\dots (29)$$

$$\text{Then; } C_p = \frac{2T_a}{\rho\pi R^2 v_t^3}; \text{ but } \frac{\omega_t}{v_t} = \frac{\lambda}{R}; \text{ Therefore,}$$

$$C_p = \frac{2T_a\omega_t}{\rho\pi R^2 v_t^3} = \frac{2T_a}{\rho\pi R^2 v_t^2}\frac{\lambda}{R} = \frac{2T_a}{\rho\pi R^3 v_t^2}\lambda$$

The above equation expresses C_p as a function of λ

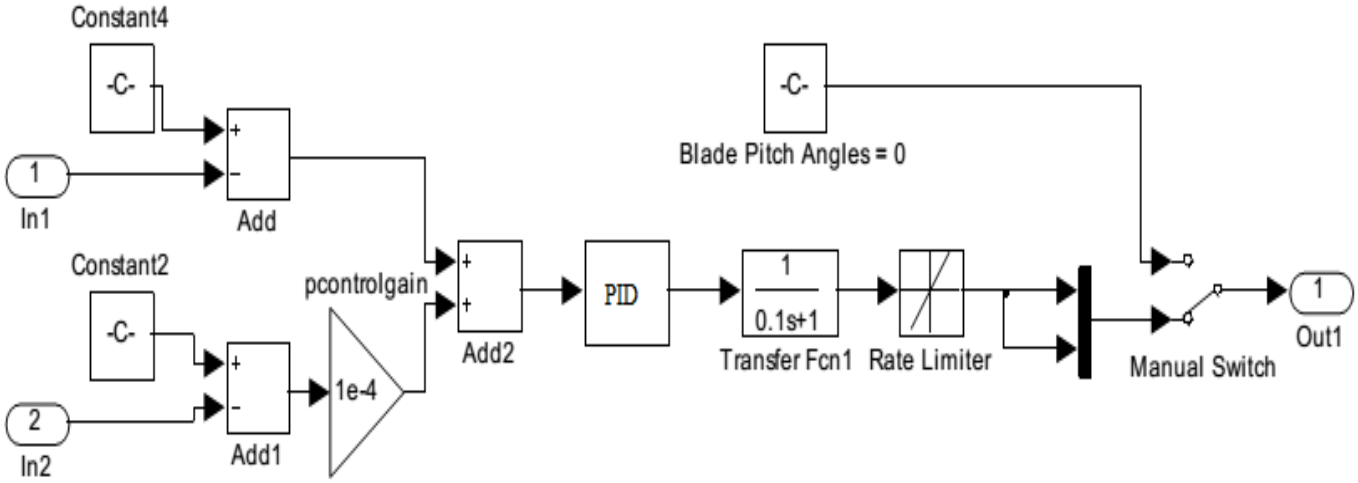

Figure 4-18 Pitch control system

The PID block settings are shown below. Essentially, a PI control is implemented. The results for the simulation are also shown for different values of pitch angleβ. From the results, it is

seen that the power coefficient C_p varies with the tip speed ratio λ but is also variant with the pitch angle. Optimal value here was 0.43.

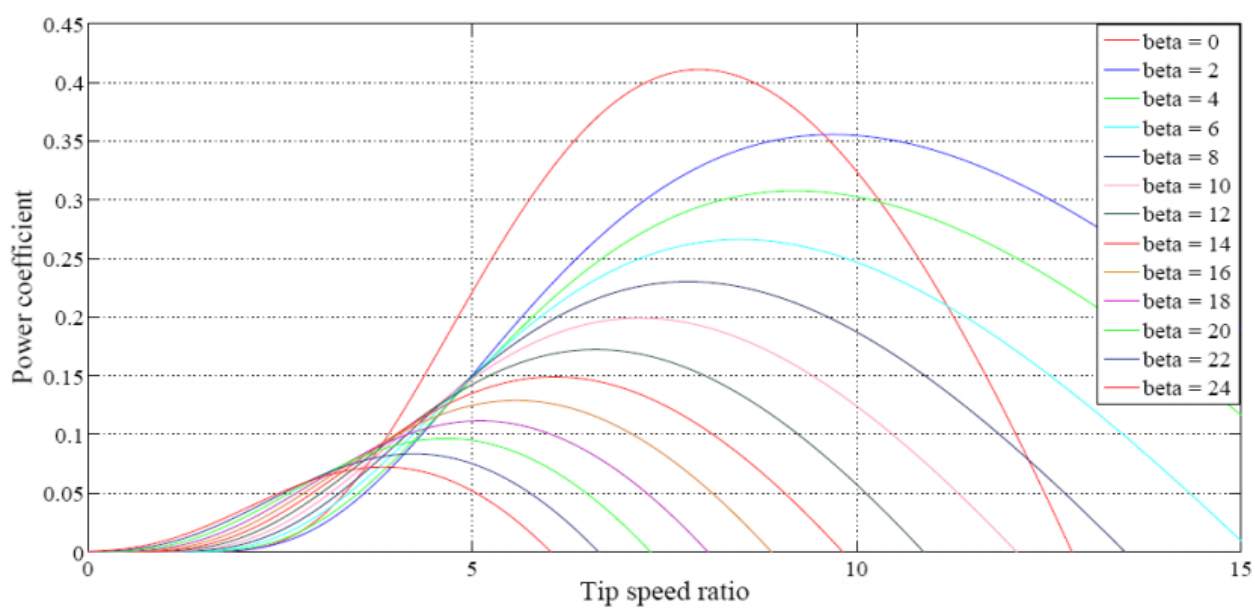

Figure 4-19 Pitch controlled angles

4.3. CONTROL SYSTEM FOR HYDRO POWER GENERATION USING PID CONTROLLERS

In reaction turbines such as overshoot wheels, Kaplan turbines, the vertical turbine configuration directly is considered an advantage as it causes rotation to be faster but inversely impact on the cost of the runner and alternator. To control the speed of the above mentioned wheels and turbines, Proportionality-Integration-Derivative controller is used in the governing system. The basic block to control a speed of a hydraulic system are: governing system, servo system, hydraulic system and turbine dynamics.

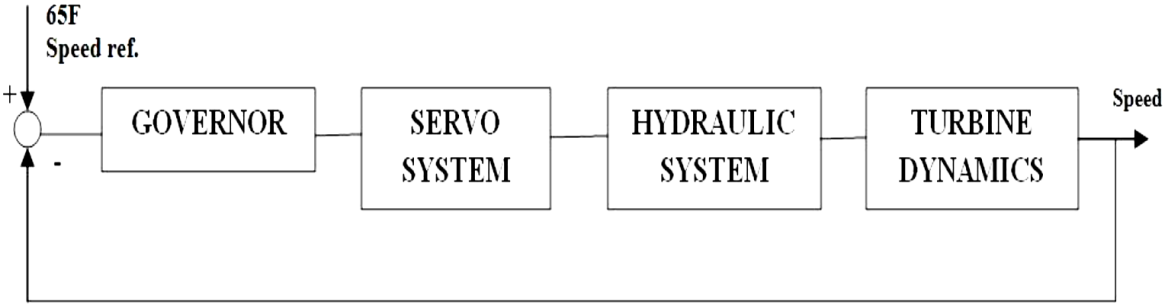

Figure 4-20 Speed control block diagram of Hydraulic systems

The main function a governing system is to control the network frequency on an isolated electrical network. This constant frequency can be brought into account if the speed is constant. The governor in a hydraulic system changes the rate of flow of water bringing the speed to a

constant value. This then provides a balance between the input and output stage of the system. Since the flow of water in small hydro increase or decrease depending on the river condition or water intake, the chance of disturbance is more. It is therefore imperative to minimise error through the Proportionality-Integration-Derivative controller used in the governor control. Figure 4-21 shows the dynamic of the PID controller where the D mode reacts fast to the change in input to the controller, I mode leads the error to zero value by increasing the control signal and P mode takes suitable action to control the error. This modes help to determine the change in water speed from its rated value thereby implementing a control mechanism to make the speed constant whilst eliminating oscillations. Stability of the system is improved by the Derivative mode which enables an increase value of gain K and also decreases integral time constant, thereby controller response speed increases.

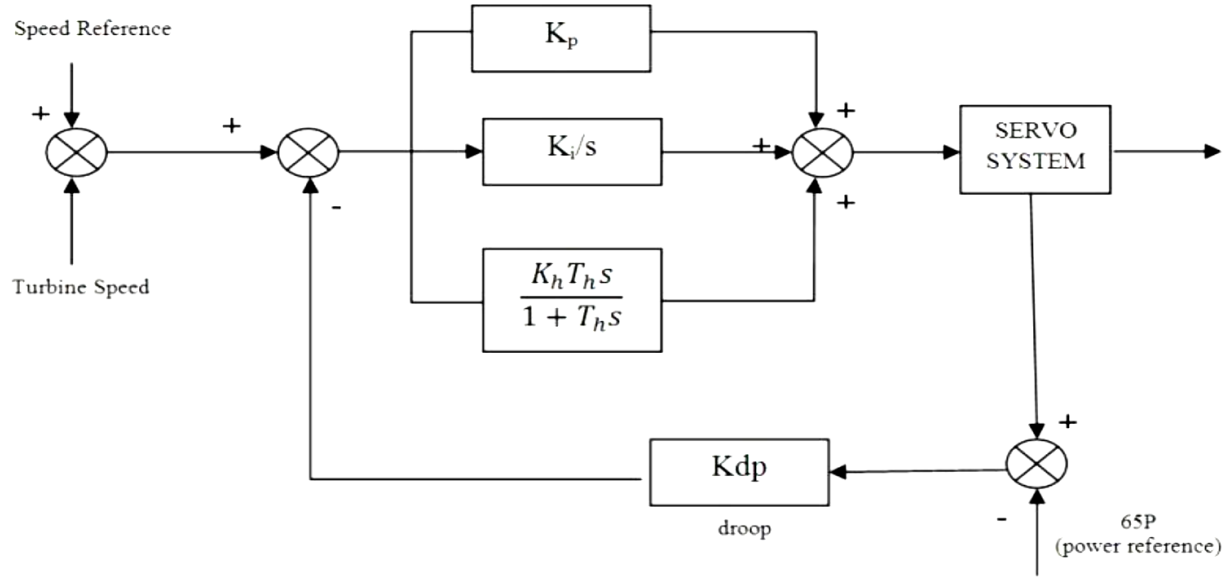

Figure 4-21Hydro PID control system

As it can be seen on figure 4-21, a servo system representing the brain of the controller is used. A servo system consist of a controller, amplifier, motor and a position sensor. The servo system receives signal from governing system. These signal are amplified and electric current is transmitted to the servo motor to produce motion which is proportional to input signal. The position sensor report the actual status of the motor. This position is compared with the input value. Any deviation in the system is identified by Proportionality-Integration- Derivative controller which responds fast to any changes at the input stage.

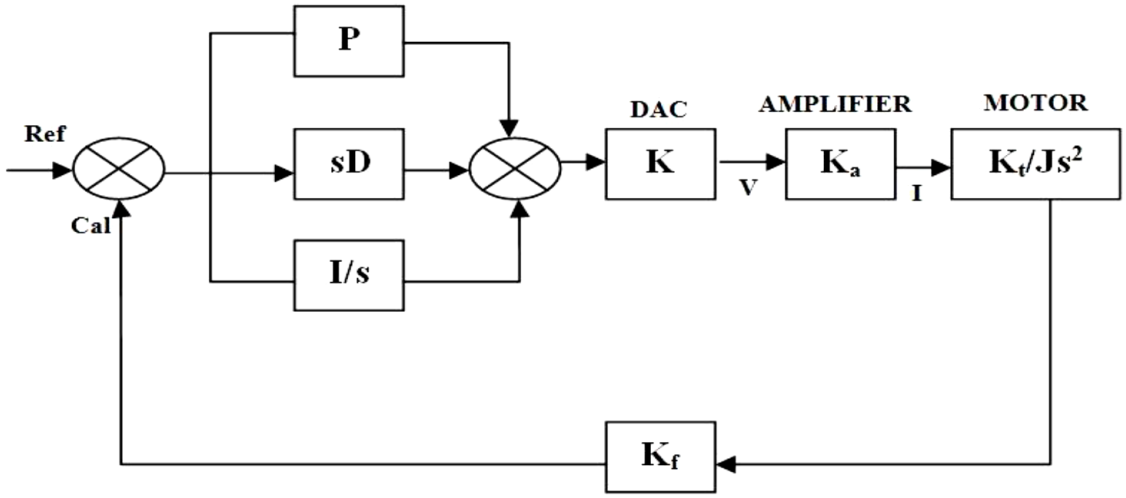

Figure 4-22 simplified diagram of the Servo system controller

- **For the servo system**

In the PID controller, the transfer function F(s), related to x number of output to "e" position error is

$$F(s) = \frac{x}{e} = P + sD + \frac{1}{s} \dots\dots\dots\dots\dots\dots (30)$$

Where

P = Proportionality gain of the controller
D = Derivative gain
I = Integral gain

In Amplification mode, the input voltage V is directly proportional to the output current

$$I = K_a V \dots\dots\dots\dots\dots\dots (31)$$

Then, Torque produced will be,

$$T_a = K_t l \dots\dots\dots\dots\dots\dots (32)$$

Where K_a is the proportionality constant,

K_t Is the Torque constant

When the total moment of inertia of load and motor is J, and T_f is the opposition friction, then total torque produced in the system is,

$$j\alpha = T_a + T_f \dots\dots\dots\dots\dots (33)$$

The angular acceleration, α is

$$\alpha = \frac{d\omega}{dt} \dots\dots\dots\dots\dots (34)$$

$$\text{Where } \omega = \frac{d\theta}{dt}$$

Taking Laplace transform of equation (18) and (19)

$$\omega = \frac{\alpha}{s} \; and \; \theta = \frac{\omega}{s} \ldots\ldots\ldots\ldots (35)$$

If T_f is negligible, substituting equation (33), and solving for θ

$$\theta = \frac{1}{S^2}\frac{K_t l}{J} \ldots\ldots\ldots\ldots (36)$$

Solving Equation (36) in equation (31), the servo system motor equation obtained is

$$\frac{\theta}{V} = \frac{K_a K_t}{JS^2} \ldots\ldots\ldots (37)$$

The encoder gain represented by K_f is equal to the number of units of feedback per one radian for a single rotation. For number of turns "n" the encoder gain will be obtained as

$$K_f = \frac{2^n}{2\pi} \ldots\ldots\ldots\ldots (38)$$

- **For the Hydraulic turbine model**

The hydraulic turbine equation for input torque changes is given as

$$\Delta U = \frac{k_1 + k_2 T_W s}{1 + k_5 T_W s}\Delta Y + \frac{k_3 + k_4 T_W s}{1 + k_5 T_W s}\Delta N \ldots\ldots\ldots (39)$$

$$k_1 \; and \; k_5 \; are \; constants \; defined \; by$$

$$k_1 = \frac{\partial U}{\partial Y}$$

$$k_2 = \left(\frac{Q}{2H} - \frac{N}{2H}\frac{\partial Q}{\partial N}\right)\frac{\partial U}{\partial Y} + \left(\frac{N}{2H}\frac{\partial Q}{\partial N} - \frac{U}{H}\right)\frac{\partial Q}{\partial Y} \ldots\ldots\ldots (40)$$

$$k_3 = \frac{\partial U}{\partial N} \ldots\ldots\ldots (41)$$

$$k_4 = \frac{Q}{2H}\frac{\partial U}{\partial N} - \frac{U}{H}\frac{\partial Q}{\partial N} \ldots\ldots\ldots\ldots (42)$$

$$k_4 = \frac{Q}{2H}\frac{\partial U}{\partial N} - \frac{U}{H}\frac{\partial Q}{\partial N}$$

$$k_5 = \frac{Q}{2H} - \frac{N}{2H}\frac{\partial Q}{\partial N} \ldots\ldots\ldots\ldots (43)$$

Where Q stands for the discharge
N stands the turbine speed

H stands for the turbine head
Y stands for the Gate position
U stands for the Torque

The hydraulic turbine equation makes mention of T_w which is basically the water inertia time constant

$$T_w = \frac{Q_n}{gH_n}\frac{L}{A} \dots\dots\dots(44)$$

Where Q_n stands for the rated discharge
H_n Stands for the rated head at the turbine entrance
L stands for the Penstock length
A stands for the cross section Area
g stands for the acceleration due to gravity
The Turbine model is represented in terms of torque and speed by ΔT *and* ΔN

$$\Delta N = \frac{\Delta U}{T_m S} \dots\dots\dots(45)$$

$$T_m = Mechanical\ starting\ Torque = \frac{\pi G D^2 N^2}{120 g U_n} \dots\dots\dots(46)$$

Where U_n stands for the rated Torque at rated speed
GD^2 Stands for the flywheel effect

$$GD^2 = \frac{1800PT}{\epsilon N^2} \dots\dots\dots(47)$$

Where P stands for the rated power
T stands for the time closure of the wicket gate
ε Stands for the coefficient for the incremental permissible speed

$$\varepsilon = \frac{\Delta N}{N} \dots\dots\dots\dots(48)$$

Figure 3-10 shows the implementation of the hydraulic turbine control system which we will test under various conditions as shown in table 1-3 below

Table 4-1 PID governor constant

Gov.	**PD**
K_p	5.0
T_h	.01
K_h	0.1
K_i	10.0
Kdp	0.04

Table 4-2 Servo system constant values

K_p	**20**
K_d	0.1
K_i	1
k	0.0488
K_a	0.5
K_t	0.1
J	0.004
K_f	565

Controller	PID
Y	0.72
K1	0.72
K2	-0.8
K3	-1.4
K4	-0.22
K5	0.76

Table 4-1 Turbine model constant

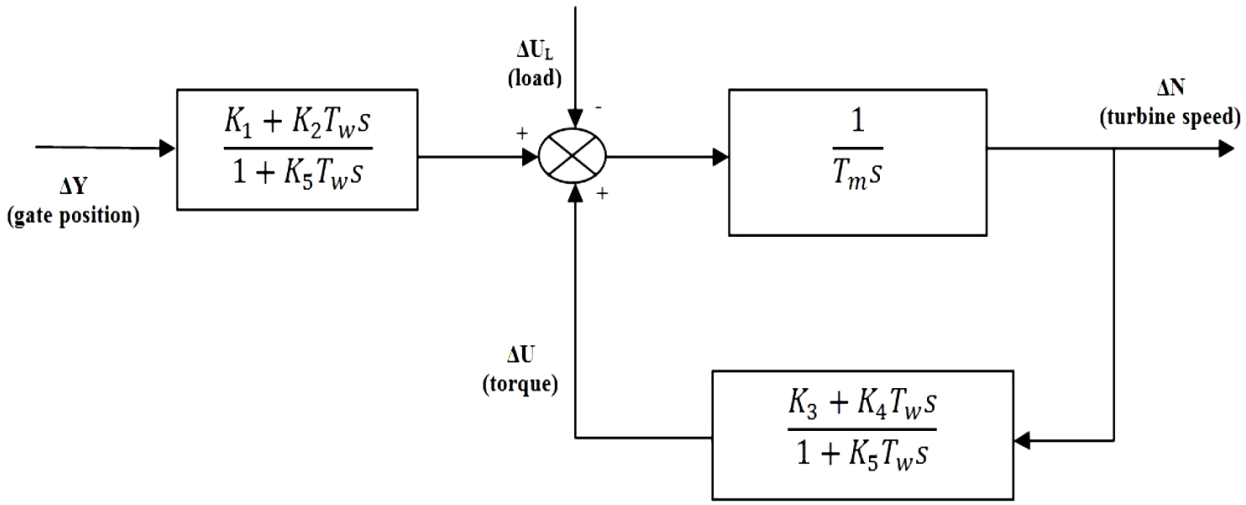

Figure 4-23 Implementation of the Hydraulic turbine system control

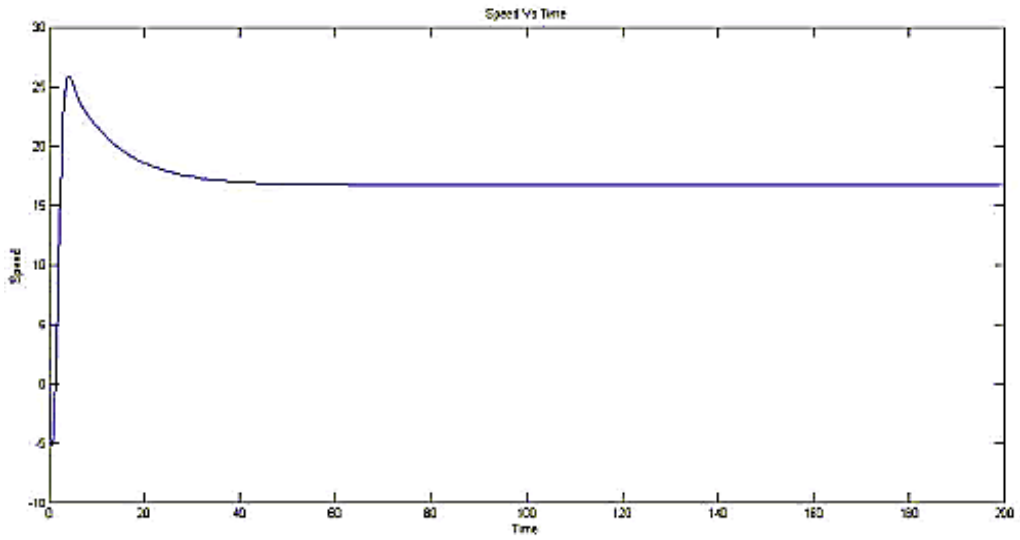

Figure 4-24 Speed versus Time for PID Servo system

Figure 4-24 shows the sharp rise in speed as soon as the servo system is applied to the system input. The application of the PID controller reacts quickly to the changes at the input stage and provide a constant speed control thereby responding to the changes. The controller brings back the speed to a constant value and the amplifier amplifies the signal avoiding the oscillation in the speed characteristic.

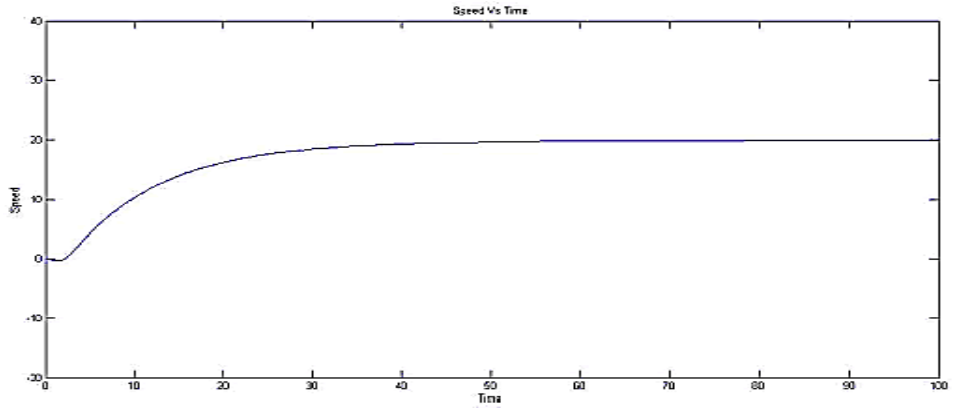

Figure 4-25 Speed Versus Time controlled graph

Figure 4-25 shows the speed versus time controlled when the PID controller is implemented. It shows that the speed becomes constant after only 30 seconds and factors such as losses and over speed are significantly controlled and reduced due to the low setting time and the controlled frequency regulated due to speed control

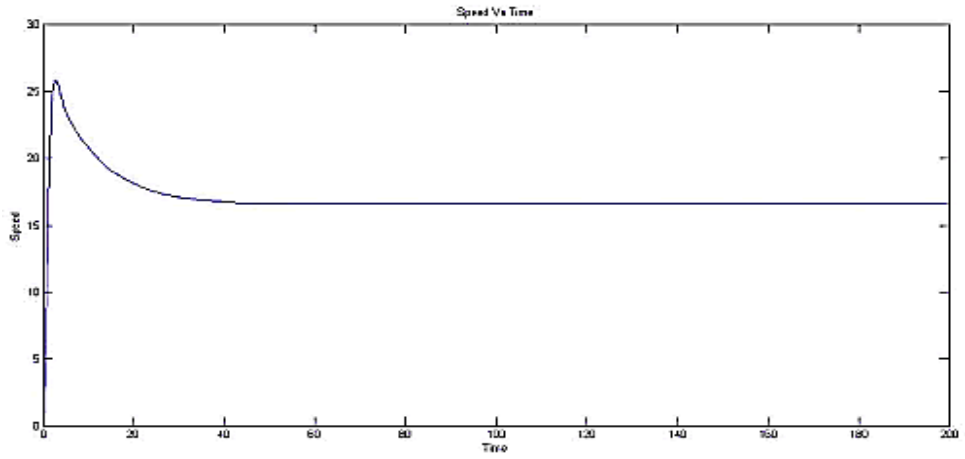

Figure 4-26 Speed versus Time in application of the PID governing system

The speed is brought back to a constant value after a sudden rise in value. This rise in speed is due to sudden force of water exerted on the turbines. Presence of permanent droop compensator determines the amount of output change in response to a change in unit speed and compensates it.

4.4. PHOTOVOLTAIC SYSTEM

The conditions for Photovoltaic (PV) cell measurement are standardized for comparison purposes but may not reflect actual operating conditions. Considering a review of few literatures, the best PV cell efficiencies are estimated at 24.2 % and the highest efficiencies devices demonstrate few practical limits without regards to cost or manufacturing considerations hence a simulation of the PV cells at average testing conditions were carried out and presented with an average output voltage of 22.5 volts at a temperature ranging from 0◦ to 25◦C.

PV Temperature & Output Voltage Analysis

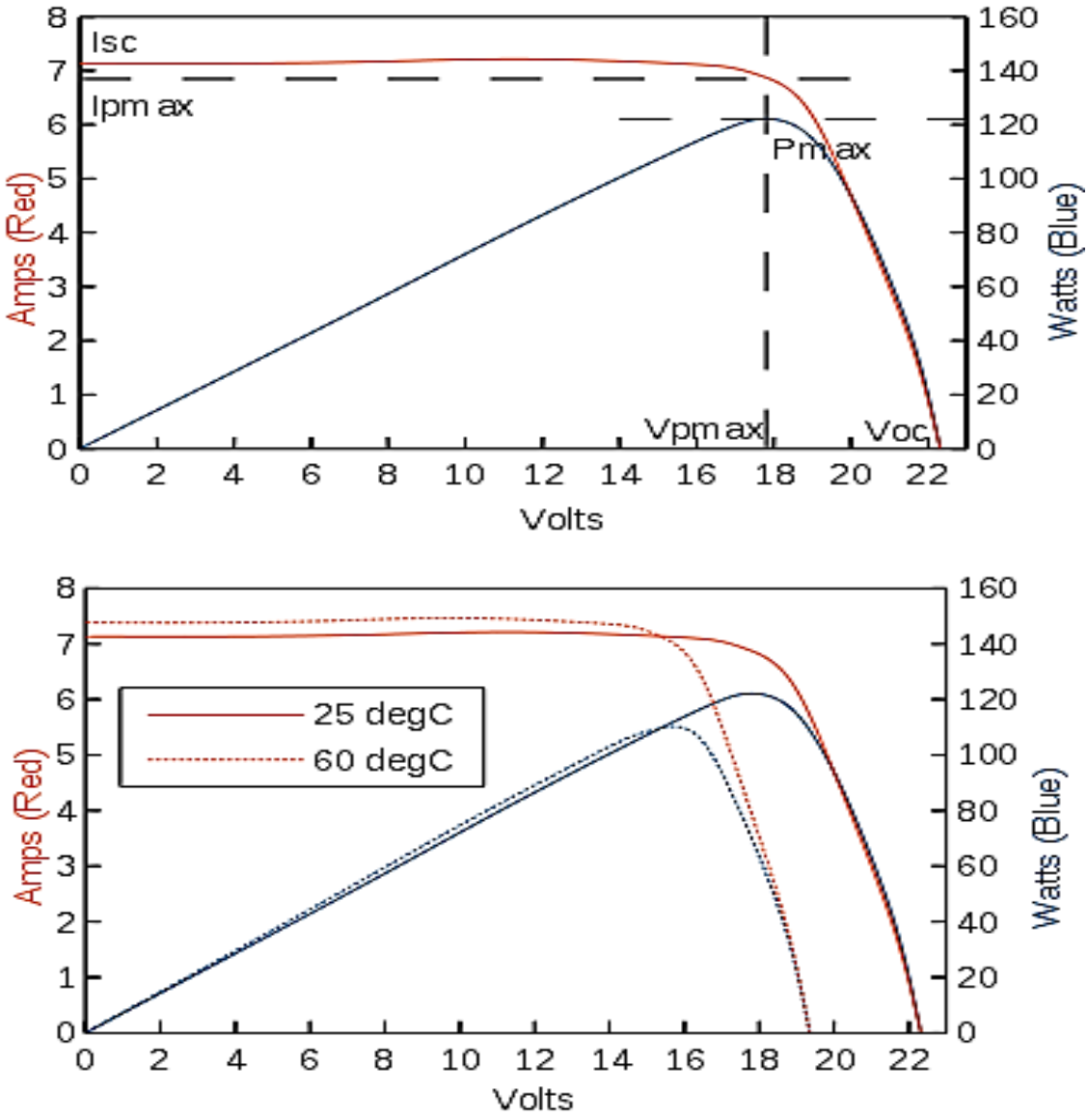

Figure 4-27 PV cell Temperature and irradiance variance test

Figure 4-27 shows the evaluation of the solar panel under ideal testing conditions, considering the voltage output and the power generated. It can define a single PV cell to produce approximately 3.15 Amps which is quite ideal for a micro power generation system.

Photovoltaic systems are systems made up of solar panel which converts light emitted from the sun to electrical energy. Each panels used is rated by its own unique DC output power. Currently the best commercial solar panel efficiency is around 17.4%. PV system output for micro scale power system can be expected to be around 24 V and upwards depending on cell sizes and irradiance. Considering our intended 3D design, a sample panel was chosen for which the technical details would be used to define its efficiency and a MATLAB/ Simulink simulation would be carried out to evaluate its output. These data would be used for the Practical design of the 3D unit

Table 4-2 PV cell Technical data

Technical details		
Cell Material		Mono Crystalline
Maximum power		20 watts
Nominal voltage		12 volts
Maximum voltage		17.6 volts
Open circuit voltage		21.8 volts
Maximum current		1.14 Amps
Short circuit current		1.25A
Maximum system voltage		600 volt
Dimensions	length	24 ½ inch
	Width	10 ¾ inch
	Thickness	1 inch
Glass thickness		3.2 mm
Maximum wind resistance		65 m/s -145 MPH

The technical details of the solar panel provided are ideal for micro power generation considering the maximum power output and the current magnitude. In order to define the

system efficiency, it would assume that the power supply needed is for 2 x 20 watt bulbs and a fan of 20 watts.

Considering a 4 hour back up time,

$$Total\ Load\ =\ 44\ h \times 40\ watts = 160 WH^{-1}\ (\ watts\ per\ hour)$$

Measure battery Ampere needed for the Load

$$Current\ (I) = \frac{160}{12} = I = 13.33\ AH$$

This means that the battery needed is a 12 volts / 14 AH

Generally, a battery charging current = 10% of its AH therefore:

$$The\ charging\ current\ (I) = \frac{13.33}{10} = 1.4\ Amps$$

$$Solar\ panel\ needed\ =\ 1.4\ A\ \times 12\ volts$$

$$Therefore\ Power\ =\ 16.8\ watts$$

From these data's it can assumed that the charge controller is 12 v/ 1.4Amps

- System loss is not added to these measurements, so as recommended a 25% system loss will be added
- Solar panel = 20 watts
- Battery= 12 volts, 15 AH
- Charge controller = 12 volts / 2Amps

The efficiency of the solar panel can then be calculated Light from sun to earth surface is estimated at $1M^2$ = 1KW

Therefore:

$$Efficiency\ = \frac{Output\ power}{Input\ power} \times 100\%\ ;\ \frac{16.8}{1000} = 16.9\% \approx 17\%$$

4.5. HYDROPOWER GENERATION SYSTEM- OVERSHOT WHEEL AND KAPLAN TURBINES

4.5.1. OVERSHOT WHEEL

Hydro turbine is a rotary engine that extracts energy from a fluid flow by transferring the potential energy to electricity generation. Depending on head and water flow rate, variation of pressure and momentum causes the runner blades to rotate. This static simulation in Solidworks studies the effects of pressure and velocity of fluid flow on blades which help in improving the hydro turbine efficiency. The computational Fluid Dynamics (CFD) was used to simulate the pressure and velocity distributions on blades of hydro bulb turbine, which consists of runner with ten blades and rotating at 500 rpm, by using Fluent Software. The Large Eddy Simulation (LES) model of turbulence flow, under the practical condition of unsteady and incompressible fluid flow, was conducted in order to study the effects of blade angles on hydro turbine earlier designed and presented in appendix D1.

At the average head of 21 m, blade twist angle of 25° and the blade camber angle of 32°, the simulation was applied on varying guide vane angle at different angles of 60° , 65° and 70° respectively for comparing the maximum and minimum pressure on blades. The simulation showed that, at guide vane angle of 60° , 65° and 70° , the maximum pressures at leading pressure side are 213 kPa, 217 kPa and 207 kPa and the minimum pressures at leading suction side are -473 kPa, - 465 kPa and -581 kPa, respectively. By adjusting the guide vane angle, it clearly affects the pressure distribution and the efficiency of the hydro turbine.

The simulation is on the hydro bulb turbine which consists of five-blade runner and rotates at 500 rpm. After meshing and specification of boundary conditions, the models are exported into Fluent Mesh program. These files are imported into file case-mesh of fluent program. The following steps had been followed:

• Set up the scale of model (Grid Mode).

• Set up and define mode.

-Viscous model

-Materials

- Boundary condition

- Grid interfaces (outlet bulb and inlet Guide Vane, outlet Guide Vane and inlet rotor, outlet rotor and inlet Draft tube)

Work is done by the fluid rotating the runner at 500 rpm. Static pressure distributions on runner blades are shown in appendix D, at different guide vane angles. The contours are showing the distribution of velocity and pressure of fluid inside the turbine. According to these contours, it implies that velocity and pressure distribution in the turbine is under acceptable condition. The maximum and minimum pressures on the blades are shown in Table 4- 5

Guide Vane Angles	RPM	Static pressure	Efficiency (T)	Efficiency (CFD)
32	500	105	96.16%	90.27%
60	319.55	213	80.79%	77.65%
65	290.7	217	77.38%	69.32%
70	218.75	207	60.58%	58.69%

Table 4-3 CFD efficiency & Theoretical efficiency

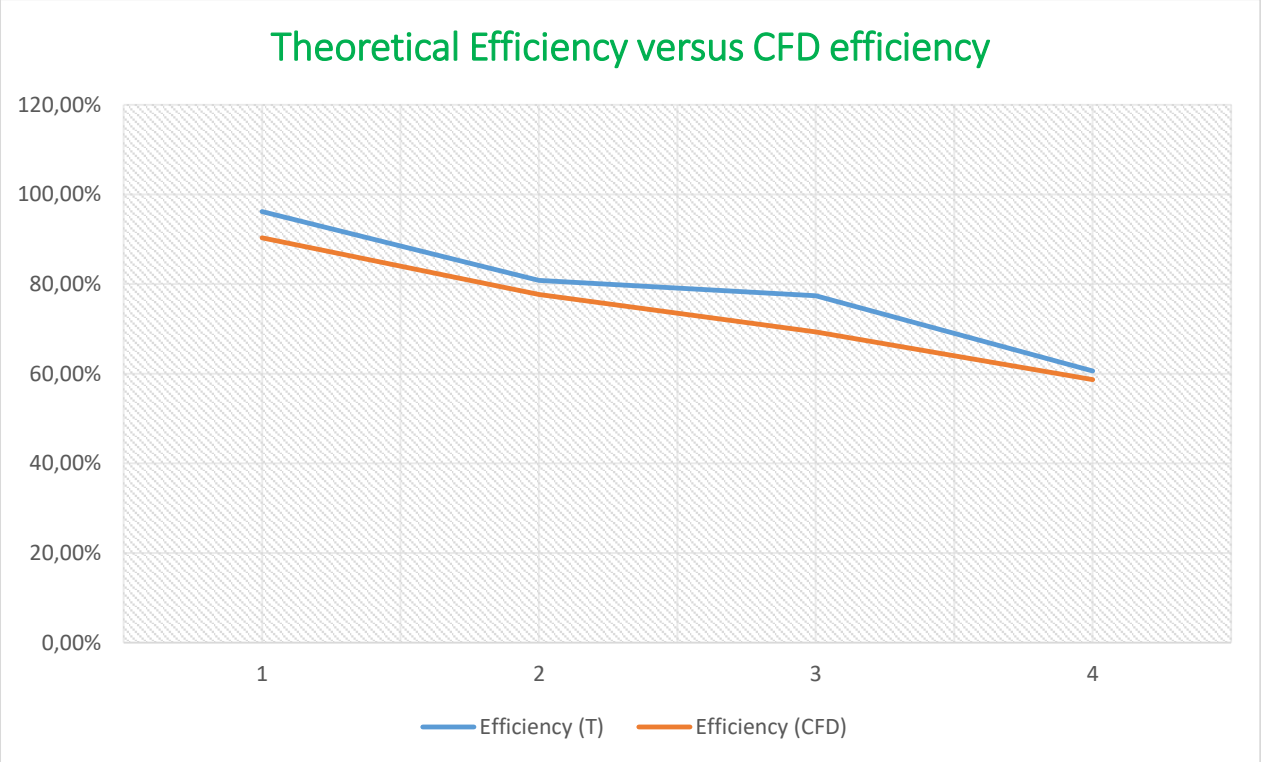

Figure 4-28 Efficiency comparison of CFD & Theoretical evaluation of Hydro wheel

Figure 4-28 graph shows the hydraulic efficiencies of the hydro systems tested under different velocity cases for theoretical and CFD. According to these graphs, it implies that the CFD and

theoretical result are very close and under acceptable conditions by the characteristics curve. These results reflected the validation of the system considering the CFD and theoretical results. The maximum efficiency regime indicated by both approaches are essentially closer to each other. The Reason behind the slight difference in efficiency computed theoretically and CFD method can be associated with human errors or to discretisation of domains and solution of differential equations in computational methods. Hence the result obtained are fairly matching, however streamlines flow in the simulation shows presence of turbulence which is due to occurrence of losses for which values are not precise at this point. Prediction of turbine performance by CFD indicates patterns of the flow behaviour inside the turbine model and the information about the intricacy of flow pattern. Considering the result obtained, the system is ideal for implementation, hence for power generation. In order to further verify this, CFD analysis and stress analysis on runner blades and guide vane blades are conducted together with fatigue analysis and factor of safety for that model. Structure analysis on the blades shows a satisfying maximum life together with a minimum potential for damages. In other hand factor of safety is at maximum implying that this model is completely safe.

4.5.2. *KAPLAN TURBINE*

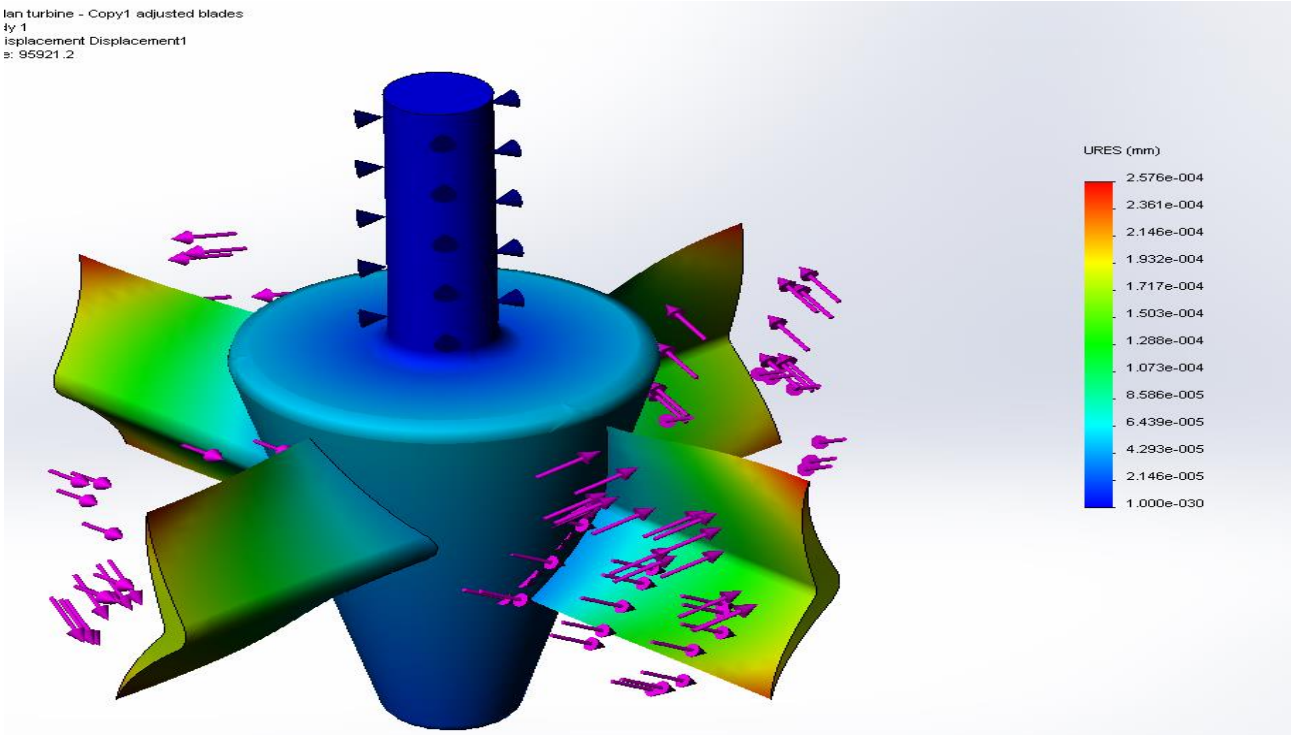

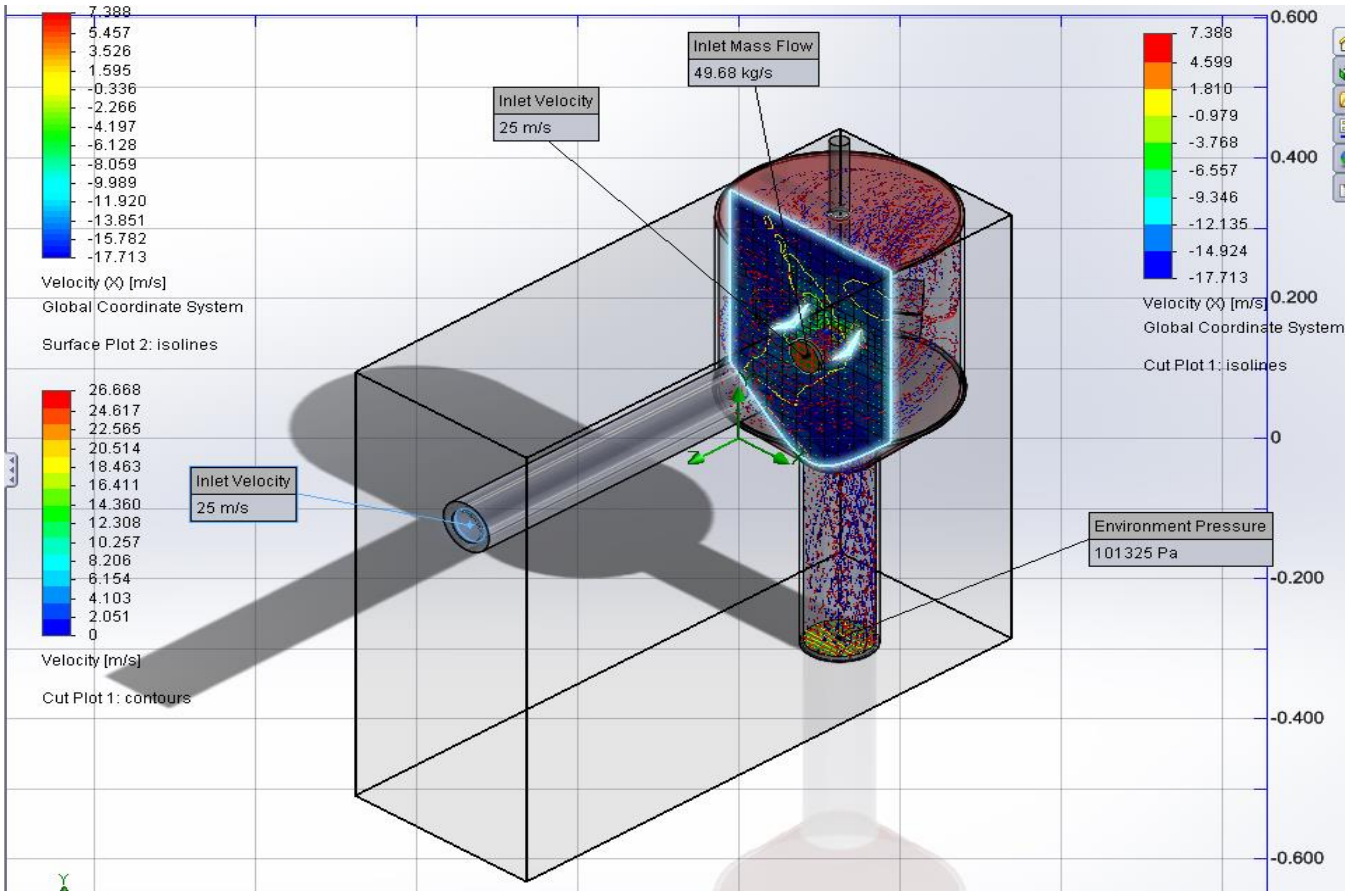

Figure 4-29 Structural and static analysis for the Kaplan turbine

Figure 4-29 shows static simulation run on the kaplan turbine. For the Kaplan turbine hydraulics a maximum efficiency of 93% (EM, 2003) could be achieved. For the purpose of an evaluation of the cavitation sensitivity of the designed runner, the Sigma value (Sigma-pHisto0.005) necessary for a guaranteed cavitation-free operation of the runner was applied. The numerical simulation results shows similar pattern for velocity and pressure variation by average circumferential area (ACA) and the distribution between hub and shroud, efficiency and also power output affected by the rotational speed of the runner. The resultant of the simulations shows static pressure fields in the volute for different Reynolds numbers. We observe that the static pressure increases with the increasing of the Reynolds numbers up to the maximum value at the volute outlet. We observe also, for the high Reynolds numbers, low pressure around the volute medium. The pressure field is almost uniform and is characterized by a strong gradient of pressure inside the region near the outlet. The volute geometry generates a dissymmetry on the pressure field inside the turbine insinuating that the static pressure is low at ring axis of the distributors. This value increases slowly up to distributor outlet. We observe

also the formation of boundaries layers showing the gradual increasing of the axial velocity from the ring axis and a gradual decreasing of the tangential velocity

Boundary wall	**Smooth with no slip**
Input boundary condition	Mass flow rate specified as 0.525 m^3/s for 35° guide vane opening 0.620 m^3/s for 40° guide vane opening 0.714 m^3/s for 50° guide vane opening
Outlet boundary condition	Specification of reference pressure at draft tube outlet as 0 atm
Stationary blade rows	Stay ring and guide vanes
Rotating blade row	Runner with rotational speed specified as 1050 rpm for 35° guide vane opening 1150 rpm for 40° guide vane opening 1375 rpm for 50° guide vane
Type of interfaces	Fluid-Fluid
Pitch change	Automatic, GGI Connection
Turbulence model	SST κ-ω model

Table 4-4 Simulation setting for Kaplan turbine simulation

Loading conditions	**Simulation Results**	**Experimental results**	**% Of error**
35° guide vane opening	89.2	91.5	2.5%
40° guide vane opening	90.3	92.0	1.8%
50° guide vane opening	88.5	90.8	2.5%

Table 4-5 Simulation and Experimental results

Figure 4-30 shows the flow velocity distributions numerically simulated and experimentally measured. They are the velocity distribution at the runner outlet. In these figures, the velocity value is normalized by the averaged axial velocity value corresponding to each operating condition, and the measure point locates 400mm downstream of the turbine centre. As for the direction of tangential velocity, the negative value designates the rotational direction of runner. It is found a satisfactory agreement between the results of numerical simulation and experiment

The efficiency obtained from numerical simulation for different guide vane openings under steady flow condition are compared with experimental results as shown in table 4-5. The efficiency obtained in case of numerical simulation is slightly higher than the experimental results because all losses may not be incorporated in numerical simulation. The high accuracy prediction method based on the whole flow passage model is applied for the study of a Kaplan turbine and the prediction accuracy is evaluated with a response surface method. As for the efficiency characteristic of a Kaplan turbine, the relation with cavitation coefficient is accurately captured by the proposed numerical method with response surface method turbulence model. The critical cavitation coefficient is predicted and the turbine efficiency breakdown is found with the pressure drop on the hub surface. As for the pressure fluctuation characteristic, RSM turbulence model is found not accurate for the prediction on a Kaplan turbine. The blade tip induced vortex is numerically damped out before reaching the runner outlet. The pressure fluctuation at the runner outlet is therefore underestimated. In essence the numerical simulation on the whole flow passage of a Kaplan turbine is carried out with proposed response surface method found sufficient to have a satisfactory accuracy on efficiency and cavitation prediction. Its accuracy replaces the burdensome preparation and cost for model test, and also facilitates future research and design works.

4.5.3. BEVEL GEAR

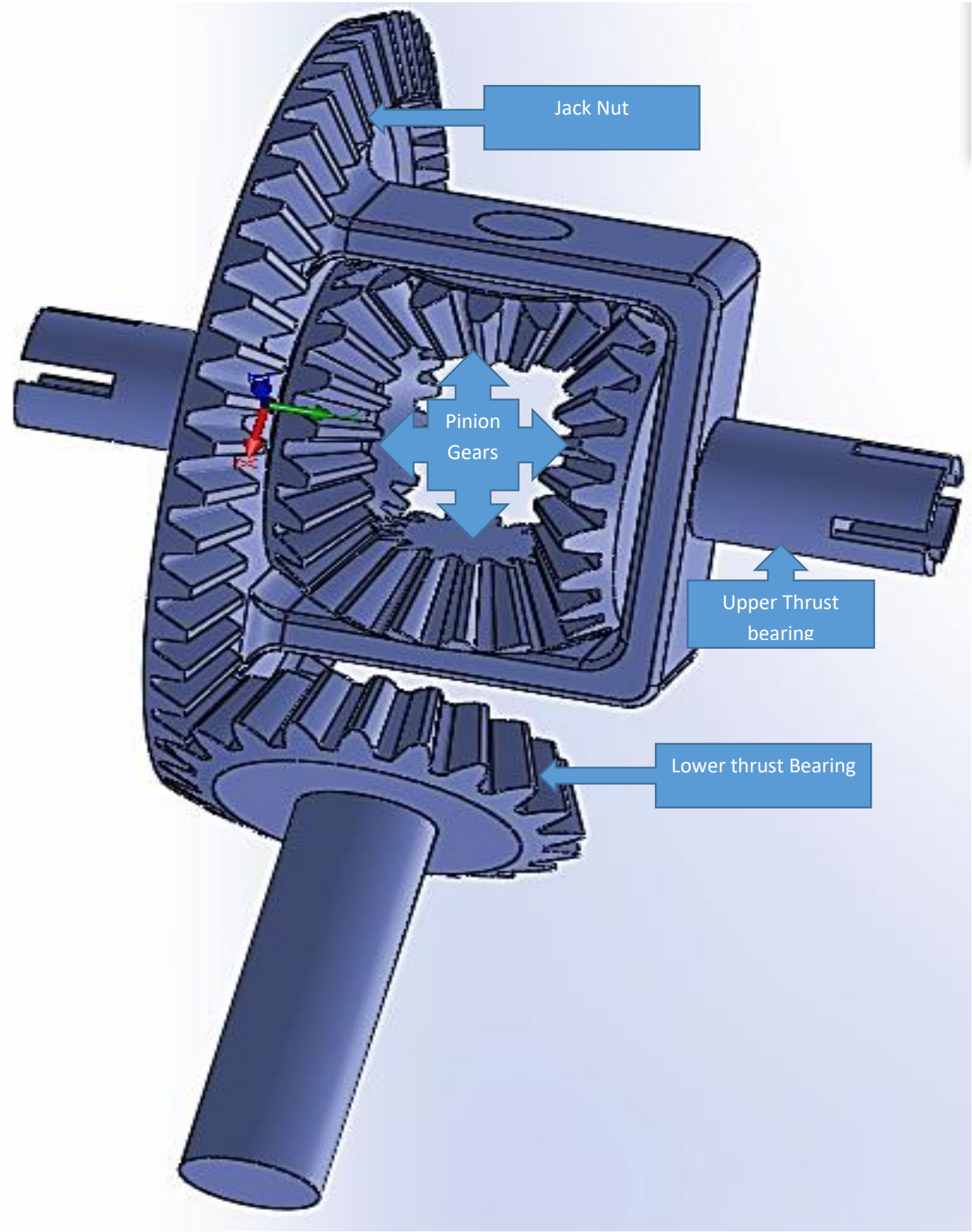

Figure 4-30 Bevel gearing system

Industrial gearboxes mainly have input shaft and output shafts for the power input and output. Input shaft are connected to the power source such as the motor via coupling and the output shaft drives the shaft that need power to be transmitted. Both input and output shafts need bearing (various types of bearings can be used based on the type of gearing and loads) supports for efficient power transmission. Bearing liners are also used to reduce the impact of bearings taking abnormal loading as opposed to liners. The objective of this design is, to strategically have a liner is that replacing a liner is cost effective as opposed to bearing and time saving process too. Further the main components include pins to hold the bearings on the planet, end caps to prevent from oil spilling from the casing. Casing (usually) in two pieces are held together via bolts. With the use of engineering analysis tools gears, for each part of the Bevel gear is designed involving sun gear, pinion and the planet. Using CES material selection tool, gear material along with gearbox casing design is carried out. Similarly like the overshot and the Kaplan turbine, the aim of using CES engineering analysis tool is to optimise the gearbox design with the aim of making the design safe. In our 3 D design, the gearbox is the main system linking the wind system and the hydro system. For this, essential considerations needs to be taken into account as the architecture of bevel gears allows for a parallel integration of both wind and Hydro systems. However, once the gearbox design is complete it is correlated to the wind blade size requirements that represents swept diameter.

Based on the assumed power requirements at 50KW for both wind and hydro systems, calculations are performed to obtain the gear teeth parameters. Considering the magnitude of power that would be transferred through the gearbox, a single stage gearbox system would suffice. Therefore, the gearbox architecture will have single input shaft, planetary gears and output shaft. The large input shaft will utilise the planets (3 gears) and act as power increaser to drive the hub on the wind turbine. The calculations of the gearing system will define the geometry for the complete rotating elements apart from the bearing selection. Bearing selection is based on the L10 hours which will usually design the bearing for one million cycles. Separate calculations are performed for bearings. Two casing designs are carried out approximately to hold the rotating elements, and are provided with horizontal mounting base plate. This will transmit the power in horizontal axis/plane. The design of gears often requires calculations that details the dimensional considerations before the gear is modelled. The design intent dimension will be used in the calculations as well to show how the values in the table are obtained. The gears involve in this design are, 1 sun gear, 4 planet gears (bevel gear) and 1 ring gear.

Sun gear: The sun gear as well as the planetary gear converts the vertical motion of a beam into circular motion within a planetary system of gearing. The sun gear used in this design will be connected to the shaft via the wind turbine. If the sun gear is in a planetary of gear train, it is regarded as a floating gear. They will have three degrees of freedom in case of planar analysis. The planetary gear on the other hand will be a set of four bevel gears and they will all be connected to a ring that will be connected to the casing and the shaft to the generator.

Module (M): The module of a gear is defined as the unit size indicated in millimetre (mm). The value is calculated by dividing the pitch (P) of the gear tooth by pie (π).

Sun gear design

The sun gear will be the gear connected to the shaft from the turbine blade and that to the generator. That is to say, the first sun gear will be connected to the shaft from the blade and the other sun gear will be connected to the shaft leading to the generator. To design the sun gear the sketch was made using the solid works to form the base of the gear, by sketching on the right plane using centre line. The base is then formed by using revolve cut feature to form the solid structure. The next stage was the formation of the second axis using right and top planes. The first plane is formed at 34.236 degree to the top plane and the second plane was formed as an offset of the first plane at 26.63mm. A sketch of the tooth is then made on the offset plane and an apex profile is mark at the midpoint of the two axis line previously formed. The lofted cut tool is used to form a half pitch of a gear tooth as shown in Appendix D4. The tooth pattern is formed by circular pattern of the lofted cut up to 22 patterns to form the sun gear teeth as shown in figure 4-10. The shaft connected to the sun gear from the blade is then extruded using the extruded boss and then a cut for the fittings is then formed using extruded cut. The images on figure D6 shows the shaft. The sun gear modelling is completed and ready for the FEA simulation. The next stage would be modelling the planet gear. The planet gears in this design had similar procedure but smaller diameter and lesser number of teeth.

The Ring gear: The ring gear in this design is the mother gear in which all the other gears will be fixed and held in place. The modelling procedure involves 10 steps. The first step was the design of the base. The sketch is made; using the revolved boss the base of the ring gear, two axes are formed in the centre using the top plane and the front plane, then the top plane and the right plane. Two planes are formed, at angle 21.80 degrees from the top plane and the other is formed as the offset of the previous plane with a distance of 53.852mm. The first tooth space width is sketched and the apex is formed at the mid-point of the two axes at distance of

44.60mm from the origin and then revolved cut is used to create the solid structure of the space width. The space width is then pattern using the pattern feature set at 50 patterns of equal space at 360 degrees on the base of the ring gear.

The next stage of the gearing system modelling was to create the structure to house the remaining of the bevel gear and to put them in place so as to avoid them falling apart. A diameter of 30mm is sketched and extruded cut at the centre of the base. Then two rectangular blocks of equal sizes are sketched and extruded by 39mm forming a diameter of 10mm. The third rectangle is then sketched and extruded by 5mm on the top to form a square box where 3 fillets are used to smoothen the sides of the rectangular beams as shown in figure 4-31

Housing is then built to enclose the gear in a cylindrical box that is made transparent so the gears are visible in the assembly. See images below on figure 4-31 show the procedure used.

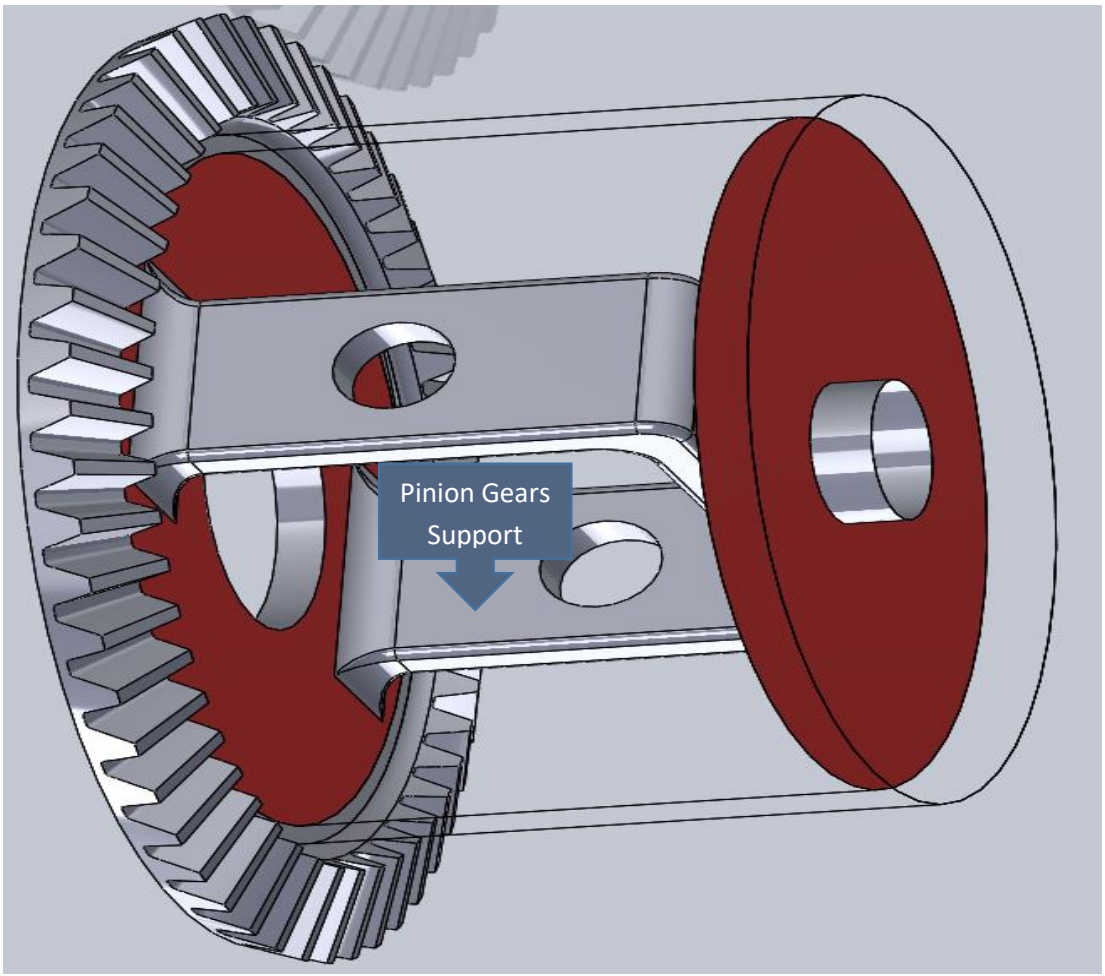

Figure 4-31 Housing formation

The housing elements was designed so as in-house the entire bevel gear unit enabling a system assembly of the 3D practical unit. Note that the ring gear has been designed as such that

additional gears could be included, if need be. However, the concept of the design is to have a simple and cost effective gear system that can transmit up to 50kw output power. From both wind and hydro systems. A unit assembly was then carried out as shown in figure 4-32 where the components of the gear system were inserted into the assembly ground and the mate used to perform the mating. There were six coincide mates and four gear mate. Two sun gears were used where the driver gear was connected to shaft from the turbine blade and the bevel gear straight to the generator. The driver sun gear is mated concisely with the sketch of the 30mm diameter of the ring gear and the bevel gear is concisely mated with the 15mm diameter on the top of the frame constructed on the ring gear. Two smaller gears are also mated on the side diameter of the frame concisely. The gear mate is used to mate the tooth of the sun gears and the planet gears. The final gear assembly is shown on the figure 4-32

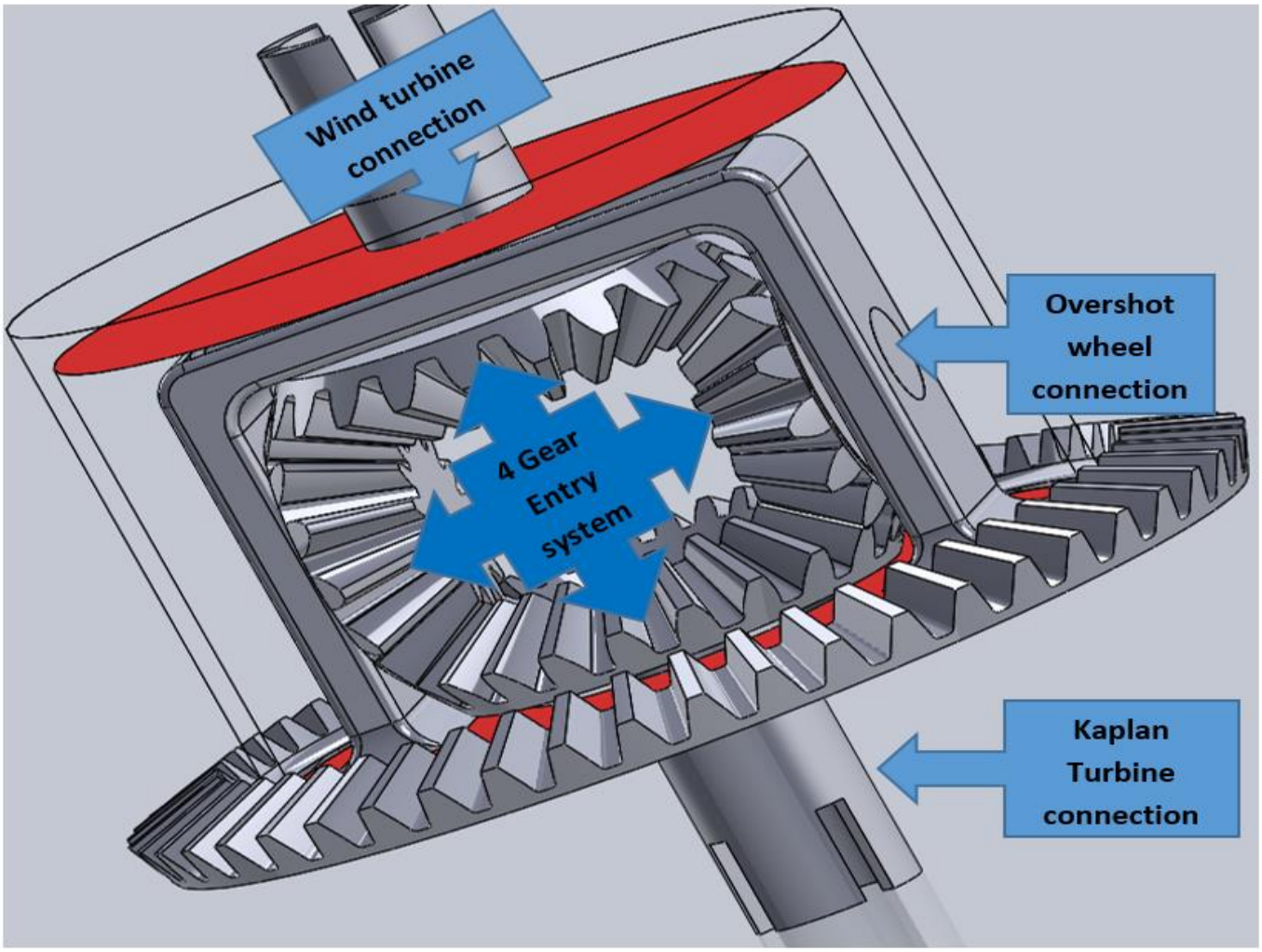

Figure 4-32 Bevel Gear systems fit for the 3D SRMPS

Figure 4-32, shows a bevel gear that has been designed and analysed using current industry standards combined with the implementation of learned methodology and test results. The gear

was designed for use in an intermediate gearbox of a medium class enabling a parallel junction of the wind and hydro system around the existing transmission components in use, specifically utilizing the current transmission housings, bearings, and seals. A detailed summary of material selection, material processing, design of gear teeth, and selection of design factors was presented in order to clarify the proper selection of certain design parameters. Upon completion of the design phase of the gear, analysis was conducted to ensure appropriate margins of safety had been implemented into the design

A bevel gear design for the overall system have been presented in Figure 4-40. The Bevel gearing system its axes and two shafts intersect and the tooth-bearing faces of the gears themselves are conically shaped. This will permit the individual rotation of both standalone Eco wheel and that of the Kaplan hydro turbine to individually rotate and direct horsepower generated to the generator. A careful analysis of the gears was done in SOLIDWORKS in order to allow a close comfortable seat and fit of the Eco wheels on the gear system.

Gear loads were calculated based on geometry of the bevel gear teeth and bearing support structure. Fatigue analysis was then conducted at the most critical sections of the gear as shown in Appendix D9-10. Margins of safety were calculated at the two critical sections and a margin of safety equal to .48 was determined insinuating that the system is very safe. Static analysis was then performed at approximately 2.5 times the endurance limit of the gear, producing a margin of safety equal to .87. A positive margin of safety was shown to provide adequate safety for operation in this application.

According to the investigation, the maximum stress of the sun gear is given as 1.495×10^{11} and the calculated allowable stress is 510.12N/mm^2. The least stress is far higher than the calculated stress as well. However, the yield strength is 6.204X10^{8}N/m^2. The displacement on the other hand shows a very high value of 3.2mm which is very high for gears of such size. The statics strain on the other hand shows similar result to the stress but the strain value is 5.324 ESTRN and it is maximum at the shaft contact to the gear and at the base of the gear and partially on the teeth. The factor of safety on the other hand is very low as compared with the calculated value. As it could be seen from the result, the factor of safety shows great safety promises and the result could be improved using another material or carrying out further design optimization on the design.

4.6. SUMMARY

Computer aided design and analysis of the front end unit of the proposed business model and 3D renewable energy platform have been carried out in this chapter. It is clearly shown that the subsystems that can control the efficiency of 3D front units can be sumarrised as follow:

Hydropower Turbine System: The design concept of the 1D Hydropower system has been completed and tested. This is comprised of a double overshoot water wheel and a Kaplan turbine for hydro turbines, Considering the Hydro power generation, the choice of turbine type, size and speed is based on the net head and maximum water flow rate, which was determined by the flow rate. The investigation into the state of the art of the hydropower technology shows that our system efficiency achieved an above average efficiency due to a better optimised design.

Wind Turbgine System: The design concept was made up of a contra rotation double wind turbine which was tested using computational fluid dynamics and a 3D Inventor modelling program using a FLUENT DDP in CFD to define the lift, drag and pressure coefficient. Initial results showed that flow conditions were steady and front rotor speed reached 600 rpm and 3.14 tip speed ratio for the rear rotor. Testing conditions shows that wind directions are of a uniform velocity. The calculation result of velocity resultant distribution along the blades showed an efficiency of about 34% at 500 rpm and 15 Nm Torque. It could then be confirmed that the methodology used for this design analysis and testing is a perfect tool for optimum blade profile where the numerical simulation was perfectly correlated for preliminary design in order to have estimated design and testing characteristic of contra rotation blade span.

2D i.e. Dual Hydropower and Wind Turbgine System system arragement: The initial results showed the importance of the approach and its smart grid application advantages. It also demonstrates the challenges that should be considered prior to building the system for reel field test. The system architecture allows for a dual renewable energy to be generated which is directly fed into the storage “battery” thereby acting a standby energy storage for meeting losses in the network with surplus power fed straight into LPN (local public network). Both active and reactive power shows that power compensation within the network is efficiently managed with the capacitive bank therefore we can then conclude that the behaviour of our 1, 2D and 3D renewable energy platform is deal for meeting the research aim.

These results provide a framework, with plausible technical recommendations and factors to be considered when the 3D proposed renewable energy system is adopted by Togo's energy sector.

CHAPTER 5

CHAPTER 5- COMPUTER AIDED DESIGN AND SIMULATION OF THE BACKEND OF SYSTEM OF THE PROPOSED RENEWABLE ENERGY PLATFORM

5.1. INTRODUCTION

This chapter focuses on three main aspects

I- The System back end with a presentation of the proposed 3D renewable energy platform, its system design, Architecture, Static simulation of the Wind and Hydro systems and parts using SOLIDWORKS

II- The System Middle end focusing on the introduction of the use of the multilevel inverter for the design and development of a 3D platform to fully utilise Togo's Renewable Energy resources into their smart grid power system infrastructure as some its features and abilities would enable extremely low distortion for the output voltage

III- The system front end represented by a friendly HMI system displaying power generated and load feeding to the grid

5.1.1. BACKEND-OF-SYSTEM

The presentation of the proposed 3D renewable energy platform and its system design; covers the components of the design and development of the 3D renewable energy platform using SOLIDWORKS, with a detailed explanation focusing on how the systems was assembled together with static simulation of the assembled system. It also looks at the laboratory facilities and elements of the practical unit assembly that will be used and proposes the technical and economic advantages the design. The presentation of the proposed 3D platform and its system design would present mechanical elements of the system with static simulations run on the hydro system and the wind system. The importance of this simulation is to present the mechanical agility of the entire 3D platform and relate simulation results to earlier feasibility studies carried out in the literature review. This also presents the overall effort invested in investigating the advantages of recent advances on design of hydro power generation namely hydro turbines and wheels and wind turbines. One of the objectives of this research was also to conduct the necessary computer simulation using CAD software that will entail simulation of the two of the three renewable energy sources (Wind-Hydro). The objectives of the

simulation will be to evaluate the power generation ability of both wind and hydro systems and confirm earlier technical evaluations carried out in the literature. This is to say that the derivatives of this simulation will represent a vendor-neutral dynamic simulation models for both fixed- and adjustable-speed for wind and hydro systems. In other words, these models simulations validate the 3D renewable energy platform through which power and control system for a combined renewable energy power system would be designed, tested and validated. The Power and control system studies fit for such models are designed to:

- Determine operating strategies and power transfer limits
- Investigate the stability of the system following disturbances (transient stability) or incremental impacts (small signal stability)
- Analyse the control of frequency and/or system voltages Thus it is very important that the models used in the above analysis be accurate.

5.1.2. FRONT END OF SYSTEM

This section introduces the function and topologies of multilevel inverter technology which has emerged as an alternative methodology in the area of high-power medium-voltage energy control. It therefore introduces the use of the multilevel inverter for the design and development of a 3D renewable energy platform to fully utilise Togo's green Energy resources into their smart grid power system infrastructure as some its features and abilities would enable extremely low distortion for the output voltage and lowerdv/dt; They draw input current with very low distortion, generate smaller common-mode (CM) voltage through sophisticated modulation methods, and eventually eliminates CM voltages.

The section is structured as such that

- A comparison of conventional inverters to new multilevel inverter topologies are examined and reported.
- A Review of Multilevel inverters based on Diode clamped; flying capacitors and cascade multilevel inverter is examined so as to define the best level of inverters needed for our design.
- A study of Control techniques based on sinusoidal pulse width modulation method, the selective harmonic elimination and space vector modulation method which are all studied so as to define the most ideal approach for our design

- A focus on Selective Harmonic Elimination considering it has low switching losses, minimum total harmonics at the output is also studied with a focus on Generic Algorithms, Newton Raphson method, Particle Swarm Optimization theories which also advocates for an efficient method in multilevel inverter controls
- A review of the IET regulations based on the [IEEE-519 standard] providing recommendations for total harmonic voltage and current distortion limitations to be ≥ 5% would be reviewed so as to ascertain which level of inverters could deliver total harmonic voltage and current distortion limitations to be ≥ 5% thereby respecting the [IEEE-519 standard] condition in view of which the design of the multilevel inverter would be finalised with appropriate simulations.

5.1.3. CONVENTIONAL INVERTERS VERSUS MULTILEVEL INVERTER

This section introduces the function and topologies of multilevel inverter technology which has emerged as an alternative methodology in the area of high-power medium-voltage energy control. It therefore introduces the use of the multilevel inverter for the design and development of a 3D renewable energy platform to fully utilise Togo's green Energy resources into their smart grid power system infrastructure as some its features and abilities would enable extremely low distortion for the output voltage and lowerdv/dt; They draw input current with very low distortion, generate smaller common-mode (CM) voltage through sophisticated modulation methods, and eventually eliminates CM voltages.

The chapter is structured as such that

- A comparison of conventional inverters to new multilevel inverter topologies are examined and reported.
- A Review of Multilevel inverters based on Diode clamped; flying capacitors and cascade multilevel inverter is examined so as to define the best level of inverters needed for our design.
- A study of Control techniques based on sinusoidal pulse width modulation method, the selective harmonic elimination and space vector modulation method which are all studied so as to define the most ideal approach for our design
- A focus on Selective Harmonic Elimination considering it has low switching losses, minimum total harmonics at the output is also studied with a focus on Generic Algorithms, Newton Raphson method, Particle Swarm Optimization theories which also advocates for an efficient method in multilevel inverter controls

- A review of the IET regulations based on the [IEEE-519 standard] providing recommendations for total harmonic voltage and current distortion limitations to be ≥ 5% would be reviewed so as to ascertain which level of inverters could deliver total harmonic voltage and current distortion limitations to be ≥ 5% thereby respecting the [IEEE-519 standard] condition in view of which the design of the multilevel inverter would be finalised with appropriate simulations

5.1.4. CONVENTIONAL INVERTERS

In conventional inverters mainly PWM inverters are used to obtain a controllable voltage (K. Jang-Hwan et al, 2008). The two level inverter is a circuit which consists of sources with some amount of voltage and many switches for controlling voltage or current. In high power and high voltage applications the conventional two level inverters is used, however, have some limitations in operating at high frequency mainly due to switching losses and constraints of the power device ratings (S. Buso, 2006).

Conventional inverters have many limitations in high-voltage and high-power applications like poor power quality, high voltage stress, EMI/EMC issue etc. (S.-K. Sul, 2010). In recent years, multilevel inverters (MLI) have been introduced as alternative controllers for high-power applications due to their ability to control and smoothen more than two voltage levels at the input and output waveforms that has lower dv/dt and lower harmonic distortions. Series and parallel combination of power switches are used in order to achieve the power handling voltages and currents (P. N. Enjeti, 2011).

In the conventional two level inverters the input DC is converted into the AC supply of desired frequency and voltage with the aid of semiconductor power switches. Depending on the configuration, four or six switches are used. A group of switches provide the positive half cycle at the output which is called as positive group switches and the other group which supplies the negative half cycle is called negative group. Some new approaches have been recently suggested such as the topology utilizing low-switching-frequency high-power devices, complex circuits can often seen in two level inverter circuits, due to its complexity and cost also increases.

Their performance is highly superior to that of conventional two-level inverters due to reduced harmonic distortion, lower electromagnetic interference, and higher dc link voltages. By using conventional method, the performance of the inverter is low. In this paper a new topology with

reversing voltage component is suggested to improve the performance of multilevel inverter. This topology requires fewer components and therefore the cost and complexity is low.

Power inverters available on the market today vary greatly in efficiency and output type. Generally, of higher end inverters, the output waveforms seen are either pure sine or modified sine. Another characteristic which determines the quality and price of an inverter is the power output in Watts (P inverters, 2015). Intelligent Inverters are currently available on the market. Microchip Technologies provides a detailed list for the functions of an intelligent inverter

- Digital On/Off control for low standby power
- Power supply sequencing and hot-swap control
- Programmable soft-start profile
- Power supply history logging and fault management
- Output voltage margining, Current fold back control
- Load sharing and balancing
- Regulation reference adjustment
- Compensation network control and adjustment
- Full digital control of power control loop
- Communications for status monitoring and control
- AC RMS voltage measurement, Power factor correction

They are designed for both grid-tie and off the grid applications. They operate much like uninterruptable power supplies (UPS). The main goal is be able to supply power to a load directly from a main power source, be it a generator (RE sources) or a wall outlet while available and continue to provide constant power when that main source of power goes offline. When connected to an established power grid (i.e., where the frequency and voltage are actively regulated), inverters typically operate as controlled current sources. This means that the high frequency switching of the inverter is controlled so that the output current from the inverter is actively forced to follow a reference signal. The design of the feedback control system that accomplishes this may differ from one manufacturer to another, but with an optimum design the output current control can be extremely fast (<1 ms response) and accurate (<1%). Furthermore, the control response can be practically unaffected by disturbances in the grid voltage.

The controlled output current of an inverter has several important implications:

As seen from the grid, the "impedance" of the inverter is very high. As a result, the inverter output current continues to follow the internal reference signal, even when power system faults cause large changes in voltage. This is generally true for positive- and negative sequence components. Most inverters provide a three-wire native output from their power electronics to an ungrounded winding on an isolation transformer, so they do not influence the zero-sequence component of output current. Thus the apparent zero-sequence impedance seen from the grid is a combination of the zero-sequence impedance of the isolation transformer plus the effect of any neutral grounding impedance. With alternative inverter topologies, it is possible for the inverter to also control the zero-sequence component, but the extra equipment expense is rarely justified. The high output impedance of an inverter is quite different from the case of a rotating synchronous machine generator, which can contribute relatively large transient output currents under fault conditions. It is important to note that, although an inverter acts as a current source with high output impedance, it also has a limited maximum output voltage available. In other words, it will not present "infinite" voltage at its terminals if an upstream feeder breaker is suddenly opened while the inverter is running. The maximum output voltage is in fact determined by a combination of the inverter DC terminal voltage and the action of the control system

The output current is limited. The internally generated current reference signal takes account of prevailing voltage variations to maintain a required power output, but it is always subject to an over-riding current limit that corresponds to the level of current needed to output rated kVA at the minimum specified working voltage, usually 0.9 per-unit (p.u). This means that with a properly designed control system, the output current from an inverter during a grid fault should not exceed approximately 1.1 p.u. In most cases, a 1.1 p.u fault contribution from distributed generators should be negligible in relation to the conventional fault contribution fed from the transmission system. Add to this the consideration that the inverter output currents are largely in phase with the system voltage, whereas the conventional fault currents are largely in quadrature, and it is safe to say that inverters contribute a negligible amount to the total fault level on a distribution feeder.

The output current can be reduced to zero in an extremely short time. If necessary, the native output current from the inverter bridge can be stopped in a few microseconds (followed by some short-lived [<1 cycle] decaying transients between the output filter and the grid). This can be very important for the protection and management of the distribution system. If the

utility is concerned about circuit breaker capacity, provisions can be made for the output current from an inverter-based generator to be stopped well before any mechanical switchgear starts to operate. In this situation, the inverter controls can autonomously initiate rapid shutdown when abnormal grid conditions are sensed, or the controls can respond to a signal from the utility (e.g., a transfer trip).

The complex (apparent) output power ($\boldsymbol{S = P + jQ}$) ***can be controlled in any of the four power quadrants.*** Because the magnitude and the phase angle of the fundamental output current relative to the grid voltage can be arbitrarily selected, the real power (P) and reactive power (Q) components of the complex output power (S) can be directly and independently controlled. The real power output is typically controlled so as to regulate another internal quantity such as the DC voltage or power generated by any RE sources. The active control of real power also allows important over-riding real-power-limiting functions, such as power curtailment and power ramping, to be implemented in response to inputs received from a remotely located system operator (e.g., via supervisory control and data acquisition or SCADA). These real power management functions are expected to become essential tools for utilities under a high-penetration scenario, especially in smaller grids (e.g., islands) where the power system may not always be able to accept additional real power and where frequency regulation is a concern. Apart from the management of real power output, the inverter has unique capabilities to generate and strategically deploy reactive power output. This topic is especially important and warrants a separate in-depth discussion in the following sections. The reactive power output that can be generated by inverters at a PV, Wind, or hydro system which are valuable resource for utilities and is expected to be crucial for regulating the voltage in a distribution system with a high penetration of renewables.

The complex output power can be controlled with very high bandwidth. In most cases it is not desirable to change real power output very rapidly because of the impact on system voltage (and frequency in weaker systems). Consequently, real power changes are usually made to follow slow time ramps whenever possible. The same consideration may often be true for reactive power. However, by means of the high bandwidth control of reactive power, the inverter can also act as a fast autonomous local voltage control system. Fast automatic response is essential for correction of the voltage deviations associated with voltage flicker, for example.

The inverter can absorb real power from the grid and deliver it to charge an energy storage device connected to the DC-side collector bus (could also be fed from any RE sources type).

This can facilitate the implementation of an energy management system in which the inverter supplies real power to the grid from storage at times when RE power is not available. To achieve different objectives, the energy storage device might be relatively small (to facilitate power ramping) or very large (e.g., for frequency regulation or power output levelling).

The inverter output current can be controlled to correct pre-existing low-order voltage (or current) harmonics on the grid. In order to do this, the inverter must deliberately produce corresponding harmonics in the output current. This rather specialized "active filter" function is sometimes performed by dedicated inverters installed specifically for this purpose. To facilitate the production of controlled harmonic output currents, an inverter would ideally switch at the highest practical frequency, and it would be designed with a small output filter inductor in order to minimize the inverter voltage needed to drive the harmonic currents. In addition, because the oscillating harmonic power produced at the AC terminals must be matched by an approximately equal harmonic power at the DC terminals, it is desirable to provide a larger-than-normal DC bus capacitance in order to minimize the corresponding harmonic voltage that develops on the DC bus. It would be relatively costly to produce a PV inverter designed to simultaneously deliver real power while also serving as an active filter. However, active-filter capability might be useful when normal RE power production is very low or zero, such as during the night.

The inverter can help to correct for unbalanced fundamental voltage at the point of connection to the grid by controlling output current to include a negative sequence fundamental component. In this mode the inverter essentially acts as an active filter for the minus-one (-1) order harmonic. The negative sequence fundamental output current produces a second harmonic power pulsation at the AC terminals, matched by a similar power pulsation at the DC terminals. As in the case of the active filter, a large DC capacitance is needed to absorb this pulsating power with acceptably small DC voltage deviation. As mentioned previously, most inverters can only correct for the negative-sequence fundamental. However, using a costlier alternative inverter topology (e.g., a four-leg inverter bridge), a similar correction could be provided for the zero-sequence components in an unbalanced system.

5.1.5. MULTILEVEL INVERTERS

A multilevel inverter is a power electronic device which is capable of providing desired alternating voltage level at the output using multiple lower level DC voltages as an input. Mostly a two-level inverter is used in order to generate the AC voltage from DC voltage. Now

the question arises what's the need of using multilevel inverter when we have two, three, five, nine etc... Level inverter. In order to answer this question, first we need to look at the concept of multilevel inverter.

First take the case of a two-level inverter. A two-level Inverter creates two different voltages for the load i.e. suppose we are providing *Vdc* as an input to a two level inverter then it will provide + *Vdc*/2 and – *Vdc*/2 at the output. In order to build an AC voltage, these two newly generated voltages are usually switched. For switching mostly PWM is used although this method of creating AC is effective but it has few drawbacks as it creates harmonic distortions in the output voltage and also has a high dv/dt as compared to that of a multilevel inverter. Normally this method works but in few applications it creates problems particularly those where low distortion in the output voltage is required.

The concept of multilevel Inverter (MLI) is slightly similar to the two-level inverter. In multilevel inverters we don't deal with the two or three level voltage; but in order to create a smoother stepped output waveform, more than two or three voltage levels are combined together and the output waveform obtained in this case has lower dv/dt and also lower harmonic distortions. Smoothness of the waveform is proportional to the voltage levels, as we increase the voltage level the waveform becomes smoother but the complexity of the controller circuit and components also increases along with the increased levels.

A multilevel converter has several advantages over a conventional two-level converter that uses high switching frequency pulse width modulation (PWM). The attractive features of a multilevel converter can be briefly summarized as follows.

● ***Staircase waveform quality:*** Multilevel converters not only can generate the output voltages with very low distortion, but also can reduce the dv/dt stresses; therefore, electromagnetic compatibility (EMC) problems can be reduced.

● ***Common-mode (CM) voltage:*** Multilevel converters produce smaller CM voltage; therefore, the stress in the bearings of a motor connected to a multilevel motor drive can be reduced. Furthermore, CM voltage can be eliminated by using advanced modulation strategies

● ***Input current:*** Multilevel converters can draw input current with low distortion.

● ***Switching frequency:*** Multilevel converters can operate at both fundamental switching frequency and high switching frequency PWM. It should be noted that lower switching

frequency usually means lower switching loss and higher efficiency. Unfortunately, multilevel converters do have some disadvantages. One particular disadvantage is the greater number of power semiconductor switches needed. Although lower voltage rated switches can be utilized in a multilevel converter, each switch requires a related gate drive circuit. This may cause the overall system to be more expensive and complex.

Plentiful multilevel converter topologies have been proposed during the last two decades. Contemporary research has engaged novel converter topologies and unique modulation schemes. Moreover, three different major multilevel converter structures have been reported in the literature: cascaded H-bridges converter with separate dc sources, diode clamped (neutral-clamped), and flying capacitors (capacitor clamped). Moreover, abundant modulation techniques and control paradigms have been developed for multilevel converters such as sinusoidal pulse width modulation (SPWM), selective harmonic elimination (SHE-PWM), space vector modulation (SVM), and others. In addition, many multilevel converter applications focus on industrial medium-voltage motor drives (Rastogi, M, 2015), utility interface for renewable energy systems, flexible AC transmission system (FACTS), and traction drive systems (Peng z et al, 2010).

This chapter reviews state of the art of multilevel power converter technology. Fundamental multilevel converter structures and modulation paradigms are discussed including the pros and cons of each technique. Particular concentration is addressed in modern and more practical industrial applications of multilevel converters and in this case with the 3D renewable energy platform to fully utilise Togo's green Energy resources into their smart grid power system infrastructure as some of its features and abilities would enable extremely low distortion for the output voltage and lowerdv/dt; They draw input current with very low distortion, generate smaller common-mode (CM) voltage through sophisticated modulation methods, and eventually eliminates CM voltages. A procedure for calculating the required ratings for the active switches, clamping diodes, and dc link capacitors including a design example is equally provided.

5.2. MULTILEVEL POWER CONVERTERS STRUCTURES

As previously mentioned, three different major multilevel converter structures have been applied in industrial applications: cascaded H-bridges converter with separate dc sources, diode clamped, and flying capacitors. Before continuing the discussion on this topic, it should be noted that the term multilevel converter is utilized to refer to a power electronic circuit that could operate in an inverter or rectifier mode. The multilevel inverter structures are the focus of in this chapter; however, the illustrated structures can be implemented for rectifying operation as well.

5.2.1. Cascaded H-bridges

A single-phase structure of an m-level cascaded inverter is illustrated in Figure 5-1. Each separate dc source (SDCS) is connected to a single-phase full-bridge, or H-bridge, inverter. Each inverter level can generate three different voltage outputs, +Vdc, 0, and –Vdc by connecting the dc source to the ac output by different combinations of the four switches, S1, S2, S3, and S4. To obtain +Vdc, switches S1 and S4 are turned on, whereas –Vdc can be obtained by turning on switches S2 and S3. By turning on S1 and S2 or S3 and S4, the output voltage is 0. The ac outputs of each of the different full-bridge inverter levels are connected in series such that the synthesized voltage waveform is the sum of the inverter outputs. The number of output phase voltage levels m in a cascade inverter is defined by m = 2s+1, where s is the number of separate dc sources. An example phase voltage waveform for an 11-level cascaded H-bridge inverter with 5 SDCSs and 5 full bridges is shown in Figure 31.2. The phase voltage van = va1 + va2 + va3 + va4 + va5

For a stepped waveform such as the one depicted in Figure 31.2 with s steps, the Fourier Transform for this waveform follows (T. G. Habetler, 2015)

$$V(\omega t) = \frac{4V_{dc}}{\pi}\sum_{n}[\cos(n\theta_1) + Cos(n\theta_2) + .. + Cos(n\theta_s)]\frac{Sin(n\omega t)}{n}, where\ n = 1,3,5,7 \ldots (eq.49)$$

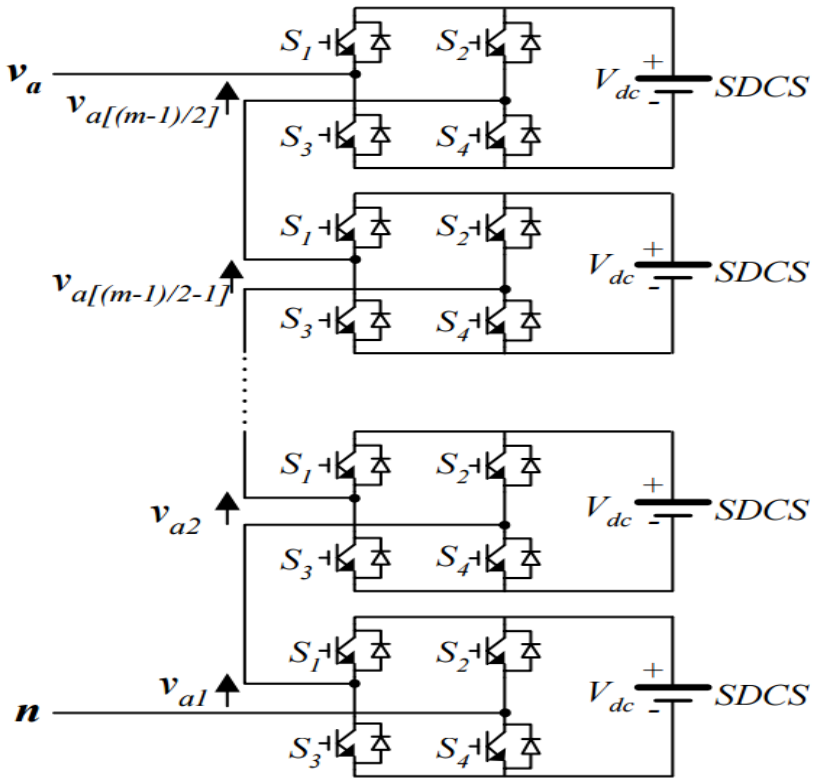

Figure 5-1 Single-phase structure of a multilevel cascaded H-bridges inverter.

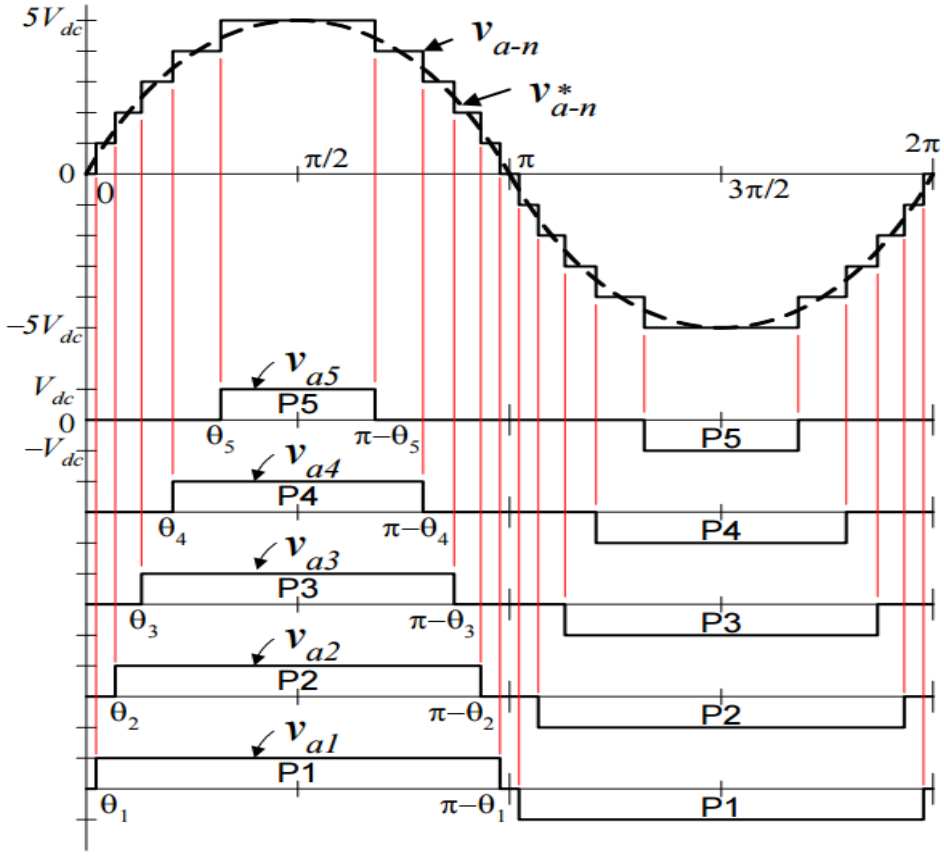

Figure 5-2 Output phase voltage waveform of an 11-level cascade inverter

From (eq. 1), the magnitudes of the Fourier coefficients when normalized with respect to Vdc are as follows:

$$H(n) = \frac{4}{\pi n}\left[\sum_{n}[\cos(n\theta_1) + Cos(n\theta_2) + .. + Cos(n\theta_s)\right]; where\ n = 1,3,5,7, \ldots (eq.50)$$

The conducting angles,θ_1, θ_2,θ_s, can be chosen such that the voltage total harmonic distortion is a minimum. Generally, these angles are chosen so that predominant lower frequency harmonics, 5th, 7th, 11th, and 13th, harmonics are eliminated (Y. Zhuang, 2011). More detail on harmonic elimination techniques will be presented in the next section. Multilevel cascaded inverters have been proposed for such applications as static VAR generation, an interface with renewable energy sources, and for battery-based applications. Three-phase cascaded inverters can be connected in wye, as shown in Figure 5-3, or in delta. Peng (2013) has demonstrated a prototype multilevel cascaded static VAR generator connected in parallel with the electrical system that could supply or draw reactive current from an electrical system (Z. Peng et al, 2013). The inverter could be controlled to either regulate the power factor of the current drawn from the source or the bus voltage of the electrical system where the inverter was connected. Peng and Joos et al (2013) have also shown that a cascade inverter can be directly connected in series with the electrical system for static VAR compensation. Cascaded inverters are ideal for connecting renewable energy sources with an AC grid, because of the need for separate dc sources, which is the case in applications such as photovoltaics or fuel cells. Cascaded inverters have also been proposed for use as the main traction drive in electric vehicles, where several batteries or ultra-capacitors are well suited to serve as SDCSs (Leon M, 2012). The cascaded inverter could also serve as a rectifier/charger for the batteries of an electric vehicle while the vehicle was connected to an AC supply as shown in Figure 5-1.

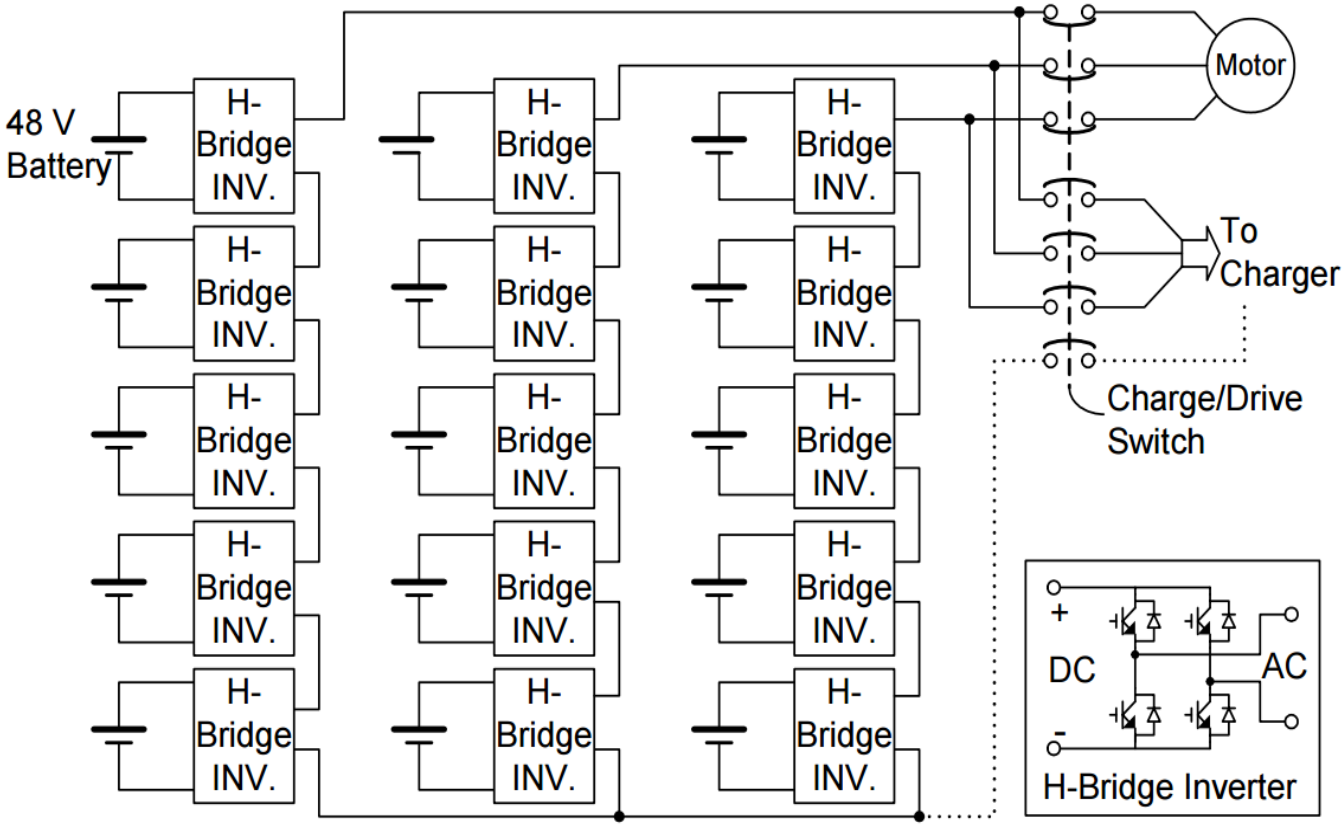

Figure 5-3 Three-phase wye-connection structure for electric vehicle motor drive and battery

Manjrekar has proposed a cascade topology that uses multiple dc levels, which instead of being identical in value are multiples of each other. He also uses a combination of fundamental frequency switching for some of the levels and PWM switching for part of the levels to achieve the output voltage waveform. This approach enables a wider diversity of output voltage magnitudes; however, it also results in unequal voltage and current ratings for each of the levels and loses the advantage of being able to use identical, modular units for each level. The main advantages and disadvantages of multilevel cascaded H-bridge converters are as follows (M. D. Manjreka, 2008).

Advantages:

• The number of possible output voltage levels is more than twice the number of dc sources (m = 2s + 1).

- The series of H-bridges makes for modularized layout and packaging. This will enable the manufacturing process to be done more quickly and cheaply.

Disadvantages:

- Separate dc sources are required for each of the H-bridges. This will limit its application to products that already have multiple SDCSs readily available.

Another kind of cascaded multilevel converter with transformers using standard three phase bi-level converters has been proposed (P. Enjeti, 2015). The circuit is shown in Figure 5-4. The converter uses output transformers to add different voltages. In order for the converter output voltages to be added up, the outputs of the three converters need to be synchronized with a separation of 120° between each phase. For example, obtaining a three-level voltage between outputs A and B, the output voltage can be synthesized by V_{ab}= Va1-b1+Vb1-a2+Va2-b2. An isolated transformer is used to provide voltage boost. With three converters synchronized, the voltages Va1-b1, Vb1-a2, Va2-b2, are all in phase; thus, the output level can be tripled (Z. Peng, 2013). The advantage of the cascaded multilevel converters with transformers using standard three-phase bi-level converters is the three converters are identical and thus control is simpler. However, the three converters need separate DC sources, and a transformer is needed to add up the output voltages.

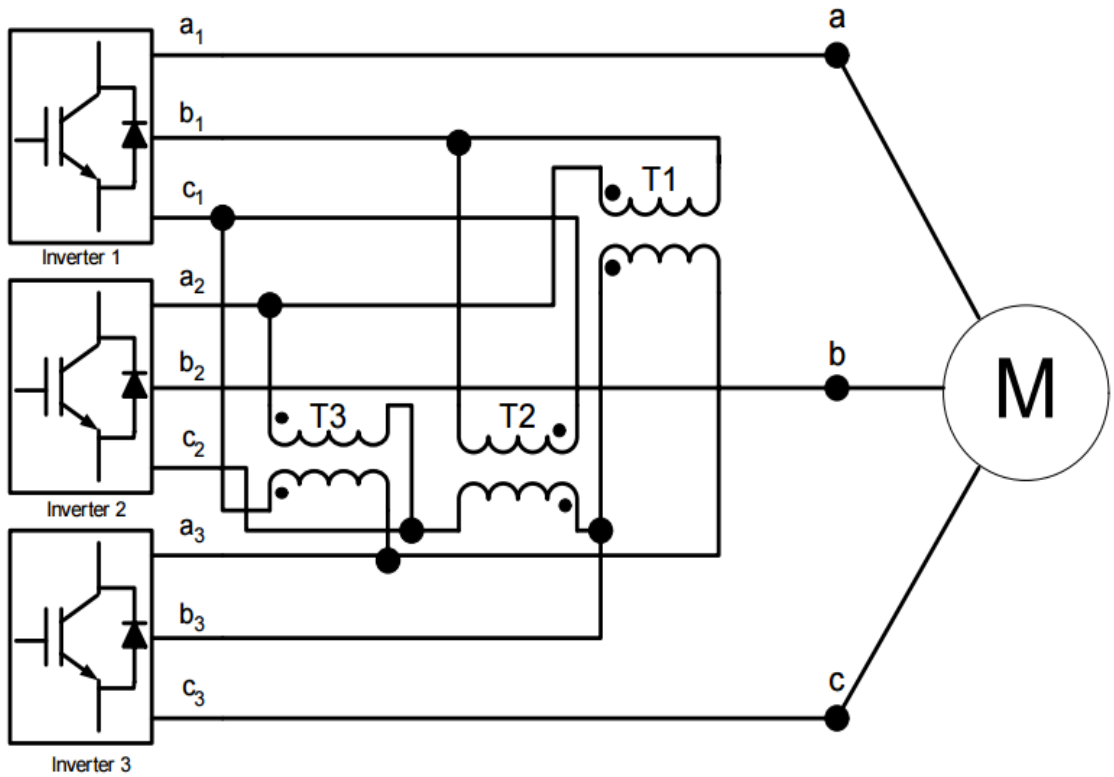

Figure 5-4 Cascaded multilevel converter with transformers using standard

5.2.2. DIODE-CLAMPED MULTILEVEL INVERTER

The neutral point converter proposed by Nabae, Takahashi, and Akagi in (1981) was essentially a three-level diode-clamped inverter (A. Nabae, 2015). In the 1990s several researchers published articles that have reported experimental results for four-, five-, and six-level diode-clamped converters for such uses as static VAR compensation, variable speed motor drives, and high voltage system interconnections (F. Z. Peng, 2015). A three-phase six-level diode-clamped inverter is shown in Figure 5-5. Each of the three phases of the inverter shares a common dc bus, which has been subdivided by five capacitors into six levels. The voltage across each capacitor is Vdc, and the voltage stress across each switching device is limited to V_{dc} through the clamping diodes. Table 5.1 lists the output voltage levels possible for one phase of the inverter with the negative dc rail voltage V0 as a reference. State condition 1 means the switch is on, and 0 means the switch is off. Each phase has five complementary switch pairs such that turning on one of the switches of the pair requires that the other complementary switch be turned off. The complementary switch pairs for phase leg a are (S_{a1},$S_{a\prime1}$), (S_{a2},$S_{a\prime2}$), (S_{a3},$S_{a\prime3}$), (S_{a4},$S_{a\prime4}$), and (S_{a5},$S_{a\prime5}$), Table 1 also shows that in a diode-clamped inverter, the switches that are on for a particular phase leg are always adjacent and in series. For a three phase three -level inverter.

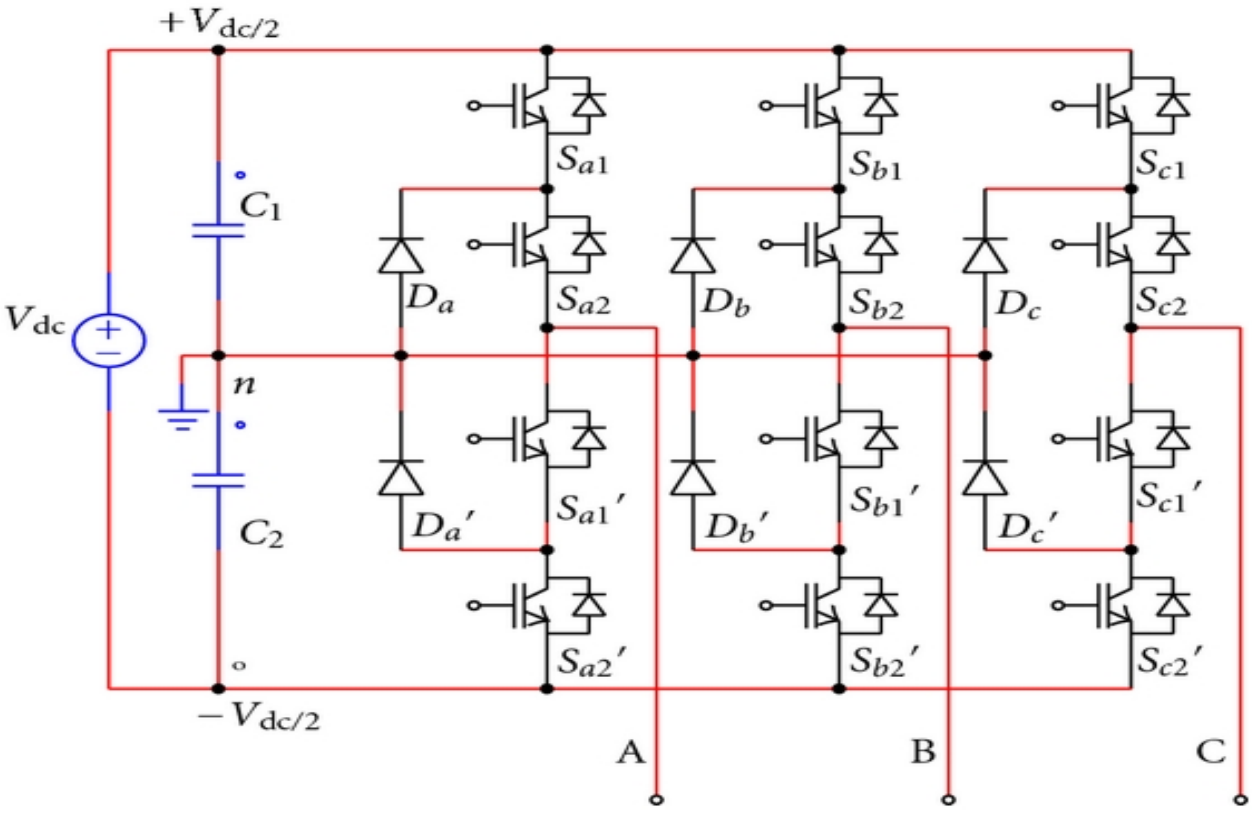

Figure 5-5 Three-phase three-level structure of a diode-clamped inverter

Voltage V_{a0}	S_{a3}	S_{a2}	S_{a1}	$S_{a'3}$	$S_{a'2}$	$S_{a'1}$
$V_3 = 3V\ dc$	1	1	1	0	0	0
$V_2 = 2V\ dc$	0	1	1	1	0	0
$V_1 = V\ dc$	0	0	1	1	1	0
$V_0 = 0$	0	0	0	1	1	1

Table 5-1 Diode-clamped six-level inverter voltage levels and corresponding switch states.

Figure 5-6 shows one of the three line-line voltage waveforms for a three-level inverter. The line voltage consists of a phase-leg a voltage and a phase-leg b voltage. The resulting line voltage is a 5-level staircase waveform. This means that an m-level diode-clamped inverter has an m-level output phase voltage and a (2m-1)-level output line voltage. Although each active switching device is required to block only a voltage level of Vdc, the clamping diodes require different ratings for reverse voltage blocking. Using phase "A" of Figure 5-5 as an example, when all the lower switches Sa'1 through Sa'3 are turned on, D3 must block 3Vdc, D2 must block 2Vdc, and D1 must block Vdc. If the inverter is designed such that each blocking diode has the same voltage rating as the active switches, Dn will require n diodes in series; consequently, the number of diodes required for each phase would be (m-1) × (m-2). Thus, the number of blocking diodes is quadratically related to the number of levels in a diode-clamped converter (J. S. Lai, 2014). One application of the multilevel diode-clamped inverter is an interface between a high voltage dc transmission line and an AC transmission line (J. S. Lai, 2014). Another application would be as a variable speed drive for high-power medium-voltage (2.4 kV to 13.8 kV) motors. Static VAR compensation is an additional function for which several authors have proposed for the diode-clamped converter. The main advantages and disadvantages of multilevel diode-clamped converters are as follows (J. Rodriguez, 2012)

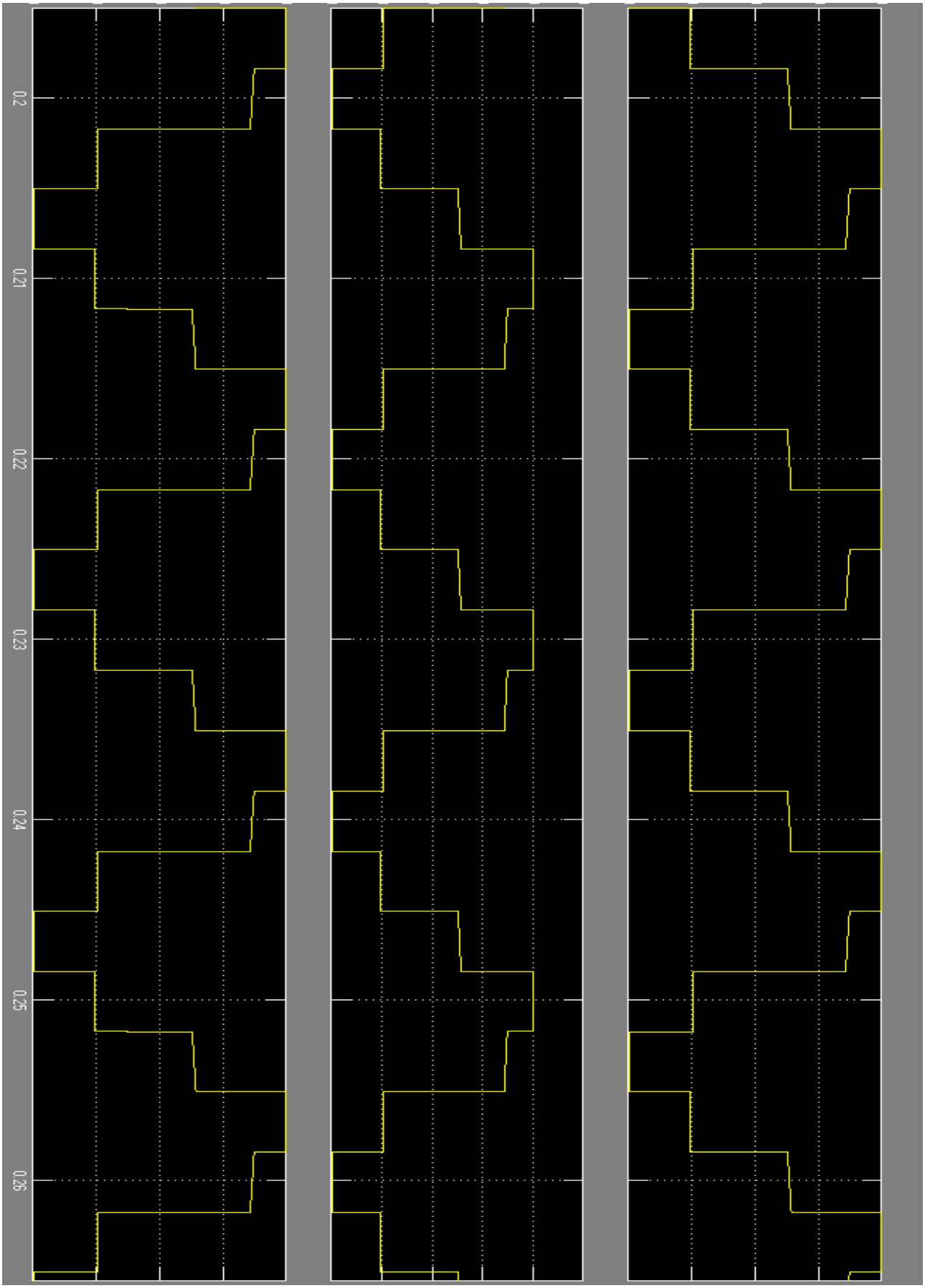

Figure 5-6 three line-line voltage waveforms for a three-level inverter

Advantages:

- All of the phases share a common dc bus, which minimizes the capacitance requirements of the converter. For this reason, a back-to-back topology is not only possible but also practical for uses such as a high-voltage back-to-back inter-connection or an adjustable speed drive.
- The capacitors can be pre-charged as a group.
- Efficiency is high for fundamental frequency switching.

Disadvantages:

- Real power flow is difficult for a single inverter because the intermediate dc levels will tend to overcharge or discharge without precise monitoring and control.
- The number of clamping diodes required is quadratically related to the number of levels, which can be cumbersome for units with a high number of levels.

5.2.3. FLYING CAPACITOR MULTILEVEL INVERTER

Meynard and Foch introduced a flying-capacitor-based inverter in 1992 (T. A. Meynard, 2012). The structure of this inverter is similar to that of the diode-clamped inverter except that instead of using clamping diodes, the inverter uses capacitors in their place. The circuit topology of the flying capacitor multilevel inverter is shown in Figure 5-7. This topology has a ladder structure of dc side capacitors, where the voltage on each capacitor differs from that of the next capacitor. The voltage increment between two adjacent capacitor legs gives the size of the voltage steps in the output waveform. One advantage of the flying-capacitor-based inverter is that it has redundancies for inner voltage levels; in other words, two or more valid switch combinations can synthesize an output voltage. Table 5-2 shows a list of all the combinations of phase voltage levels that are possible for the five-level circuit shown in Figure 5-7. Unlike the diode-clamped inverter, the flying capacitor inverter does not require all of the switches that are on (conducting) be in a consecutive series. Moreover, the flying-capacitor inverter has phase redundancies, whereas the diode clamped inverter has only line-line redundancies (G. Sinha, 2014). These redundancies allows a choice of charging/discharging specific capacitors and can be incorporated in the control system for balancing the voltages across the various levels. In addition to the (m-1) DC link capacitors, the m-level flying-capacitor multilevel inverter will require (m-1) × (m-2)/2 auxiliary capacitors per phase if the voltage rating of the capacitors is identical to that of the main switches.

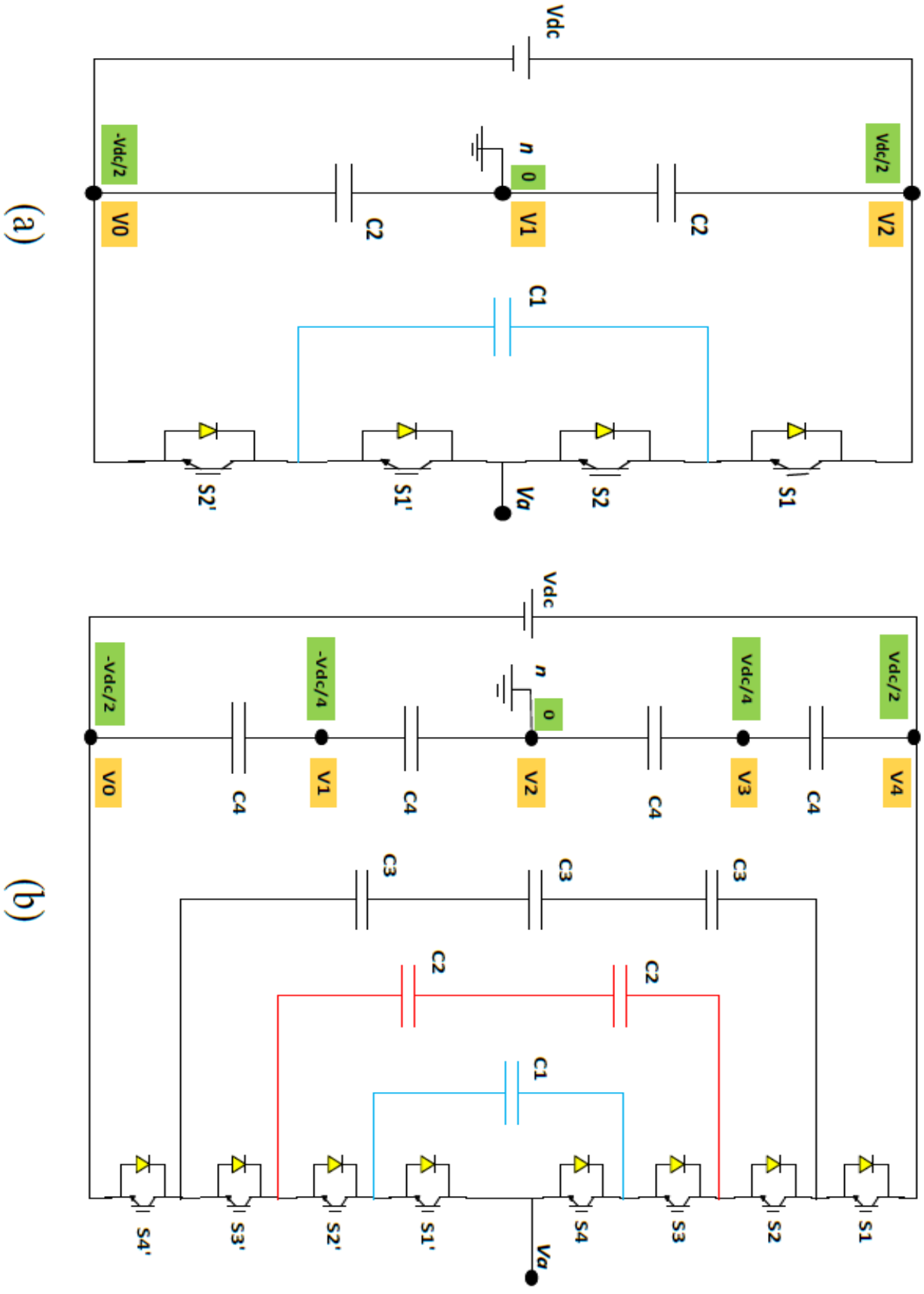

Figure 5-7 flying capacitor multilevel inverter circuit layout for a) 3-levels, and b) 5-levels.

One application proposed in the literature for the multilevel flying capacitor is static VAR generation. The main advantages and disadvantages of multilevel flying capacitor converters are as follows (T. Habetler, 2009).

Advantages:

- Phase redundancies are available for balancing the voltage levels of the capacitors.
- Real and reactive power flow can be controlled.
- The large number of capacitors enables the inverter to ride through short duration outages and deep voltage sags.

Disadvantages:

- Control is complicated to track the voltage levels for all of the capacitors. Also, pre-charging all of the capacitors to the same voltage level and start up are complex.
- Switching utilization and efficiency are poor for real power transmission.
- The large numbers of capacitors are both more expensive and bulky than clamping diodes in multilevel diode-clamped converters. Packaging is also more difficult in inverters with a high number of levels.

Output voltage Level	V_{an} Value	Switch state (5 level)							
V_4	$V_{dc}/_2$	1	1	1	1	0	0	0	0
V_3	$V_{dc}/_4$	1	1	1	0	1	0	0	0
		0	1	1	1	0	0	0	1
		1	0	1	1	0	0	1	0
V_2	0	1	1	0	0	1	0	0	1
		0	0	1	1	0	0	1	1
		1	0	1	0	1	0	1	0
		1	0	0	1	0	1	1	0
		0	1	0	1	0	1	0	1
		0	1	1	0	1	0	0	1

V_1	$-V_{dc}/4$	1	0	0	0	1	1	1	0
		0	0	0	1	0	1	1	1
		0	0	1	0	1	0	1	1
V_0	$-V_{dc}/2$	0	0	0	0	1	1	1	1

Table 5-2 Switching states for 5-level fly capacitor multilevel inverter

5.3. GENERALISED MULTILEVEL TOPOLOGY

Existing multilevel converters such as diode-clamped and capacitor-clamped multilevel converters can be derived from the generalized converter topology called P2 topology proposed by Peng (F. Z. Peng, 2010) as illustrated in Figure 5-8. The generalized multilevel converter topology can balance each voltage level by itself regardless of load characteristics, active or reactive power conversion and without any assistance from other circuits at any number of levels automatically. Thus, the topology provides a complete multilevel topology that embraces the existing multilevel converters in principle. Figure 5-8 shows the P2 multilevel converter structure per phase leg. Each switching device, diode, or capacitor's voltage is 1Vdc, for instance, 1/ (m-1) of the DC-link voltage. Any converter with any number of levels, including the conventional bi-level converter can be obtained using this generalized topology (F. Z. Peng et al, 2010)

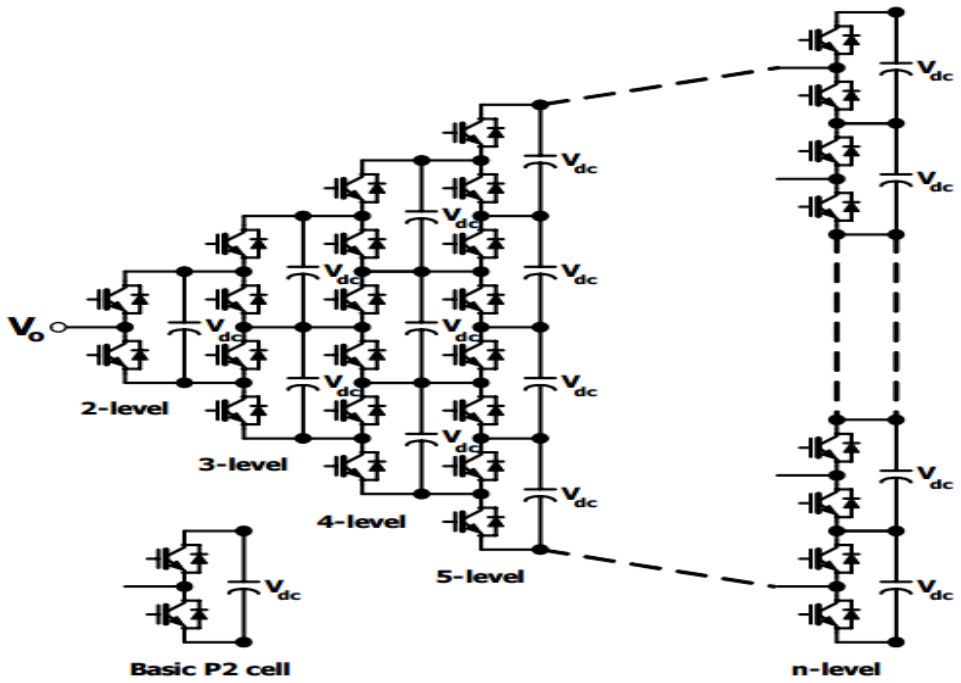

Figure 5-8 Generalized P2 multilevel converter topology for one phase leg.

5.3.1. MIXED-LEVEL HYBRID MULTILEVEL CONVERTER

To reduce the number of separate DC sources for high-voltage, high-power applications with multilevel converters, diode-clamped or capacitor-clamped converters could be used to replace the full-bridge cell in a cascaded converter ((F. Z. Peng et al, 2010). Figure 5-9 shows a nine-level cascade converter incorporates a three-level diode-clamped converter as the cell. The original cascaded H-bridge multilevel converter requires four separate DC sources for one phase leg and twelve for a three-phase converter. If a five-level converter replaces the full-bridge cell, the voltage level is effectively doubled for each cell. Thus, to achieve the same nine voltage levels for each phase, only two separate DC sources are needed for one phase leg and six for a three-phase converter. The configuration has mixed-level hybrid multilevel units because it embeds multilevel cells as the building block of the cascade converter. The advantage of the topology is it needs less separate DC sources. The disadvantage for the topology is its control will be complicated due to its hybrid structure.

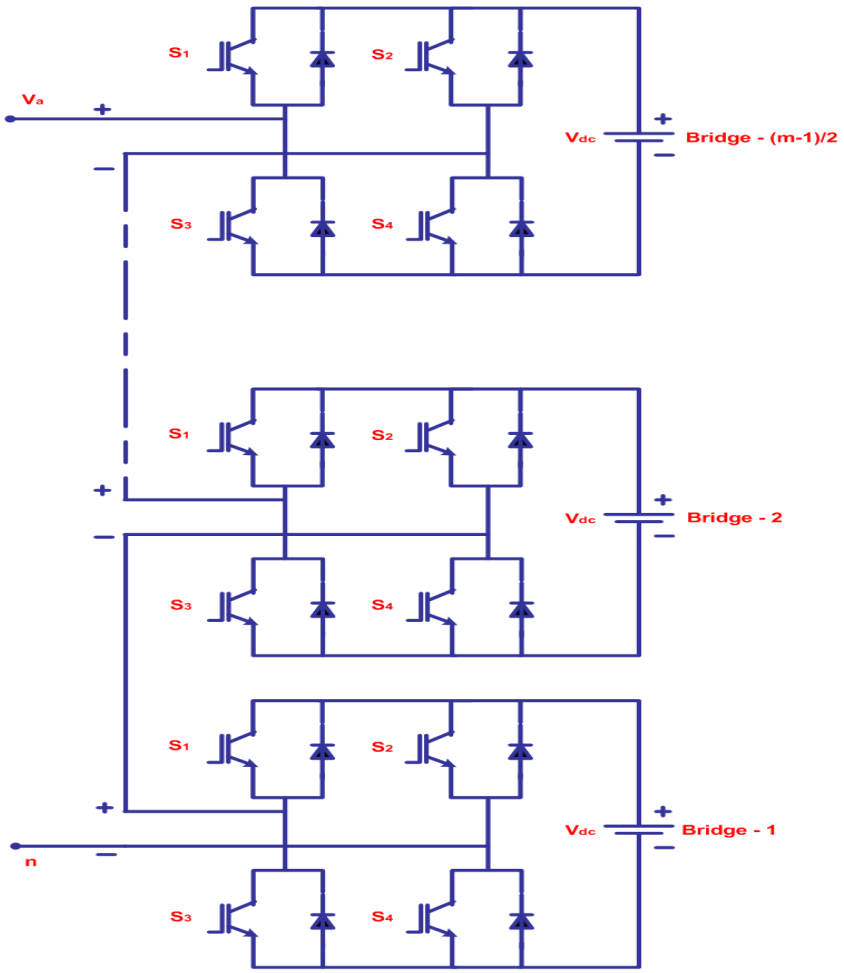

Figure 5-9: Multilevel cascaded unit configuration using the three-level diode-clamped converter to increase the voltage levels.

5.3.2. SOFT-SWITCHED MULTILEVEL CONVERTER

Some soft-switching methods can be implemented for different multilevel converters to reduce the switching loss and to increase efficiency. For the cascaded converter, because each converter cell is a bi-level circuit, the implementation of soft switching is not at all different from that of conventional bi-level converters. For capacitor-clamped or diode-clamped converters, soft-switching circuits have been proposed with different circuit combinations. One of soft switching circuits is a zero-voltage-switching type which includes auxiliary resonant commutated pole (ARCP), coupled inductor with zero-voltage transition (ZVT), and their combinations (B. M. Song et al, 2005)

5.3.3. BACK-TO-BACK DIODE-CLAMPED CONVERTER

Two multilevel converters can be connected in a back-to-back arrangement and then the combination can be connected to the electrical system in a series-parallel arrangement. Both current demanded from the utility and the voltage delivered to the load can be controlled at the same time. This series-parallel active power filter has been referred to as a universal power conditioner (H. Fujita et al, 2011) when used on electrical distribution systems and as a universal power flow controller (Y. Chen, 2012) when applied at the transmission level. Previously, Lai and Peng (2010) proposed the back-to-back diode-clamped topology for use as a high-voltage dc inter connection between two asynchronous ac systems or as a rectifier/inverter for an adjustable speed drive for high-voltage motors. The diode-clamped inverter has been chosen over the other two basic multilevel circuit topologies for use in a universal power conditioner for the following reasons:

- All six phases (three on each inverter) can share a common dc link. Conversely, the cascade inverter requires that each dc level be separate, and this is not conducive to a back-to-back arrangement.
- The multilevel flying-capacitor converter also shares a common dc link; however, each phase leg requires several additional auxiliary capacitors. These extra capacitors would add substantially to the cost and the size of the conditioner.

Because a diode-clamped converter acting as a universal power conditioner will be expected to compensate for harmonics and/or operate in low amplitude modulation index regions, a more sophisticated, higher-frequency switch control than the fundamental frequency switching method will be needed. For this reason, multilevel space vector and carrier-based PWM

approaches are compared in the next section, as well as novel carrier-based PWM methodologies.

5.4. CONTROL TECHNIQUES – SINUSOIDALE PULSE WIDTH MODULATION, SELECTIVE HARMONIC ELEMINATION & SPACE VECTOR MODULATION

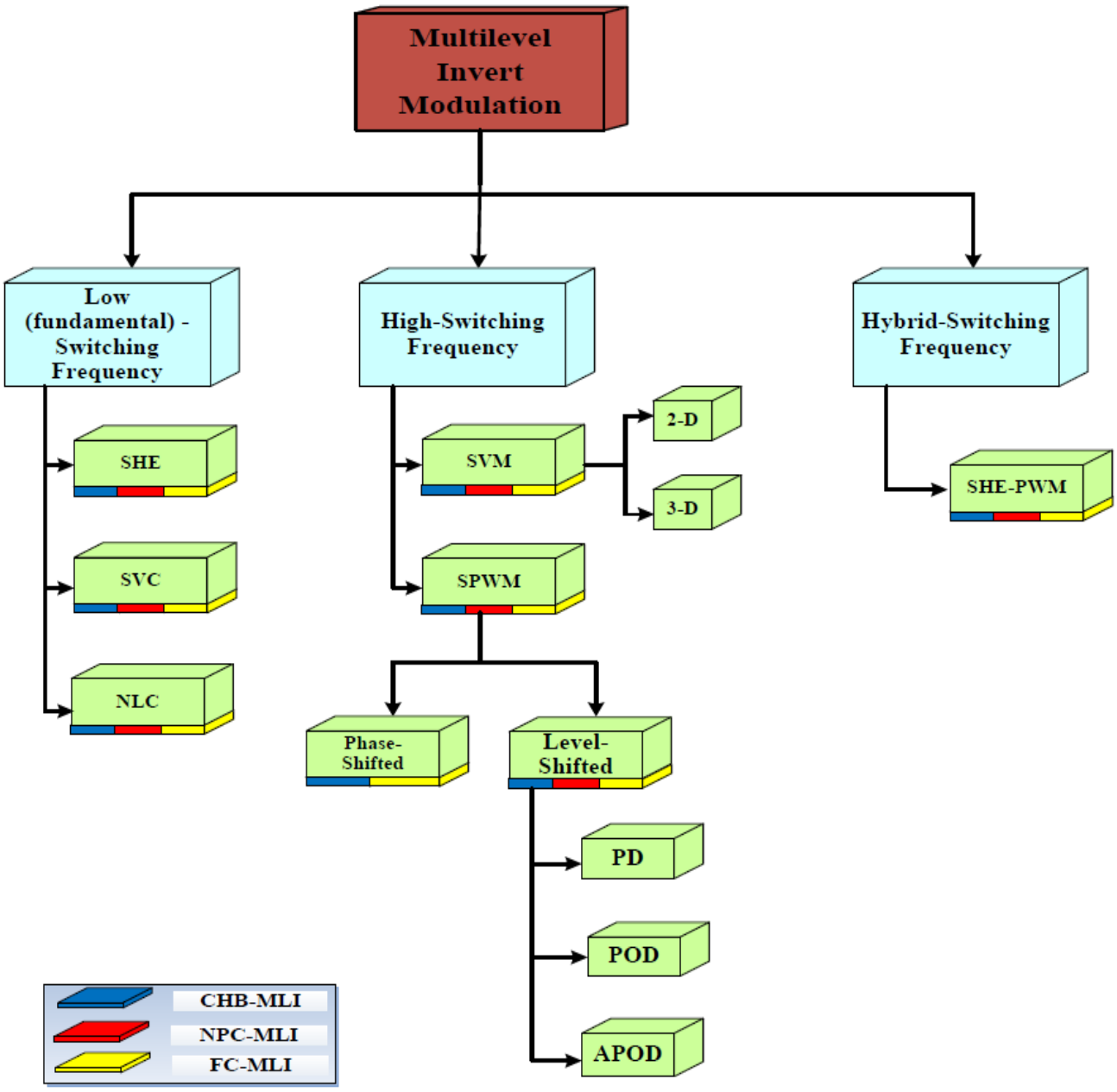

Figure 5-10 Classifications of control Techniques (A, Basem, 2016)

By increasing the number of levels in the inverter, the output voltages have more steps generating a staircase waveform, which has a reduced harmonic distortion. However, a high number of levels increases the control complexity and introduces voltage imbalance

problems. The modulation methods used in multilevel inverters can be classified according to switching frequency (N. Celanovic, 2015). Methods that work with high switching frequencies have many commutations for the power semiconductors in one period of the fundamental output voltage. A very popular method in industrial applications is the classic carrier-based sinusoidal PWM (SPWM) that uses the phase-shifting technique to reduce the harmonics in the load voltage (Y. Liang, 2014). Methods that work with low switching frequencies generally perform one or two commutations of the power semiconductors during one cycle of the output voltages, generating a staircase waveform. Representatives of this family of multilevel are the selective harmonics elimination (SHE), the space vector control (SVC), and the sinusoidal multicarrier based pulse width modulation (SPWM). Three different topologies have been proposed for multilevel inverters with the aforementioned modulation methods as shown in figure 5-10, thus, Low- (fundamental-) switching frequency modulation, High-switching frequency modulation, Hybrid-switching frequency modulation (A. Basem et al, 2016)

5.4.1. SINUSOIDAL MULTICARRIER BASED PULSE WIDTH MODULATION

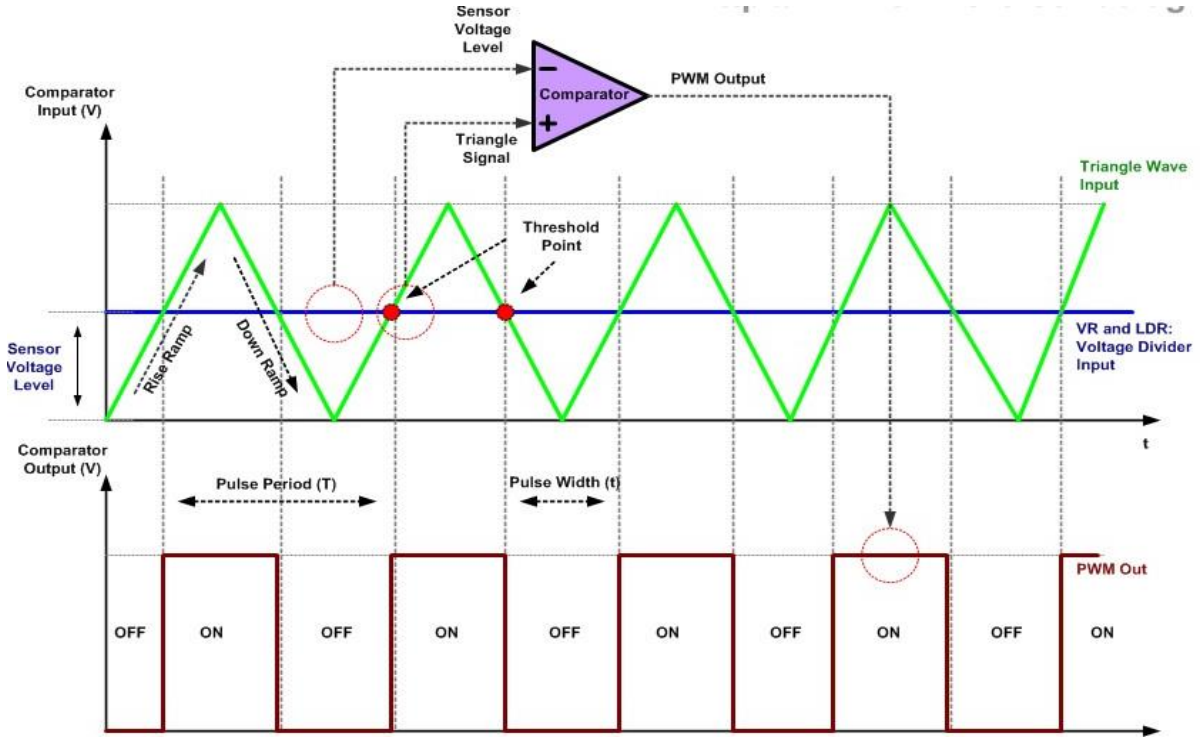

Figure 5-11 Basic principle of PWM control (PIC12F683).

In reference to the SPWM, it is evident that the most popular control methodology recommended by researchers and adopted by engineering practitioners for multilevel inverter control is the SPWM. In effect, it is a fact that SPWM does produce pulses through the

comparison of a sinusoidal reference waveform with a triangular carrier waveform, as it could be seen in figure 5-11. Sinusoidal Pulse Width Modulation (SPWM) is the name of a technique to generate low frequency output signals from high frequency pulses. Rapidly switching the output voltage of an inverter leg between the upper and lower DC rail voltages, the low frequency output can be though as the average of the voltage over a switching period. In its simplest form SPWM output signals are constructed by comparing two control signals, a carrier signal and a modulation signal. This is known as carrier-based SPWM. The carrier signal is a high frequency (switching frequency) triangular waveform. The modulation signal can be any shape. If the peak of the modulation is less than the peak of the carrier signal, the output will follow the shape of the modulation signal. If instantaneous magnitude of the modulation signal is greater than the carried signal at a point in time, the output voltage of the inverter leg should be connected to the positive side of the DC link.

Phase-Shifted SPWM

Considering the phase shifted technique, all the triangular carriers have the same frequency and same peak-peak amplitude; but there is a phase shift between any two adjacent carrier waves. For "m" Voltage levels (m-1) carrier signals are required and they are phase shifted with an angle of θ= (360°/m-1). The gate signals are generated with proper comparison of carrier wave and modulating signal. Considering minimum distortion is part of the aim here, it is noteworthy to accommodate the idea that to obtain the minimum distortion at the output waveform for an inverter with $Ncells$, the carrier signals should be shifted by a displacement angle $\theta =$ =360°/$N_{cells.}$ The illustration of this modulation method is shown in Figure 5-12 below

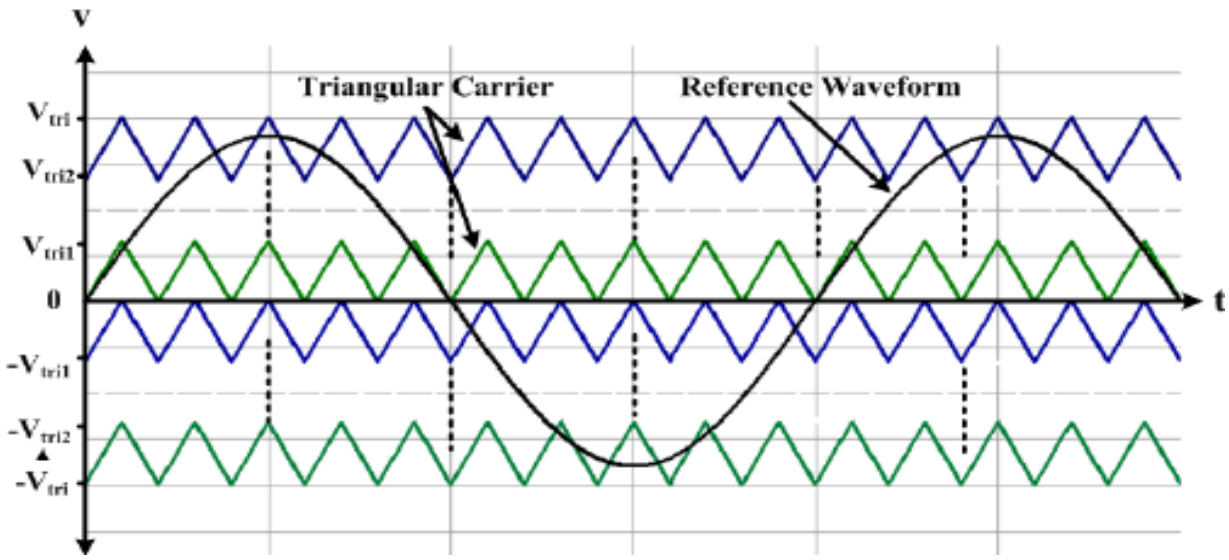

Figure 5-12Phase level shifted Modulation simulation

Level-Shifted SPWM

For carrier's signals, the time values of each carrier waves are set to [0 1/600 1/300] while the outputs values are set according to the disposition of carrier waves. After comparing, the output signals of comparator are transmitted to the IGBT. This technique is divided into 3 types

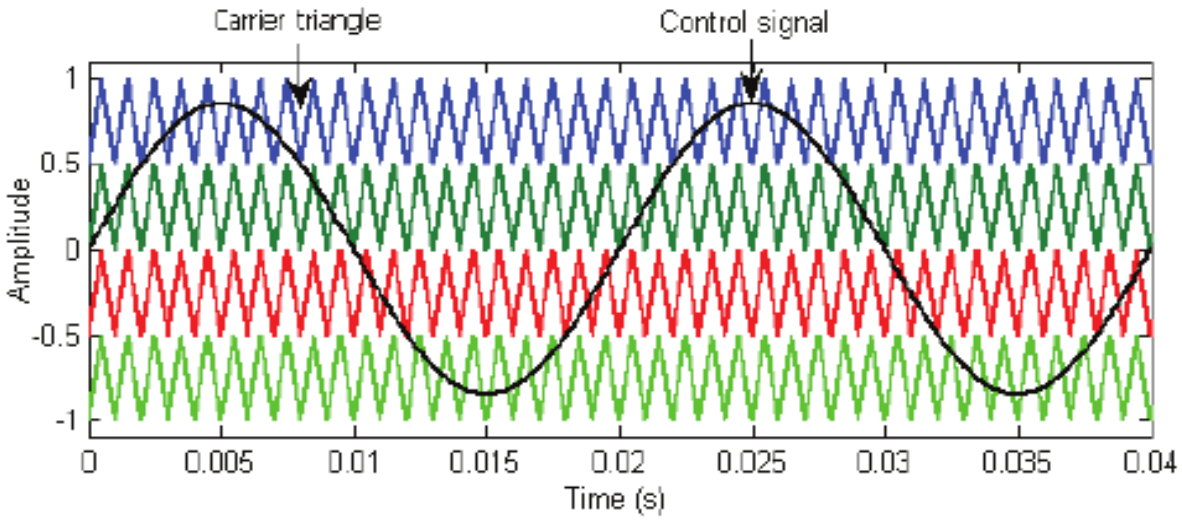

Figure 5-13 Level shifted Modulation simulation

The modulating signal of each phase is displaced from each other by 120°. All the carrier signals have an equal frequency and amplitude. The carrier waves and the modulating signals are compared and the output of the comparator defines the output in the positive half cycle the comparator output will have the value high, if the amplitude of the modulating signal is greater than that of the carrier wave and zero otherwise. Similarly, for the negative half cycle, if the modulating signal is lower than the carrier wave the output of the comparator is high and zero otherwise. The particularity of the application of this modulation technique is that all the carriers are in phase but vertically disposed and placed in such a way that they cover the entire amplitude range of the inverter (Basem A, 2017).

5.4.2. MULTILEVEL SPACE VECTOR PULSE WIDTH MODULATION

Choi et al (2003) was the first author to extend the two-level space vector pulse width modulation technique to more than three levels for the diode-clamped inverter. Figure 5-14 shows what the space vector d-q plane looks like for a six-level inverter. Figure 5-15 represents the equivalent dc link of a six-level inverter as a multiplexer that connects each of the three output phase voltages to one of the dc link voltage tap points (G Sinha, 2015). Each integral point on the space vector plane represents a particular three-phase output voltage state of the inverter. For instance, the point (3, 2, and 0) on the space vector plane means, that with respect

to ground, a phase is at $3V_{dc}$, b phase is at $2V_{dc}$, and c phase is at $0V_{dc}$. The corresponding connections between the dc link and the output lines for the six-level inverter are also shown in Figure 15 for the point (3, 2, 0). An algebraic way to represent the output voltages in terms of the switching states and dc link capacitors is described in the following.

For n = m-1 where m is the number of levels in the inverter:

$$V_c = [V_{c1}\ V_{c2} \dots \dots V_{cn}]^T;\ H_{abc} = \begin{bmatrix} h_{a1} & h_{a2} & h_{a3} \dots . h_{an} \\ h_{b1} & h_{b2} & h_{b3} \dots . h_{bn} \\ h_{c1} & h_{c2} & h_{c3} \dots . h_{cn} \end{bmatrix}, V_{abc0} = \begin{bmatrix} V_{a0} \\ V_{b0} \\ V_{c0} \end{bmatrix} and$$

$$h_{aj} = \sum_{j}^{n} \delta(h_a - j),$$

Where h_a is the switch state and j is an integer from 0 to n, and where

$$\delta(x) = 1\ if\ x \geq 0, \delta(x) = 0\ if\ x < 0$$

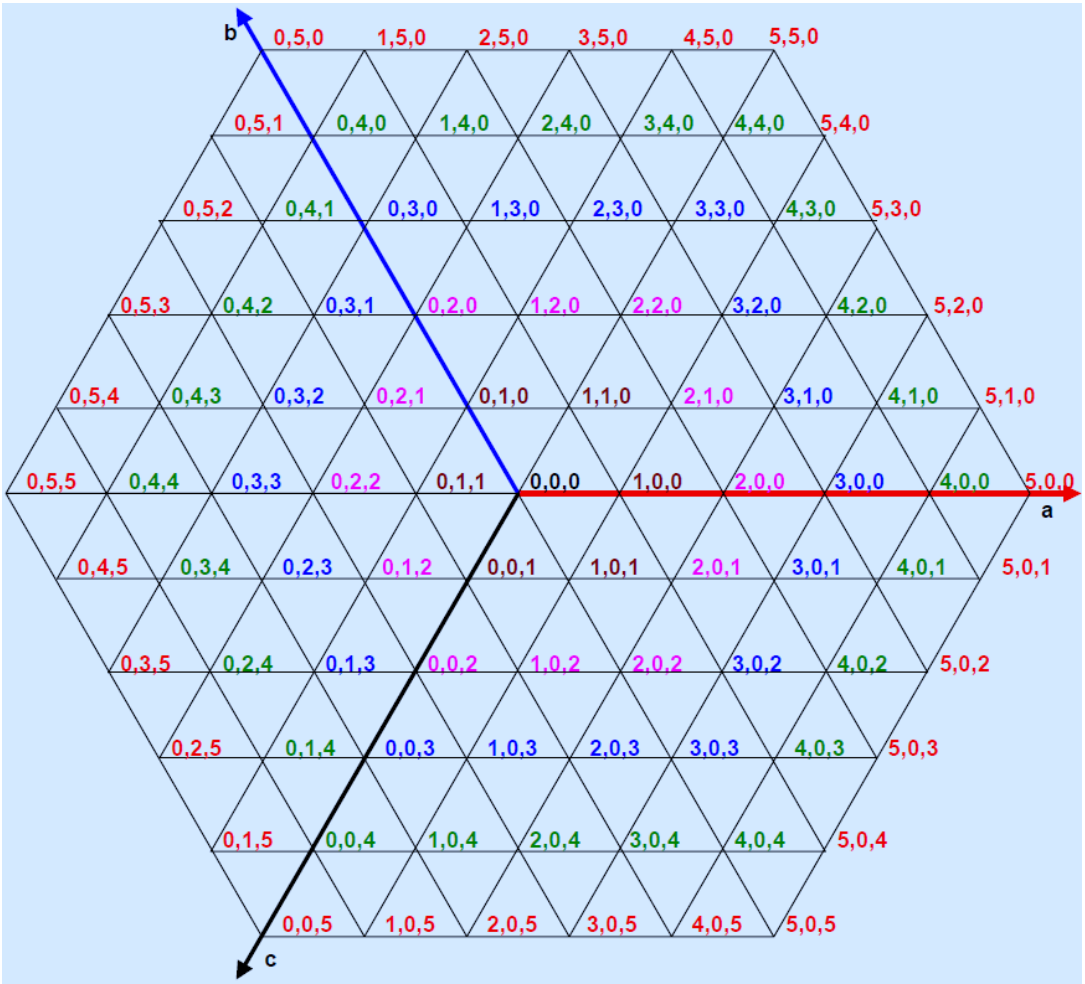

Figure 5-14 Voltage space vectors for a six-level inverter.

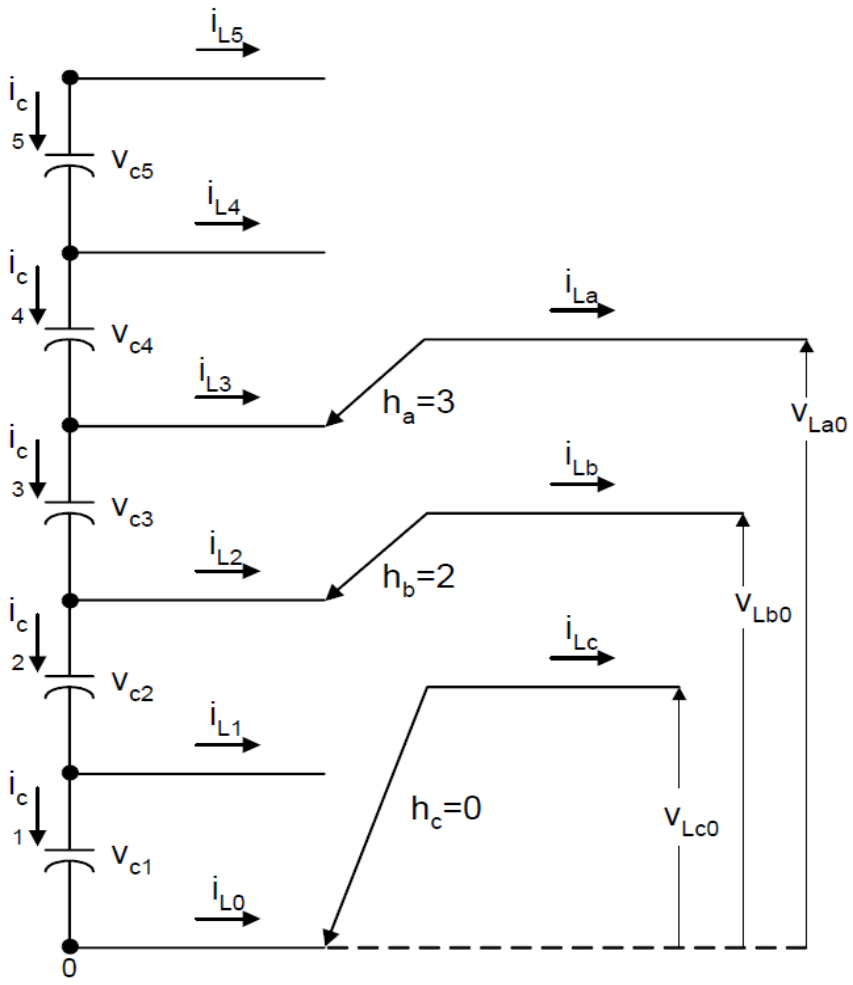

Figure 5-15 multiplexer model of diode-clamped six-level inverter.

Besides the output voltage state, the point (3, 2, and 0) on the space vector plane can also represent the switching state of the converter. Each integer indicates how many upper switches in each phase leg are on for a diode-clamped converter. As an example, for $h_a = 3$, $h_b = 2$, $h_c = 0$, the H_{abc} matrix for this particular switching state of a six-level inverter would be

$$H_{abc} = \begin{bmatrix} 0 & 0 & 1 & 1 & 1 \\ 0 & 0 & 1 & 1 & 1 \\ 0 & 0 & 1 & 0 & 0 \end{bmatrix}$$

Redundant switching states are those states for which a particular output voltage can be generated by more than one switch combination. Redundant states are possible at lower modulation indices, or at any point other than those on the outermost hexagon shown in Figure 31.23. Switch state (3, 2, 0) has redundant states (4, 3, and 1) and (5, 4, 2). Redundant switching states differ from each other by an identical integral value, i.e., (3, 2, 0) differs from (4, 3, 1) by (1, 1, 1) and from (5, 4, 2) by (2, 2, 2). For an output voltage state (x, y, and z) in an m-level diode-clamped inverter, the number of redundant states available is given by

m – 1 – max(x, y, z). As the modulation index decreases (or the voltage vector in the space vector plane gets closer to the origin), more redundant states are available. The number of possible zero states is equal to the number of levels, m. For a six-level diode-clamped inverter, the zero voltage states are (0, 0, 0), (1, 1, 1), (2, 2, 2), (3, 3, 3), (4, 4, 4), and (5, 5, 5). The number of possible switch combinations is equal to the cube of the level (m^3). For this six-level inverter, there are 216 possible switching states. The number of distinct or unique states for an m-level inverter can be given by $m^3 - (m-1)^3 = [6\sum_{n=1}^{m-1} n] + 1$

Therefore, the number of redundant switching states for an m-level inverter is$(m-1)^3$. Table 5- 3 below summarizes the available redundancies and distinct states for a six-level diode-clamped inverter.

Redundancies	Distinct states	Redundant states	Unique state coordinates: (a,b,c0 where 0≤a,b,c≤5
5	1	5	(0,0,0)
4	6	24	(0,0,1),(0,1,0),(1,0,0),(1,0,1),(1,1,0),(0,0,1)
3	12	36	(p,0,2),(p,2,0),(0,p,2),(2,p,0),(0,2,p,),(2,0,p) where p≤2
2	18	36	(0,3,p),(3,0,p),(p,3,0),(p,0,3),(3,p,0),(0,p,3) where p≤3
1	24	24	(0,4,p),(4,0,p),(p,4,0),(p,0,4),(4,p,0),(0,p,4) where p≤4
0	30	0	(0,5,p),(5,0,p),(p,5,0),(p,0,5),(5,p,0),(0,p,5) where p≤5
Total	91	125	216 total states

Table 5-3 available redundancies and distinct states for a six-level diode-clamped inverter.

In two-level PWM, a reference voltage is tracked by selecting the two nearest voltage vectors and a zero vector and then by calculating the time required to be at each of these three vectors such that their sum equals the reference vector. In multilevel PWM, generally the nearest three triangle vertices, V_1, V_2, and V_3, to a reference point Vf are selected so as to minimize the harmonic components of the output line-line voltage (L Liu, 2014). The respective time duration, T_1, T_2, and T_3, required of these vectors is then solved from the following equations:

$$T_s = T_1 + T_2 + T_3$$

Where T_s is the switching period, therefore;

$$\begin{bmatrix} T_1 \\ T_2 \\ T_3 \end{bmatrix} = \begin{bmatrix} V_{1d} & V_{2d} & V_{3d} \\ V_{1q} & V_{2q} & V_{3q} \\ 1 & 1 & 1 \end{bmatrix}^{-1} \begin{bmatrix} V_d T_s \\ V_q T_s \\ T_s \end{bmatrix}$$

Redundant switch levels can be used to help manage the charge on the dc link capacitors (Sinha G, 2015). Generalizing from Figure 5-15, the equations for the currents through the dc link capacitors can be given as

$$i_{cn} = -i_{Ln}, and$$

$$i_{c(n-j)} = i_{L(n-j)} + i_{c(n-j+1)} where\ j = 1,2,3, \ldots\ldots, n-1$$

The dc link currents for $h_a = 3$, $h_b = 2$, $h_c = 0$ would be $i_{c5} = i_{c4} = 0$, $i_{c3} = -i_a$, $i_{c2} = -i_a - i_b$, $i_{c1} = -i_a - i_b$. To see how redundant states affect the dc link currents, consider the two redundant states for (3, 2, 0). In state (4, 3, 1), the dc link currents would be $i_{c5} = 0$, $i_{c4} = -i_a$, $i_{c3} = -i_a - i_b$, $i_{c2} = -i_a - i_b$, $i_{c1} = -i_a - i_b - i_c = 0$; and for the state (5, 4, 2), the dc link currents would be $i_{c5} = -i_a$, $i_{c4} = -i_a - i_b$, $i_{c3} = -i_a - i_b$, $i_{c2} = i_{c1} = -i_a - i_b - i_c = 0$.

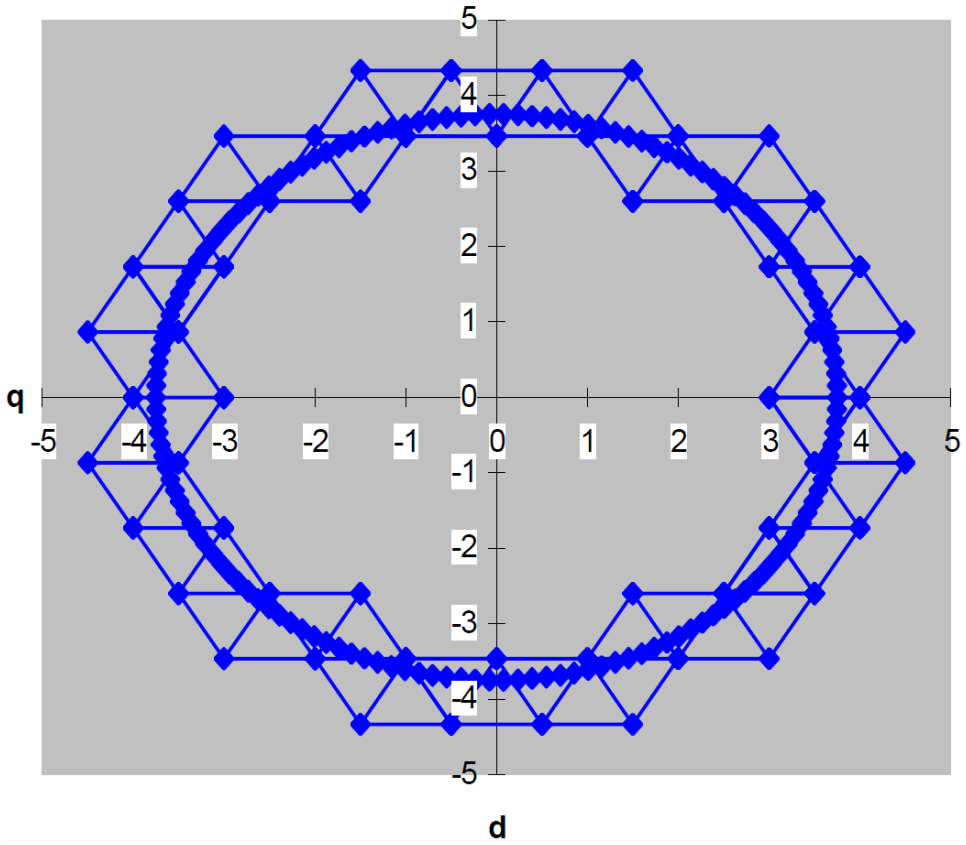

Figure 5-16 Sinusoidal reference and inverter output voltage states in d-q plane.

From this example, one can see that the choice of redundant switching states can be used to determine which capacitors will be charged/discharged or unaffected during the switching period. While this control is helpful in balancing the individual dc voltages across the capacitors that make up the dc link, this method is quite complicated in selecting which of the redundant states to use. Constant use of redundant switching states also results in a higher switching frequency and lower efficiency of the inverter because of the extra switching's. Recently, optimized space vector switching sequences for multilevel inverters have been proposed by researchers as well (McGrath, B. P., 2010)

5.4.3. SELECTIVE HARMONIC ELIMINATION

The selective harmonic elimination method is also called fundamental switching frequency method based on the harmonic elimination theory proposed by Patel et al (1974). The Selective Harmonic Elimination (SHE) for multilevel inverters is presented here. This section investigates the Selective Harmonic Elimination (SHE) to eliminate harmonics produced by Pulse Width Modulation (PWM) inverter. The selective harmonic elimination method for Multilevel Inverter is generally based on ideas of opposite harmonic injection. In this proposed scheme, the lower order harmonics (3rd, 5th, 7th, and 9th) are eliminated by the dominant harmonics of same order generated in opposite phase by Sinusoidal Pulse Width Modulation (SPWM) inverter and by using this scheme the Total Harmonic Distortion (THD) is reduced. Analysis of Sinusoidal Pulse Width Modulation (SPWM) technique and Selective Harmonic Elimination (SHE) is simulated using MATLAB/SIMULINK model. Since most existing multilevel inverter topologies belong to either a diode clamped configuration or a cascaded H bridge configuration, they both have the drawback of their high number of switching devices. Selective harmonic elimination applied to these configurations using traditional techniques will add to the overall system complexity.

Newton Raphson (NR), Genetic algorithms (GAs), Particle swarm optimisation (PSO) are stochastic optimization techniques. They are simple, powerful, general purpose, derivative free, stochastic global search algorithms inspired by the laws of natural selection and genetics. They follow Darwin's theory of evolution, where fitter individuals are likely to survive in a competing environment (Basem A, 2016). These algorithms derived from these techniques are derivative free in the sense that they do not need functional derivative information to search for a set solution that minimizes (or maximizes) a given objective function. The properties of Gas, NR or PTO reduce the computational burden and search time and also enable them to solve complex objective function

The implementation of the Selective harmonic elimination in this modulation is to predefine the switching angles using Fourier analysis based on the magnitude of the output signal, which results in eliminating a number of unwanted low-order harmonics, whilst simultaneously synthesizing the desired multilevel fundamental-voltage waveform. All the switching angle calculations are performed offline, so it is a pre-calculated control technique and can be classified as an open-loop control.

In the application of the selective harmonic elimination, the Total Harmonic Distortion (THD) for 3rd, 5th, 7th and 9th order harmonics is firstly defined followed by the amplitude of these order (3rd, 5th, 7th, and 9th) harmonics with help of Total Harmonic Distortion (THD). After calculating amplitude, the same order of harmonics is injected in opposite amplitude so as the resultant disorder sine wave is compared with triangular waveform and results generated in pulse so as to allow switching. This method is simple and easily implemented to achieve a reduced Total Harmonic Distortion (THD). The simulation of three phase voltage source inverter by using selective harmonic elimination method is done in MATLAB/SIMULINK software and shown in 5-17.

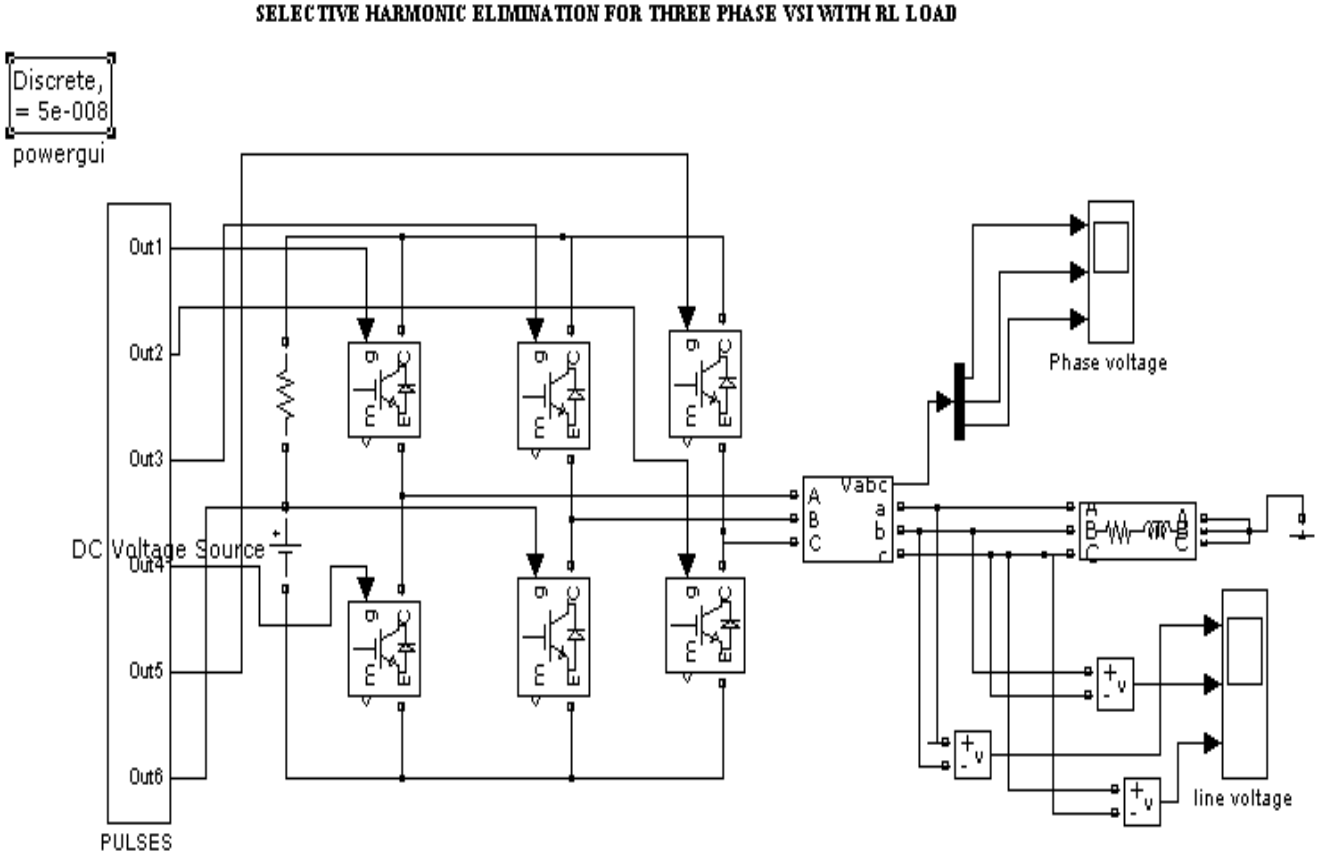

Figure 5-17 three phase voltage source inverter by using selective harmonic elimination

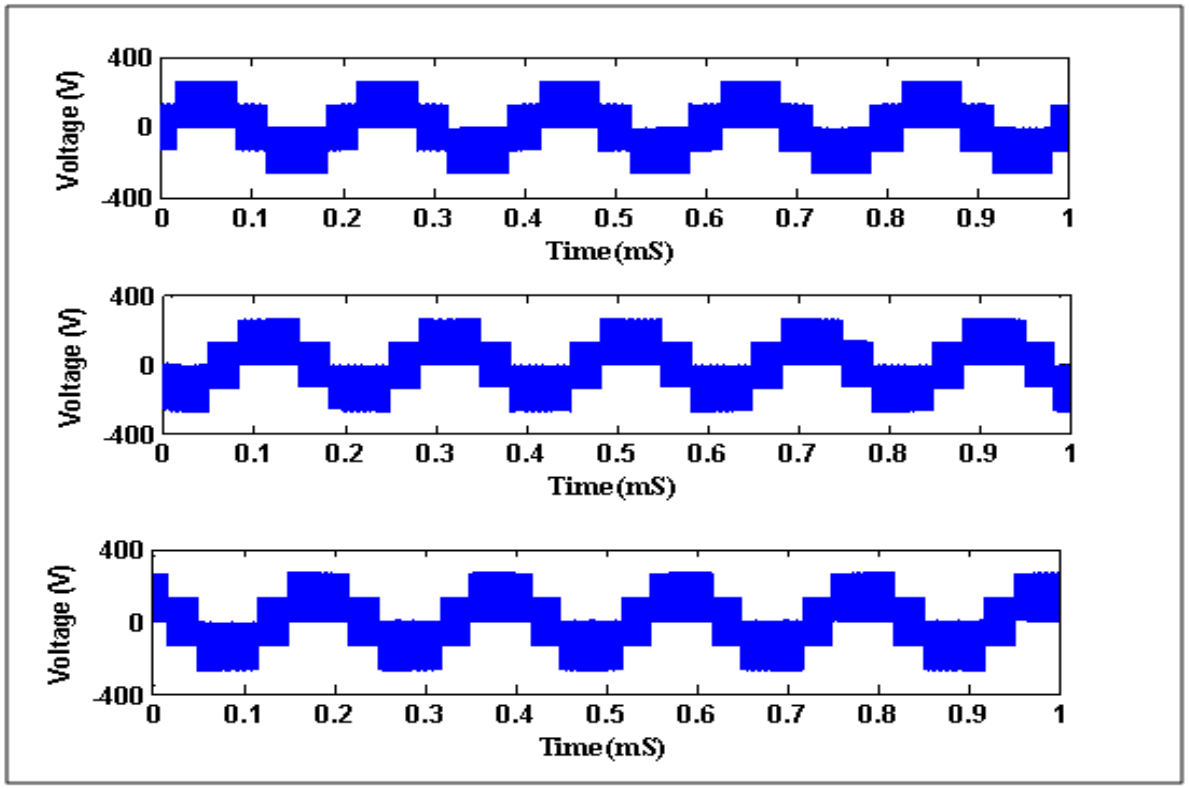

Figure 5-18 Phase voltage output waveform

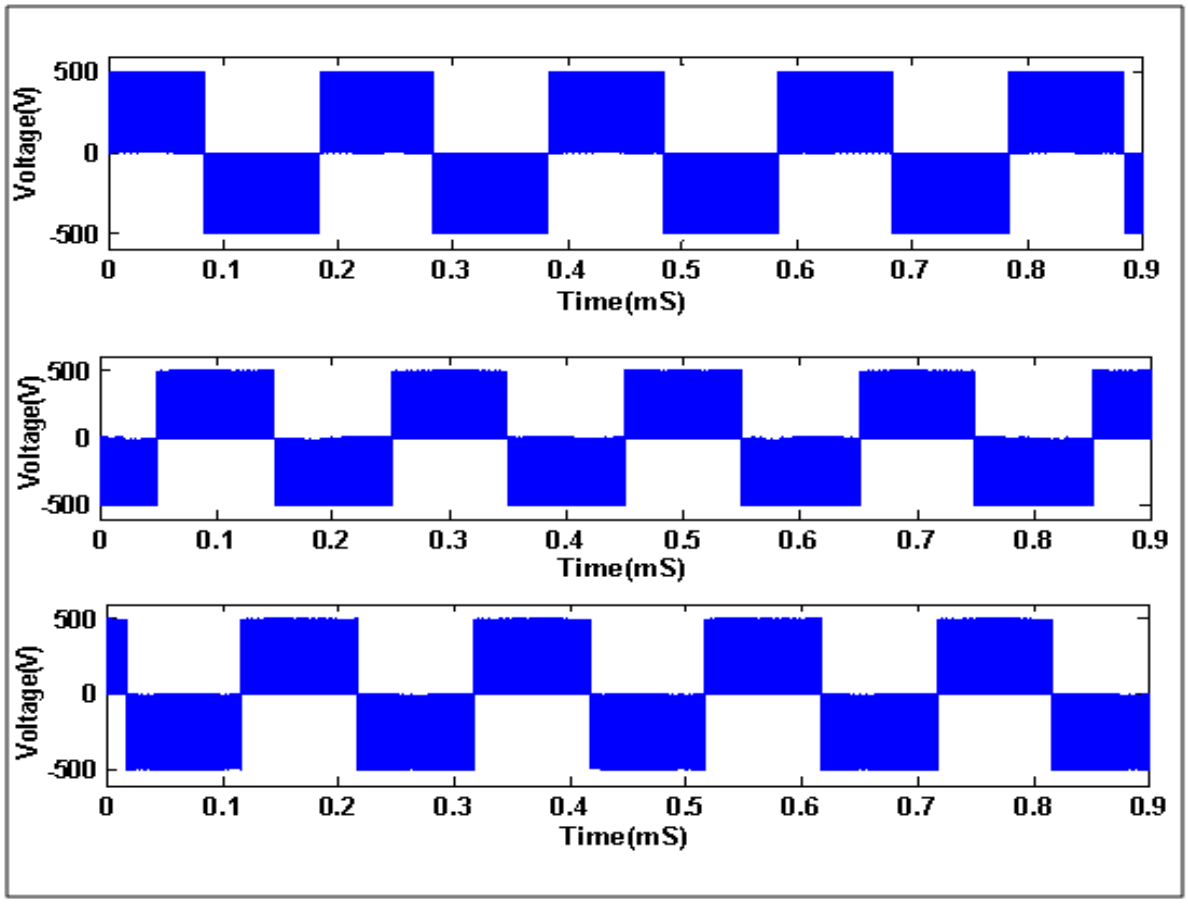

Figure 5-19 Line voltage output waveform

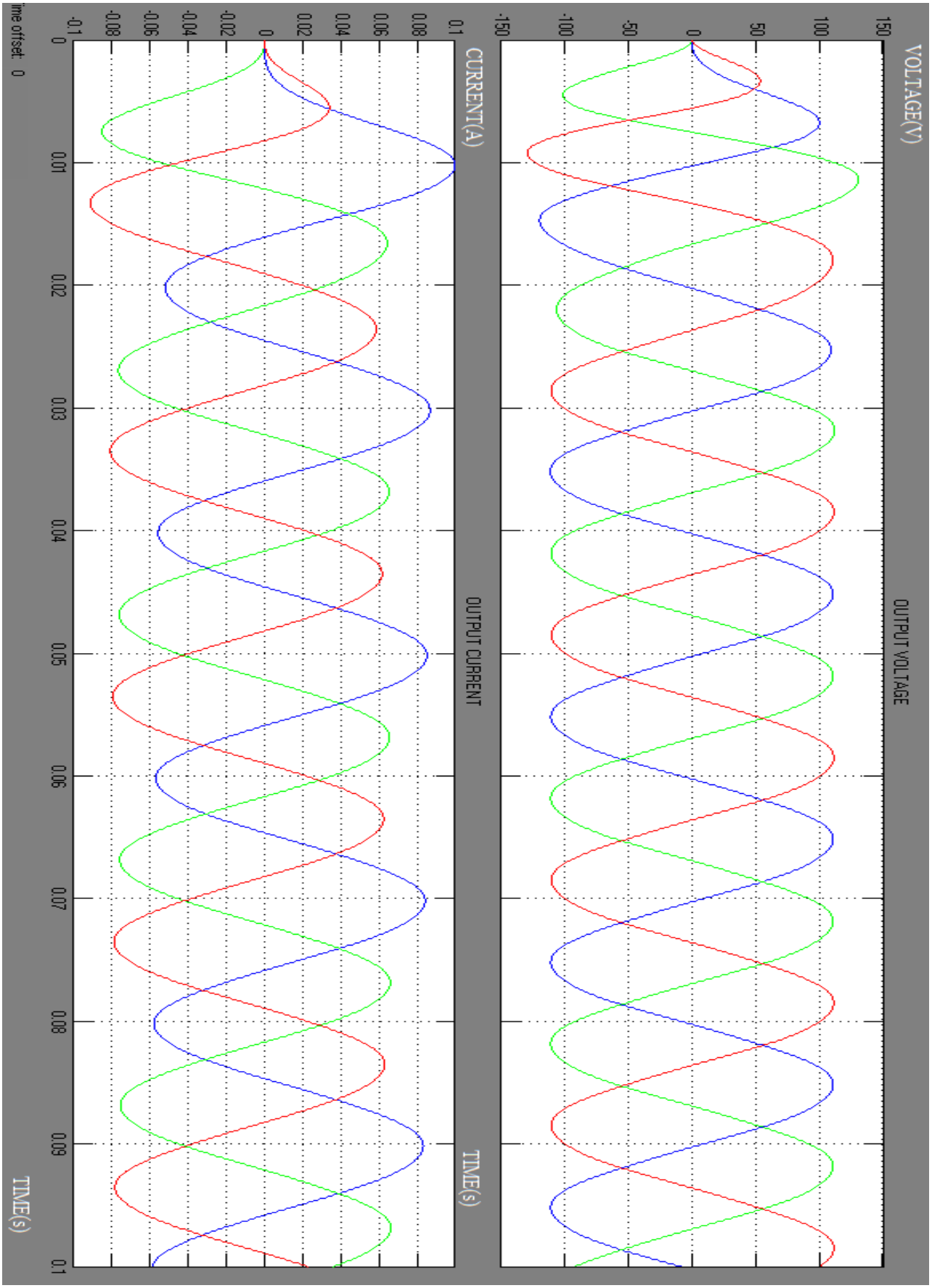

Figure 5-20 Output waveform for Selective Harmonic Elimination (SHE) with filter

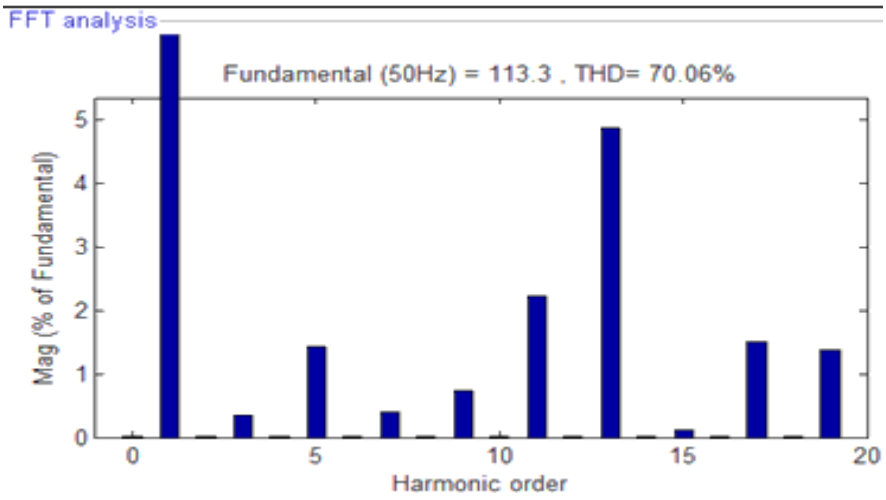

Figure 5-21 FFT analysis for Sinusoidal PWM Technique

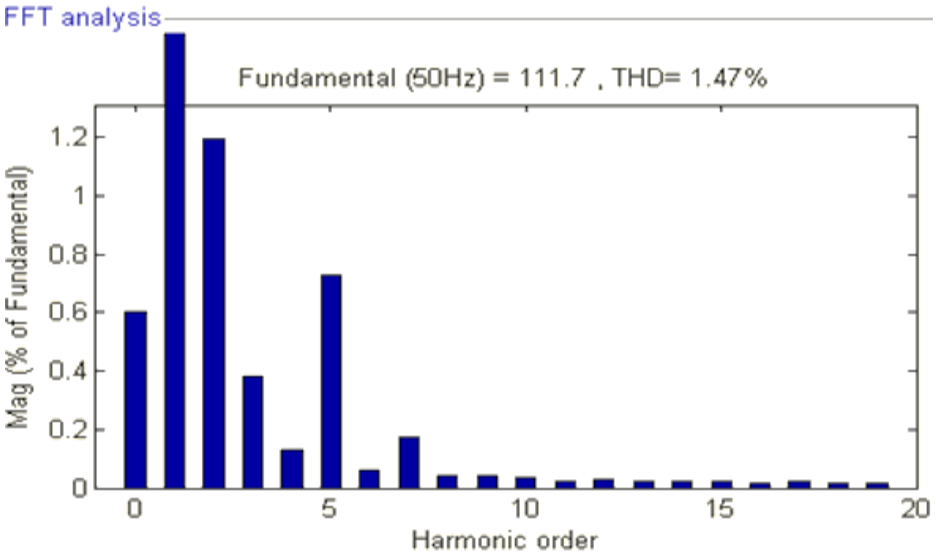

Figure 5-22 FFT analysis for Selective Harmonic Elimination (SHE)

As shown in figures 5-20, the generation of lower order harmonics, Dominant harmonics, Phase angle output wave forms, and Line voltage output wave forms are obtained by the Matlab Simulink model. Fast Fourier Transform analysis are also obtained. Figure 5-18 represent the phase voltage output waveform where the amplitude and time in period represented in obtaining the opposite phase to eliminate the harmonics generated whilst figure 5-19 illustrates the line voltage output wave form, injecting the same order of harmonics in opposite amplitude Thus the resultant disorder sine wave is compared with triangular waveform and results in pulses are produced. Figure 5-20 represents the output wave form for Selective Harmonic Elimination (SHE) with LC-section, this shows RGB Harmonics of amplitude in Voltage vs. Output Current in Time (ms). Figure 5-21 shows the FFT analysis of Selective Harmonic Elimination (SHE) with fundamental frequency of 50 Hz we got 113.3 and the Total Harmonic

Distortion of 70.06% this is obtained by without using the LC filter. Fig 5-22 FFT analysis of Selective Harmonic Elimination (SHE) with fundamental frequency of 50 Hz we got 113.3 but the Total Harmonic Distortion is reduced up to 1.47% this results is produced by using the LC filter. Thus the result shows that the Selective Harmonic Elimination (SHE) technique is improved by reducing the Total Harmonic Distortion (THD) up to 1.47%.

The above presented shows a selective harmonic elimination application technique for three phase voltage source inverter with the RL load. A Three phase Voltage Source Inverter (VSI) changes DC input voltage to a three phase variable frequency variable voltage output. The elimination of specific low-order harmonics from a given voltage/current waveform achieved by Selective Harmonic Elimination (SHE) technique. We unite the inductor filter with the capacitor the ripple aspect will turn out to be more or less autonomous of the load filter. Finally Analysis and comparison of Total Harmonic Distortion (THD) for sinusoidal Pulse Width Modulation (PWM) technique and selective harmonic elimination technique has been done. From the comparison it is very apparent that the Total Harmonic Distortion (THD) for selective harmonic technique is less than that of sinusoidal Pulse Width Modulation (PWM) method.

5.4.4. OVERVIEW OF GA, NR AND PSO

Various modulation techniques are used in controlling the effects of output voltages of a typical multilevel inverter (MLI). According to research, these modulation methodologies can be classified considering the magnitude of the switching frequency depending on the techniques used for either low or high frequencies (Liu H, 2015). Research also advocates for the space vector control and the selective harmonic elimination for being the most ideal techniques with the lowest switching of about one or two times during a cycle therefore making the technique an ideal one to be used for our MLI.

Eliminating the specific harmonics especially low-order harmonics of the output voltage of a Multilevel inverter using SHE-PWM control scheme is investigated. Harmonic minimization is the intricate optimization problems because the nonlinear transcendental equations have multiple local optima (A Ajani, 2013). Increasing the degrees of freedom in the suggested method means that the number of switching angles increases (Olla A, 2015). The suggested method is able to eliminate high number of undesired harmonics through the application of SHE which results in lower switching losses and less EMI due to its low switching (A Ajani, 2013). Furthermore, it can eliminate some of the dominant low order Harmonics and hence minimize the size of the required filter at the inverter output.

5.4.5. SELECTIVE HARMONIC ELIMINATION USING GENETIC ALGORITHM

The main problem with the selective harmonic elimination method is how to solve the nonlinear equations. Analytical approaches can find solutions of these equations, but if switching angles needs to be determined are increased, the system becomes very complex to solve (Almari B, 2015). Thus, optimization algorithms can be very useful. Genetic Algorithm has three major differences from other traditional optimization methods. It can process an encoding set of parameters, it searches a population of points in parallel, and it uses probabilistic rules rather than deterministic rules (Rashad M, 2015). GA is considered simple and easy to implement as it does not include complex derivations or mathematical modelling. It can therefore be easily applied to solve the problem of selective harmonic elimination. Its implementation consists of: 1) Initialization of the population, 2) Evaluation of fitness function, 3) Selection, and 4) Apply genetic operators. Figure (5-23) presents a general flow chart for genetic algorithm.

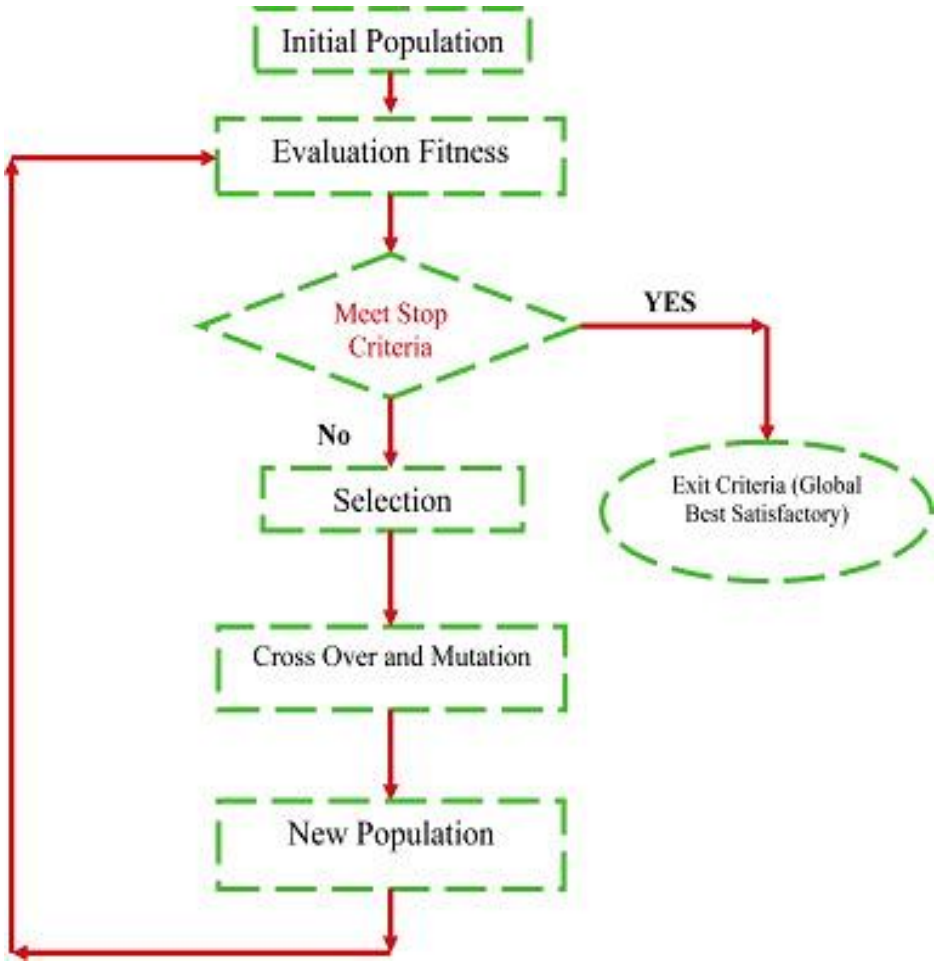

Figure 5-23Flow chart of the GA optimization technique

- ***Initialisation of the population:*** Initial population plays an important role in heuristic algorithms such as GA as it helps to decrease the time those algorithms need to achieve an acceptable result. Furthermore, it may influence the quality of the final answer given by evolutionary algorithms. Parameters of the optimization problem are coded in a binary or floating-point string followed by a set of solutions which is randomly generated based on the coded parameters referred to as "initial population" (Pi)
- ***Evaluation of fitness Function:*** The most vital item for the GA to evaluate the fitness of each chromosome is the cost function. The purpose of this study is to minimize specified harmonics; therefore, the fitness function has to be associated to THD. In this work the fifth, seventh, eleventh, and thirteenth harmonics at the output of an eleven-level inverter are to be minimized.

$$FV = \frac{\sqrt{\sum n = 5,7,11,13,21(\frac{1}{n}\sum_{k=1}^{5}\cos(n\alpha K))^2}}{\sum_{k=1}^{5} Cos\alpha k} \ldots\ldots\ldots\ldots (51)$$

For each chromosome a multilevel output voltage waveform is produced using the switching angles in the chromosome and the required harmonic magnitudes are calculated using FFT techniques. GA is typically set to run for a certain number of iterations to get an answer. After the first iteration, FV's are used to determine new offspring. These go through crossover and mutation operations and a new population is created which goes through the same cycle starting from FV evaluation (Kumar D et al, 2012).

- ***Selection:*** At selection stage, parents are chosen based on selection rules to produce offspring chromosomes (Almari B, 2015). The selected parents are the main contributors to form the next generation. In this the fittest individual are likely to survive and the less fit are eliminated.
- ***Crossover & mutation:*** Crossover is the most significant operation in GA. It creates a group of children from the parents by exchanging genes among them. The new offspring contain mixed genes from both parents. By doing this, the crossover operator not only provides new points for further testing within the chromosomes, which are already represented in the population, but also introduces representation of new chromosomes into the population to allow further evaluation on parameter optimization (Kumar D et al, 2012. Mutation is another vital operation. It works after crossover operation. In this operation, there is a probability that each gene may become mutated when the genes are being copied from the parents to the offspring. This process is

repeated, until the preferred optimum of the objective function is reached (Singh H et al, 2014).

- ***New Population:*** New population is when a solution has been reached basing this on the fact that the algorithm should stop after 100 iterations are performed which in some cases, the algorithm finds a solution much earlier before 100 iterations converges, it tells the algorithm when to stop and terminate. Hence, it decides the optimum solution as an output.

5.4.6. SELECTIVE HARMONIC ELIMINATION USING NEWTON RAPHSON METHOD

Selective Harmonic Elimination technique has been applied on chosen multilevel inverter configuration and nonlinear transcendental SHE equations set have been developed. In order obtain analytical solution during whole range of modulation index from 0 to 1, deterministic and stochastic algorithms have also been developed. Newton-Raphson method is one of the traditionally preferred iterative methods to solve non-linear transcendental equations. This method based on calculus approach is a fast iterative method with fast convergence to reach global minimum, begins with an initial guess and generally converges at a zero. Newton's method was first described by Isaac Newton in 1969, twenty years later Joseph Raphson got close to Newton's approach but only for polynomials of degree up to ten. Finally in 1740, Thompson Simpson explained NR method as an iterative method to solve optimization problems by setting the gradient to zero (BBC, 2016). H. S. Patel et al (1973), first applied NR method to solve SHE equations to eliminate harmonics in the half-bridge and full bridge inverter output waveforms. Later in literature several authors have used NR method to solve non-linear transcendental SHE equations (Rashad M, 2015). Though, this technique is an extremely powerful and fast iterative method to solve non-linear equations, it suffers from the drawback of requirement of good initial guess. If the initial guess is good, rate of convergence is fast and computational time is reduced (H. S. Patel et al, 1973). Providing good initial guess is greatly dependent on previous history. However, probability of providing good initial guess is very low in most cases. Since the search space of the SHE problem is unknown, and one does not know whether a solution exists or not, and if exists, what is the good initial guess (Liu H, 2005). Hence, in order to overcome the above mentioned drawback, Jagadeesh Kumar et al (1985) have used an approach of "any random initial guess" to obtain analytical solution for solving SHE equations by using Newton-Raphson method. Figure 5-24 shows Newton Raphson method

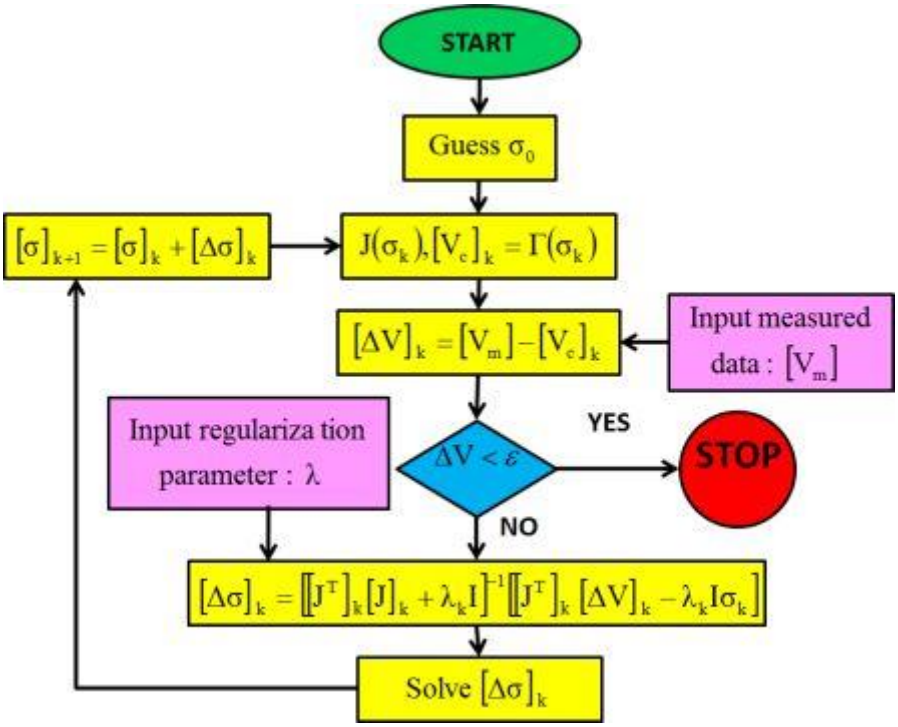

Figure 5-24 Flow chart of the NR optimization technique

Main steps for NR method are

Step 1: Assume any random Initial Guess (say α_0)

Step 2: set $M_I = 0$

Step 3: Calculate $F(\alpha_0), B(M_I)$ and Jacobian Matrix J (α_0)

Step 4: Calculate error $\Delta\alpha = \alpha_0 \left[\frac{\delta F}{\delta \alpha}\right]^{-1} [B[M_I] - F[\alpha_0]]$

Step 5: Update the switching angle i.e.$\alpha(n+1) = \alpha(k) + \Delta\alpha(n)$

Step 6: repeat the steps (3) and (5) for sufficient number of iterations to attain error goal

Step 7: Increment M_I by a fixed step

Step 8: repeat steps (2) to (7) for complete range of M_I

Where (B) represent the values of required harmonic amplitudes, (M) Modulation index, (f) frequency

5.4.7. SELECTIVE HARMONIC ELIMINATION USING PARTICLE SWARM OPTIMISATION (PSO)

Particle swarm Optimization is a computational method used for optimizing a problem by iteratively solving the candidate solution (S Selvaperumal et al 2012). It is a metaheuristic approach as it makes few or no assumptions about the problem to be optimized. The system was initialized with a population of random solution and optimized by updating generations. PSO had no evolutionary operators such as crossover and mutation (S. Muralidharan et al, 2015). PSO had been successfully applied in many areas like function optimization, artificial neural network training, fuzzy system controller etc. (BBC, 2016).

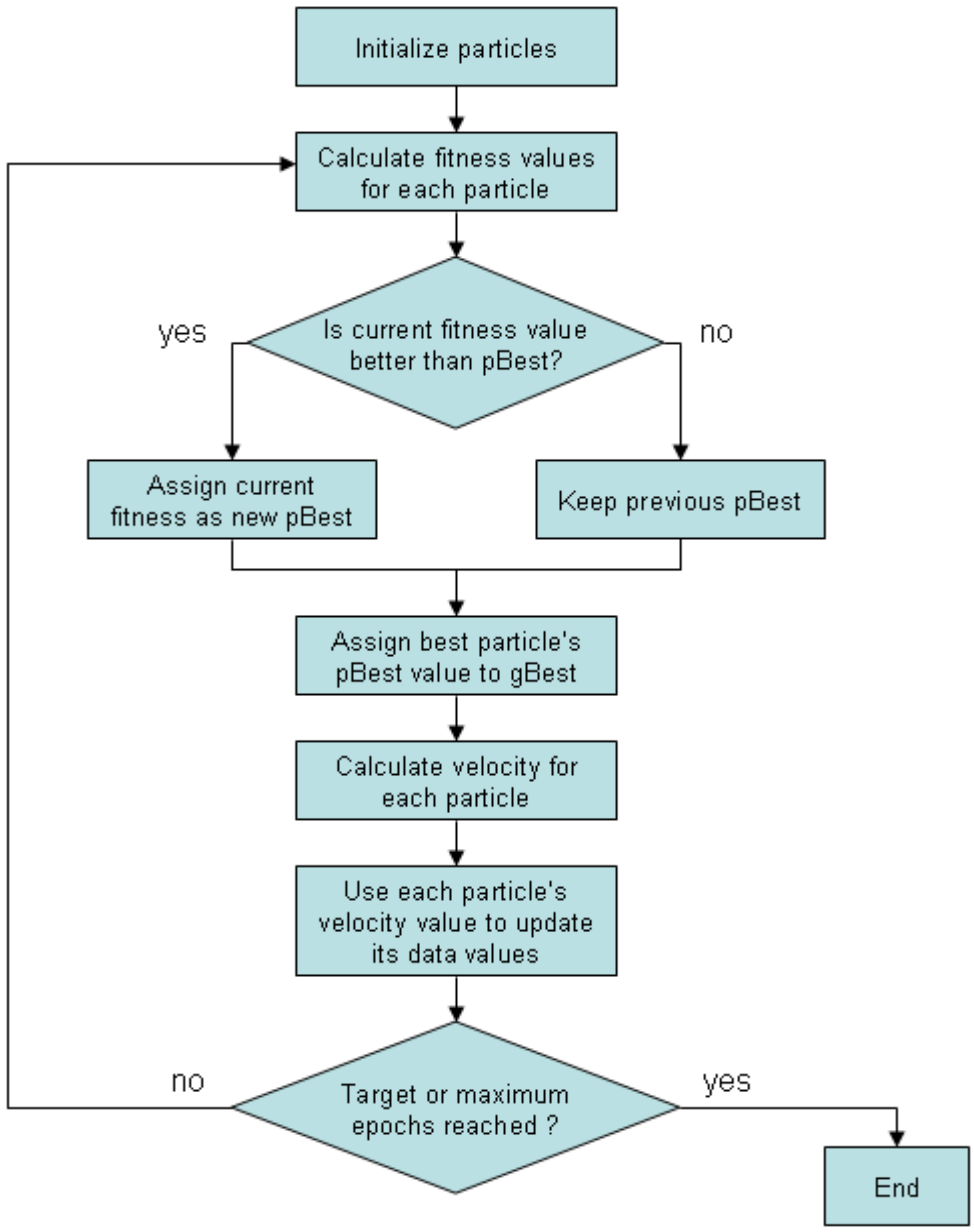

Figure 5-25 Flow chart of the PSO technique

At first, PSO algorithm was used to discover the birds flying patterns and their sudden route alteration. Swarm members called particles can be led to obtain the best solution using the experiences of all particles or social intelligence approach (M. Omid, 2013). Since all particles cooperate to reach the aim, this method is more effective than the methods which individual agents act (M. Yousefi, 2013). In fact, the particles reform their movement toward the aim according to the best previous position of themselves and other neighbours in every iteration. In PSO, the velocity and position of particles are updated using the following equations respectively. These equations are the main part of updating particles experiment in searching space.

$$V_i(t+1) = w \times V_i(t) + C_1 \times rand_1\big(Pbest_i(t) - x_i(t)\big) + C_2 \times rand_2(Gbest_i^{(t)} - x_i^{(t))} \ldots (52)$$

$$x_i^{(t+1)} = x_i^{(t)} + V_i^{(t+1)} \ldots . (53)$$

where 'i', 't', 'v', 'x', 'rand', 'Pbest' and 'Gbest' are particle number, iteration number, particle velocity, particle position, random function, the best position ever visited by particle i and the best position discovered so far, respectively. In addition, 'w', 'C1' and 'C2' are positive constant, which are called inertia weight and acceleration coefficients. Figure 5-25 provides PSO flowchart for which

Step 1 **-** Initialize swarm: Randomly generate bounded real values to form initial swarm of particles. Each particle represents the unknown parameters of neural network. The initial swarm is scattered enough for better search space for the algorithm

Step 2 -Initialization: Following parameter values assigned for algorithm execution. Set the number of flights. Set the fitness limit and start cycle count. Set the values of individual best and global best acceleration factors. Set the value of inertia weight ω and maximum velocity vmax.

Step 3- Fitness Evaluation: Calculate fitness by using the fitness function given in the expressions below

$$e_1^j = \frac{1}{N}\sum_{i=0}^{8}\left[D^v \hat{y}(t_i) - f\left(t_i, \hat{y}(t_i), D^n \hat{y}(t_i)\right)\right]^2 j \ldots . (54)$$

Where s is the number of time steps,y, $D^n\hat{y}$ $D^v\hat{y}$ are the linear combination of the networks. The value of s is adjusted as a trade-off between the computation complexity and the accuracy of algorithm. Similarly e_1^j is linked with initial and boundary conditions and can be written as

$$e_2^{=j} = \frac{1}{N}\sum_{k=0}^{N-1}\left[D^k \hat{y}(0) - c_k\right]^2 + \frac{1}{N}\sum_{k=0}^{N-1}\left[D^k \hat{y}(t_b) - b_k\right]^2 j \ldots . (55)$$

Step 4-Ranking: Rank each particle of the swarm on the basis of minimum fitness values. Store the best fitness particle.

Step 5 - Termination Criteria: Terminate the algorithm if either predefined fitness value, i.e., MSE $10^{-8}$for linear FDEs and $10^{-4}$for non-linear FDEs is achieved or number of maximum flights/cycles is reached. If yes go to Step 7 else continue.

Step 6- Renewal: Update the Velocity using Equation (49). Update the position using Equation (5.3). Repeat the procedure from Step 3 to Step 6 until total number of flights is reached.

Step 7- Refinement: MATLAB optimization toolbox is used for simulating annealing algorithm for further fine-tuning by taking the best fitted particle as start point of the algorithm. Store the value of fitness along with the best particle for this run. Stop.

As a preliminary study of this research work, the ability of NR, PSO and GA to solve the SHE problem of a seven-level CHB-MLI was investigated

5.4.8. Evaluation of GA, NR, PSO

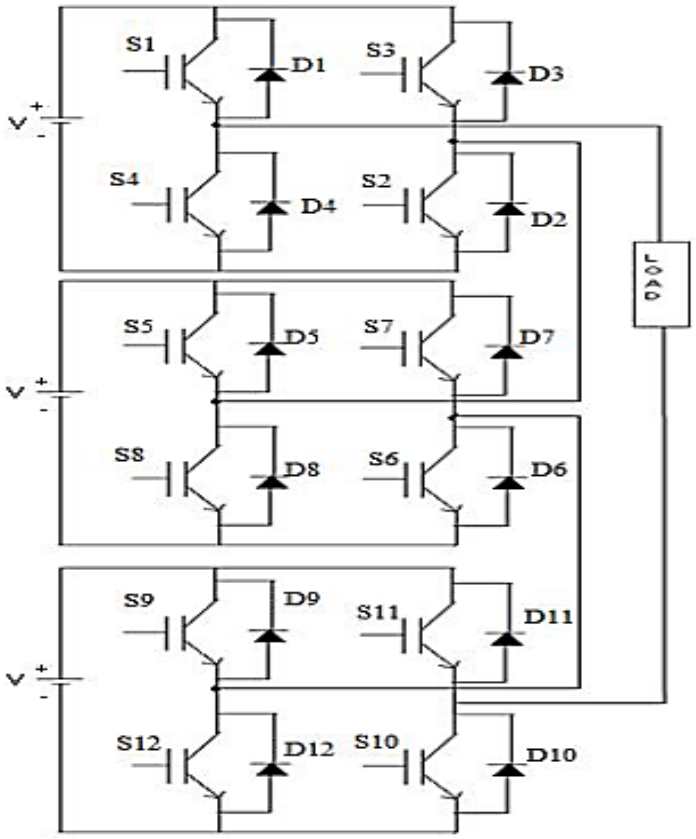

Figure 5-26 Single-phase 7-level cascaded H-bridge inverter

Figure 5-26 shows a single phase 7-Level CHB-MLI for which the switching devices have been selected as an IGBT type. Each cell in the system is connected to a separate dc link supply of potential difference 100 V. The Modulation index is set to vary over a modulation range of (0 to 1) throughout the analysis.

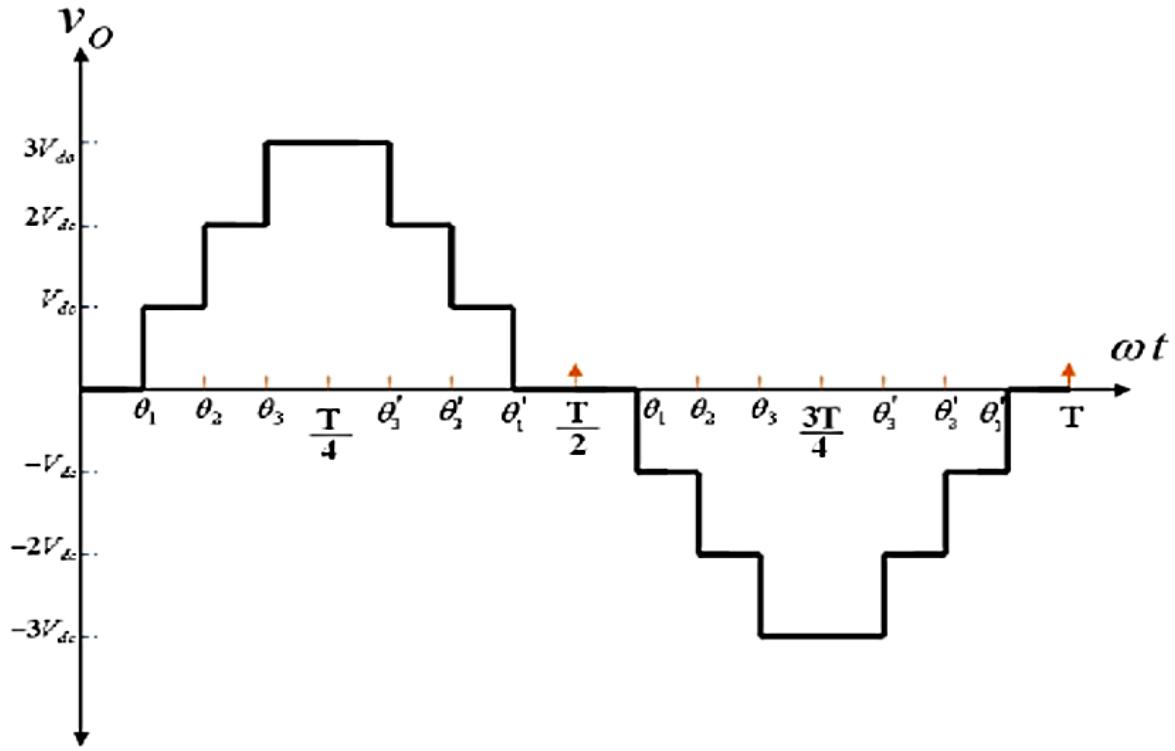

Figure 5-27 Output voltage of the 7-level asymmetric cascade inverter

Selective harmonics elimination uses pre-defined switching angles in order to form the anticipated multilevel fundamental voltage and thereby supress low order harmonics in order to achieve a minim harmonic distortion in total (THD). In this system, the switching angles are pre-calculated off-line therefore it is considered an open loop control technique. In our endeavour to achieve low THD, we applied Fourier's expansion, so as the asymmetric cascade inverter stepped voltage wave form can be expressed in sum of sine and cosine periodic signals and a constant. As one can notice, due to the quarter symmetry of the waveform, the even harmonics and the dc constant are cancelled therefore, only odd harmonics are considered. For balanced three phase systems all tripled harmonics are zero. Ideally, the output voltage waveform can be written as:

$$v_{an}(wt) = \sum_{K=1,3,5}^{\infty} \frac{4V_{dc}}{k\pi}[\cos(k\alpha_1) + Cos\,(k\alpha_2) \ldots . + Cos\,(k\alpha_2)]Sin(kwt) \ldots (56)$$

Where (S) is the number of H-bride cells of the inverter

Considering the output voltage of the 7 level asymmetric cascade inverter, we can deduct that the switching angles are less than a right angle and in ascending order. As it must be with a 7 level MLI, $\theta 1$ is < $\theta 2$ is < $\theta 3$ is < 90°. The fifth and seventh harmonic were also eliminated using non-linear equations approach where the modulation index was introduced and used in our equations. This system of equations are highly non-linear and are also called transcendental equations. Resolving such systems, therefore requires the application of different techniques. The most common algorithms in solving SHE have already been investigated thus Newton-Raphson (NR), Genetic Algorithm (GA) and Particle Swarm Optimization (PSO). The results obtained by these techniques are compared and discussed using Matlab –Simulink has been used considering a modulation index ($M_i = 0.05\ to\ 1.0$)

Table (5-4), shows the detailed calculations of switching angles and THD at each modulation index value with the "**" indicating that the algorithm failed to find a feasible solution at that point of modulation index

CALCULATION OF SWITCHING ANGLES AND THD OBTAINED USING DIFFERENT SOLVING TECHNIQUES

B. Alamri and M. Darwish, "Optimum Switching Angles Determination for Cadcaded H-Bridge Multilevel Inverters Using Genetic Algorithm (GA)", ResCon, Brunel University, London, UK, 2014. [Accessed 10 May 2017].

CONTENT REMOVED FOR COPYRIGHT REASONS

Table 5-4 calculation of switching angles and THD obtained using different solving techniques

Using data in table 5-4, comparison graphs were plotted as it can be seen from figure 5-28 and 5-29. The simulations showed that the application of the Newton Raphson method was not the most ideal solution for this MLI as it was unable to find a solution for the complete range of modulation index thus (0.05 to 1) but does find a solution for the modulation index range ranging between (Mi = 0.3 to 0.9).

The application of the Genetic Algorithm and the Particle Swarm Optimisation however were able to define solutions for the complete range of modulation index (Mi = 0.05 to 1.0). It is to be noted that the Newton Raphson method was excellently ideal in eliminating the selected harmonics, whilst the Genetic Algorithm and the Particle Swarm Optimisation were capable of minimizing the THD thereby eliminating the harmonics. It is therefore easy to say that the application of the Genetic Algorithm and the Particle Swarm Optimisation in this case were much suited in minimizing the THD as compared to the Newton Raphson method. Figure (28) present a comparison of THD obtained for different modulation index values using NR, GA and PSO with NR having the worst THD profile and GA being the most ideal approach to minimising THD. Figure (29) on the other hand presents the THD for each solving method used.

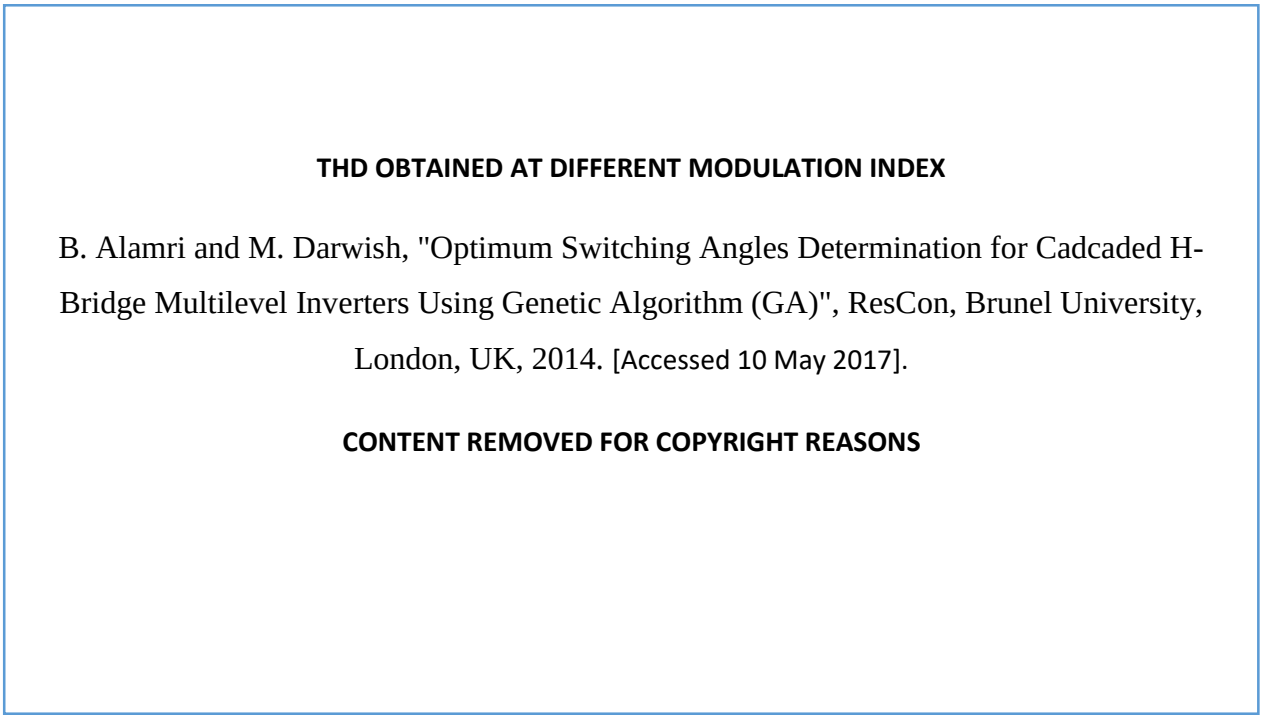

Figure 5-28 THD at different modulation index values

THD PROFILE OBTAINED FOR EACH SOLUTION

B. Alamri and M. Darwish, "Optimum Switching Angles Determination for Cadcaded H-Bridge Multilevel Inverters Using Genetic Algorithm (GA)", ResCon, Brunel University, London, UK, 2014. [Accessed 10 May 2017].

CONTENT REMOVED FOR COPYRIGHT REASONS

Figure 5-29 THD profile for each solving technique.

SWITCHING ANGLES OBTAINED FOR NEWTON RAPHSON, GENETIC ALGORITHMS, PARTICLE SWAM OPTIMISATION

B. Alamri, A. Sallama and M. Darwish, "Optimum SHE for Cascaded H-Bridge Multilevel Inverters Using: NR-GA-PSO, Comparative Study," AC and DC Power Transmission, 11th IET International Conference on, Birmingham, pp. 1-10. 2015,

[Accessed 10 May 2017].

CONTENT REMOVED FOR COPYRIGHT REASONS

Figure 5-30 Switching angles using NR-GA-PSO.)

HARMONIC PROFILES OBTAINED FOR NEWTON RAPHSON, GENETIC ALGORITHMS, PARTICLE SWAM OPTIMISATION

B. Alamri, A. Sallama and M. Darwish, "Optimum SHE for Cascaded H-Bridge Multilevel Inverters Using: NR-GA-PSO, Comparative Study," AC and DC Power Transmission, 11th IET International Conference on, Birmingham, pp. 1-10. 2015,

[Accessed 10 May 2017].

CONTENT REMOVED FOR COPYRIGHT REASONS

Figure 5-31 Harmonic profile using NR-GA-PSO.

Figure (5-30) above shows a comparison of all the calculated switching angles obtained for NR, GA and PSO. The analysis of this shows that the application of the GA and PSO results partly in similar switching angles. The comparison of harmonic profile however in figure 5-31 shows that considering the 5th harmonic, the Newton Raphson method had the lowest value of THD whilst the Particle swarm optimisation had the highest THD in comparison with the other methods. We can easily say at this point that the application of the GA technique has the best performance for Selective Harmonic Elimination whilst NR technique had the worst performance in this case. Considering the investigation for this 7 level MLI, we can say that the problem of SHE into an optimization problem is made possible through the application of heuristic algorithms such as GA, PSO, and NR.

5.5. OVERVIEW OF FILTERS IN MULTILEVEL INVERTERS

Power quality and their steady state have become topics of research interest because of widespread use of nonlinear loads such as diode / thyristor rectifiers, SMPS, UPS, induction motor drives etc. (Alexander B, 2003). These nonlinear loads effect in harmonic or distortion current and reactive power problems (Joseph W, 1990).

The harmonics induce malfunctions in sensitive equipment, overvoltage by resonance, increased heating in the conductor, harmonic voltage drop across the network impedance and affect the other customer loads at the point of common coupling (W. M. Grady, 2000).

Traditionally passive filters have been used to compensate the harmonic distortion and the reactive power; but passive filters are large in size, have aging and tuning problems and resonate with the supply impedance (F. Barrerro, 2000). Recently Active Power Line Conditioners (APLC) or Active Power Filters (APF) overcome these problems and are used for compensating the current harmonics and suppressing the reactive power simultaneously due to fluctuating loads (Bhim Singh, 1999).

It is therefore important to understand the role played by both active and reactive power filters in Multilevel inverters especially considering IEE 519 regulations stipulating that for electrical systems that include both linear and nonlinear loads IEEE Recommended Practices and Requirements for Harmonic Control In Electric Power Systems for voltages levels up to 69 kV, THD_v should be kept under 5%, and non-individual voltage harmonics should exceed 3%. Similarly, THD_i follows the standards limits according to the system short-circuit ratio (IEEE, 1992).

5.5.1. PASSIVE FILTERS

SHUNT FILTERS

B. Alamri, A. Sallama and M. Darwish, " Losses investigation in SPWM-controlled cascaded H-bridge multilevel inverters," Power Engineering Conference (UPEC), 2015 50th International Universities, Stoke on Trent, pp. 1-5. 2015

[Accessed 10 May 2017].

CONTENT REMOVED FOR COPYRIGHT REASONS

Figure 5-32 Shunt Filters

Figure 5-32 shows the a summary of a series of passive filters selection matrix based on various conditions namely RL series, RLC shunt tuned and RLC high pass.

RL Series filters are used to block a single harmonic current (such as the third harmonic) and are especially useful in a single-phase circuit where it is not possible to take advantage of zero sequence characteristics. The use of the series filters is limited in blocking multiple harmonic currents. Each harmonic current requires a series filter tuned to that harmonic. A series passive filter is connected in series with the load. The inductance and capacitance are connected in parallel and are tuned to provide a high impedance at a selected harmonic frequency. The high impedance then blocks the flow of harmonic currents at the tuned frequency only. At fundamental frequency, the filter would be designed to yield a low impedance, thereby allowing the fundamental current to follow with only minor additional impedance and losses The ideal harmonic filter can be seen as a device that is capable of completely eliminating reactive current whilst a low pass RL filter is required at the output terminal of inverter to reduce harmonics generated by the pulsating modulation waveform. While designing R-L filter, the cut-off frequency is chosen such that most of the high order harmonics are eliminated.

The RLC Shunt Harmonic Passive Filter (SHPF) as shown in Figure 5-32 is generally a series RLC circuit configured in parallel arrangement with the AC to DC converter. Its application ensures low impedance path to the harmonic currents flowing into the Power distribution system connected with nonlinear loads. The Impedance – frequency characteristics describe that impedance value exponentially decreases with the increase in the frequency and it ceases at 5th harmonic frequency but later on, linearly increases for higher frequencies.

RLC High pass is generally a series RLC circuit configured in parallel arrangement with the AC to DC converter. The filter passes signals with a frequency higher than a certain curt off frequency and attenuates signals with frequencies lower than the cut-off frequency. High-pass filters are the second category of shunt filters. Its operation principle is to provide low impedance for a wide spectrum of frequencies higher than the cut-off frequency but its implementation is considered mostly due to the filter providing high impedance for frequencies lower than the cut-off frequency

5.5.2. ACTIVE FILTERS

SHUNT FILTERS

B. Alamri, A. Sallama and M. Darwish, " Losses investigation in SPWM-controlled cascaded H-bridge multilevel inverters," Power Engineering Conference (UPEC), 2015 50th International Universities, Stoke on Trent, pp. 1-5. 2015

[Accessed 10 May 2017].

CONTENT REMOVED FOR COPYRIGHT REASONS

Figure 5-33 Shunt Filters (Almari B, 2016)

The major problems caused by the mains harmonic currents are those associated with the harmonic currents themselves, and those caused by the voltage waveform distortion resulting from the harmonic currents flowing in the supply source impedance. This distortion of the voltage waveform can cause, e.g. serious effects in direct on-line induction motors, ranging from a minor increase in internal temperature through excessive noise and vibration to actual damage; electronic power supplies may fail to operate adequately; increased earth leakage current through EMI filter capacitors due to their lower reactance at the harmonic frequencies. To minimize these effects in electricity distribution systems (non-sinusoidal voltages, harmonic currents, unbalanced conditions, power de-rating, etc.) different types of compensators have been proposed to increase the electric system quality, (Bollen, 1999, Hingorani & Gyugyi, 1999). One of those compensators is the active power filter (APF), (Atagi et al., 1984).

An active power filter is a high performance power electronics converter and can operate in different modes: harmonics elimination, power factor correction, voltage regulation and load unbalance compensation. Different control approaches are possible but they all share a common objective: imposing sinusoidal currents in the grid, eventually with unity power factor, even in the case of highly distorted mains voltage. Figure 5-33 analyses and compares different approach to be used based on semiconductor devices in the control of an active power filter and provides system advantages and disadvantages. Different approaches such as notch filter, (Newman et al., 2002), scalar control, (Chandra et al., 2000), instantaneous reactive power theory, (Furuhashi et al., 1990, Akagi et al., 2007), synchronous detection method, (Chen et al., 1993), synchronous d–q frame method, (Mendalek et al., 2003), flux-based control, (Bhattacharya et al., 1996), and closed loop PI, (Bhattacharya et al., 1996), internal model control, (Marconi et al., 2007), and sliding mode control, (Saetieo et al., 1995), can be used to improve the active filter performance. Also, the direct power control method has found application in active filters, (Chen & Joós, 2008). Specific harmonics can be cancelled out in the grid using the selective harmonic elimination method (Lascu et al., 2007). In all cases, the goal is to design a simple but robust control system for the filter. Usually, the voltage-source is preferred over the current-source to implement the parallel active power filter since it has numerous advantages, (Routimo et al., 2007). Using higher voltages in the DC bus is desirable and can be achieved with a multilevel inverter (Lin & Yang, 2004).

It is clear that the filter dynamics depends on the switching frequency; higher frequencies given better results but also higher losses. In particular, selective harmonic elimination methods can bring additional performance (Routimo et al., 2007). Also, multilevel based topologies allow the APF to reach higher voltages and power and so give the filter the possibility of being applied in the power systems domain.

Based on this review of filters, the composite PPF was proposed for optimum multilevel inverter design as it features a cost-effective harmonic-elimination solution, a simple structure, reliability and easy implementation. Furthermore, the passive filter has excellent harmonic-mitigation performance compared to active filters and does not require any complex control. In addition, the shunt-tuned and high-pass PPF do not carry full-load current, which considerably reduces power loss and component weight and size.

5.6. Multilevel inverter for the proposed 3D renewable energy platform

In order to define the ideal multilevel inverter system for our proposed 3D renewable energy platform, it is essential to consider the system topology prior to designing and testing. In adopting a system topology, a comparison of the three classical multilevel inverter topologies namely NPC-MLI; FC-MLI, CHB-MLI have been analysed so as to choose the ideal one that fit the aim of this research. A comparison of the Neutral point lamped -MLI; Flying capacitor-MLI, and Cascaded High Bridge-MLI can be found in table 5-5 below.

Figure 34 provides a complete general block diagram for the proposed methodology adopted for the MLI design. The application of this should enable us to have a complete performance evaluation of the MLI for our proposed 3D renewable energy platform

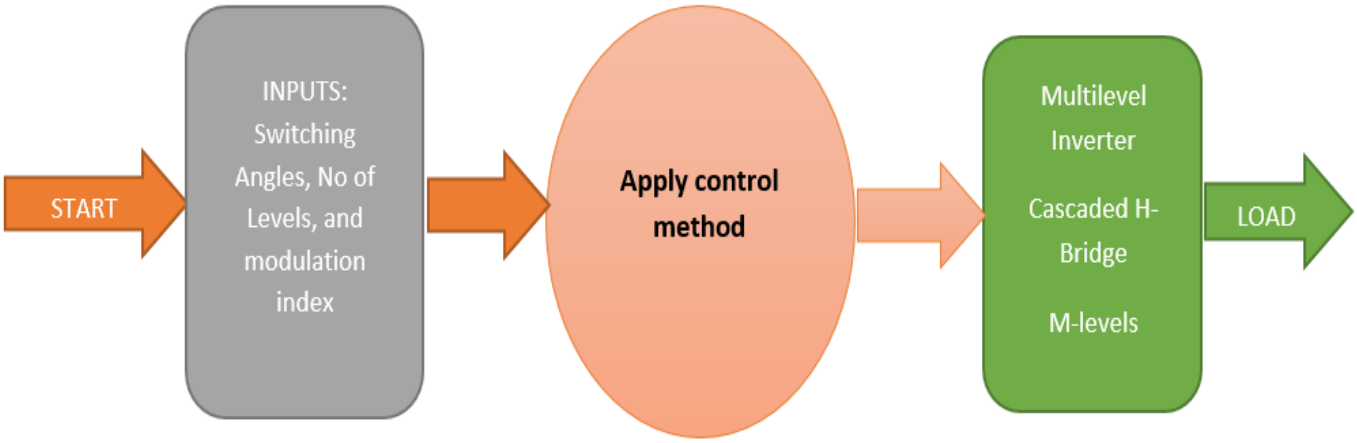

Figure 5-34 General flow model of proposed methodology for MLI design

5.6.1. COMPARISON OF CLASSICAL MULTILEVEL INVERTER

CLASSIC MULTILEVEL INVERTERS COMPARISON

B. Alamri and M. Darwish, "Enhancing Power Quality of Distributed Generator Systems Using Multilevel VSC", ResCon, Brunel University, London, UK, 2013.

[Accessed 10 May 2017].

CONTENT REMOVED FOR COPYRIGHT REASONS

Table 5-5 multilevel inverter topologies (Almari B, 2016)

We could deduct from the findings that for high-power and medium-voltage applications the most ideal topology is the CHB-MLI which in essence represents a realistic and feasible topology compared to other multilevel topologies. The choice of this is mainly due to the fact that in contrast with the use of a two, three or five-level inverter a series of connected semiconductors contributes to unequal voltage-sharing between connected devices therefore bringing reliability issues within the entire system ((Lascu et al., 2007).Considering the neutral-point clamped multilevel inverter (NPC-MLI), it is easy to see that its application is mostly suitable for three levels MLI and design become more complex due to the number of diodes with higher levels MLI. Similar operation and designs are observed with the flying capacitor (FC-MLI) as it needs more capacitors for higher levels leaving us with a clear conclusion that The CHB-MLI topology is ideal for high-power and high-voltage applications.

5.6.2. MODULATION INDEX

As previously discussed, the application of heuristic algorithms provides an efficient solution to SHE challenges than iterative methods. Using MATLAB, simulations are carried out to eliminate low-order harmonics and minimise the %THD by varying the modulation index from 0 to 1. Figure 5-35 shows the application of heuristic solutions thus NR, PSO, GA in order to define which best finds a solution for the entire modulation index. The simulation results as shown in figure 35 proves that the NR was the least heuristic solution for the entire modulation index whilst GA and PSO were able to effectively do that. Nevertheless, results shows that GA has significant advantages as aforementioned and in this case GA is said to be the most efficient solution for the entire modulation index. We can then conclude by saying that the proposed GA could solve the switching angles even in higher levels and implement the optimal SHE control for different inverter levels.

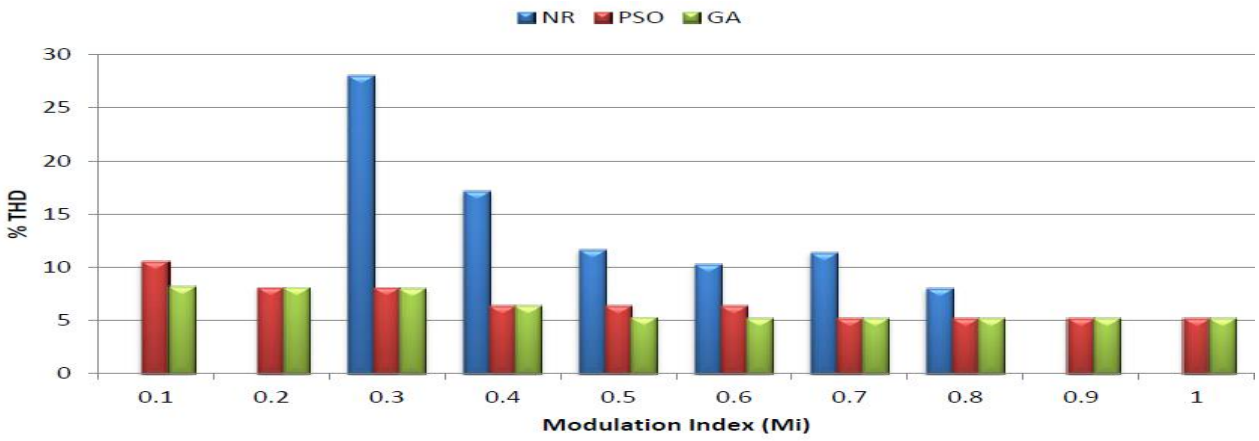

Figure 5-35 Minimum THD obtained for defining SHE solutions using NR-PSO-GA

Applying GA over a number of Inverter number of levels, we were able to generate GA's response and confirm its ability to provide an efficient solution for our proposed 3D renewable energy platform and compared this with the IEEE 519 standard. Figure 5-36 shows at modulation index 0.9 the THD percentage against the number of levels. Our findings shows that when the SHE control is applied, the %THD of the inverter was less than 5%, which is the IEEE-519 standard recommendation for a nine-level inverter and above.

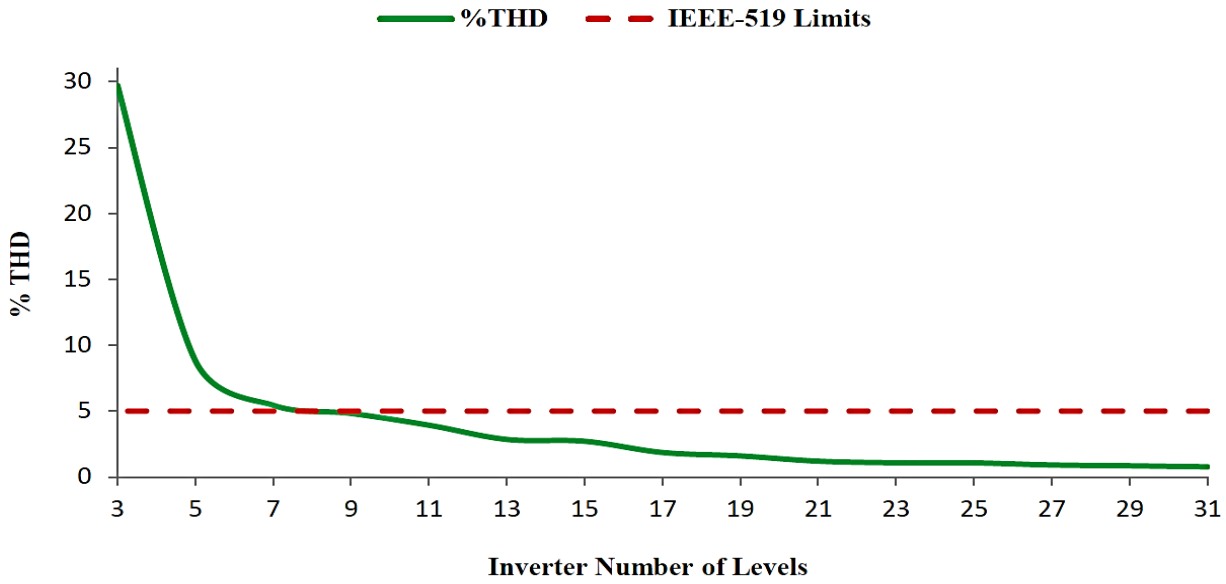

Figure 5-36 %THD versus inverter number of levels at Modulation Index 0.9

5.6.3. SWITCHING ANGLES

Multilevel inverters provide a less THD than other inverters and it can improve with more levels added. One of the drawbacks is the calculation of the switching angles since the more levels are needed, more angles must be calculated and more time is spent in calculation as explained in section 5.7.5 of this report. One of the most used techniques for finding the switching angles is to use the Fourier coefficients to eliminate some harmonics. The number of harmonics to be eliminated is equal to the number of switching angles to be calculated minus one, with this technique. THD for p switching angles is

$$THD = \frac{\sqrt{\frac{\pi^2 P^2}{8} - \frac{\pi}{4}\sum_{I=0}^{P-1}(2i+1)_{a_i+1} - (\sum_{i=1}^{p} Cos(\alpha_i))^2}}{(\sum_{i=1}^{p} Cos(\alpha_i)} \dots\dots (57)$$

Equation (5.7) can be used to minimize THD assuming$0 < \alpha_i < \alpha_{i+1} < {}^{\pi}/_{2}, for\ 1 \le i \le p.$ A computer program can be used to find the switching angles for the minimum THD using the same equation, nevertheless the amount of time of calculation increases with the number of

angles. Calculation of THD requires computing of p cosines, two square roots, 2p summations, p+2 multiplications, and one division, where p is the number of angles to be calculated. Calculation of the minimum THD depends on angle resolution. For one degree resolution the first angle goes from 1° to 89° in steps of 1°, the second angle goes from 2° to 89° and so on, so that for p angles it is needed$\prod_{n=1}^{p}(90-n)/p$. The flowchart of the program is shown in figure 37. The more switching angles are needed, the more for loops must be nested and the program can spent a lot of time running. Applying this technique $\%THDMin = 121.62 \times m^{-1.479}$ where m is the number of inverter levels. Table 6 and 7 provide the optimum switching angles from 3 to 31 different inverter levels solved by Genetic algorithms with a selected modulation index of 0.95 and 0.90 as they have the least %THD as earlier shown in table 4.

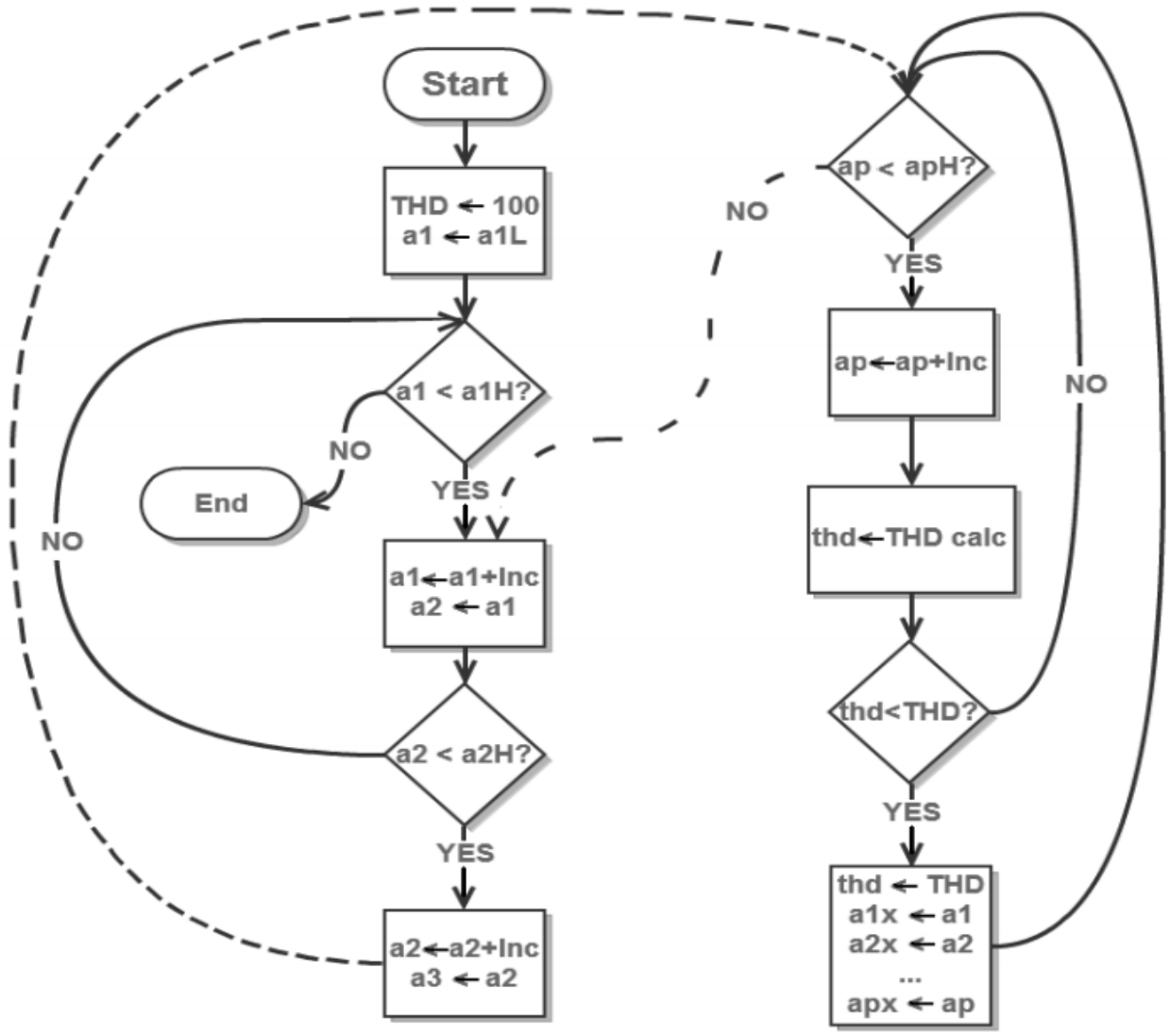

Figure 5-37 Flowchart for switching angles calculation

No of levels	3	5	7	9	11	13	15	17	19	21	23	25	27	29	31
α_1	29.67	9.11	5.56	5.30	3.13	3.54	3.27	2.91	3.82	1.12	2.34	1.62	1.25	1.79	0.72
α_2		26.73	16.68	11.80	8.89	8.55	7.83	5.54	4.29	5.12	3.87	3.96	4.03	2.91	3.26
α_3			35.81	23.07	18.18	12.86	9.65	10.04	8.52	7.95	7.32	7.04	5.69	5.83	5.73
α_4				38.67	27.31	23.08	18.65	14.96	13.44	11.65	10.65	9.22	9.10	8.13	7.71
α_5					41.00	28.83	23.01	19.95	17.25	14.68	13.01	12.66	10.57	10.63	10.10
α_6						42.35	31.62	26.18	22.44	20.24	17.36	14.93	14.12	12.25	11.52
α_7							41.49	32.66	27.73	23.69	21.13	18.97	16.94	16.19	14.78
α_8								42.39	34.28	28.88	25.34	22.67	20.62	17.74	16.13
α_9									43.20	35.12	30.01	26.76	23.54	22.30	20.03
α_{10}										43.5	35.8	31.71	27.83	24.22	22.58
α_{11}											43.1	36.55	31.72	28.74	25.93
α_{12}												43.46	36.94	32.26	29.26
α_{13}													43.53	37.44	33.05
α_{14}														43.41	37.73
α_{15}															43.18
%THD	29.78	8.8	5.31	4.70	3.66	2.31	2.71	1.79	1.76	1.31	1.06	1.01	0.95	1.00	1.08

Table 5-6 Optimum SHE Switching Angles for t Inverter Levels (3-31) with Mi =0.95, Solved by GA

No of levels	3	5	7	9	11	13	15	17	19	21	23	25	27	29	31
α_1	29.69	9.03	5.09	3.29	3.67	4.19	1.52	2.74	2.79	1.23	2.70	0.94	0.64	1.22	1.69
α_2		26.82	16.92	13.24	8.79	8.25	8.48	6.10	4.67	4.65	3.56	4.63	4.15	3.20	2.95
α_3			35.71	23.14	19.89	13.08	10.46	9.80	9.44	9.47	8.00	6.51	6.40	6.71	5.54
α_4				39.96	25.81	23.89	18.63	16.32	13.23	10.56	10.29	9.80	8.53	7.74	8.32
α_5					41.92	28.32	24.21	20.89	18.65	16.28	15.02	13.04	12.91	11.17	9.43
α_6						43.14	32.32	27.07	23.07	20.37	18.24	17.02	14.93	14.80	13.03
α_7							42.88	34.55	28.89	24.75	22.38	19.82	18.65	16.52	15.80

α_8								44.94	35.78	30.61	26.97	23.93	22.03	20.26	18.25
α_9									45.24	36.34	31.83	28.20	25.42	23.35	21.84
α_{10}										45.11	38.32	32.77	29.87	26.80	24.05
α_{11}											46.82	39.04	34.25	31.10	28.32
α_{12}												47.21	40.53	35.14	31.63
α_{13}													48.39	41.30	36.08
α_{14}														48.83	41.46
α_{15}															47.86
%THD	29.78	8.83	5.28	4.70	3.45	2.85	2.97	1.68	1.34	0.99	0.96	0.74	0.63	0.64	0.45

Table 5-7 Optimum SHE Switching Angles for t Inverter Levels (3-31) with Mi =0.90, Solved by GA

Table 5-6 and 5-7 show the optimum SHE switching angles with modulation indexes 0.95 and 0.90. The results validation has been done considering the output voltage waveforms of inverter levels varying from 3 to 31 which were modelled and simulated (please refer to Appendix).

5.6.4. PROPOSED PASSIVE FILTER

In order to propose an ideal filter that would serve as a base line for the design of a 3D renewable energy platform, it is essential to understand electrical distribution network in Togo. Figure 5-38 shows Togo power system from the generating station to consumer's home through a very systematic distribution network. Depending on distribution transformers, 22, 11 or 6.6Kv are used therefore an example of a PPF fit to handle either 6.6,11 or 22KV would suffice in validating the PPF. We therefore consider a 5 MW load at a lagging power factor of 0.8 at the output of CHB-MLI with a rated line-to-line voltage of 11 kV. The ultimate outcome of this, would be to have a PPF at the output of a 17, 19 and 21 levels of CHB-MLI topologies where its implementation should improve the lagging power factor to between (0.92 and 0.98) and reduce the %THD in general.

TOGO POWER DISTRIBUTION NETWORK

Compagnie Energie Electrique du Togo. 2018. [ONLINE] Available at: http://www.ceet.tg/tg/. [Accessed 10 August 2016].

CONTENT REMOVED FOR COPYRIGHT REASONS

Figure 5-38 Togo Power system

Proposed Passive power filter for 17 Level CHB-MLI (11KV L-L)	
Filter Type	High pass
Order	>19th
Size (KVar)	2100
C(µF)	18.41
L(mH)	1.52
R(Ω)	9.1
Quality factor	5
Total Filter Size (kVar)	2100
THD Before Filter (%)	3.06
THD After Filter (%)	1.31

Table 5-8 Proposed Passive power filter for 17 Level CHB-MLI (11KV L-L)

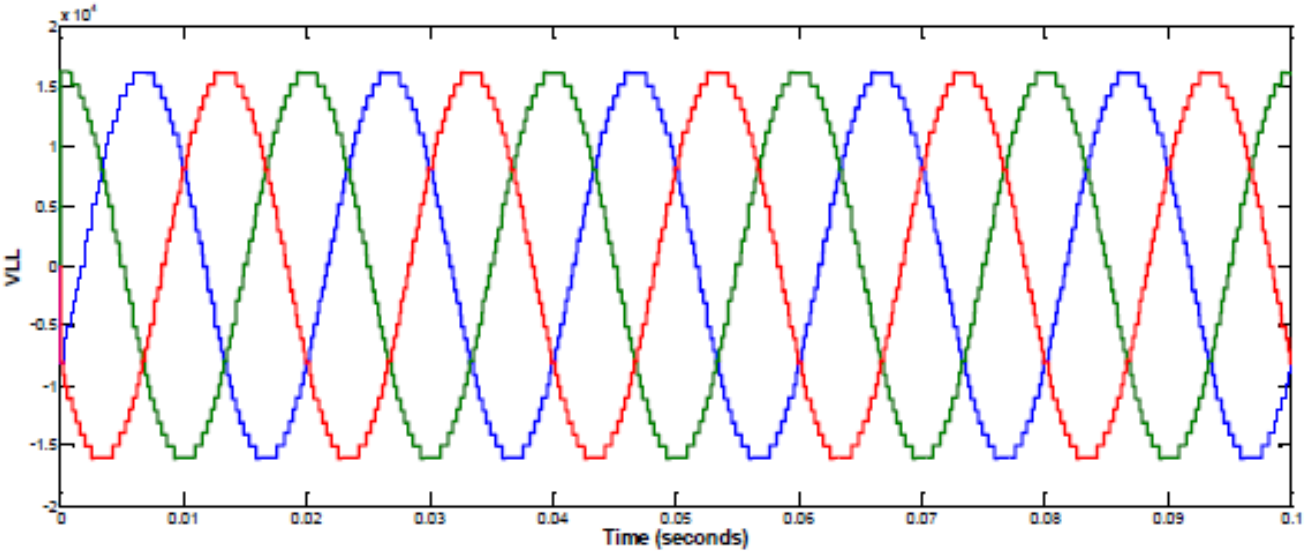

Figure 5-39 Output three-phase voltage before filtering

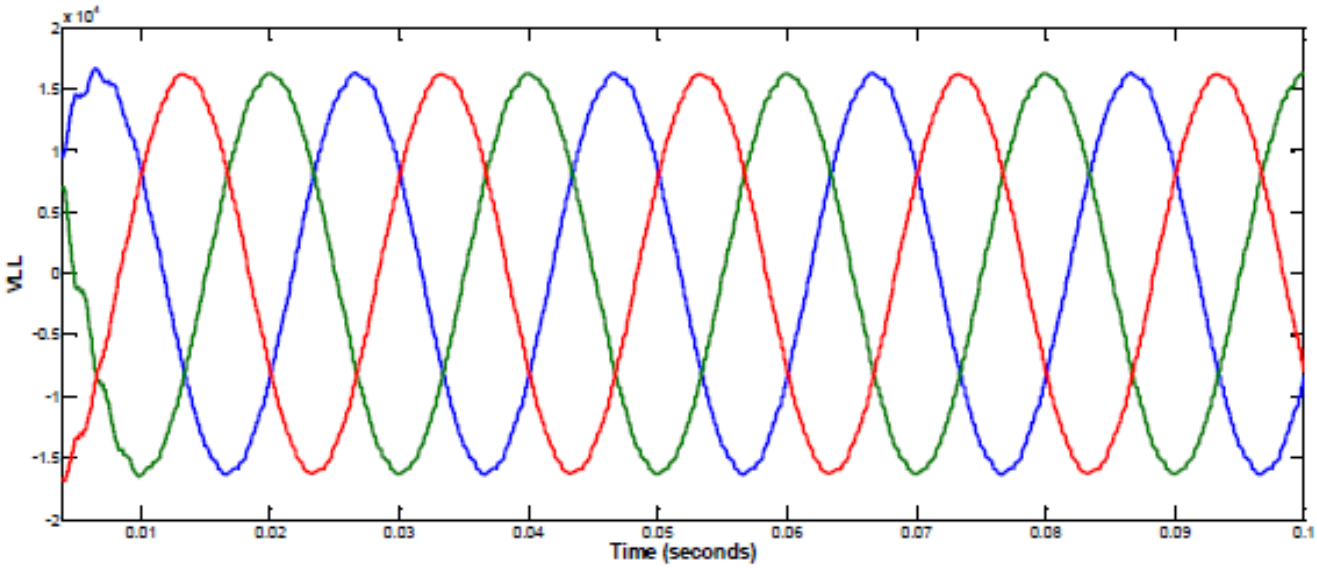

Figure 5-40 Output three-phase voltage after filtering

Proposed Passive power filter for 19 Level CHB-MLI (11KV L-L)	
Filter Type	High pass
Order	>19th
Size (KVar)	1800
C(µF)	15.78
L(mH)	1.78
R(Ω)	10.61

Quality factor	5
Total Filter Size (kVar)	1800
THD Before Filter (%)	2.82
THD After Filter (%)	1.25

Table 5-9 Proposed Passive power filter for 19 Level CHB-MLI (11KV L-L)

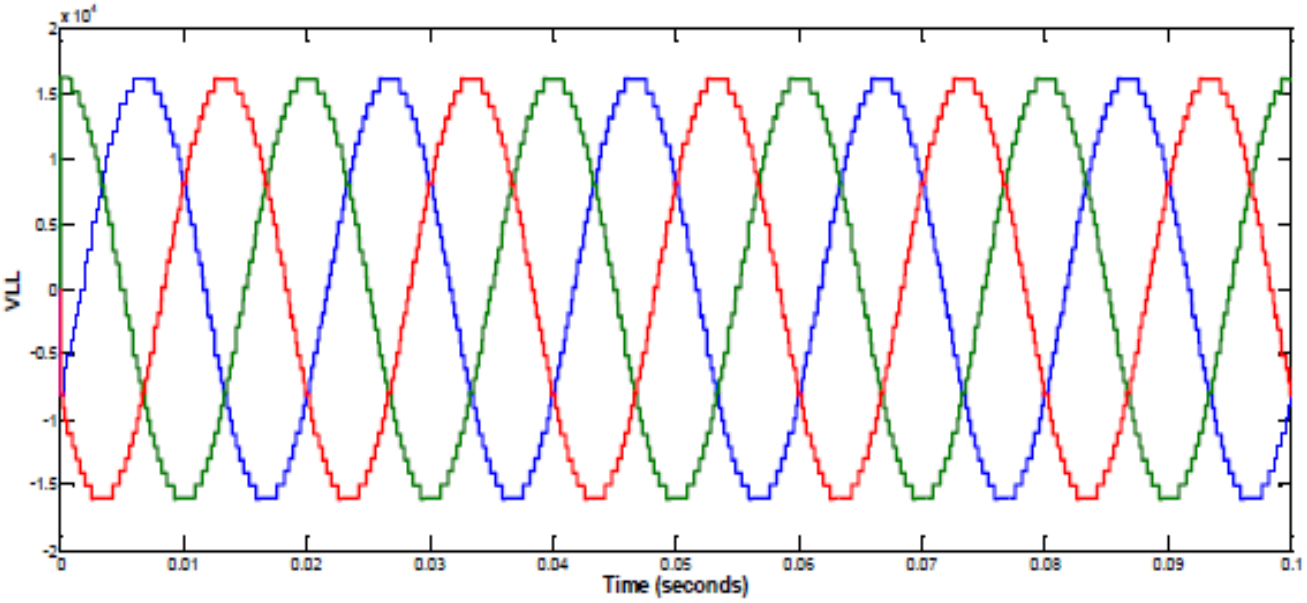

Figure 5-41 Output three-phase voltage before filtering

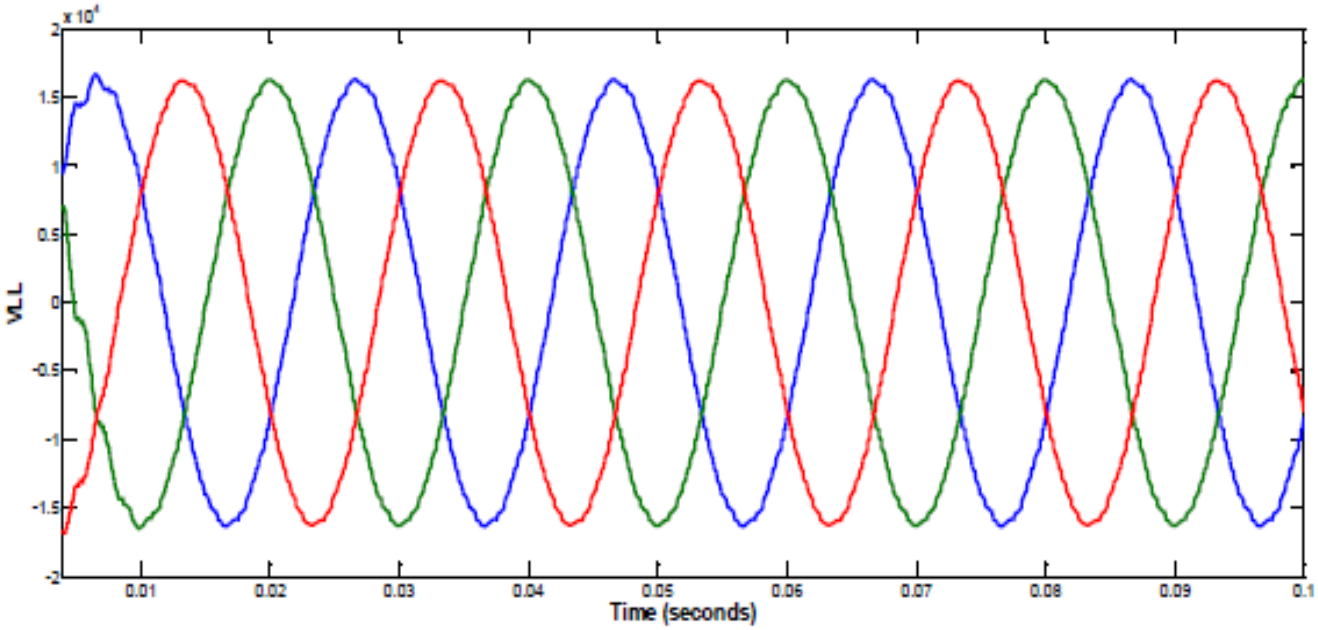

Figure 5-42 Output three-phase voltage after filtering

Proposed Passive power filter for 21 Level CHB-MLI (11KV L-L)	
Filter Type	High pass
Order	>19th
Size (KVar)	1750
C(µF)	1.83
L(mH)	15.34
R(Ω)	10.91
Quality factor	5
Total Filter Size (kVar)	1750
THD Before Filter (%)	2.64
THD After Filter (%)	1.29

Table 5-10 Proposed Passive power filter for 21 Level CHB-MLI (11KV L-L)

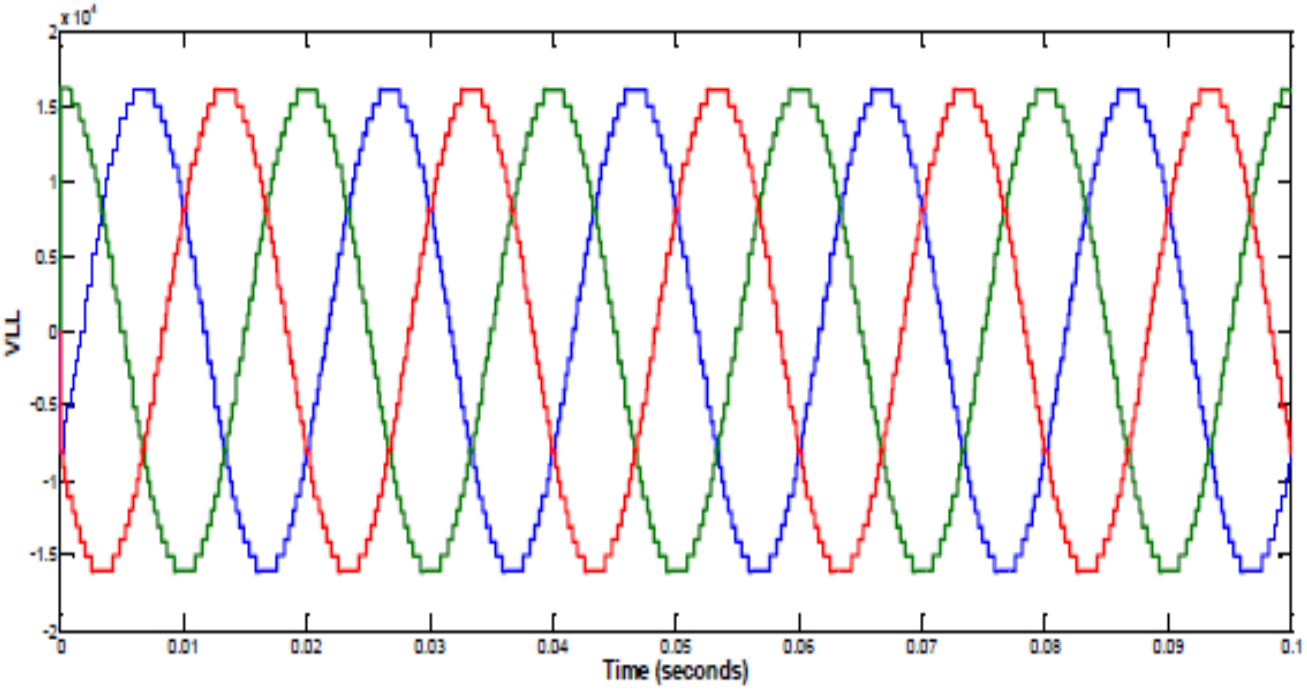

Figure 5-43 Output three-phase voltage before filtering

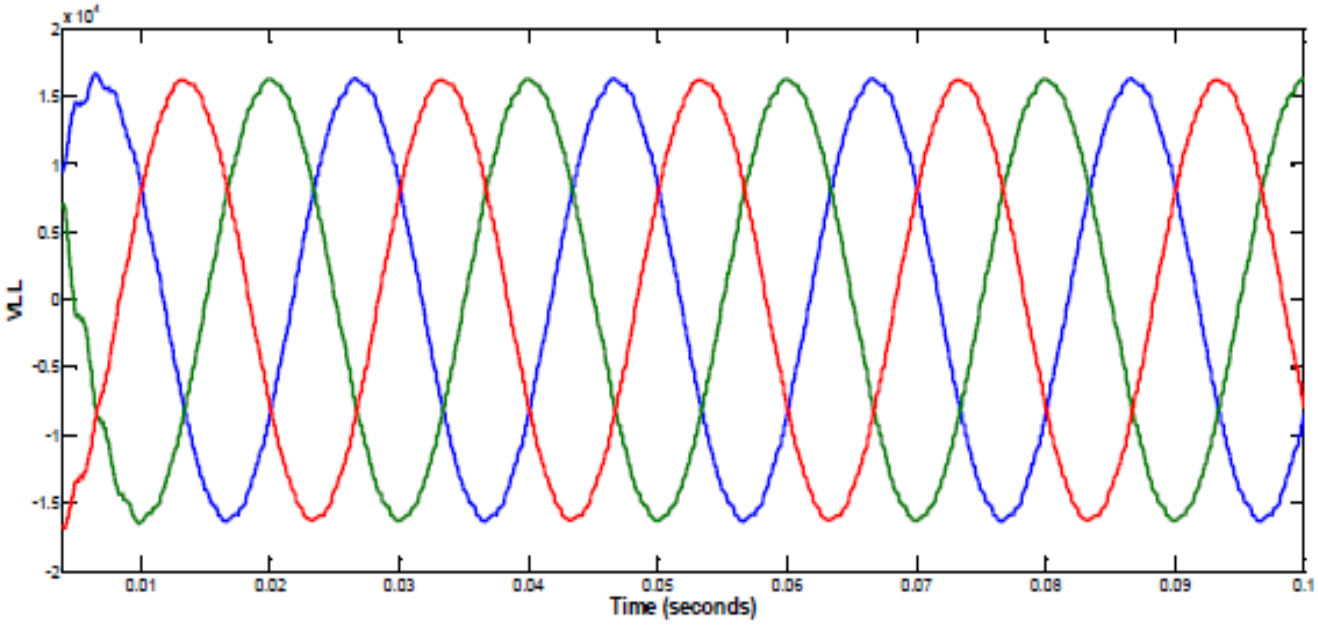

Figure 5--44 Output three-phase voltage after filtering (B Almari, 2016)

Figure 5-39 to 5-44 goes to show the great impact of the PPF over the three phase output voltages. Considering the simulations results, we can say that the three-phase line-to-line voltage waveforms and the associated harmonic profile provides basis for choosing the 21 level multilevel inverter for our design considering its lowest %THD and also the cost associated in designing it. A study conducted on CHB-MLI using SHE further confirms this choice as provided in figure 45 below.

No. Levels	5	7	9	11	13	15	17	19	21
Device Counts	48	36	48	60	72	84	96	108	120
% THD	9.95	6.28	5.7	4.85	4	3.61	3.06	2.82	2.64
P_{loss} (kW)	17.431	16.128	17.467	21.847	26.219	29.018	33.363	24.28	26.92
P_{loss} Cost (£)	87,171	80,657	87,351	109,255	131,119	145,117	166,846	121,422	134,625
IGBT Cost (£)	54,000	72,000	54,000	51,300	61,560	31,500	36,000	23,004	25,560
Total Cost (£)	141,171	152,657	141,351	160,555	192,679	176,617	202,846	144,426	160,185

Figure 5--45 Key Measures of Performance Calculated for Designed Inverters at Different Levels (B Almari et al, 2017)

5.7. SIMULINK MODEL OF PROPOSED 21 LEVEL INVERTER

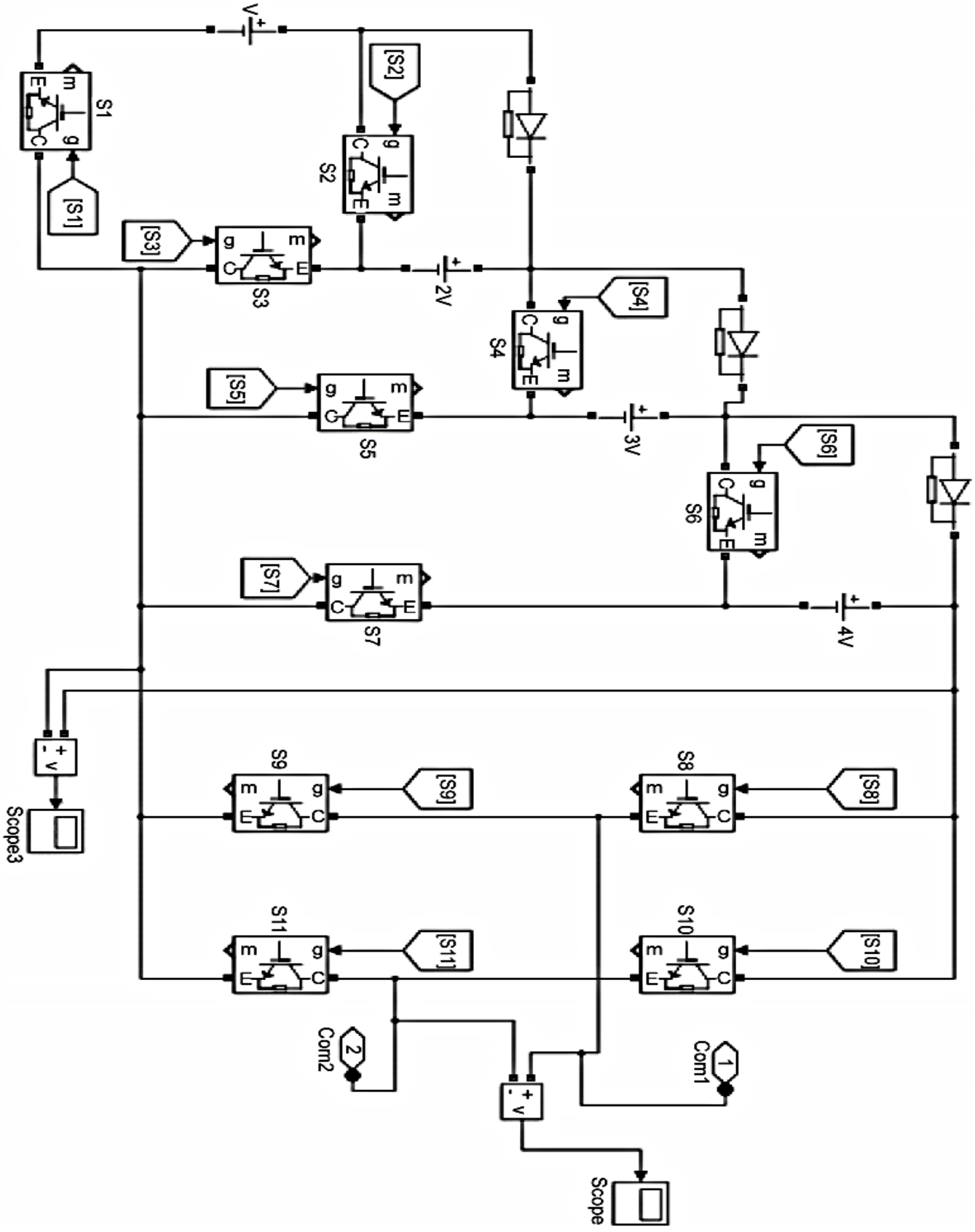

Figure 5-46 Simulink model of proposed 21 level inverter

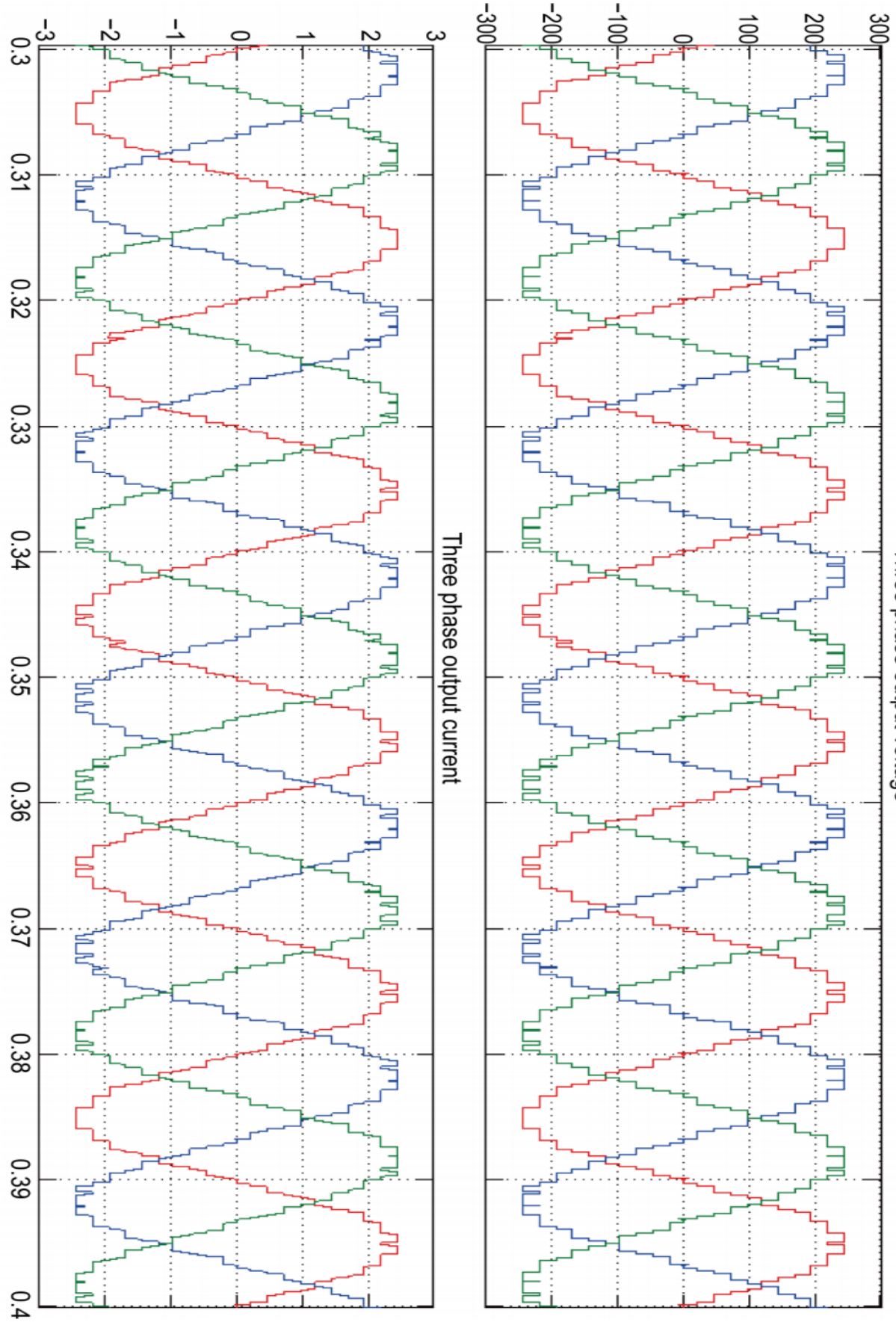

Figure 5-47 simulated three-phase output voltage analysis for 21-level CHB-MLI

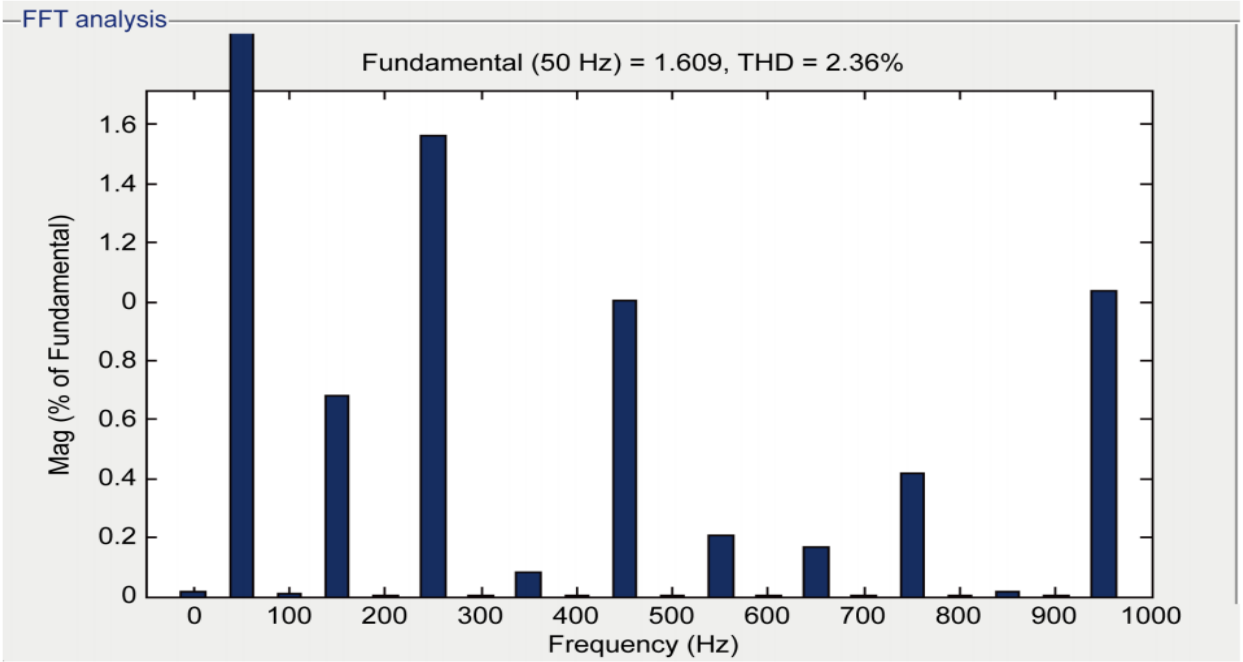

Figure 5-48 simulated three-phase harmonic distortion analysis for 21-level CHB-MLI

1- The proposed model as shown in figure 5-46 uses only 11 switches and diodes with four asymmetrical voltage sources to 21 levels in the output voltage waveforms. The main inverter produces only positive voltage of levels 1 to 10. The auxiliary inverter converters it positive ten levels, negative ten levels along with one zero level to produce an output of 21 levels at their output voltage. Figure 5-46 shows the simulation circuit of the proposed inverter. It has 11 switches numbered from S1 to S11. The Switches S1 to S7, along with three diodes D1, D2 and D3 with four asymmetric voltage sources which forms the main inverter whose output will be in positive regions only. The switch S8 to S11 forms the auxiliary inverter which is a PWM 3D converter. When switch S8 and S11 is on it produce the positive voltage levels and when S9 and S10 are on it produces the negative voltage. Figure 5-48 shows the total harmonic distortion present in the output voltage of the proposed multilevel inverter reveals that THD has been reduced by using the proposed PPF. The proposed asymmetric cascaded multilevel inverter produces multilevel output with minimum number of power semiconductor device. The simulation also proves that if any failure occurs in any one of the switches it is still capable of producing multiple voltage levels without shunt downing the entire systems. The multilevel inverter was successfully controlled by using GA and was used to achieve control of the multilevel output steps both in linear and nonlinear loads. The

simulation result also proves the effectiveness of the proposed multilevel inverter which uses less number of power semiconductor devices compared to the conventional one

5.8. Summary

The Computer Aided Design, simulation and Modelling of the Backend of System (BoS) of the proposed renewable energy platform i.e. control system, multi-level converted and relevant filtration system have been investigated and presented in this chapter. The investigation and work carried out recommended that the possible BoS that can suit the proposed 3D renewable energy system are:

- The adoption of Genetic algorithms and the Particle Swarm Optimisation in this case were much suited in minimizing the THD as compared to the Newton Raphson method but for the 21 level multilevel inverter, the THD was lower hence the Genetic algorithms were chosen
- The adoption of the CHB-MLI was ideal for connecting renewable energy sources with an AC grid, because of the need for separate dc sources, which is the case in applications such as photovoltaics or fuel cells. Cascaded inverters have also been proposed for use as the main traction drive in electric vehicles, where several batteries or ultra-capacitors are well suited to serve as separate DC sources

The simulation is done in various nonlinear load conditions. The proportional integral control based compensating cascaded passive filter made balance responsibility even when the system is nonlinear load. FFT analysis of the passive filter brings the THD of the source current less than 5% as recommended with IEEE 519 1992 and IEC 610003 standards harmonic under nonlinear and/or unbalanced load conditions.

The multilevel system including the proposed control method is validated through extensive simulation with results revealing that the cascaded passive power filter effectively filters the harmonics and compensates reactive volt amperes. The measured total harmonic distortion of the source currents was found to be 2.36% that is in compliance with IEEE 5191992 and IEC 610003 standards for harmonics

CHAPTER 6- INTEGRATION OF THE PROPOSED RENEWABLE ENERGY PLATFORM INTO SMART GRID

6.1. INTRODUCTION

This chapter introduces system integration of the proposed renewable energy platform into the smart grid. The chapter gives a good introduction about the smart grids, relevant technology development, and the steps that can be taken to integrate the proposed renewable energy platform into the grids. The micro-grid is formed by interconnection of small voltage generators, storage and controllable load distribution systems and can be connected to the main power network or be operated autonomously, similar to power systems of physical islands. For controlling a micro-grid some strategies can be used, namely; Supervisor Control, Local Decentralized Control, Centralized/decentralized Load Dispatching. Usually these strategies can be combined in applications which results in a number of combinations of possible to control types. The Chapter concluded with a computer simulation and analysis model of the system that shows the dynamic behaviour of the proposed model which is examined under different operating conditions.

6.2. SMART GRID SYSTEM

Smart grid is a concept by which the existing electrical grid infrastructure is being upgraded with integration of multiple technologies such as, a two-way power flow, two-way communication, automated sensors, advanced automated controls and forecasting system. Smart grid enables interaction between the consumer and utility which allow the optimal usage of energy based on environmental, price preferences and system technical issues. This enables the grid to be more reliable, efficient and secure, while reducing greenhouse gases. This paper presents a survey of the recent literature on integrating renewable energy sources into smart grid system. Various management objectives, such as improving energy efficiency, maximizing utilization, reducing cost, and controlling emission have been explored.

Considering the increasing demand in energy and the persistent dependency on fossil fuel it has become important that efforts be conjugated into the adoption of renewable energy as a sustainable way of supplying energy but also cutting down on carbon emission (Zhang, P 2010). The dependency on renewable energy therefore made important, it must be understood

that its integration of these intermitted nature sources into existing electrical grid would need serious improvements and modifications which must be considered in order for the system to be efficient.

Smart grid therefore brings efficient monitoring, system management, control and communication capabilities to the national electrical power generation and delivery infrastructure to meet grid demand around as efficiently and economically as possible. With the use of smart grid, smart home technologies and time-varying energy pricing models, there is need for smart energy management system (Siano P et al, 2012). The application of smart grid system therefore responds to varying cost of energy, by reducing or shading the peak demand automatically, reducing the number of required standby power plants, and therefore saving utility and user costs which are very much some of the advantages of smart grid systems (variaya P, 2011). A comparison between the traditional grid and smart grid is shown in Fig.6.1 below

SMART GRID VERSUS TRADITIONAL GRIDS

ASEA BROWB BOVERI| ABB. 2018. Power grid | ABB. [ONLINE] Available at: https://new.abb.com/grid/stronger-smarter-greener/digital-grid. [Accessed 10 September 2018].

CONTENT REMOVED FOR COPYRIGHT REASONS

Figure 6-1 from traditional to Smart grid (ABB, 2015)

One of the advantages of using smarter grids is its ability to be a Two-way communication. In Smart grid systems, a two-way communication facilitates the cooperation between utility company and subscribers. This cooperation increases the reliability and efficiency of the power grid, minimizes power loss, vanishes peak hours, and minimizes subscriber's total electricity cost (Z Fan et al, 2011). Demand-Side Management (DSM) is commonly a program used to manage energy consumption at the subscriber's side. Residential homes usually use DSM

programs to manage their consumption patterns according to varying electricity prices over time (P siano, 2012). Subscribers can participate in DSM in different ways like reducing their load demand, shift their load demand to off-peak hours, and rely on renewable energy to limit their dependence on grid energy. The technology of smart grid requires the integration of the knowledge and expertise from many different fields to design an efficient system. One of these fields is mathematical optimization. Linear Programming is a mathematical optimization method introduced by George B. Dantzig in 1947 (Jarvis JJ et al, 2011). It is used to optimize (maximize or minimize) a linear objective function, under linear equality and linear inequality constraints. Renewable energy is a promising option for electricity generation especially solar PV, wind and hydro energy systems as they are clean energy sources. Today, the integration of renewable energy sources into smart grid system is increasingly gaining importance and widely studied by many researchers (De Castro L et al, 2013). A Renewable Energy and Smart Grid Interfacing Options Integrating renewable energy sources into the smart grid system enables the reduction of the cost associated with sources required for building extra power generators, improves power quality and reliability

Figure 2 shows a clear difference between the traditional grid and the smart grid system. The parameters of the traditional gird definitely pose challenges to the implementation of renewable energy system due to the fact that it uses a number of sensors application only leading to automation of the system being inefficient and also its features allow efficient performance only under a centralised power generation system. Renewable energy power generation is dependent on nature hence couldn't be considered as a stable power production system hence decentralisation of power plants becomes a strategic approach towards efficiently avoiding losses during distribution.

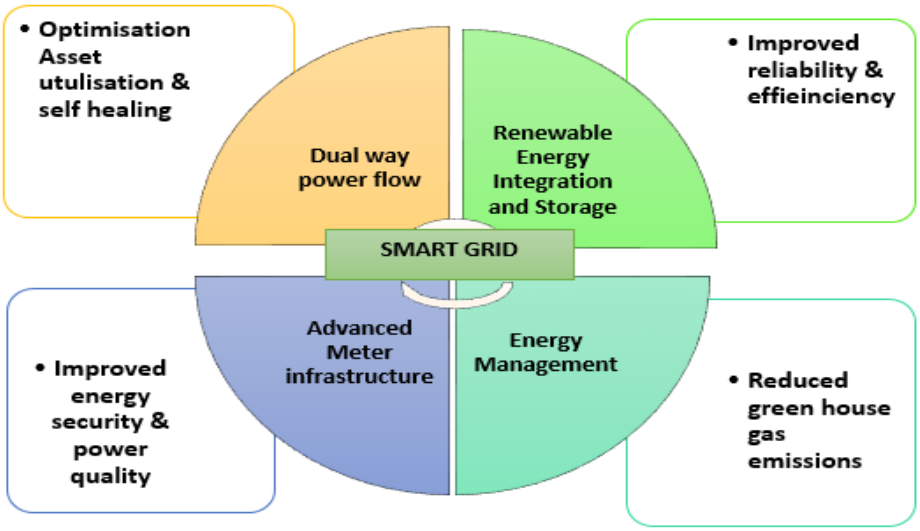

Figure 6-2 Smart grid challenges and benefits

There are many challenges that can be addressed based on smart grid technology which can be summarized in Fig 6-2. Renewable energy integration and energy management are the major challenges for developers and practitioners of smart grid system (Fadaeenejad, M., et al, 2014).

6.3. SMART GRID TECHNOLOGY DEVELOPMENT

Smart grid control gives the capability of maintaining system operation, predicting system behaviour, anticipatory operation, reduce the cost of operation, handling distributed resource, security, stochastic demand and optimal response to smart appliances (Shahraeini, M., et al, 2010) The self-managing and reliable smart grid is seen as the future of protection and control systems (Liserre, M., et a, 2010). Smart grid systems consist of digitally based sensing, communications, and control technologies and field devices that function to coordinate multiple electric grid processes. A more intelligent grid includes the application of information technology systems to handle new data and permit utilities to more effectively and dynamically manage grid operations. The information provided by smart grid systems also enables customers to make informed choices about the way they manage energy use.

ARCHITECTURE OF A SMART GRID CONTROL SYSTEM

ESNA a vision for the future grid. 2018. ESNA a vision for the future grid. [ONLINE] Available at: http://www.esna.org/2011/october/article21/index.html. [Accessed 10 September 2018].

CONTENT REMOVED FOR COPYRIGHT REASONS

Figure 6-3 Smart Grid control Architecture (ESNA, 2015)

Figure 3 shows the basic smart grid architecture when implemented as an energy control system. The true smart grid creates an energy network that will detect and address emerging problems in the system before they negatively affect service. It will be able to respond to local and system-wide inputs, provide much more information about broader system problems and, most importantly, be able to immediately react to or resolve problems that do occur. For example, demand response (DR) is becoming instrumental in managing the growing demand for energy, especially where it is combined with new and innovative pricing plans and consumer energy use portals. The combination of heightened awareness, an ability to track and manage energy use and financial incentives will give consumers a sense of "energy empowerment" that they have never before experienced. This requires smart metering and smart grid systems that offer distributed local intelligence at the neighbourhood transformer to effectively manage the edge of the grid thus where decentralized generation, electrical vehicles and customers must constructively co-exist.

6.4. DEPLOYMENT AND INTEGRATION OF DISTRIBUTED RESOURCES AND GENERATION

Distributed energy resources are small sources of power that can help meet regular power demand. Distributed energy resources such as storage and renewable technologies facilitate the transition to Smart Grids. The coming in of renewable energy sources as distributed generators can help mitigate the problems of depleting fossil reserves and the growing consumer demand.

Distributed generation which include wind generators, photovoltaic generators, hydropower generators and battery storage systems may incorporate thermal generation and electric vehicles. The aggregation of these sources, however, also means that tremendous amounts of data would need to be handled and processed. Empirical evidence also shows that individual intelligent nodes control of a number of electric assets within the grid, instead of being centralized could be a key solution to resolving smart grid challenges. (Penya et al, 2012)

While many renewable energy studies have been conducted to explore additional sources of clean energy, integrating renewable energy sources into the power system is one of the challenges in the modernization of the electric grid and making the grid smart. Some grids are already highly congested and moving power from wind farms into the grid for consumption can be difficult. Renewable energy sources are intermittent and inherently variable. Traditionally, electricity has flowed one way, from a power station to a customer. With additional sources coming from alternative sources, electricity has to enter the grid from multiple locations. Grid automation, two-way power flow and modern controls are needed to bring wind, solar and other alternative sources into the distribution grid and move it to its destinations. Coordinated efforts are needed to adapt solar photovoltaic, wind, hydro energies and new devices in Smart Grid systems in a smart way that they must be able to be easily integrated with existing equipment and communicate freely. Computer tools for analysing the integration of renewable energy into smart grids are also available. These energy tools are diverse in terms of applications, corresponding technologies and objectives they realize but due to the research aim and objectives, these will not be critically analysed.

6.5. POSSIBILITIES OF INTEGRATING OF THE 3D RENEWABLE ENERGY PLATFORM INTO A SMART GRID

Evidently, the findings based on the integration of renewable energy into smart grid is a very smart and futuristic solution that will help in meeting current and future energy challenges associated with fossil fuel power generation and its subsequent exponential and continuously increasing carbon dioxide level. The 3D renewable energy platform is made up of distributed and varied generation system for which a buck converter was implemented in its control strategy so as to ensure a minimum level of power delivery constantly as long as a single energy is being harnessed from either of the 3 sources or jointly.

Empirical evidences show that the integration of renewable energy into smart grid system is definitely possible, an example of this this is the work of (Penya et al, 2012) on the distributed semantic architecture for smart grid where the implementation of renewable energy power generations are introduced into smart grid system through individual intelligent nodes control. Although made easy when being implemented into a new smart grid system, similar operations in existing grid poses challenges such as

- Managing variably and uncertainty during the continuous balancing of the system
- Balancing supply and demand during generation scarcity and surplus situations
- Challenges related to high peak load during periods of low variable RE production are less technically demanding and are primarily economic challenges related to market solutions chosen to remunerate reserve capacity or demand response activities.

This being said, it goes to show that although feasible variable renewable energy sources are uncertain and more variable than conventional generators. System operators and energy planners therefore must overcome several challenges when integrating high penetrations of variable renewable energy. These challenges can be roughly grouped as either technical or economic, policy, and regulatory in nature. Solutions to four specific challenges are emerging, and will be important to watch in coming years:

- Technical: Managing variability and uncertainty during the continuous balancing of the system
- Technical: Balancing supply and demand during generation scarcity and surplus situations
- Economic, Policy, and Regulatory: Deferring or avoiding capital-intensive grid upgrades
- Economic, Policy, and Regulatory: Enhancing Renewable Energy project returns to enhance the investment environment.

Fortunately, there already exist a variety of potential technology and practical solutions that can be used to overcome these challenges, such as improved forecasting, smart inverters, demand response, storage (distributed and large-scale), real-time system awareness, and dynamic line rating. New advanced energy management protocols in the transmission and distribution operator interfaces can also support flexible integration of variable Renewable

Energy hence it is quite possible that a large scale version of our 3D renewable energy platform may be a contributor to defining solutions to current and future energy challenges.

This 3D renewable energy platform integration into smart grids would contribute to the solution of the vulnerability of the power system and its potential environmental and social impacts can be mitigated through diversification of the hybrid power generation. Diversity is attained when the hybrid generation has variety in the number of options that can utilised, disparity among the options (different generation sources and technologies), and balance in the contribution of the options (K, Moglo et al, 2016). The importance of hybrid systems has therefore grown as they appeared to be the right solution for a clean distributed energy production. It has to be mentioned that new implementations such as hybrid systems, require special attention on analysis and modelling. The system integration therefore focuses on the development and optimisation of the possible business and technical model of 3D platform.

6.5.1. PV system

The conditions for Photovoltaic (PV) cell measurement are standardized for comparison purposes but may not reflect actual operating conditions. Considering a review of few literatures, the best PV cell efficiencies are estimated at 24.2 % (GPPE, 2017) and the highest efficiencies devices demonstrate few practical limits without regards to cost or manufacturing considerations hence a simulation of the PV cells at average testing conditions were carried out and presented with an average output voltage of 22.5 volts at a temperature ranging from 0◦ to 25◦C. Photovoltaic systems are systems made up of solar panel which converts light emitted from the sun to electrical energy. Each panels used is rated by its own unique DC output power. Currently the best commercial solar panel efficiency is around 17.4%. PV system output for micro scale power system can be expected to be around 24 V and upwards depending on cell sizes and irradiance levels. Considering our intended 3D renewable energy platform, a sample panel was chosen for which the technical details would be used to define its efficiency and a MATLAB/ Simulink simulation would be carried out to evaluate its output. These data could be used for Practical implementation for the 3D platform

Figure 6-4 The PV arrays and technical details

Technical details		
Maximum power		20 watts
Nominal voltage		12 volts
Maximum voltage		17.6 volts
Open circuit voltage		21.8 volts
Maximum current		1.14 Amps
Short circuit current		1.25A
Maximum system voltage		600 volt
Dimensions	length	24 ½ inch
	Width	10 ¾ inch
	Thickness	1 inch
Glass thickness		3.2 mm
Maximum wind resistance		65 m/s -145 MPH

Table 6-1PV cell Technical data

The technical details of the solar panel provided are ideal for micro power generation considering the maximum power output and the current magnitude.

MATLAB/ Simulink Design & Simulation

Since the field tests can be expensive and depend primarily on weather conditions it is very convenient to have simulation models to enable work at any time. For this reason the research investigates a simple one-diode solar cell mathematical model, which was implemented applying MATLAB script. The model can be considered as an easy, simple, and fast tool for characterization of different types of solar cells, as well as, determines the environmental conditions effect on the operation of the proposed system. It can conclude that the changes in irradiation mainly affect the output current, while the changes in temperature mainly influence the output voltage.

Solar Converter System

The controller senses the grid voltage and current and gives the corresponding grid active and reactive power. The power controller senses the inverter output voltage and current and gives the corresponding active, reactive power. The current controller is mainly used for getting a triggering pulse as per the reference value. Using the Proportional Integral (PI) controller as shown in Figure 4(a) the reference current (Idref) is obtained with the load voltage, load current which is used to determine the RMS value of the load. By using PI controller we can get quadrature axis reference current which is another input of current controller.

The single stage solar converter model simulates one complete AC cycle for a specified level of solar irradiance and corresponding optimal DC voltage and AC RMS current. Using this model, the optimal values have been determined as 23V DC and 3.15A AC for an irradiance of 1000W/m^2 and panel temperature of 33 degrees Celsius. Efficiency is determined in two independent ways. The first compares the ratio of AC power out to DC power in. The second calculates losses by component by making use of Simscape logging. The small difference in calculated efficiency value is due to differences between trapezoidal integration used by the script and the greater accuracy achieved by the Simulink variable-step solver.

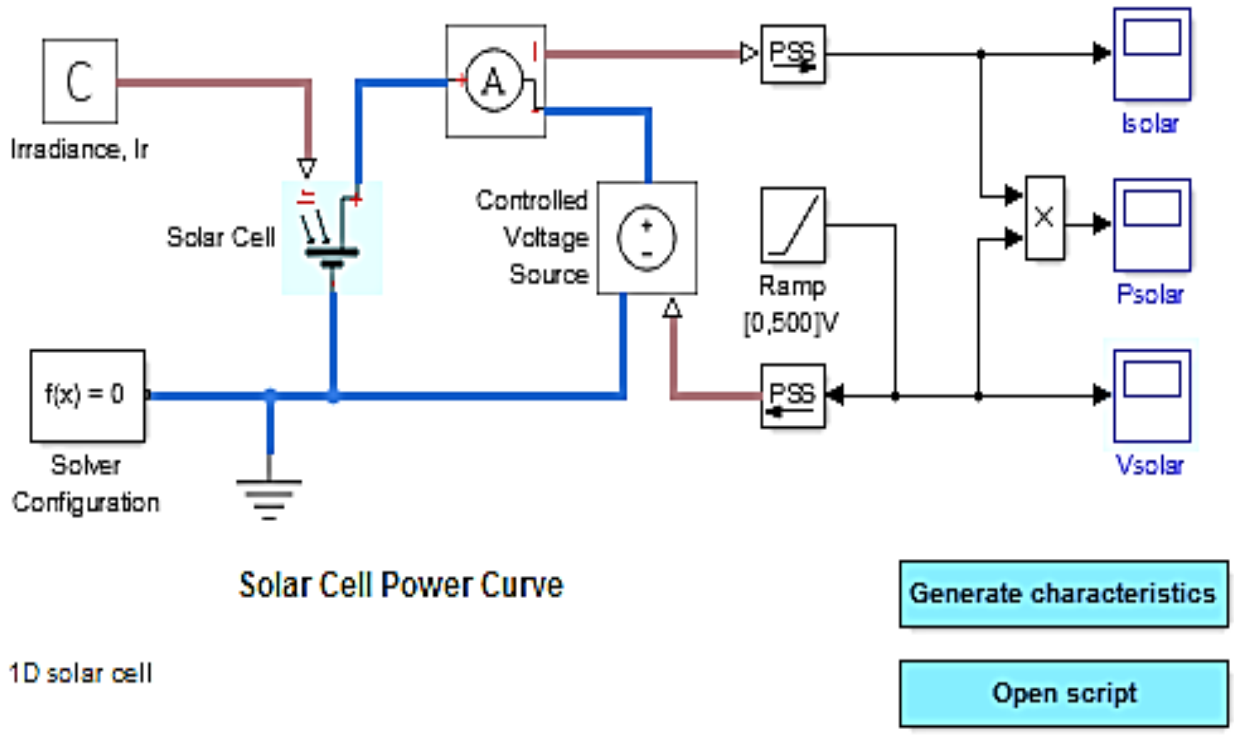

Figure 6-5 PV system

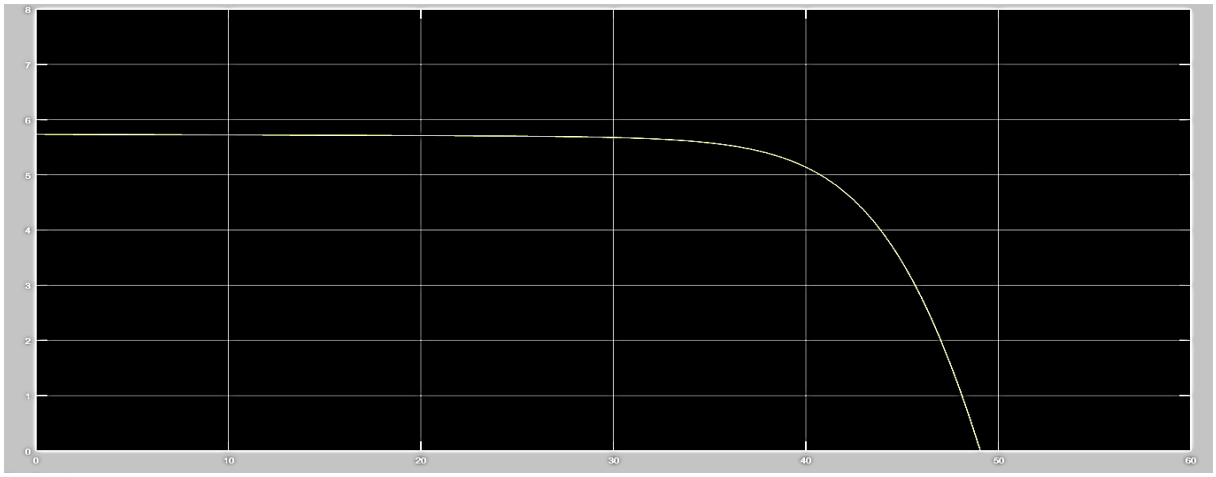

(a) Output Current (I)

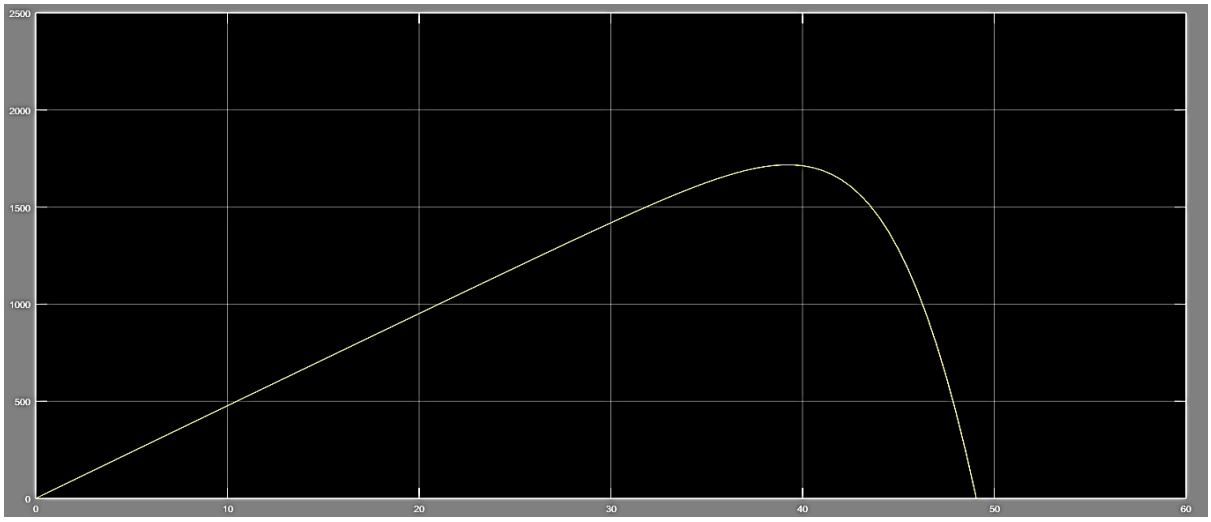

(b)Output power (w)

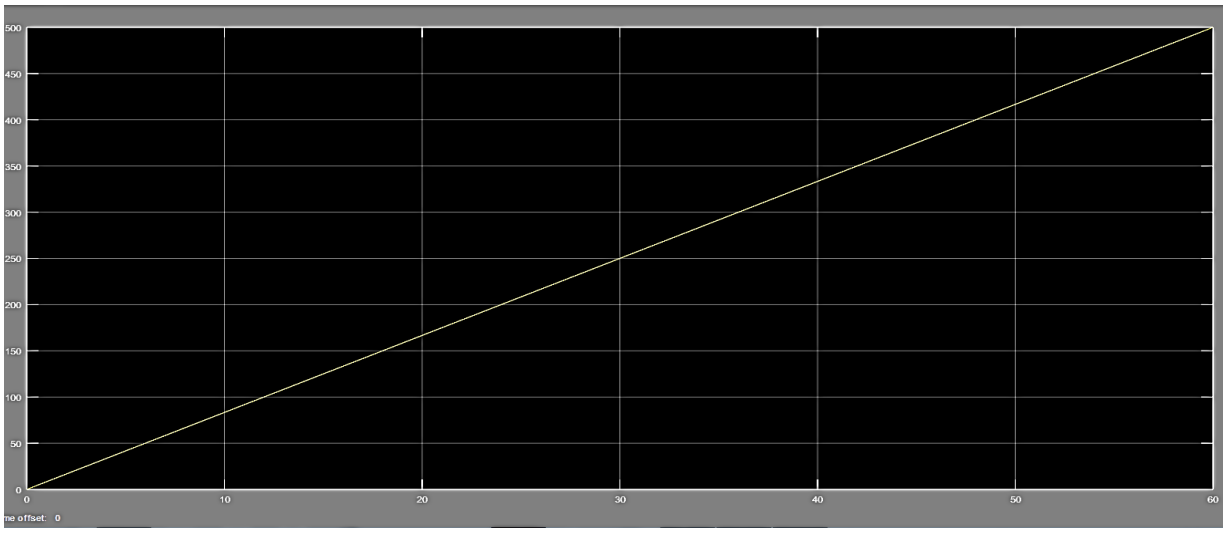

(c) Output Voltage (V)

Figure 6-6 a) Current, (b) Power, (c) Output Voltage characteristics

The characteristics of Solar PV system behaviour have been developed. The results of the solar PV system provide the current and the inverter tracks the reference current from the solar PV and supplies to the grid. The simulation of the power converter shown in Figure 4 shows the representation of the PV system. The simulation shows the DC voltage being the first simulation, the Demanded AC RMS current, the AC voltage and AC current. The simulated PV module circuit helps in understanding the PV characteristics, DC to DC converter topologies, component calculation & circuit design. A step by step procedure of modelling the PV module is shown. In the simulation model, the curve between P-V & V-I is shown in Figure 6-6 for varying temperature & varying irradiance. It was then interfaced with a buck-boost converter. The results obtained from the model show close correspondence to manufacturer's curve. The results as it can be seen provides a clear and concise understanding of the I-V and P-V characteristics of PV module which will serve as the model for the 3D design modelling

6.5.2. Hydro system

Evaluation of the Hydro system:

This section focuses on the analysis of the power generation feasibility of both a pump as turbine (PAT) and an experimental propeller turbine, when applied to water supply systems. This is completed through an analysis of the electrical generation aspects of the PAT's induction motor and of a permanent magnet DC motor, which was connected to the propeller turbine. The collected data allows for parameter optimization, adequate generator choice and computational modelling. These tests constitute a good sample of the range of applicability of small scale turbines as valid solutions for micro-hydro systems. It is also possible to consider multiple scenarios, such as rescaling/resizing, for larger turbines and systems, and the use of power electronics for further efficiency enhancing.

6.5.3. Hydro Turbine modelling

The free flows of water caused due to gravity from higher to lower geodesic points have various yet specific kinetic and potential energies. For a stationary hydro system, lossless and friction- free flow with incompressibility are mostly experienced (K Moglo et al, 2016), the difference of energy between the two geodesic points can be calculated using Bernoulli pressure equation:

$$p + \rho_{water} gh + \ + \rho_{water} v_{water}^2 = constant \ldots\ldots\ldots\ldots (58)$$

Bernoulli's equation can be transformed so that the first, second and third term expresses the pressure level, the level of the site and the water velocity level respectively.

$$\frac{p}{\rho_{water} g} + h + \frac{1}{2}\frac{v_{water}^2}{g} = constant$$

The practical difference in head measurement (h_r) can be defined through a gradient definition of the difference in pressure, in height and in velocity of the water flow:

$$h_r = \frac{p_2 - p_1}{\rho_{water} g} + (h_2 + h_1) + \frac{v_{water1}^2 - v_{water2}^2}{2g} \ldots\ldots\ldots (59)$$

Considering Bernoulli's pressure equation, the power generated by the water could be expressed as P_{water} which magnitude can actually be determined by using:

$$P_{water} = \rho_{water}\, g q_{water} h_r \ldots\ldots\ldots\ldots (60)$$

"q_{water}" considered as the volumetric related flow rate, one can then use the Bernoulli's equation to determine the power generated considering the volume of flow and the practical head. One must then consider on a more practical approach two different heads of the river in order to define the power by doing:

$$P_{water} = \rho_{water}\, g q_{water}\, (h_2 - h_1)$$

Considering the Micro hydro turbine, the energy generated through the rotational movement of the turbines is converted into a mechanical power with some micro losses during conversion described by the turbine efficiency $n_{turbine}$ where the power available at the turbine shaft is given as:

$$p_{turbine} = n_{turbine}\, \rho_{water}\, g q_{water} h_r$$

Where the torque of the turbine can be found by:

$$T_{turbine=} \frac{p_{water}}{\omega r} \ldots\ldots\ldots\ldots (61)$$

Where: ωr represents the rotor angle speed.

In micro hydro power generation system such as the one presented in this design, the height is kept constant by the use of a fore-bay tank, while the volume- related water flow can be adjusted manually using an upstream guide vane. To avoid the repercussions of load

variation on the generator dummy load, load controller or ballast load are used for power balancing when the system is used as stand-alone.

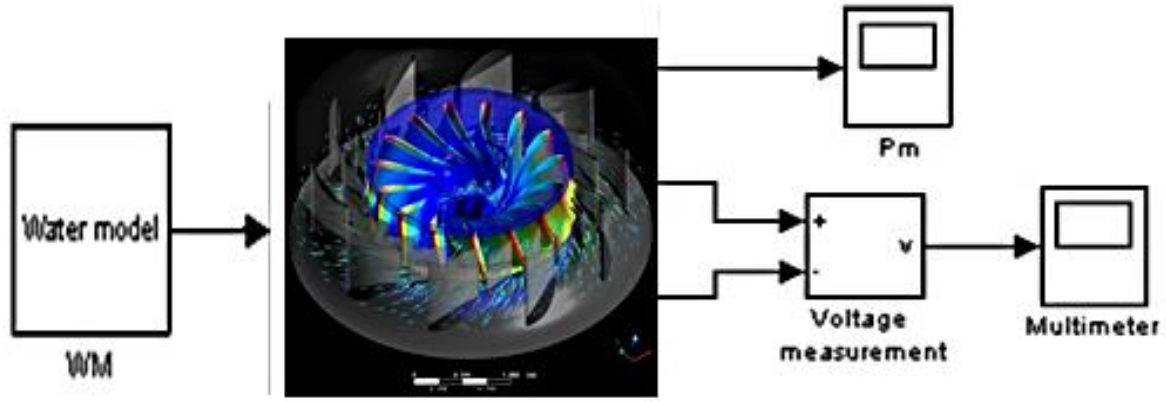

Figure 6-7 Micro Hydro power induction generator/ turbine (Simulink)

The modelling and simulation of the micro hydro turbine was carried out done in this paper using MALAB/Simulink tools. The simulation results as shown in figure 5 shows that with proper choice of governing system, the micro hydropower system leads to proper load sharing, constant voltage output and constant speed with variation of load values. This leads to an economical operation of the system. The modelling of this system can be made more accurate and attractive by introducing a voltage regulator block, a battery for storage system, a reactive power control block … etc. The introduction of a control device block to control the power quality of the system may be incorporated in the modelling. Given the results obtained in laboratorial testing and due to the nature of water supply systems, the chosen (and simulated) control method was the one resorting to flow control valves. The objective of these simulations was to control and avoid a runaway situation, which results from a load withdrawal on the generator. MATLAB/Simulink was used. The control scheme is described below and the simulation results are presented.

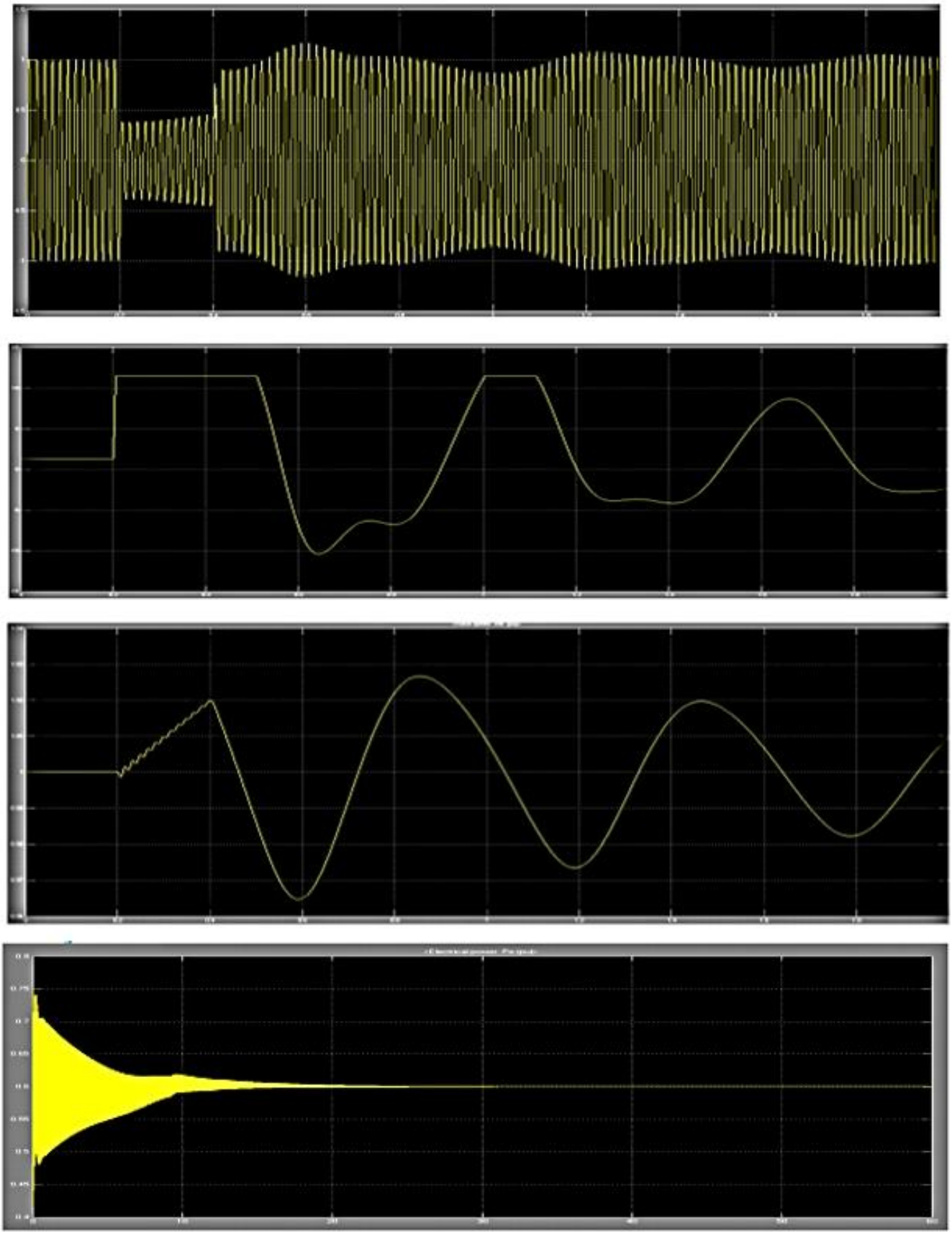

Figure 6-8 Output waveforms (a) Output voltage of generator (va); (b) Excitation voltage (vf), (c) Speed characteristics vs time; (d) Active power

The system capacity may be enhanced up to 100kW (maximum limit of micro power generation) and other option for connecting other renewable energy sources may be exercised. This may be tested for some realistic load patterns of some chosen areas. As it can be noted from the output waveforms, active power characteristics Figure 6-8 (d) of the synchronous generator, shows a steady state value of 0.6 p.u i.e. 1800 W which is nothing but the actual load connected to the hydro system. It is observed that the steady state is obtained around 27 sec. To reach the stable operating point on power - angle characteristics, few oscillations around this point occurs. This leads to initial overshoots of the power characteristics of the micro hydro turbine system.

6.6. Contra rotation double rotor wind turbine system

The most used and conventional type of wind turbine are made up of large sized wind rotors that are known for spawning high outputs even in the presence of moderately strong winds. Considering this theory, the relative output of a smaller wind size turbine is micro generated as the blades respond mostly to weaker winds. The theory then suggests that the application or decision of wind size blades is a direct result of the wind presence and its studies in different areas. The conformity of wind turbine size to potential wind circumstances are equipped with brakes or pitch control mechanism strategies enabling them to exercise control of turbine speeds and protect the generator when in abnormal rotation due to wind speed.

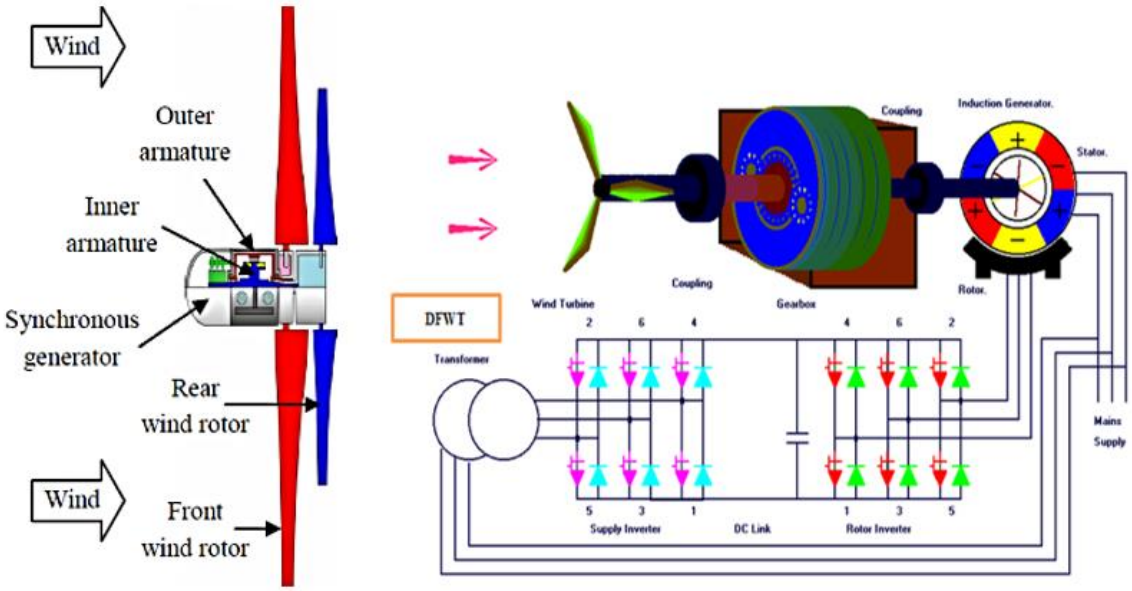

Figure 6-9 Contra rotation Double rotor wind turbine

The contra rotation double wind turbine however is made up of a double rotor wind turbine that initially rotates at low wind speed namely but one of the rotors mostly the smaller turbine, rotates against the front wind turbine. As wind speed increases, both rotors speed increases but the smaller turbines are the rear is even faster due to its smaller size and also due to the direction of winds hitting the blade.

Operation of contra rotation double rotor wind turbine

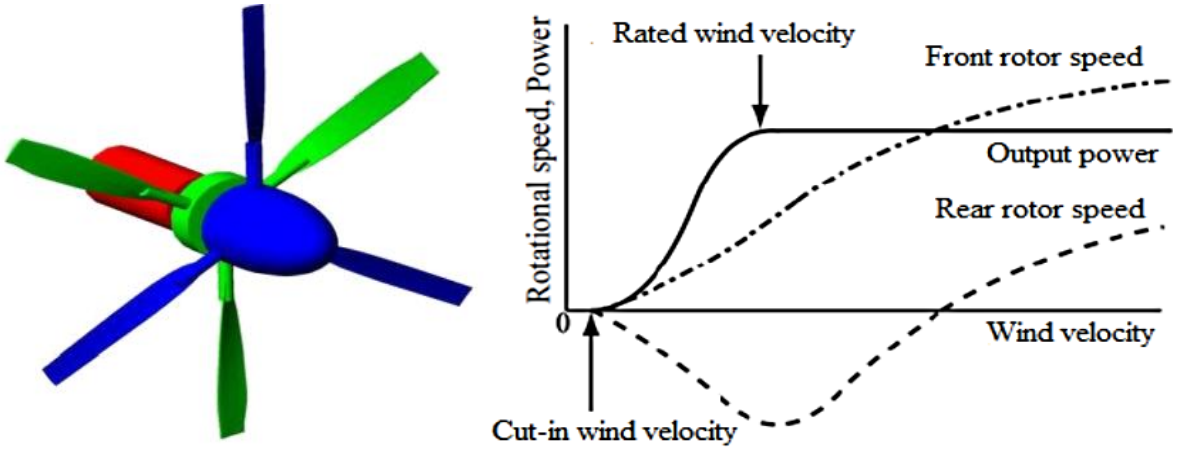

Figure 6-10 Contra rotation Double rotor wind turbine front & rear blades Isometric and front view with Operational mode

In order to understand the operation of the contra rotation double rotor wind turbine, a simulation using computational fluid dynamics and a 3D Inventor modeling program (Inventor 2008) version was used for the two and three dimension wind turbine. It then used FLUENT DDP in CFD to define the lift, drag and pressure coefficient. The same tool was used to define force components which show the impact of velocity increase, wake and wind energy turbulence. Considering the aerodynamic analysis conducted, a flow determinant issue was found around the distribution of velocity, and pressure variance in axial direction. Initial simulation made considered 60cm diameter for the front rotor placed in a wind tunnel of a 150×300. Initial results showed that flow conditions were steady and front rotor speed reached 600 rpm and 3.14 tip speed ratio for the rear rotor. Testing conditions shows that wind directions are of a uniform velocity prior to hitting both rotors hence the boundary conditions for the rear blade are initial velocity vectors for the front rotor. The pickup boundary Three dimension wind turbine rotor is produced using.

Simulation results:

Using the 3D FLUENT DDP, the two/three dimension rotors were tested and simulated using optimum blade designs methods showing excellent results and similitude. The analysis carried out and compared by fluent shows that there is a slight difference between the resultant velocities which is indeed normal as the velocity at the rear turbine would essentially be different from the front turbine. The calculation result of velocity resultant distribution along the blades as well show similar differences where the torque is 15 Nm and the efficiency is ≈ 34% at 500 rpm. Using numerical simulation Fluent, the torque obtained is approx. 13 Nm and the efficiency is ≈29% at 500 rpm. Similarly both efficiencies for the contra rotation double rotor wind turbine calculated using calculations and fluent shows similar results and trend. As one can deduct from Figure 9, both rear and front rotor have similar order of torque which is an ideal performance for this wind system. Considering all, it could say that the methodology used for this design analysis and testing is a perfect tool for optimum blade profile where the numerical simulation is perfection for preliminary design in order to have estimated design and testing characteristic of contra rotation blade span.

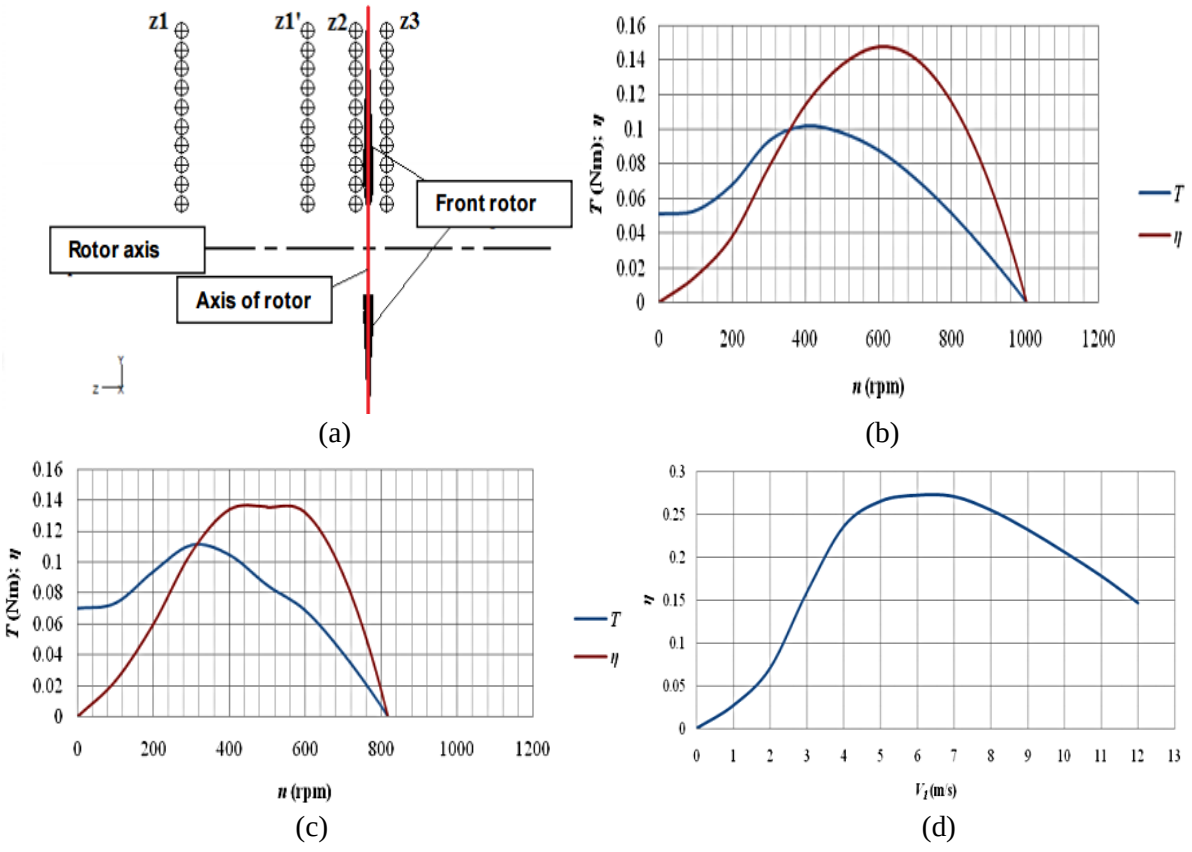

Figure 6-11 (a) Position of pick up velocities & (b; c) torque/efficiency vs rotational speed (Front & rear) (d) efficiency vs wind velocity

6.7. MATLAB/ SIMULINK DESIGN & SIMULATION

Isolated micro-grid makes a great sense of supplying power in the area without large power grid covers. In this section, an isolated operating micro-grid model is built based on the Matlab/Simulink environment, which contains miniature wind power system, PV system and energy storage system. In order to improve the quality of electrical energy, a composite control method with PI controller and neural network is designed. Simulation result shows the presented control method is effective. The 3D system architecture shown in figure 3-15 was modelled as such that the primary energy sources with different parameters, and converters could easily be integrated making the system an innovative sustainable and smart hybrid system with different topologies of the local distribution system and last but not least different types of consumers with linear or nonlinear characteristic. It shows the amalgamation of three renewable energy sources representing a novel adaptive system for efficient sustainable energy production and management.

Like wind power system, variable step perturbation and observation method is used for tracking the maximum power point of the PV generator system, and Boost circuit is also taken for stepping the voltage. Energy storage model is established by the super capacitor, and the super capacitor is paralleled to DC bus, which is the output of PV generation system and wind power system. The super capacitor of DC side can eliminate the ripple by using its energy storage characteristics, and it can make the DC voltage has little pulse and to be stable. The super capacitor model can be simplified as a serial structure of an ideal capacitor and an equivalent resistance, which can also accurately reflect the external electric characteristics in the process of charging and discharging. The single phase bridge PWM inverter circuit is selected, and IGBT is taken as the switching device. The control aim of inverter is to ensure the stability of the micro-grid voltage. PI controller has the virtues of simplexes and easy to be adjusted, so it is widely used in the application. Due to the small capacity of the isolated micro-grid, the load fluctuation and carrying capacity change in energy storage unit could cause the distortion of the voltage. In order to improve the quality of electric energy, a compose method of PI and BP neural network is adopted. The prediction model of BP neural network is built firstly. The inputs are the DC voltageU_{dc}, filter capacitor voltageU_c, inverter voltageU_o, inverter current I, duty cycle D at the K moment, the estimated inverter voltage Uo and inverter current I at the K+1 moment. Three-layer structure is adopted, so the input layer contains 7 neurons, the hidden layer contains 9 neurons, and the output layer contains 1 neuron. Tansig function is taken as the transfer function of hidden layer, and the purelin function is taken as the transfer function

of output layer. Taking the output of the model as a feed forward and add it to the output of the single closed-loop PI controller, a compound control method is constructed.

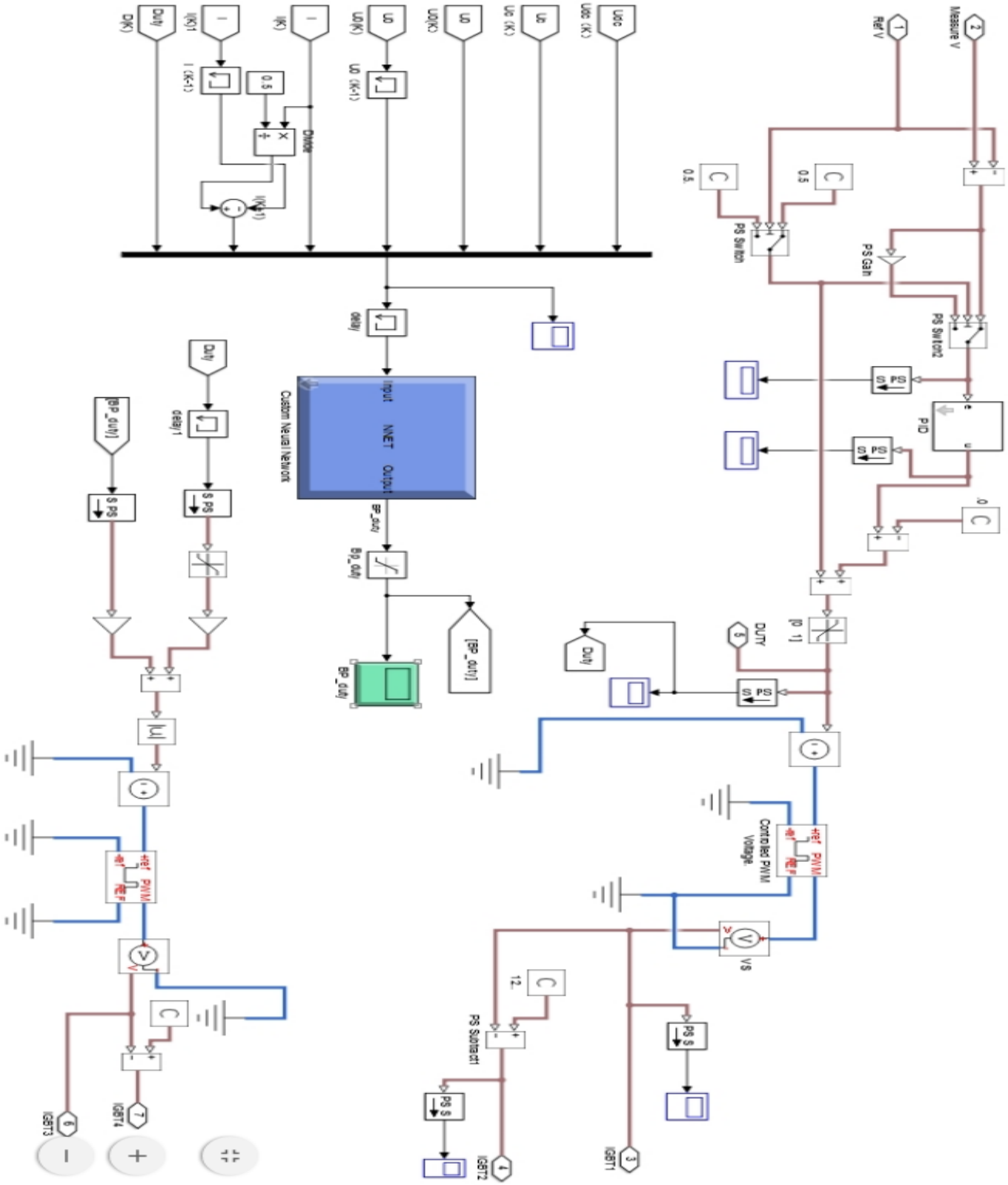

Figure 6-12 3D MATLAB simulation

Figure 6-12 shows the dynamic behaviour of the proposed model which is examined under different operating conditions. Real-time measured parameters are used as inputs for the developed system. The proposed model and its control strategy offers a proper tool for optimizing hybrid power system performance, such that it may be used in smart-grid applications. SIMULINK models are developed; using MATLAB simulations software to highlight the characteristics of the output power characteristics. In addition, reactive power compensation of the electric grid is included, operating simultaneously and independently of the active power generation. In order to be able to simulate the system, power generation blocks (PV, wind / hydro, battery blocks) were used together with measurement tools for power, current and voltages. An AC/DC voltage bus bar and voltage regulator blocks were also used.

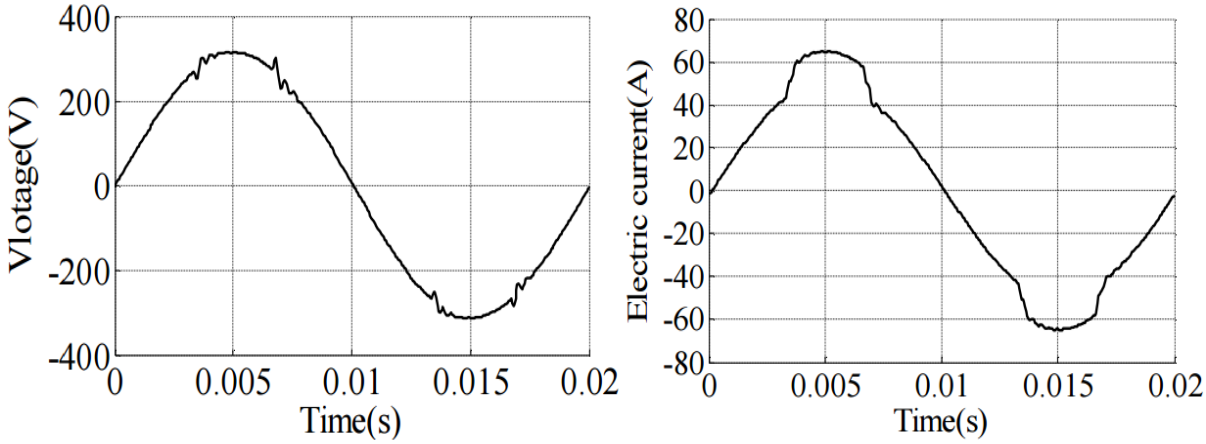

Figure 6-13 Current and Voltage output

The simulation results show the output of the 3D renewable sustainable micro power station for smart grid, house and industrial applications. Figure 6-13 shows the voltage and current produced through Simulink simulation generated form the three renewable energy sources (PV, wind, hydro). As one can note from the architecture, the energy generated is directly fed into the storage "battery" where load power is driven from. This also is ideal for meeting losses in the network where the surplus power generated is directly injected into LPN (local public network). Active power shows approximately $3 \times 10^4\ W$ generated for both active and reactive power which shows that power compensation within the network is efficiently managed with the capacitive bank within the network. The research undertaken to design and develop a 3D renewable energy platform for smart grid applications introduces a solution to challenges in the energy generation sector which do not only refrain only to the safe supply of clean Energy. A major importance for the theoretical study of this innovative systems, based on renewable energy is the availability of the models that can be utilized to study the behaviour

of hybrid systems and most importantly, computer aided design simulation tools. As the available tools are quite limited, the technical evaluations were presented using the most current and up to date model in Simulink. The 3D renewable energy platform architecture is presented with initial results showing the importance of the approach and its smart grid application advantages. It also demonstrated the challenges that should be considered prior to building the system for field test evaluations. To typify this feature, studies were considered for the suitability of using solar, wind and hydro resources available in Simulink tool allowing the development of the simulation model referred to steady, transient systems, with the possibility of active and reactive power flowing evolution. It is worth noting the importance of the presented model considering its usefulness tool in energy management system domain and its technological advantages for future sustainable, hybrid, and smart applications developments.

6.8. Design Optimisation and Evaluation of the 3D renewable energy platform for Smart Grid Applications

The design and development of a 3D renewable energy platform for smart grid applications focuses on the design optimization process of the station model. It looks at the evaluation of its productivity, discussing the possible applications including smart grid application. An investigation into the current state of the art of wind, hydro and solar energy conversion system have previously been considered and linearization around various outputs and a set of control equilibrium techniques is discussed. This is aiming to obtain a linear parameter variable model from a nonlinear system regulating the output of the 3D renewable energy platform. The initial simulation and practical results of this system based on some experimental measurements of the efficiency and possible power level that can be delivered is also presented.

6.8.1. Model description

A computational hybrid system has been developed, agent based, system modelling and simulation method, as a valuable tool for analysis, design and validation of micro-grids. Trying to simplify the exposition and the result analysis, and also for didactic reasons, the method is applied to a rather simple one. The model has been built in AnyLogic and is composed of 7 Active Object classes: Battery, Bus, Diesel, Load, Multiplug, PV and Wind besides the Main class. Figure 6-17 shows that Once all the objects had been created it is possible to connect them and run simulation. Any number objects can be connected to DC bus. The displayed

figure represents the AnyLogic simulation window of a simple example with 5 generator elements and three loads.

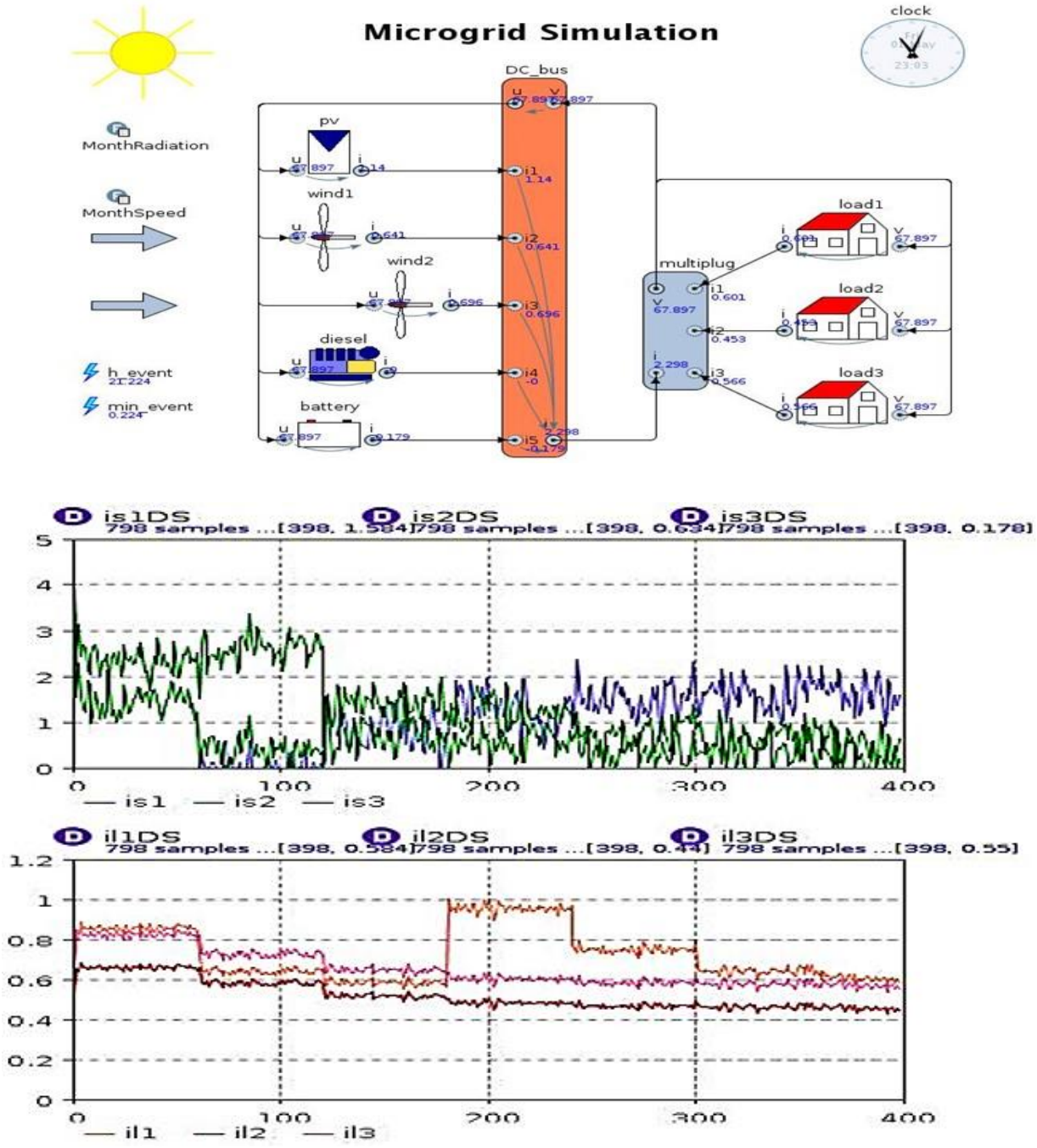

Figure 6-14 3D renewable energy platform smart grid integration system and simulation

Figure 6-14 shows the design of the 3D renewable micro power station implemented into "Anylogic" software with a photovoltaic generator (PV), two wind turbines (wind1 and wind2), a diesel generator (diesel representing the Hydro system) and a battery as an accumulator. This mode of operation is characterized by both generation subsystems set to operate at their maximum energy conversion points. Moreover, the battery bank in the system is able to revert

its energy flow, acting as a power supplier instead as a recipient of energy. This has been introduced as an effective way of meeting power fluctuations and shortcomings of the renewable energy sources. Operation in state Wind, Battery (hydro) is maintained as long as the energy available in the battery bank is about a fixed percentage (i.e. 24%) of maximum stored energy, otherwise the diesel generator is connected to fulfill the load demand.

6.9. SUMMARY

The Smart Grid concept has evolved from a vision into a goal that is slowly being realized. As technology grew, devices and systems are able to support the formation of a more intelligent grid. Concrete energy policies facilitate Smart Grid initiatives. Smart Grid practices in different regions barely indicate competition but rather an unordered community of similar aspirations and shared lessons. The basic idea of the Smart Grid is not enough when embarking on this complex system. Even with experiences and technologies that are available for reference, the Smart Grid pursuit is an investment of time, money and continuous investigation and testing. With large efforts put forth for Smart Grid research, the Smart Grid can be more effective in helping attain energy sustainability and environmental conservation and preservation. The exact future of the Smart Grid may be difficult to predict, but recent innovations display a dynamic merging of sectors, mechanics and communities.

An agent based model for micro-grids has been implemented here using AnyLogic. The model is mainly intended to design and try micro-grids and it can be used as a tool for design, development and demonstration of control strategies specially Centralized Supervisor Control and Decentralized Load-Dispatch Control, design and demonstration of micro-grid operation strategies, design and trying of micro-grid communication buses, micro-grid optimal design, and economic benefits demonstration. The model can be used to analyse a number of topic design of micro-grids like as Design, development and demonstration of control and operation strategies, design and trying of micro-grid communication buses, optimal micro-grid design and economic benefits demonstration. The system hereby presented will help in balancing out short-term fluctuations and ensure sustainable and consistent power supply are supplied as needed. Technically the design and development of the 3D renewable energy platform represents the amalgamation of smart innovative technologies which today dispels arguments that the availability of electricity from renewable energy sources is too dependent on meteorological influences.

CHAPTER 7 -VALIDATION AND EVALUATION OF THE PROPOSED RENEWABLE ENERGY PLATFORM

7.1. INTRODUCTION

This chapter presents the laboratory validation and evaluation of the proposed renewable energy platform. It demonstrates a series of experimental evaluation into the dynamic response of the system, stability of the system and its output and control capability as a validation of the developed systems. The chapter focuses on the laboratory validation and evaluation of the proposed renewable energy platform. The design procedure for this type of renewable energy platform is discussed. One of the most innovative approach introduced in this laboratory validation and evaluation system is the application of a smart control system able to track for each source of the 3D renewable energy platform their maximum delivery point so as to ensure maximum efficiency at all stages in power generation and transportation and delivery.

The control system is applied for the PV system, the Hydro system and the wind turbine. The technique implemented is developed so as to ensure that the needs of the output voltage or load demand from the back end systems is potentially tracked efficiently and delivered. The use of converters are also necessary to step down back end systems voltages and step up the current to meeting load demand conditions. With the application of a microcontroller, the PWM (pulse width modulation) is configured upon back end systems converters parameters and it's controlled through the algorithms written for the microcontroller so as to deliver maximum efficiency.

7.1.1. SYSTEM ARCHITECTURE OF LABORATORY EVALUATION

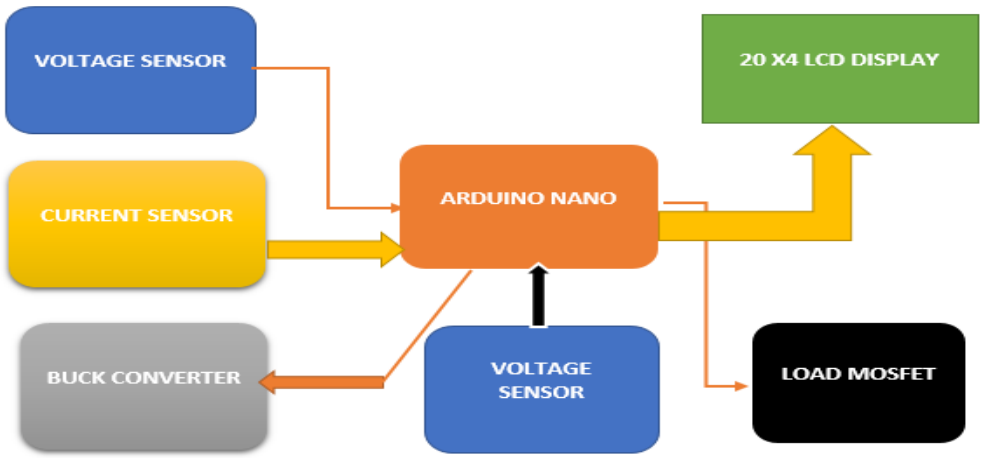

Figure 7-1 sustainable renewable micro power station - front end unit

The architecture presented above consists of examining renewable energy and its control as a viable option and obtaining the maximum amount of 'green' energy, thus getting the maximum power from the 3D sources at any given time. This is obtained by keeping the 3D power sources generated, generating at their Maximum Power Point (MPP) continually. On researching this, it has been found that some major factors come into account when the MPP is continually trying to deliver its maximum efficiency. This study looks at issues of Maximum Power Point Tracking (MPPT) and comes up with a valid solution to overcome the problem and obtain the MPP without interruption. To achieve MPPT there are a number of options available to date, these are the Perturb and Observe (P&O) MPPT method and Incremental Conductance (IC) MPPT method. Extensive research has been carried out on these two MPPT methods and a detailed account of the findings is documented.

7.1.2. POWER SUPPLY

Power supply used here is made up of a 3D distinctive renewable energy system comprised of the wind power generator, hydropower and photovoltaic power generation system as clearly expatiated in this report. Its combination has been implemented with the ideology of providing an uninterrupted output power to load and through the implementation of smart control system meet various load conditions through efficient generations and delivery. This represents the system front end as earlier explained and this is backed up by a battery system that stores energy generated when load demand is low so as to complement the demand later on when load demand increases and natural phenomenon does not allow full power generation from the 3D renewable energy platform. The 3D renewable energy platform generation systems have been presented with technical feasibilities covered thereby confirming the potential of each source and their relevant output power delivery. It is therefore important to understand each part of this controlled system to as to attempt field testing.

7.1.3. VOLTAGE SENSOR

For the proposed system, two voltage sensors are used in the setup. One of the voltage sensor is connected at the input just after the solar panel terminals, this sensor will provide us with the value of the voltage obtained from each of the 3D renewable energy sources and feed it to the Arduino analogue input pins. Other sensor including the current sensor are connected from the input of the buck converter and measures the voltage being fed the battery so that full tracking of the input and output voltages are measured and compared.

The voltage sensor is a simple voltage divider that steps down the voltage of the power amplifier to something between 0V and 5V so that it can be fed into one of the analogue inputs of the Arduino. This will measure the voltage provided by each of the 3D sources. A 100k potentiometer is used to achieve this. To calibrate it, 30V was fed into it and a multimeter took a voltage reading from the wiper. The potentiometer was then adjusted until the multimeter read 4V. Pin 1 is connected to ground, pin 2 in the new output voltage which is connected to pin 3 of the Arduino, while pin 3 is the original input voltage.

7.1.4. BUCK/BOOST CONVERTER

Buck converter Design Parameters

Calculations were carried out to find the correct value of components needed. The inductor used was an EPCOS product with model number B82721-K with an inductance of 400µH. The diode used in the circuit is a schottky diode which has a low forward voltage drop and a fast switching action. The capacitor which was used had a value of10µF as calculated above. A MOSFET is used in this circuit which acts as a switch. The MOSFET used is a 2.5A, 500V n-channel MOSFET with model number IRF 820. This requires a gate driver circuit, which incorporates a way to drive the gate voltage from the source. The driver chip used to do this is a half bridge driver, IRS2003, which outputs reads between 10-20 volts which is perfect to drive the MOSFET. The DC to DC buck converter also known as the voltage converter is equally based on switching principles and conversion of different voltage magnitude. Buck converter for the purpose of this design is used to convert the voltage from a higher level to a fixed and stable low level voltage. The voltage from each of the 3D sources is considered at a high state in the 1st stage of power generation and also variable, therefore with the use of a buck converter, a steady output voltage is obtained and fed to the load or battery. The buck converter circuit consists of a MOSFET, an inductor, a capacitor, a diode and a resistor as shown in the circuit. The MOSFET operation is considered as a switch in the case, where a PWM signal is driven to the MOSFET, where it operates as a switch to open and close the circuit. As the switch is turned ON, the diode in the circuit is open because of the reverse biased current flowing through the diode and the inductor where energy is stored as a result of the electrons generated from presence of the magnetic field. When the switch is turned OFF, this means the circuit is open. This is due to the forward bias nature of the diode which makes short circuit and the current in the inductor decrease and discharge its stored energy.

7.1.5. CIRCUIT PARAMETERS

- Maximum Solar Panel Power: 80W
- Maximum hydro output power:
- Maximum wind output power
- Maximum circuit output voltage: 25V
- Minimum circuit input voltage: 15V
- Battery bank: 12V
- Output desired voltage: 12V
- PWM Switching Frequency: 15KHz

To find the maximum current output:

$$I_{max} = \frac{Power}{Voltage} = \frac{P_{max}}{V_{max}} = \frac{80}{12} = 6.6A$$

Duty ratio calculations:

To determine the duty ratio for ON and OFF condition states, the following equation is used:

$$D = \frac{V_0}{V_{in}} = \frac{12}{15} = 0.8$$
$$D = 80\%$$

Inductor Value Calculations:

To determine the value of inductor, first there should be high switching frequency and it's assumed as 15 KHz using the equation below:

$$L = \frac{D(V_{in} - V_{out})}{\Delta L \times f}$$

Where, D is duty cycle, F frequency switching, and ΔL is the current ripple of the maximum current calculated above. This ripple current in good circuit designs varies between 40% and 20%, for our design 25% where chosen $\Delta L = 0.25$.

$$\Delta L = current\ ripple\ ratio\ \times I_{max}$$

$$\Delta L = 0.25 \times 6.6 = 1.65A$$

Substituting in the equation to find L:

$$L = \frac{D(V_{in} - V_{out})}{\Delta L \times f} = \frac{0.8(15 - 12)}{1.65 \times 15 \times 10^3} = 0.000096H = 96\mu H$$

To work out the inductor current, using the following equation:

$$Inductor\ Current = \frac{\Delta L + I_{max}}{2} = \frac{1.65 + 6.6}{2} = 4.125$$

The value of the inductor chosen to accommodate our design 100µH and 6A for better current rating.

Capacitor Value Calculations:

To determine the value of the capacitor, the equation below is provided:

$$Capacitor\ (C) = \frac{\Delta I}{8\, f \Delta v}$$

Where, (f) is switching frequency, ΔI is current ripple, and Δv is voltage ripple. The voltage ripple assumed to be 15mv.

$$Capacitor\ (C) = \frac{1.65}{8\ \times 15 \times 10^{3} \times 15 \times 10^{-3}} = 0.000916F = 916\mu F$$

The values of the capacitor chosen for our design is 1000µF and 100V working voltage for better charging and discharging in coupling for better performance.

The selection of the diode based on higher current rating and performance, as the type of the MOSFET and they are commonly used in solar power applications and designs.

7.1.6. MOSFET DRIVER

In power electronics, MOSFET does not use voltage control but rather uses the current drive for switching "ON" the high output current totem pole of gate driver will have fast switching frequency. Therefore the function of gate driver is charging up the junction capacitor. Known as the opto-isolator, the MOSFET driver transmits a beam of light from the emitting part and send signals between two electronic devices to provide coupling and these can be found in electrical isolations circuits between the inputs and the outputs. The principle applied therefore reside in protecting the system from any sudden changes that will endanger the system especially when using high voltages in passing signal from/to a microcontroller unit driving MOSFET to switch between different step sizes.

The photo-coupler which is essentially a chip consists of two main components, an LED (light emitting diode) which is the source of the beam and a photo-sensor represented by a photo resistor or transistor, with both components isolated with a barrier from a non-conducting material (dielectric). When current flows through the LED, the diode will emit an infrared beam detected by the photo-transistor allowing current to pass though the output of the MOSFET.

With our system however, the Arduino microcontroller board cannot provide enough current for the MOSFET to switch and this is due the capacitive gate of the MOSFET. Due to this misfortune, the MOSFET driver chip is required to deliver the current for switching purposes

where varying the PWM signal steps will be done and supplied to the buck converter circuit, so the driver will make good isolation for the MOSFET ground and source.

7.1.7. PULSE WIDTH MODULATION

It is very important to understand the role played by the pulse width modulation. Considering the application of the DC to DC converter, there are two main operations required in the switching mechanism, the initial one occurs at the Controller stage which supervises the power supply precision showing a regulated voltage and the PWM keeping the voltage regulated. In theory the PWM provides an analogue results from a digital signal in a square-wave from as shown in Appendix C. The Arduino microcontroller board has a set of PWM pins already integrated providing the required switching mechanism. In essence we could say that the PWM operated by varying the duty ratio of the switching mechanism provides a constant voltage at the output stage.

When the duty ratio is 0%, this means there is no signal and the circuit is grounded to 0V signifying that the circuit output would give its maximum voltage if the duty ratio selected was 100%. Reminding ourselves that the main aim of implementing this design is to obtain the maximum power point (MPP) for charging the battery and supplying enough power to the load at the same time, therefore the PWM controller will control the signal driven to the MOSFET and would also control how much the switch would be fully ON or fully OFF for. In programming the Arduino microcontroller, the PWM has to set to operate in both auto and a manual setting. The auto setting will work its way from the P&O algorithm to find the maximum power by varying the PWM and switch the MOSFET into different steps. The manual setting on the other hand would focus on observation and endeavour to maximise the power to its peak value.

7.1.8. PROPOSED TECHNOLOY FOR SYSTEM PROTECTION

This system was designed specifically to provide protection in order to ensure safety at all stages of the system against any changes in the load demand or at the source. The hereby proposed system offers protection that can be used for hybrid and system.

Short circuit current protection& Battery Protection- reverse polarity

To protect the circuitry system from short circuit or overcurrent effects, a fuse can be used between the circuit and the load output. In essence, all electronics products have some sorts of protection. Considering the complexity of our system however, it is important to consider reverse polarity protection due to the fact that there is a chance of getting at the back end of the buck converter a reversed current when connecting the battery in reverse, so to drive away high current from the inductor which may otherwise result in splitting the diode apart. Overcoming this issue would mean implementing an efficient protection system through a circuit using a couple of poly-fuses PPTC (Polymeric Positive Temperature Coefficient) in parallel for producing any current limit needed for the system. An LED is connected to show when in operation and also when the fuses are blown and the circuit is open. They will stay open because of the high current passing through them until a low temperature is reached enabling conduction

Low Voltage Protection

This type of protection is very useful if the batteries became numb, this implies the use of a Fuse MOSFET disconnecting the battery from the load whenever the battery the load decreases below threshold level. The application of the Arduino implies that the MOSFET can be switched ON or OFF based on the output magnitude from the battery voltage level.

High voltage protection

Whenever the battery voltage level increases over the limit, the system becomes inefficient, and overcharging the battery would mean reducing its life expectancy. It is therefore important that when designing a system such as ours, a full range of protections from the low to the high voltage be implemented so as to ensure good function of the system. Using the Arduino control programmed system, we will be monitoring and controlling the level of the battery between the normal and expected ranges and whenever a high voltage is detected at the battery the MOSFET will switch off and disconnect the battery form the charging controller circuitry.

7.1.9. SYSTEM INDICATOR UNITS

The system has the following monitoring and indications components.

Nokia 5110 LCD for control display

This type of LCDs is very small having about 1.5” diameter based on an 84x84 pixel monochrome display. The LCD has a backlight making data reading easily even in the dark. A graphic LCD means we can view characters of different inputs and displays ranging from the

voltage sensor, the current sensor, the power, the duty ratio selected, and the efficiency obtained using the PWM and the MPPT methods from the 3D sources input and from the battery to load side.

ARDUINO NANO MICROCONTROLLER

The microcontroller to be used to implement the required algorithm is the Arduino. The decision to use this microcontroller was made after carrying out an extensive research on it and also on the 8051 microcontroller. The Arduino is relatively simple and is perfectly able to implement the type of algorithm that is ideal for our system. On researching the 8051 microcontroller it was found that it was a lot more complicated than the Arduino and may prove hard to for the algorithms to be implemented, if chosen.

The main reasons for choosing the Arduino Nano is that:

- It is Inexpensive, most Arduino starter kits cost between £30-40.
- The Arduino will work on Windows, Mac and Linux.
- Simple clear and open source programming environment. Software for the programming of the Arduino can be obtained online for free and the programming environment is relatively simple with the language being a mix of C and C++.
- It has a 6 analogue inputs.
- Its operating voltage is ≈ 5 volts.
- DC current I/O pin 40mA.
- Flash memory of 32kb (0.5kb used by the boot loader).
- Input voltage maximum of 6-20 volts, recommended to use 7-12 volts
- 14 digital outputs, 3 of which are pulse width modulators (providing 8 bit pulse width modulation).
- Board can be powered by the USB port from a computer, 2.1mm centre positive plug in the board, or the 5 volt and the 3.3 volt connection on the board.
- Clock speed of 16MHz

7.1.10. LIMITATIONS OF ARDUINO

Logic expressions such as "&&, ||0, !" which are AND OR and NOT logical operators respectively, were used in when writing the code to program the microcontroller. Operators such as these saved time and cut down on the amount of code written. Algorithms like the one employed in this project can sometimes be difficult to implement using the Arduino due to

inner workings not being exposed. The Arduino's relatively inaccurate timer's means that systems have to be ran for a greater number of samples to get accurate results. Interrupt commands in the Arduino are hard to implement successfully and the open identification of variables between loops can sometimes cause confusion when the microcontroller is being programmed. For the program that was used in this study, initially arrays of 100 samples were taken to get accurate readings, on testing the software it was found that the code would only run correctly up to a certain point. After much research and reading on the principles of operations of the Arduino it was found that the SRAM (Static RAM) part of the memory, which is used to store these arrays, has a limit of 2k. The arrays in the code were 101 elements with each element being a float of 4 bytes long, therefore each array is 404 bytes. The SRAM has a limit of 2k which is equal to 2048 bytes. Therefore after the fifth array, an error would occur due to the capacity of the memory being used up. The code is made up of 9 arrays as well as other variables, so it was decided to decrease the number of samples taken to 10 samples. This provides a less accurate solution but solves the problem with the memory's capacity. Another possible solution to the problem was found during data sheet analysis, consisting of using the flash program memory, where the Arduino sketch is stored instead of SRAM, where the Arduino sketch creates and manipulates variables when it runs. This is done using the PROGRAM keyword as the variable modifier, for this the library in which the PROGRAM is part of must first be included by including at the top of the sketch:

#include <avr/pgmspace.h>

And then putting whatever data required to go into the flash memory into it, using the following form: data Type variable Name [] PROGMEM = {dataInt0, dataInt1,dataInt3...};

Where data Type is the memory variable type and variable Name is the name of the array that is required to be put in the alternative memory.

7.1.11.ARDUINO CODING

Coding was done using the Arduino software, which holds all the functions to program the chip. Since the P&O algorithm is used to track the 3D sources power production, it was selected for its simplicity. The program structure for the P&O algorithm will track whenever the voltage or the current from the 3D sources changes thus either increases or decrease. The resultant power therefore is measured and recorded. If the power decreases, the algorithm will

change its increments in the opposite direction based on the expected output curve of the 3D sources. When the maximum power is determined the tracker will hold that peak value and will keep oscillating around this value. This is done by selecting the sampling time using the PWM adjustment with the Arduino microcontroller capability of implementing this feature and uploading it to the system. When the PWM is 100%, it means that the MOSFET is switched ON completely and when at a maximum power it ensures full power delivery to the battery. The algorithm tracking principle keeps feeding the battery with the maximum power obtained from the 3D sources and if any changes occur thus if the current or voltage drops down, the PWM will switch between different duty to find a sufficient range that can deliver a stable amount of power where the algorithm will keep on running simultaneously so as to obtain the maximum power possible.

7.1.12. SYSTEM INTEGRATION FOR SIMULATION AND FIELD TESTING

For the purposes simulation and Field testing, the above mention parts making up the system entire architecture has to be put up together. The Arduino Nano was connected between the sensors to measure and record the current and the voltage from a single source of the 3D this being either the solar, wind or hydro. This then means that 3 of these systems were built to deliver maximum efficiency of the each of the 3D sources with a unified control system taking readings from the output of each of the 3D controller terminals which are fed to a battery for field test purposes and could also be fed to a load. The circuit was primarily design to confirm feasibilities studies through simulation and was later built and tested. Appendix C shows the overall circuitry designed in PROTEUS software powered with a DC battery at the input representing either the solar source, wind or hydro and a battery at the output with a load connected to it.

The current and voltage reading at the solar panel end and the battery end was monitored and displayed on the LCD. However, tracking mode of maximum power can be manually set through calculations and assumptions or could be set to automatic. The Automatic mode is literally where the potentiometer is ON and set at a max of 100%, meaning that when varying the potentiometer, different switching modes will be applied to the MOSFET to operate in different duty cycles and this can be monitored as well in the LCD with the MOSFET defining the maximum efficiency or minimum efficiency for balancing the overall system between the input power (solar, wind, hydro) to the output power. As shown in the simulation circuit, the voltage at the input reads 34.9V with a current 0.06A and power of 0.6W and at the output a

voltage delivery of 21.8V with a current 0.06A and power of 2.1W and 49% efficiency therefore balancing the system and delivering the maximum power possible. Further test revealed when 34.47 volts was generated by the solar panel end terminals representing the input a 25.00 volts being fed to the battery with a power of 2.6 watts at a 69% efficiency. To test the switching modes of the MOSFET, an oscilloscope was connected to the MOSFET gate with simulation results showing in Appendix C. Following this, the potentiometer was set to 33% and the output driven to the MOSFET gate displayed on the oscilloscope. The potentiometer was set to 66% and the output driven to the MOSFET gate displayed on oscilloscope, showing switching operation mode. The potentiometer was set to 0% and the output driven to the MOSFET gate shown as part of the simulation results.

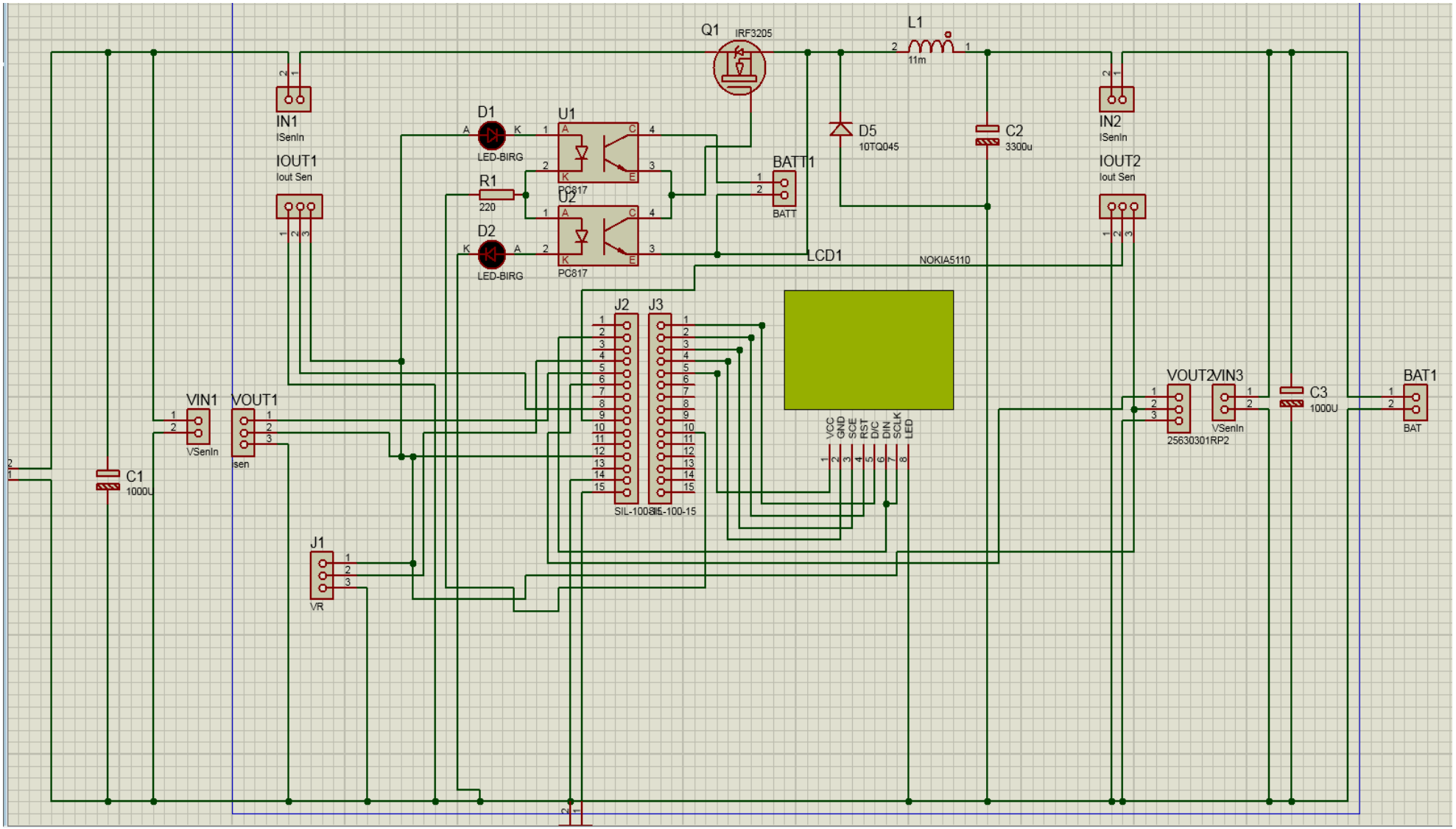

Figure 7-2 Overall MPPT System Connection for Simulations

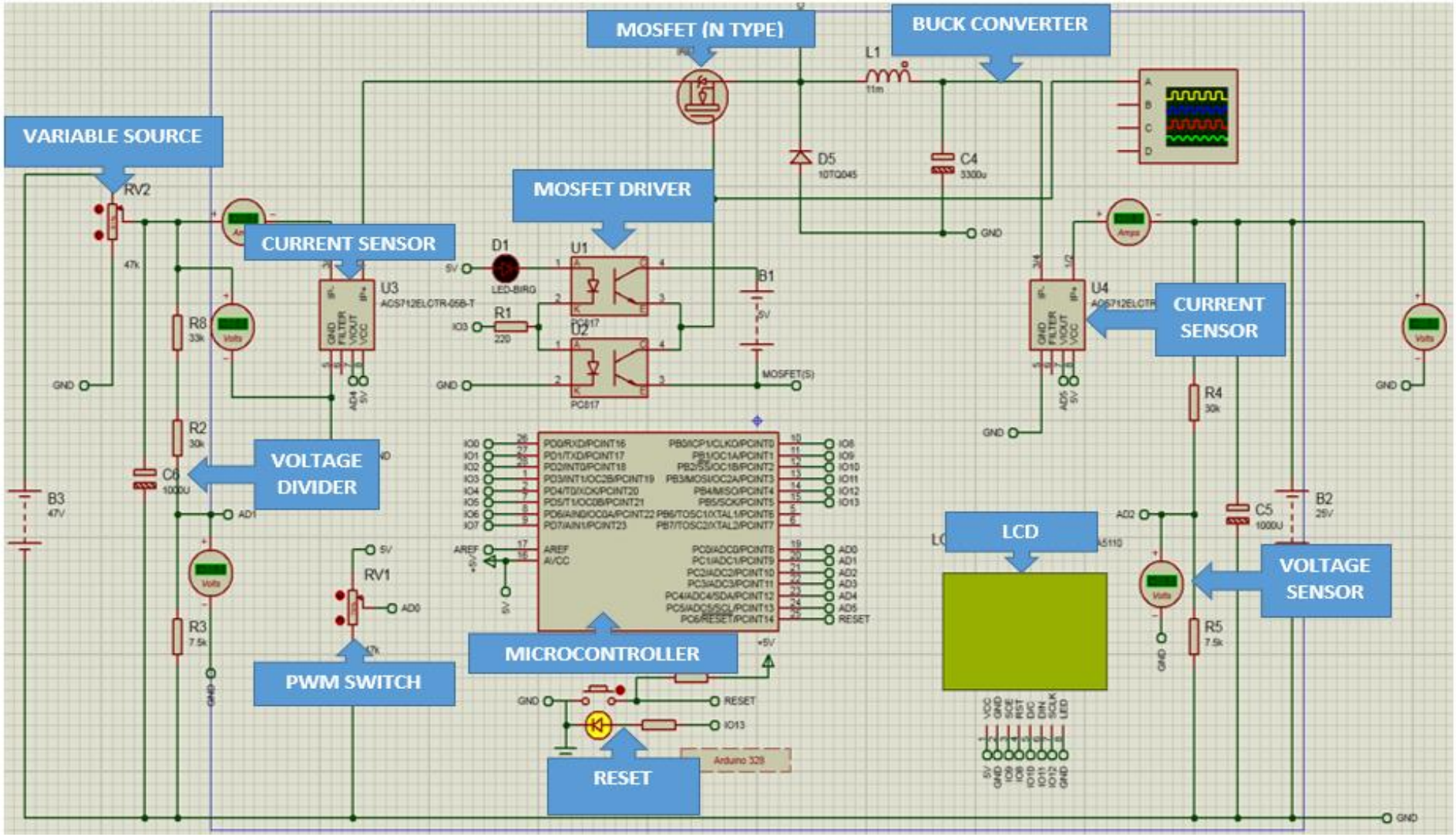

Figure 7-3 Overall MPPT System Connection for Simulations showing each block diagram

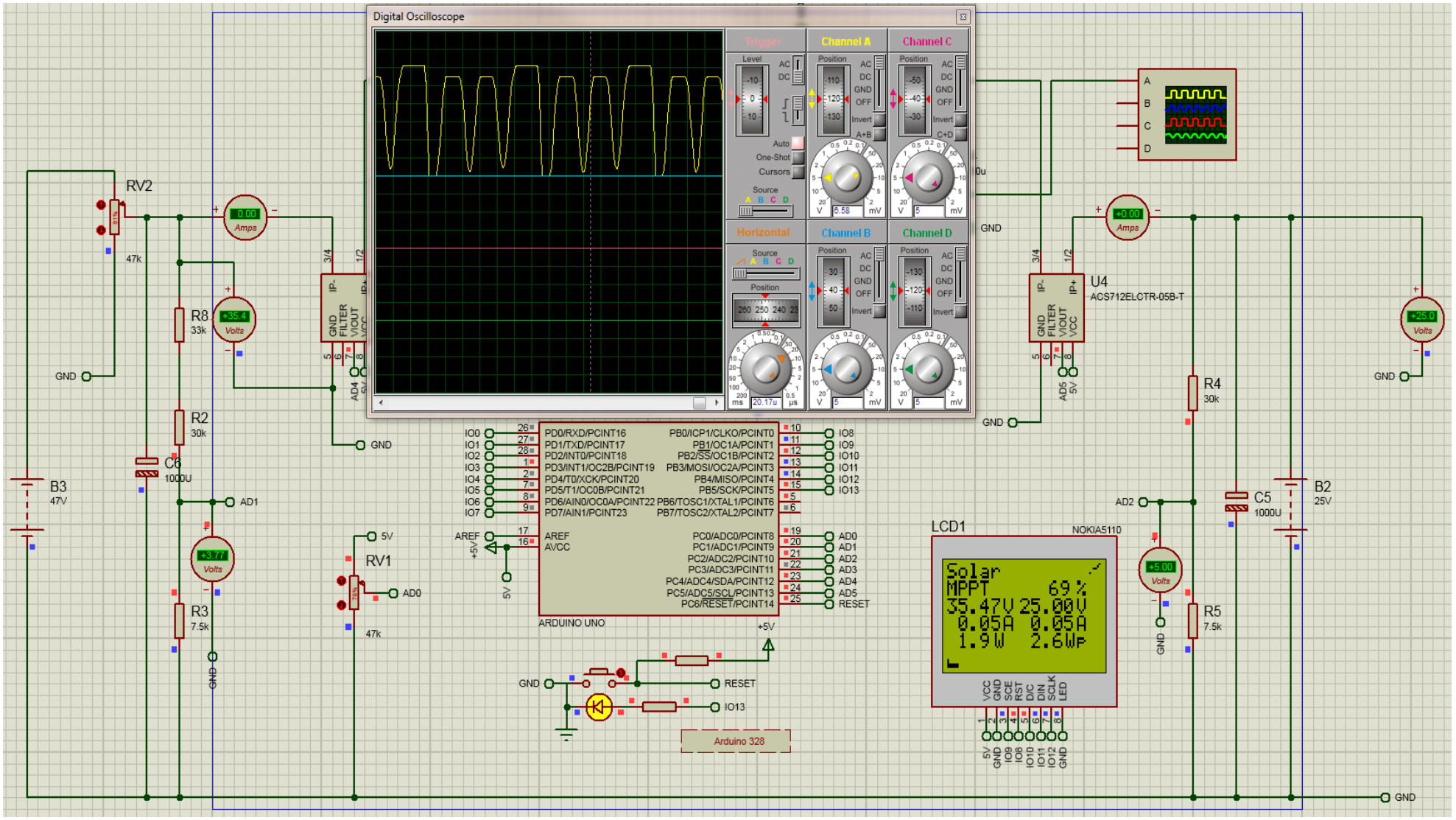

Figure 7-4 Overall MPPT System Simulation

Buck converter operation

The Buck converter circuit operation principle is to drive and supply a stable DC output voltage, where the value of this voltage is dependent on the input signal and the duty cycle switched from the MOSFET. If the duty cycle selected was 50% and the input supply voltage from the solar panel was 35.47V, in this case the output voltage would be half the input voltage using the following equation to determine the output voltage but in this case we see more than half of the input voltage being fed to the load or battery showing maximum tracking and efficient delivery to the output load or battery.

$$V_{out} = V_{in} \times Duty\ Cycle \dots\dots\dots (62)$$

$$V_{out} = 35.47 \times 50\% = 35.47 \times 0.5 = 17.7V\ versus\ 25\ V\ fed\ to\ battery$$

It is to be noted that the source of the solar panel for the purpose of simulation was based on a variable power supply using a potentiometer and a DC battery source. With variation of the power supply, the potentiometer slider, the step duty cycle and the P&O algorithm balance in operation is made easy noticing that on the LCD display, the power of the input parameters and the battery is balanced with a max efficiency obtained. As generation began and the P&O kicked in, the system became much balanced and delivered a stable power to the battery and the load, thus a power of 12.06 watts at an efficiency of about 84.35%.

Recorded measurement

Input Parameters (PV/Wind)			Output Parameters (Battery End)			
Voltage (V)	**Current (A)**	**Power (W)**	**Voltage (V)**	**Current (A)**	**Power (W)**	$= \frac{Efficiency\ Power\ Battery}{Power\ Solar} \times 100$
16.83	0.73	12.29	10.41	0.96	9.99	81.34%
10.50	0.90	9.45	8.20	1.12	9.18	97.19%
10.43	0.89	9.28	5.54	1.37	7.60	81.87%
15.37	0.93	14.29	6.28	1.92	12.06	84.35%

Table 7-1 Measurement Result Table

7.2. PRACTICAL SYSTEM IMPLEMENTATION

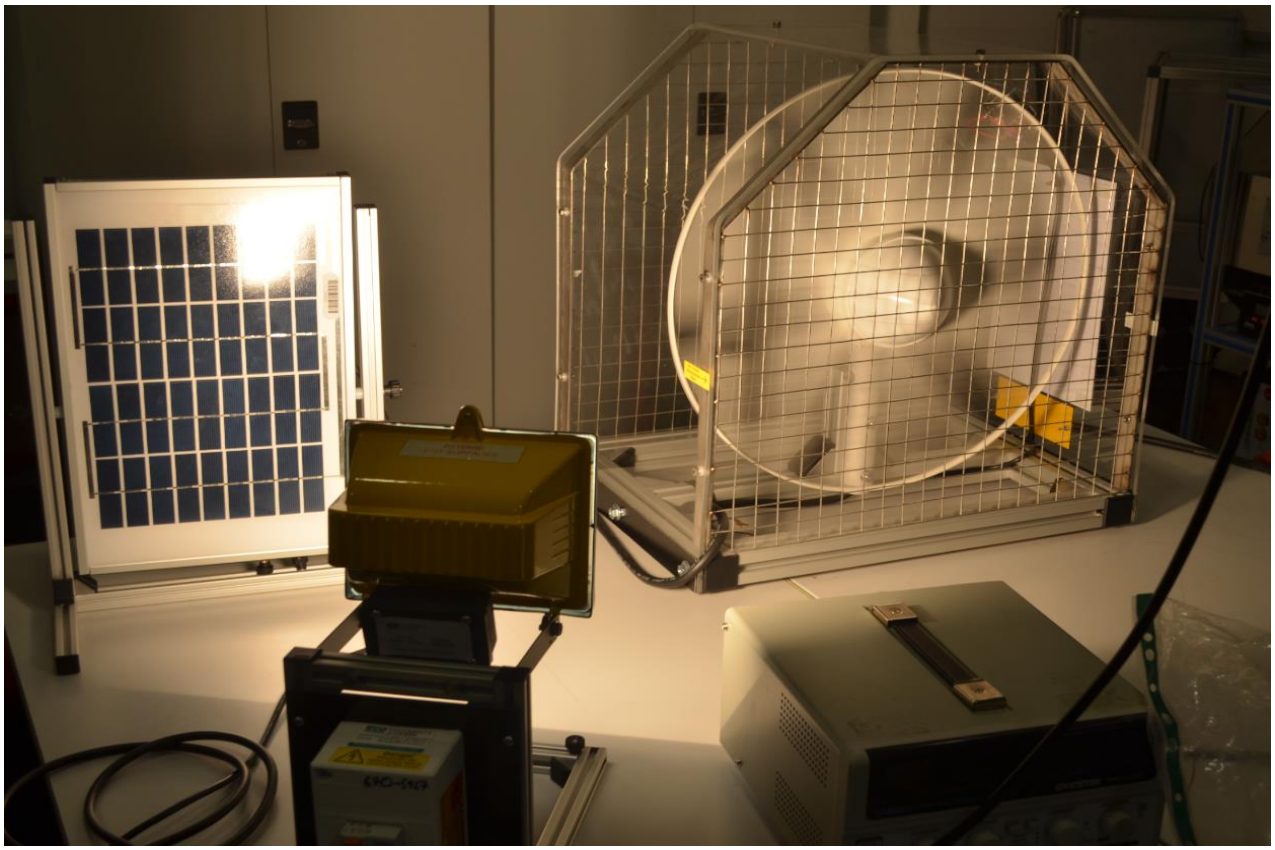

Figure 7-5 3D renewable sources Practical system unit assembly under testing conditions

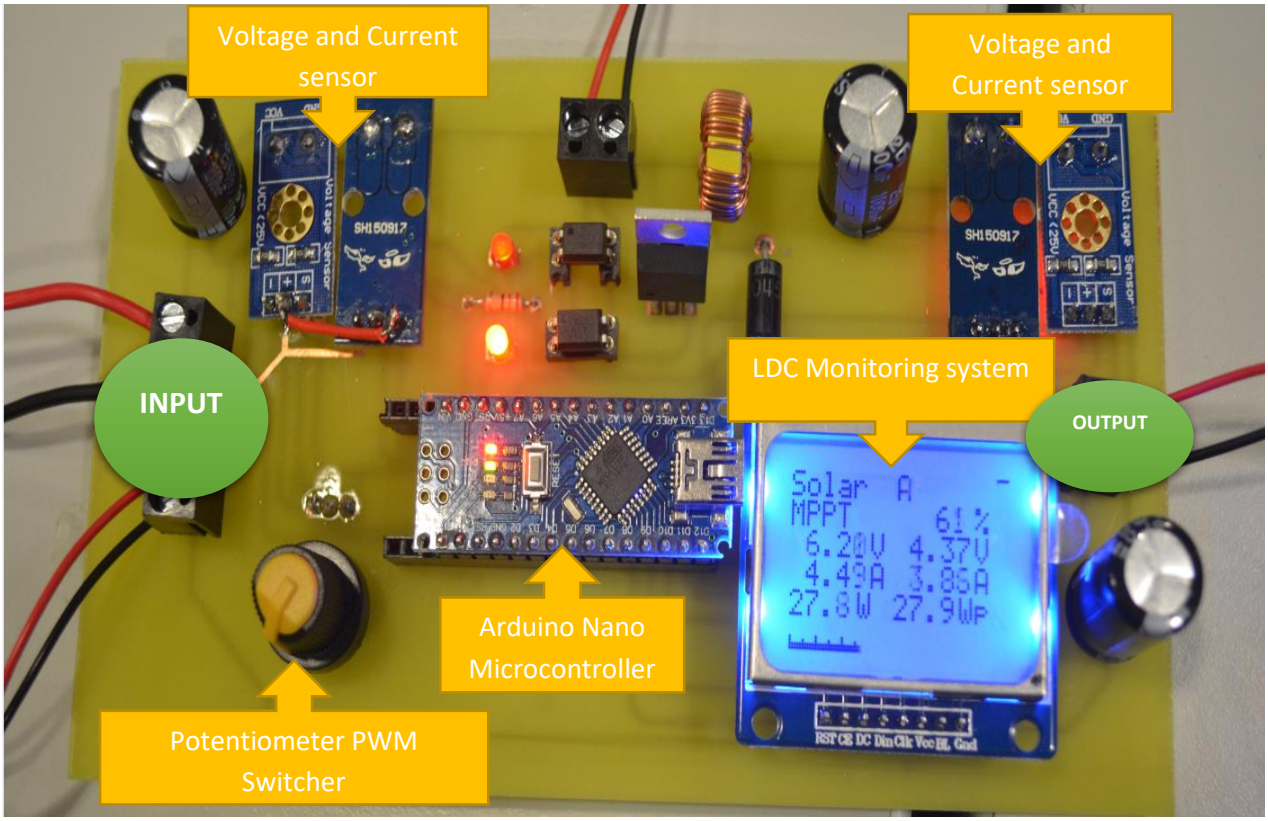

Figure 7-6 3D renewable energy platform laboratory evaluation (solar output- System front end)

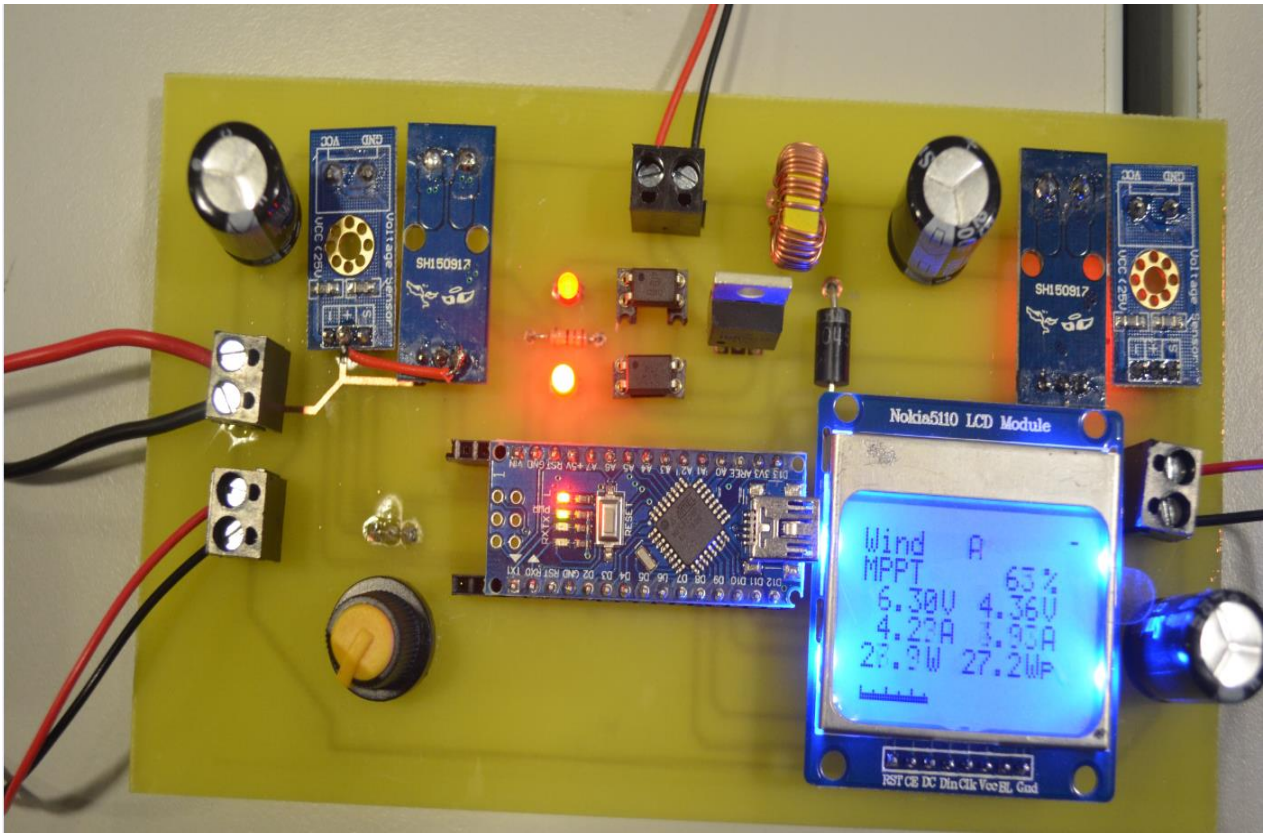

Figure 7-7 3D renewable energy platform (Wind turbine output- System front end)

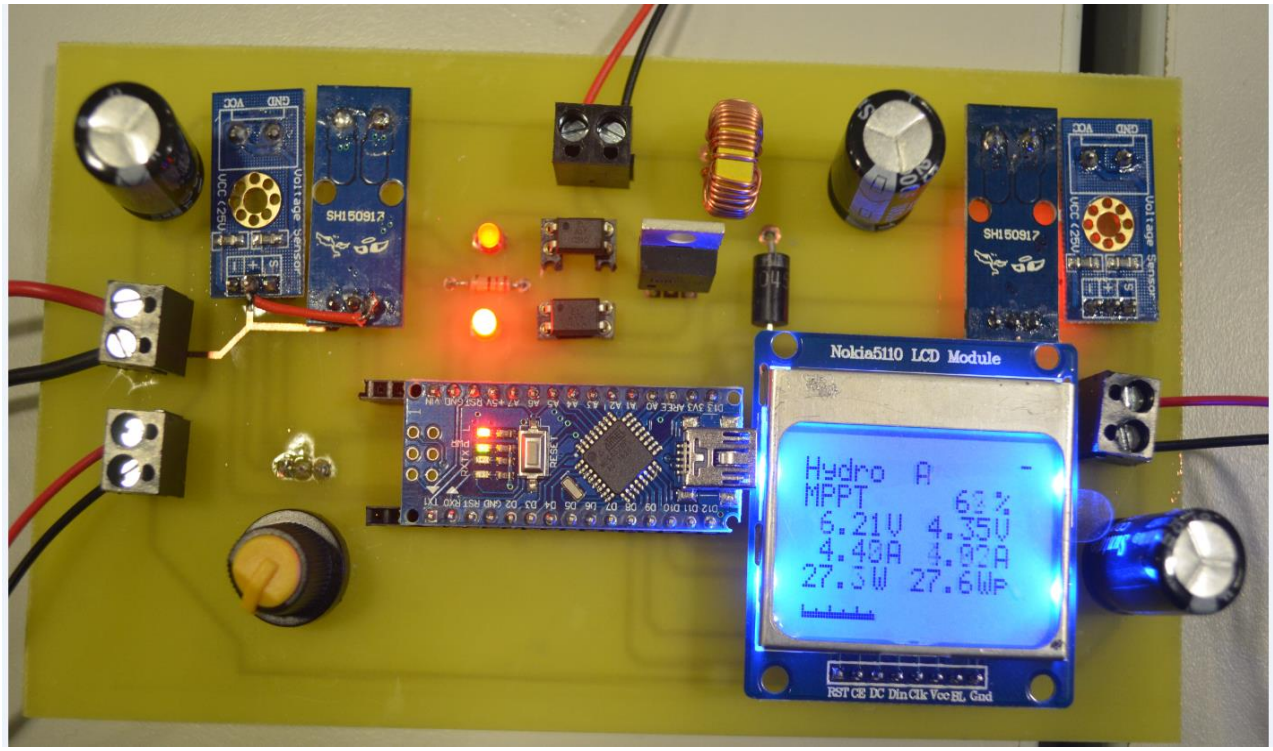

Figure 7-8 3D renewable energy platform (Hydro output- System front end)

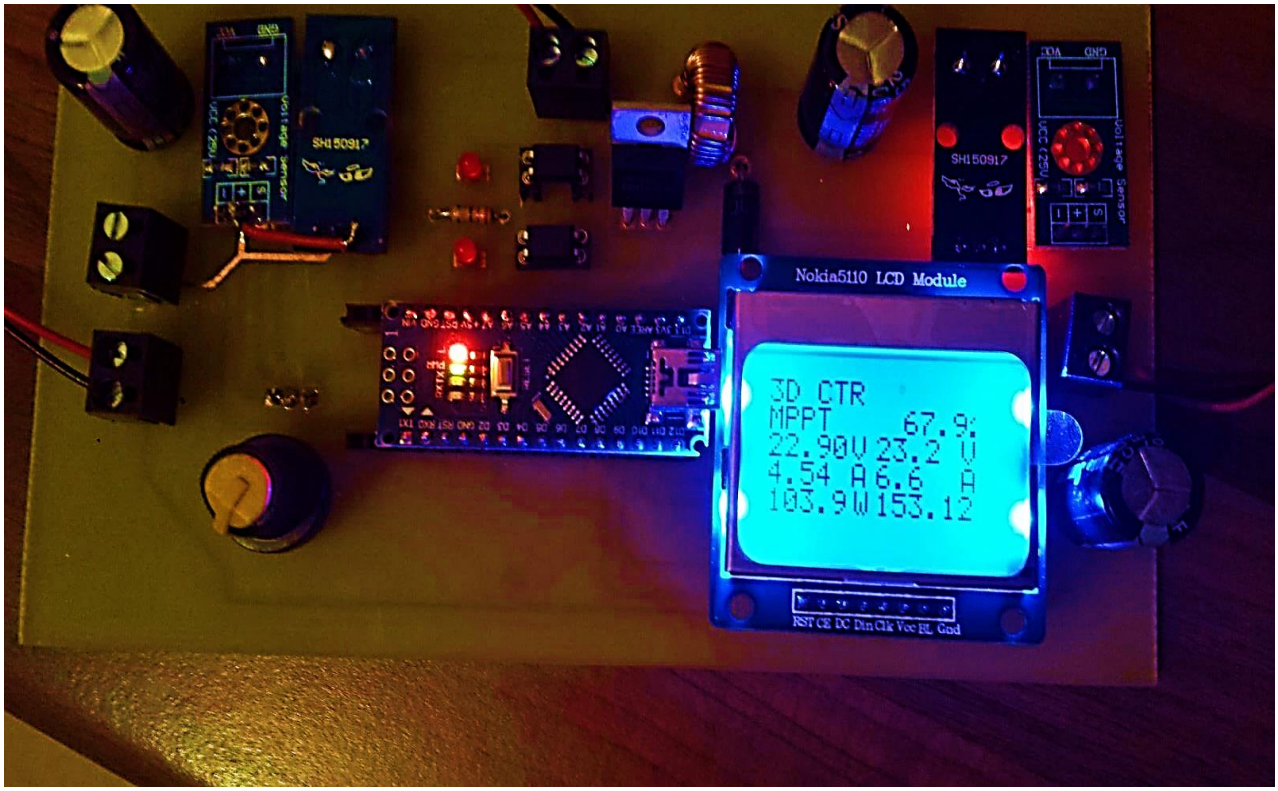

Figure 7-9 3D renewable energy platform (Combined 3D output- System front end)

7.2.1. SOLAR CONTROLLER

Figure 7-6 shows the controller for the photovoltaic system. At the input stage the designed and built controller tracks a maximum of 6.20 volts at a 61% efficiency and a current generated at 4.49Amps with a load delivery of 3.86 Amps. The demand conditions thus the battery draws up the output current and voltage needed from the maximum tracked voltage and current at the input stage. The application of the microcontroller and that of enables this to be proportionally made as demand is fed according to how much power is needed whilst the rest is strategically stored in a battery used as a backup of the entire system. Readings on the LCD shows a power delivery of 27.9 watts with the potentiometer PWM switch set to Automatic meaning maximum delivery is tracked constantly as solar rays or daylight changes during the day. Under laboratory conditions light were partly shaded on the solar panels so as to generate between 5-6 volts at the input for safety purposes and to maintain continuous operation so as to get a generalised output on the main 3D controller.

7.2.2. WIND CONTROLLER

Figure 7-7 shows the controller for the Wind turbine system. . At the input stage the designed and built controller tracks a maximum voltage of 6.30 volts at a 63% efficiency and a current generated at 4.23 Amps with a load delivery of 3.93 Amps. The demand conditions thus the

battery draws up the output current and voltage needed from the maximum tracked voltage and current at the input stage. The application of the microcontroller and that of enables this to be proportionally made as demand is fed according to how much power is needed whilst the rest is strategically stored in a battery used as a backup of the entire system. Readings on the LCD shows a power delivery of 27.2 watts to the load with the potentiometer PWM switch set to Automatic meaning maximum delivery is tracked constantly as wind speed was controlled using a regulated transformer delivering a 12 volts to the laboratory fan .

7.2.3. HYDRO CONTROLLER

Figure 7-8 shows the controller for the Hydro turbine system which was represented by the DC power supply. At the input stage, a maximum of 6.21 volts at a 62% efficiency was obtained and a generated current of 4.40 Amps delivering 4.02 Amps. The demand conditions thus the battery draws up the output current and voltage needed from the maximum tracked voltage and current at the input stage. The application of the microcontroller and that of enables this to be proportionally made as demand is fed according to how much power is needed whilst the rest is strategically stored in a battery used as a backup of the entire system. Readings on the LCD shows a power delivery of 27.6 watts to the load and a generated power supply of 27.3 watts

7.2.4. 3D CONTROLLER

The controller output is shown in figure 7.9. In essence, the 3D controller unit sums up power, voltages and current generated at the solar, wind and hydro output terminals and tracks the maximum point delivery of each of the sources and deliver this to the load and in case load demand is low, this is fed to a standby battery for charging purposes. The generated output of the 3D sources shows a cumulated and maximum tracked power of 22.90 volts with a delivery of 23.2 volts whereas a 4.56 amps is obtained at the input and 6.6 amps is delivered to the battery. The maximum power delivered was found to be 153.12 watts. The entire system efficiency was found to be 67.9% which shows an above average efficiency of the entire system.

Input Parameters			Output parameters			Efficiency %
Voltage (V)	Current (I)	Power (W)	Voltage (V)	Current (I)	Power (W)	
16.83	0.73	12.29	10.41	0.96	9.99	81.34
10.50	0.90	9.45	8.20	1.12	9.18	97.19
10.43	0.89	9.28	5.54	1.37	7.60	81.87
15.37	0.93	14.29	6.28	1.92	12.06	84.35
17.37	1.00	17.37	8.28	2.10	17.39	100.12

7.3. SUMMARY

The practical or field testing of our 3D renewable energy platform has been tested under laboratory conditions. The 3D sources were each represented by factory manufactured systems for which their specifications and technical parameters were provided in this chapter. Joined as single system, the power generation ability of the 3D sources were correlated accordingly together with a central control unit enabling full control of the 3D renewable energy platform. This 3D central control unit focused on the development of maximum power point tracking system using Perturb and Observation (P&O) method. The system consists of a DC-DC buck converter circuit which converts the high/not stable voltage obtained from each of the 3D sources panel and either charges the battery when load demand conditions are low or supplies the load with enough power needed. This system features the use of embedded system based on Arduino microcontroller which plays the main part of the system. The microcontroller processes all the data and the sensors signal such as the temperature sensor, current sensor, and voltage sensors for three of the sources and at the battery terminals. The program runs on the chip based on P&O which executes continuously and switches between different duty cycles to the MOSFET gate, for maximising the power from the solar, wind and hydro systems and maintain a balanced system at the maximum power point obtained.

CHAPTER 8 - GENERAL CONCLUSION, DISCUSSIONS & RECOMMENDATIONS FOR FUTURE WORK

A highly efficient renewable energy platform that could suit Togo's power system infrastructure and industrial application have been developed and presented in this thesis. The developed platform presents an innovative approach to overcome the barriers for implementing the renewable energy resources into Togo's power sector and introduces a new approach based on modular form. The modular form of the 3D platform would allow Togo's power sector and other nation adopting such approach to utilise the technology using a number of configurations i.e. 1D, 2D and 3D. This is mainly dependent on the renewable energy resources available, geographical location, power demand, possible industrial load nature and applications.

The development process of the proposed system has passed through a number of stages. These included:

An investigation into the governmental reports, key database, publications, technical reports and case studies, related areas to the current research programme. This was concluded with the possible recommended business model and renewable energy platform.

Computer Aided Design and Analysis of the front End renewable energy resources of the proposed platform. This was mainly aiming to investigate the possible factors of improving the efficiency of the front end units. The computer aided design and analysis has been carried to Hydropower units (water wheels, Kaplan turbine, dual feed arrangement for both water wheel and Kaplan turbine …etc.), Wind turbine units, 2D arrangements i.e. wind and hydropower …etc.

Computer Aided Design, simulation and Modelling of the Backend of System (BoS) of the proposed renewable energy platform i.e. control system, multi-level converted and relevant filtration system. This concluded with the possible recommendation of multi-level converter, relevant filtration system based on possible load nature and applications.

System integration of the proposed renewable energy platform into the smart grid. This concluded with a computer simulation and analysis model of the system that shows the dynamic behaviour of the proposed model which is examined under different operating conditions.

Carry out laboratory validation and evaluation of the proposed renewable energy platform. This demonstrated the dynamic response of the system, stability of the system and its output and control capability of the proposed system.

Togo for years has been in serious energy deficiency due to many factors ranging from bad energy management to failure to invest into renewable energy sources. The country electricity supply is mostly based on fossil fuel thus 78% and 33 % hydro. Based on an Area of 56600Km^2, the country is faced with rapid growth and new industrial investment and project coming in due to new government legislation facilitating trade (Rep of Togo, 2010). In addition, the country imports hydrocarbons in order to produce electricity (ECOWAS, 2005) making the country succumb to the fluctuation effect of oil price on international markets thereby making it very difficult to attain full electricity generation efficiency leading to serious disturbances in the country. The country geographical position is an advantage for renewable energy exploitation and implementation as the country aims to attain at least 75 % of full electrification by 2030 (ECOWAS white paper, 2010). Considering the country's aim to attain full electrification in few years, it is important to consider other and cleaner sources of generating energy. It is in this light that this research was aimed at providing a system by name "Computer aided design of a 3D renewable energy platform to fully utilise Togo's renewable energy resources into their smart grid power system infrastructure" that will efficiently help the country in attaining its energy and electrification target. This application of this highly efficient system would not only be beneficial to Togo only but will go a long way to help any other country, government, institutions that will feel this innovative technology will help them in one way or the other in generating clean energy and meeting up demands of a particular city, country or community.

The research undertaken therefore to provide a "Computer aided design of a 3D renewable Energy platform to fully utilise Togo's renewable energy resources into their smart grid power system infrastructure" introduces a solution to challenges in the energy generation sector which do not only refrain to the safe supply of clean Energy but also aim to contribute towards providing a sustainable solution to current environmental challenges. A major importance for the theoretical study of hybrid systems, based on renewable energy (photovoltaic, wind, hydro system) in relation to this research is the availability of the models that have been utilized to study the behaviour of hybrid systems and most importantly, computer aided design simulation tools. As the available tools are quite limited, this research has presented the most current and

up to date model which can be used for the simulation purposes of the 3D renewable energy platform integration as well as for educational purposes. A research methodology needed to defined the research strategy and after careful consideration, the research onion model was used considering it helped defining in clear terms the methods and processes that can be implemented for a successful research. The research methods therefore used for this research were Exploratory, Constructive and empirically based. The three methods allowed me to meet the research objectives through a step by step procedure, whilst identifying the application design specifications, the development of the system architecture, the system main hardware & software units, development of a finite solution by obtaining an outline design, and then test the feasibility of the design using empirical evidence. A prototype has also been developed and tested based on design specifications and needs to verify the potential of the technology from an economic, social and policy point of view. The development plan of this PhD research was split into three main stages. The initial stage consisted of conducting a feasibility study and conduct the literature survey that covered all the elements of the research, a focus on the definition of the 3D renewable energy station model system needs, design specification and architecture. The second stage consisted of designing and developing the system hardware and software units and the last stage focused on the system Integration and Field test validations

The outcome of the initial stage showed that amalgamation of renewable energy and the use of an energy mixed model was plausible based on the fact that empirical evidences showed already existing model of the use of a dual renewable energy source based system and the possibilities of adding more renewable energy sources to existing technologies considering system control have been duly adjusted to cope with this. Simulation and CAD models as earlier mentioned were also encouraging factors as efficient tools to carry out design and feasibilities studies of each models and design was part of the university available software tools.

The outcome of literature survey was also very interesting as Togo's Total energy consumption in 2012, was estimated at 2 056370 toes (0.31 toes per capita), of which 67% was from biomass and 29% from Oil, for which electricity occupied 4% of annual energy consumption. The national electrification rate has been stagnant at a 27% rate for a decade now for which 50% were concentrated in urban areas and 5% in rural areas. The Government of Togo (according to its national strategy SCAPE 2013-2017) expects to achieve a rate of 50% of national electrification by 2024. Final energy consumption is mainly distributed between households (64%), transport (24%), market and public services (9%), and industry accounts for 3%.

Analysis carried out also showed great potential for solar energy harnessing for photovoltaic power generation application with global solar energy irradiation on a horizontal plane estimated at 4.5 kWh/m²/day with an average of 10-12 hours of sun rays available daily. Wind potential was also investigated with Togo being ranked amongst the quiet geographical areas in Africa, although transient spikes wind can reach high values up to 4m/s in some areas especially in the northern part of the country during harmattan period. Only the coastal area of the country has favourable evidence with wind speeds of 7m/s on average making the development of wind power a viable alternative source to consider. Hydropower potential was also investigated with studies showing at least 40 sites of which 23 sites have potentials greater than 2 MW of energy production totalling 850 GWh for an installed capacity of about 224 MW. The country equally has a wonderful coastline that extends to about 55 Km on the Atlantic sea, River Oti and Mono of which water flow strength could be great for hydro and tidal power generation.

The literature survey also showed encouraging energy policy focusing on the development and adoption of an investment code or law which includes tax and incentives for the promotion of renewables energies; the development and adoption of rules defining the conditions for production of renewable energy and connection to the national network at a discounted price; and the development and adoption of a law to define energy efficiency policy by promoting equipment using low energy. The outcome of this concluded Togo's energy regulatory framework and policies analysis which are definitely encouraging factors for the implementation of the 3D renewable energy platform.

Nevertheless, the business model currently adopted in Togo satisfies current Energy demand but does not take into account future challenges, energy demand and grid expansion. The criticism of this business model would go to the cost incurred by the purchase of Diesel from Nigeria using the West African power pool pipeline for the 6 Tri fuel diesel engines plant for contour global and the cost incurred originally in the building of a Diesel power plant instead of an investment into renewable energy power expansion considering the potentialities of renewable energy sources in Togo. Considering all of the above, it is apparent that efforts needs to be conjugated to meet future power demands hence the full optimisation and implementation of renewable energy systems for sustainable energy production for which a new business model focusing on the integration of Independent power producers and policies focused on subsidising the renewable energy sector creating opportunities for efficient cash flow from investors. With these changes, the costs of renewable electricity can be lowered by up to 20%,

where customers can benefit from values they lend to the system, and take advantage of new markets able to reduce the cost of integrating renewable energy sources, improving reliability and accelerating innovation. The findings of this litterature goes to show that Togo indeed has some serious energy defficiency issues together with an average power gneneration system used in meeting current energy demands in the country. The cost associated with this however is unnimaginable and couldn't be evaluated considering unavailability of data and also due to the fact that ever changing pices of fossil fuel related products. The technical feasability of the 3D renewable energy platform has also been conducted in Matlab simulink and simulation result shows that the amalgamation of these three sources represents the advanced stage in hybrid power generation systems with litteratures showing easy integration into smart grid enabling use to define this innovative 3D renewable energy platform as a contributor to the solutions to Togo's energy issues. The current business model also shows significant encouragement from the government for IPP's to be integrated and for the promotion of renewable nergy power generation

8.1. MAJOR CONTRIBUTIONS OF THIS RESEARCH WORK

The work discussed in this thesis presented contributions in the fields of renewable power generation systems, smart grid systems, and power electronics. These are summarised as followed

- The design and development of a 3D renewable energy platform that could be used for industrial, commercial and domestic applications.
- An innovative design focused on the used on the doubly fed wind turbine for the 3D system enhancing the efficiency of the entire 3D sustainable renewable micro power micro station
- The design of an overshot water wheel with an average efficiency reaching 85% for better hydropower production
- The implementation a triple fed Hydro generator namely (02 overshot water wheel; 01 Kaplan turbine) enabling hydropower production to be the most efficient system of our 3D renewable energy platform
- The implementation of many innovative ideas that presents an entirely new perspective on the possible usage of a 3D central control unit focused on the development of maximum power point tracking system using Perturb and Observation (P&O) method consisting of a DC-DC buck converter circuit which converts the high/unstable voltage

obtained from each of the 3D sources into a much improved and regulated. This system features the use of embedded system based on Arduino microcontroller which mainly represented the system intelligence as it processes all the data and the sensors signal such as the temperature sensor, current sensor, and voltage sensors for three of the sources and at the battery terminals equally.

- The thesis presented a viable idea into the implementation of the a 3D Renewable energy platform to fully utilise green energy resources into smart grid power system infrastructure" through individual intelligent nodes control enabling efficient management of the variable nature of the generated power and uncertainty during continuous balancing of the system; a balancing of the supply and demand during generation scarcity and surplus situations and a solution to challenges related to high peak load during periods of low variable RE production.

8.2. LIMITATIONS OF THE CURRENT DESIGN

The limitations and technical problems faced were purely in the development of the control system and the practical unit assembly of the 3D renewable energy platform

Challenges in the control system:

The challenges associated with the control system was also in the laboratory validation and assembly unit. Initial testing of the control system were inconclusive as the output didn't deliver the expected output which was due to connections error within the assembly of the control system. A power management circuit such as ours was designed to rectify the input voltage, if necessary and regulates the output voltage to the desired level to charge the battery or feed the load. The core part of this control system is the buck converter, and the key requirement for the control system to maximize the net energy harvested by (i) transferring maximum power from the source to the storage device and (ii) dissipating minimal power. Meeting the two requirements needed a trade-off in the control circuitry design for small scale energy harvesting. To transfer the maximum power, the load impedance was to match the source impedance, and the source impedance changes as operating conditions changes. Matching between the source and load were the most complicated but was resolved using maximum power point tracking (MPPT), which dynamically adjusts the load impedance (or the load voltage for each of the three sources), specifically the input impedance of the buck converter. To minimize power dissipation therefore we selected a unique MPPT algorithm judiciously by considering the type of transducer, the amount of energy available, and its

application. We also noted that when the storage is drained completely, the control system fails to start. Two solutions were adopted; one is to provide a dedicated backup battery for cold start, and the other one use the source power to start. Both approaches have pros and cons as a controls system for energy harvesting such as ours should be able to harvest energy from a low input voltage and should have low standby power dissipation, and desirably a battery controller circuit. Some design challenges of control circuitries are specific to energy sources. For example, a rectifier circuit for a piezoelectric and electromagnetic generator causes a substantial loss for small scale vibration energy harvesting. Implementation of a power efficient MPPT is difficult for such vibration energy, and incorporation of a sleep mode may be necessary.

Measurements:

Considering the challenges associated with the control system, measurements within this current area of research is still a very sensitive area. Specialist equipment's are not needed to measure outputs per say but essentials and accurate measurement from the sensors are still a very much sensitive which needs constant improvements and research in order to improve sensors efficacy and efficiency. Majority of the measurements carried out in this research were taken using available facilities and basic principles of measurement which in fact was a major reason to carry out these measurements a few times to ensure that high precision of measurements has been recorded

CHAPTER 9 - RECOMMENDATIONS & FUTURE WORK

The research work has significant contribution in the field of renewable energy systems, methodology for modelling and design, implementation of specific control circuity system fit for a micro or large scale renewable energy harvesting system. Subsequently, numerous technical points have been duly raised in this area of research and applications and the possibility to extend this system to cover different applications is quite viable as one could deduce from the outcome of this research.

Further research work and experimental work is however required to fully implement the capability of a developed renewable energy system with their unique control systems. There are various ways our proposed system could be developed in order to increase its scope and applicability further. These may include the incorporation of further algorithms for system stability. This therefore shows a necessity for future work to be focused on the following questions

- Can this innovative and energy miscegenation system work with same efficiency if the load demand increases?
- Would the parallel operation of all the three renewable energy system (3D) have the same effectiveness even in off grid paradigm.
- The efficiency of solar power system need to be increased over 60%.
- The size of the system need to be as such that it can be constructed in nearly all possible terrains with a single control system embedded within its architecture enabling its mobility and facilitate usage for the end user
- Could artificial intelligence system enable an automatic adjustment and stability of the system with various load demands and automatic assessment of the system for maintenance purposes?

A fully practical assembled unit of the 3D unit for micro, mini, medium and large scale 3D platform couldn't have been done yet, hence practical efficiency level using our proposed system for various energy deficiency issues couldn't possibly be confirmed. But once completed we need to investigate how well our solution method works practically for a medium and large scale applications. This would mean that for Mega systems, new mathematical model enabling linearity's of non-linear signals from the input must be determined clearly for more accurate study of system dynamic

References

A Lucero Tenorio,'Hydro turbine and Governor modelling', Norwegian University Science & Technology, 2010

Ahmad Al Nabulsi, and R. Dhaouadi, Efficiency Optimization of a DSP- Based Standalone PV System Fuzzy Logic and Dual-MPPT Control", IEEE Transactions On Industrial Informatics, Vol. 8, No. 3, 2008.

Advanced Inverter technology for high penetration levels of PV generation in distribution systems, [online] available at http://www.nrel.gov/docs/fy14osti/60737.pdf accessed on 01/08/2017

Asgeirsson, H., "Distribution automation—the foundation for the smart grid at DTE energy," Power and Energy Society General Meeting, IEEE, pp. 1-3, 2010,

Atsushi Izena, Hidemi Kihara, Toshikazu Shimujo, Kaiichirou Hirayama, 'Practical hydraulic turbine Model.' , IEEE Conference on, 2006.

Atwa, Y., et al., "Optimal renewable resources mix for distribution system energy loss minimization," Power Systems, IEEE Transactions on, vol. 25 (1), pp. 360-370, 2010.

Atwa, Y., et al., "Optimal renewable resources mix for distribution system energy loss minimization," Power Systems, IEEE Transactions on, vol. 25 (1), pp. 360-370, 2010.

Ayompe, L., et al., "Validated real-time energy models for small-scale grid-connected PV-systems," Energy, vol. 35 (10), pp. 4086-4091, 2010.

B. Alamri and M. Darwish, "Enhancing Power Quality of Distributed Generator Systems Using Multilevel VSC", ResCon, Brunel University, London, UK, 2013.

B. Alamri and M. Darwish, "Optimum Switching Angles Determination for Cadcaded H-Bridge Multilevel Inverters Using Genetic Algorithm (GA)", ResCon, Brunel University, London, UK, 2014.

B. Alamri and M. Darwish, "Power Loss Investigation for 13- level Cascaded H-Bridge Multilevel Inverter", Vol. 2, No. 6 , pp. 230-238 J. Energy Power Sources, 2015

B. Alamri and M. Darwish, "Power loss investigation in HVDC for cascaded H-bridge multilevel inverters (CHB-MLI)," PowerTech, 2015 IEEE Eindhoven, pp. 1-7. Eindhoven, 2015

B. Alamri and M. Darwish, "Precise Modelling of Switching and Conduction Losses in Cascaded H-bridge Multilevel Inverters", Int. Power Engineering Conference (UPEC), 49th International Universities, Cluj-Napoca, pp. 1-6. IEEE, 2014.

B. Alamri, A. Sallama and M. Darwish, "Optimum SHE for Cascaded H-Bridge Multilevel Inverters Using: NR-GA-PSO, Comparative Study," AC and DC Power Transmission, 11th IET International Conference on, Birmingham, pp. 1-10. 2015,

B. Alamri, S. Alshahrani and M. Darwish, "Losses investigation in SPWM-controlled cascaded H-bridge multilevel inverters," Power Engineering Conference (UPEC), 2015 50th International Universities, Stoke on Trent, pp. 1-5. 2015,

B.Vairamohan: State of Charge Estimation of Batteries, A Thesis Presented for the Master of Science Degree, The University of Tennessee, Knoxville, U.S.A., 2002

Bakker, V., et al., "Demand side load management using a three step optimization methodology," IEEE International Conference on Smart Grid Communications (SmartGridComm), pp. 431-436. 2010

Balijepalli, V. M., et al., "Deployment of microgrids in India," IEEE Power and Energy Society General Meeting, pp. 1- 7. 2010

Bernard, 2010 Bernard Equer, Energie solaire photovoltaïque (Ellipses 2010).

Bică, C. D. Dumitru, A. Gligor, A.-V. Duka – Renewable energy.Isolated hybrid solar-wind-hydro renewable energy systems, Ed. Intech, Vukovar, Croaţia, p.297-316; 2009

C.Jaliu, I. Visa, D. Diaconescu, R. Saulescu, M. Neagoe,'Dynamic Model of a Small Hydropower Plant', Optimization of Electrical and electronic parameters IEEE, pp.258-358, 2014

Carmen L.T Borges and Roberto J. Into, 'Small hydro power plants energy availability modelling for generation reliability evaluation', IEEE (85), pp.258-365, 2013

Cecati, C., et al., "Smart Grids Operation with Distributed Generation and Demand Side Management," Modeling and Control of Sustainable Power Systems, ed: Springer, pp. 27-46.2012,

Celli, F. Pilo, G. Pisano, and G. G. Soma, “Optimal Planning for Active Networks,” in 16th Power Systems Computation Conference (PSCC), Glasgow, Scotland, 2008.

Chen, S.-y., et al., "Survey on smart grid technology," Power System Technology, vol. 33 (8), pp. 1-7, 2009.

Chian-Song Chiu, Ya-Lun Ouyang, and Chan-Yu Ku, 'Terminal Sliding Mode Control for Maximum Power Point Tracking of Photovoltaic Power Generation Systems', Solar Energy, 86 pp. 2986-95. (2012)

Clastres, C., "Smart grids: Another step towards competition, energy security and climate change objectives," Energy Policy, vol. 39 (9), pp. 5399-5408, 2011.

Cook, T.C., G.E. Hecker, H.B. Faulkner, and W. Jansen. 1997. Development of a more fish tolerant Turbine runner-advanced hydropower project hydroelectric power efficiency improvement

Crow, M. L., et al., "Intelligent Energy Management of the FREEDM System," Power and Energy Society General Meeting, IEEE, pp. 1-4., 2010

D. P. Hohm, and M. E. Ropp, 'Comparative Study of Maximum Power Point Tracking Algorithms Using an Experimental, Programmable, Maximum Power Point Tracking Test Bed', in Photovoltaic Specialists Conference, 2000. Conference Record of the Twenty-Eighth IEEE, pp. 1699-702. 2000.

D. W. Hart, Power Electronics, McGraw-Hill, 2011.

D.S. Morales, “Maximum Power Point Tracking Algorithms for Photovoltaic Applications” [Master’s Thesis], Aalto University, Faculty of Electronics, Communications and Automation, 2010.

De Brito, M.A.G., Sampaio, L.P., Junior, L.G., Canesin, C.A., 2010, " Evaluation of MPPT techniques for photovoltaic applications ", IEEE International Symposium on Industrial Electronics, PP. 1039-1044, IEEE Publisher., London 2010

De Brito, M.A.G., Sampaio, L.P., Luigi, G., e Melo, G.A., et.al, 2011 "Comparative analysis of MPPT techniques for PV applications ", International Conference on Clean Electrical Power (ICCEP) , PP. 99-104, IEEE Publisher, London 2011.

De Castro, L. and J. Dutra, "Paying for the smart grid," Energy Economics, vol. 40, pp. S74-S84, 2013.

De Jong, S. and J. Wouters, "Making the Transition: EU-China Cooperation on Renewable Energy and Carbon Capture and Storage," Leuven Centre for Global Governance Studies Working Paper, (66), 2011.

Dorin Petreus, Toma Patarau, Stefan Daraban, Cristina Morel, and Brian Morley, 'A Novel Maximum Power Point Tracker Based on Analog and Digital Control Loops', Solar Energy, 85 pp. 588-600. (2011)

Dr. B. R Gupta 'Generation of Electrical Energy', Sixth Edition, ISBN: 81-219-0102-2, by Eurasia Publishing House.

Drouilhet, S.; Muljadi, E.; Holz, R.; Gevorgian, V. Optimizing Small Wind Turbine Performance in Battery Charging Applications. NREL/TP-441-7808. Golden, CO: National Renewable Energy Laboratory, 1995.

Drouilhet, S.; Muljadi, E.; Holz, R.; Gevorgian, V. Optimizing Small Wind Turbine Performance in Battery Charging Applications. NREL/TP-441-7808. Golden, CO: National Renewable Energy Laboratory, 1995.

E. Ortjohann, O. Omari, R. Saiju, N. Hamsic, D. Morton, A Simulation Model For Expandable Hybrid Power Systems. University of Applied Sciences Sudwestfalen, Division Soest, Laboratory of Power ¨ Systems and Power Economics. Internal Report.

Earle, R., et al., "Measuring the capacity impacts of demand response," The Electricity Journal, vol. 22 (6), pp. 47-58, 2009.

Electronic Equipment, IEEE trans. Pp: 1217-1223, 2010

Elgendy, B. Zahawi, and D. J. Atkinson, 'Assessment of Perturb and Observe MPPT Algorithm Implementation Techniques for PV Pumping Applications', Sustainable Energy, IEEE Transactions on, 3 pp. 21-33. (2012)

Employee engagement and its various impact, [online] available at http://business.kingston.ac.uk/cress/employee-engagement-consortium Accessed on 25/04/12

Employee engagement at university, [online] available at http://www.employee-engagement-surveys.com/employee-engagement-university.html Accessed on 20/04/12

Employee engagement- general survey, [online] available at http://staff.napier.ac.uk/services/hr/workingattheUniversity/Pages/EmployeeEngagementSurvey.aspx Accessed on 15/04/12

Employee engagement news, Kent survey, [online] available at http://www.kent.ac.uk/kbs/ecg/news-events/esrc-employee-engagement.html Accessed on 25/04/12

Employee engagement survey, [online] available at http://www.gre.ac.uk/offices/hr/ere/employee-surveys Accessed on 22/04/12

Employee engagement, HR perspective, [online] available at http://www.gallup.com/consulting/52/employee-engagement.aspx Accessed on 15/04/12

Energy crisis awareness in Africa [internet], available at http://www.ofid.org/publications/PDF/pamphlet/ofid_pam_39_EP.pdf Accessed on 10/01/12

Energy crisis in Africa, [internet] available at http://africa-toolkit.reeep.org/modules/Module12.pdf Accessed on 15/01/2012

Energy crisis on the Gulf of Guinea, focus on Nigeria Energy [internet], available at http://www.africapeace.org/home/content/o/l/u/oluwakorede/html/images/file/strategic%20perspective%20onnigeria.pdf Accessed on the 20/01/2012

Energy demand and supply [online], available at http://www.econstor.eu/bitstream/10419/19387/1/357.pdf Accessed on 11/07/12

Engineering Society 2004 General Meeting, , IEEE, 6-10 June, 2004

EPRI (Electric Power Research Institute) (2006), Hydro wheels self-reliance, experience with micro Hydro generators, a US micro Hydro Power Technology Report, Volume 2, New York, US

EPRI (Electric Power Research Institute) (2006)Hydro wheels self-reliance, experience with micro hydro generators, , Rehabilitating and Upgrading Hydro Power Plants - a US micro Hydro Power Technology ound-Up Report, Volume 2, New York, US

F. Valenciaga, P.F. PulestonSupervisor Control for a Stand-Alone Hybrid Generation System Using Wind and Photovoltaic Energy. IEEE Transactions on Energy Conversion, VOL. 20, NO. 2, JUNE 2005.

Fadaeenejad, M., et al., "The present and future of smart power grid in developing countries," Renewable and Sustainable Energy Reviews, vol. 29, pp. 828-834, 2014.

Farhangi, H., "The path of the smart grid," Power and Energy Magazine, IEEE, vol. 8 (1), pp. 18-28, 2010.

Femia, G. Petrone, G. Spagnuolo, and M. Vitelli, 'Optimization of Perturb and Observe Maximum Power Point Tracking Method', Power Electronics, IEEE Transactions on, 20 pp. 963-73. (2005),

Fred Prillwitz, Salah Eddin Al-Ali, Torsten Haase, Harald Weber, Lutfi Saqe,'Simulation model of the hydro power plant Shkopeti', EUROSIM

Garrity, T. F., "Getting smart," Power and Energy Magazine, IEEE, vol. 6 (2), pp. 38-45, 2008.

Gaviano, A., et al., "Challenges and Integration of PV and Wind Energy Facilities from a Smart Grid Point of View," Energy Procedia, vol. 25 pp. 118-125, 2012

Global Energy Network Institute, [internet], available at http://www.economist.com/debate/days/view/159 Accessed on 10/01/2012

Goudar, M.D., Patil, B.P., Kumar, V. , 2011, " Adaptive MPPT Algorithm for a Distributed Wireless Photovoltaic Based Irrigation System ", International Conference on Devices and Communications (ICDeCom), PP. 1-4, IEEE Publisher.

H. Hussein, I. Muta, T. Hoshino, and M. Osakada, 'Maximum Photovoltaic Power Tracking: An Algorithm for Rapidly Changing Atmospheric Conditions', Generation, Transmission and Distribution, IEE Proceedings-, 142, pp. 59-64. (1995)

H. Patel and V. Agarwal, “Maximum Power Point Tracking Scheme for PV Systems Operating Under Partially Shaded Condition,” IEEE Transactions on Industrial Electronics, vol. 55, no. 4, April 2008.

H. Weber, F. Prillwitz ,'Simulation models of the hydro power plants in Macedonia and Yugoslavia', IEEE Bologna powerTech Conference,

Hannes Knopf, "Analysis, Simulation, and Evaluation of Maximum Power Point Tracking (MPPT) Methods for a Solar Powered Vehicle ", 1999, MSc Thesis, Portland State University.

Holst, M. Golubovic , H. Weber, 'Dynamic model of hydro power plant', International Youth Conf. on Energetic, 31 May-2 June, 2007

Hui Hu @ Iowa State University 2017. [ONLINE] Available at: http://www.aere.iastate.edu/~huhui/DRWT.html. [Accessed 18 February 2017]

Human resource survey, employee engagement, [online] available at http://www.mmu.ac.uk/humanresources/devandtrain/docs/employee-engagement-strategy-29-01-10.pdf Accessed on 17/04/12

IEEE Transactions on Power Electronics, vol. 26, no. 4, pp. 1010-1021, April 2011.

"IEEE Guide for Smart Grid Interoperability of Energy Technology and Information Technology Operation with the Electric Power System (EPS), End-Use Applications, and Loads," IEEE Standards Coordinating Committee 21, 2011.

International Energy Agency (IEA) (2010), Energy Technology & Hydropower generation Perspectives 2010, IEA, Paris, 2010

IPCC, 2007 Climate change 2007: the physical science basis. Contribution of Working Group I to the Fourth Assessment Report of the Intergovernmental Panel on Climate Change Cambridge University Press Cambridge, UK, 2007

IPCC, 2007 Climate change 2007: the physical science basis. Contribution of Working Group I to the Fourth Assessment Report of the Intergovernmental Panel on Climate Change Cambridge University Press Cambridge, UK, 2007

Islam, M.R., Youguang Guo, Jian Guo Zhu , Rabbani, M.G. , 2010, "Simulation of PV array characteristics and fabrication of microcontroller based MPPT ", International Conference on Electrical & amp; Computer Engineering, PP.155-158 (ICECE 2010),

J. E. Huber and J. W. Kolar, "Optimum number of cascaded cells for high-power medium-voltage multilevel converters," in 2013 IEEE Energy Conversion Congress and Exposition, pp. 359-366.2013

J. Ramu, S. Parkash, K. Srinivasu, R. Ram, M. Prasad and M. Hussain, "Reducing Switching Losses in Cascaded Multilevel Inverters Using Hybrid-Modulation Techniques," IJESE, vol. 2, pp. 26-36, 2012.

J.M. Undriil and J.L Woddward 'Non-Linear Hydro Governing Model and Improved Calculation for determining temporary droop', IEEE

J. Rodriguez, J. S. Lai and F. Z. Peng, “Multilevel Inverters: Survey of Topologies, Controls, and Applications,” IEEE Transactions on Industry Applications, vol. 49, no. 4, Aug. 2002, pp. 724-738.

J. S. Lai and F. Z. Peng, “Multilevel Converters-A new Breed of Power Converters,” IEEE Trans. Ind. Applicat., vol.32,pp. 509-517, May/June 1996.

K. Abdelsalam, A. M. Massoud, S. Ahmed and P. N. Enjeti, “High-Performance Adaptive Perturb and Observe MPPT Technique for Photovoltaic-Based Microgrids,”

Kaltschmitt, Renewable energy. Isolated hybrid solar-wind-hydro renewable energy systems, Ed. Intech, Vukovar, Croaţia, 2010, p.297-316;

Kauppert et al 2003, water wheels Efficiency Curve,– Britain’s new source of energy, Proc. ICE Civ. Eng., Vol. 150, No. 4, 178-186., London, 2003

Khan, M.I. et.al. "Photovoltaic Maximum Power Point Tracking Battery Charge Controller", 2009, 1st International Conference on the developments in Renewable Energy Technology (ICDRET), IEEE Publisher.

Khurana, S. and Anoop Kumar: "Small hydro power – A review", International Journal of Thermal Technologies, Vol. 1, NO. 1, pp. 107-110, December, 2011.

Kohsri, S. and B. Plangklang, "Energy Management and Control System for Smart Renewable Energy Remote Power Generation," Energy Procedia, vol. 9, pp. 198-206, 2011.

Koichiro Furukawa, Atsushi Izena,, Toshikazu Shimujo, Kaiichirou Hirayama, 'Governor control study at the time of a black start', by Power

Lee, P. and L. Lai, "A practical approach of smart metering integration in micro-grid," Power and Energy Society General Meeting, 2010 IEEE, 2010, pp. 1-5.

Lee, P. and L. Lai, "A practical approach of smart metering integration in micro-grid," Power and Energy Society General Meeting, 2010 IEEE, 2010, pp. 1-5.

Li, L., "The Effect Research of Smart Grid to Residential Users Intelligent Response Behavior," Advanced Materials Research, vol. 860, pp. 2452-2455, 2014.

Liserre, M., et al., "Future energy systems: Integrating renewable energy sources into the smart power grid through industrial electronics," Industrial Electronics Magazine, IEEE, vol. 4 (1), pp. 18-37, 2010.

Liu Xuejun, “An Improved Perturbation and Observation Maximum Power Point Tracking Algorithm for PV Panel” [Master’s Thesis], Concordia University, Department of Electrical and Computer Engineering, 2004.

Lopez-Lapena, O. , Penella, M.T. , Gasulla, M.A., 2010 "New MPPT Method for Low-Power Solar Energy Harvesting", IEEE Transactions on Industrial Electronics, Volume: 57 Issue: 9 Pages.

Lotfi Khemissi, Brahim Khiari, Ridha Andoulsi, and Adnane Cherif, 'Low Cost and High Efficiency of Single Phase Photovoltaic System Based on Microcontroller', Solar Energy, 86 pp. 1129-41.(2012)

Louis N. Hannett, B. Fardanesh, 'Field test to validate Hydro Turbine Governing Model structure and parameter', IEEE Trans. On Power

L. M. Tolbert, F. Z. Peng, “Multilevel Converters as a Utility Interface for Renewable Energy Systems,” in Proceedings of 2000 IEEE Power Engineering Society Summer Meeting, pp. 1271-1274.

L. M. Tolbert, F. Z. Peng, and T. Habetler, “Multilevel Converters for Large Electric drives,” IEEE Trans. Ind. Applicat.,vol.35,pp. 36-44, Jan./Feb. 1999.

M. Abdulkadir, S. Samosir and A. H. M. Yatim, “Modelling and Simulation of Maximum Power Point Tracking of Photovoltaic System in Simulink model,” 2012 IEEE International Conference on Power and Energy (PECon), 2-5 December 2012.

M. Ahmed, and M. Shoyama, 'Highly Efficient Variable-Step-Size Maximum Power Point Tracker for PV Systems', in Electrical and Electronics Engineering (ISEEE), 2010 3rd International Symposium on, 2010), pp. 112-17.

M. Darwish, B. Alamri and C. Marouchos, "OrCAD vs Matlab Simulink in teaching power electronics," Power Engineering Conference (UPEC), 2015 50th International Universities, Stoke on Trent, 2015, pp. 1-5.

M. Jantsch1, M. Real, H. Häberlin, C. Whitaker, K. Kurokawa, G. Blässer, P. Kremer, and C.W.G. Verhoeve, 2008, "Measurement of PV Maximum Power Point Tracking Performance ".

M. Komlanvi & M. Shafik & J. Garza Reyes, M. Elvis Ashu,” Computer simulation & modelling of a Micro-hydro power generator using Kaplan turbine for domestic & industrial building applications” International Conference in Sustainable design and Manufacturing, Cardiff, Wales, UK, 28-30 April 2014.

M. Komlanvi & M. Shafik &, M. Elvis Ashu, (2015), ‘3D sustainable Renewable Micro-power station for smart grid Industrial Applications’, International Journal of Robotics and Mechatronics, http://ojs.unsysdigital.com/index.php/ijrm, Vol. 2, Issue 4, 27th of December 2015.

M. komlanvi, M. shafik , M.A. Elvis, (2015), “Development of a 3D sustainable power station model using renewable energy resources”, Proceedings of the Business Innovation and Technology Management conference, ISBITM, UK, July 01-03 2013

M. komlanvi, M. shafik , M.A. Elvis, (2015), “Micro-hydro generator using eco-wheel system for domestic and industrial building applications”, International journal of Robotics and Mechatronics, IJRM, UK, December 2014

M. Lokanadham and K. Vijaya Bhaskar, “Incremental Conductance Based Maximum Power Point Tracking (MPPT) for Photovoltaic System,” International jurnal of Engineering research and Applications, vol. 2, no. 2, pp. 1420-1424, March-April 2012.

M.K. Deshmukh, S.S. Deshmukh. Modeling of hybrid renewable energy systems. Renew-able and Sustainable Energy Reviews 12 (2008) 235-249

M.K. Deshmukh, S.S. Deshmukh. Modeling of hybrid renewable energy systems. Renewable and Sustainable Energy Reviews 12 (2008) 235–249

Masafumi Miyatake, Tooru Kouno, and Motomu Nakano, 2002, "A Simple Maximum Power Point Tracking Control Employing Fibonacci Search Algorithm for Power Conditioner of

Matthew Buresch, 1983, "Photovoltaic Energy Systems ", McGraw-Hill, Inc.

Maximum Power Point Tracking,” IEEE Transactions on Industrial Electronics, vol. 54, no. 3, June 2007.

Models for system dynamic studies' Power systems, IEEE Trans.Vol.7, Issue 1 p.167-179., 1992.

Mohamed A. El-Sayed, and Osama A. Al-Naseem, 'Efficient Utilization of Photovoltaic Energy for Supplying of Remote Electric Loads', Universities' Power Engineering Conference (UPEC), Proceedings of 2011 46th International (2011), pp. 1-5.

Mohibullah, M. A. R. and MohdIqbal Abdul Hakim: "Basic design aspects of micro-hydro-power plant and its potential development in Malaysia", National Power and Energy Conference (PECon) Proceedings, Kuala Lumpur, Malaysia, 2004.

Molderink, A., et al., "Management and control of domestic smart grid technology," IEEE Transactions on Smart Grid, vol. 1 (2), pp. 109-119, 2010.

Muller W. 2003, Overshot water wheel buckets design specifications, Die Wasserräder, The water Wheel, Reprint of the 2nd Ed, Moritz Schäfer Verlag, Detmold, Germany.

N. Femia, G. Petrone, G. Spagnuolo, and M. Vitelli, 'Optimizing Duty-Cycle Perturbation of P&O MPPT Technique', in Power Electronics Specialists Conference, 2004. PESC 04. 2004 IEEE 35th Annual, Vol.3, 2004), pp. 1939- 44.

N. Femia, G. Petrone, G. Spagnuolo, and M. Vitelli, 'Optimizing Sampling Rate of P&O MPPT Technique', in Power Electronics Specialists Conference, 2004. PESC 04. 2004 IEEE 35th Annual, Vol.3, 2004), pp. 1945-49.

N. Khaehintung, C. Kangsajian and P. Sirisuk, “Grid-connected Photovoltaic System with Maximum Power Point Tracking using Self-Organzing Fuzzy Logic Controller,”

N. Mutoh, M. Ohno, and T. Inoue, 'A Method for MPPT Control While Searching for Parameters Corresponding to Weather Conditions for PV Generation Systems', Industrial Electronics, IEEE Transactions on, 53 (2006), pp. 1055-65.

Nabil Karami, Nazih Moubayed, and Rachid Outbib, 'Analysis and Implementation of an Adaptative PV Based Battery Floating Charger', Solar Energy, 86 (2012), pp. 2383-96.New Delhi-110001

O. Aashoor and F. V. P. Robinson, “A Variable Step Size Perturb and Observe Algorithm for Photovoltaic Maximum Power Point Tracking”.

OSSBERGER, 2012 A study conducted on the Efficiency curve of the Kaplan turbine, [accessed on April 11, 2014] VIEW ITEM

Overshot water wheel buckets design specifications MÜLLER W., 1939, Die Wasserräder, The water wheel, Reprint of the 2nd Ed, Moritz Schäfer Verlag, Detmold, 2009

P.S Nigam 'Handbook of Hydro power electric engineering', Second Edition, NAbhi Publication, N-101A second Floor, Munshiram Building,

Papavasiliou, A. and S. S. Oren, "Large-Scale Integration of Deferrable Demand and Renewable Energy Sources," IEEE Transactions on Power Systems, vol. 29 (1), 2014.

Patel and V. Agarwal, “MATLAB-Based modeling to Study the Effects of Partial

Petreus, D. , Daraban, S. , Cirstea, M., Patarau, T., et al. , 2011, "A novel implementation of a Maximum Power Point Tracking system with digital control ", IEEE International Symposium on Industrial Electronics, PP. 977-982, IEEE Publisher.

Photovoltaic Generators ", EPE-PEMC 2002.

Power Engineering Society- Overview of Hydroppower generations, 1999 Winter Meeting, IEEE, Vol.1, p: 646-650, 31 Jan-4 Feb, 1999

Power Point Tracking', Renewable Power Generation, IET, 4 (2010), pp. 317-28.

R. Billinton, H. Chen and R. Ghajar, Time-series Models for Reliability Evaluation of Power Systems Including Wind Energy, Microelectron. Reliability, Vol.36. No.9. 1996, pp 1253-1261.

R. Klempka, "Passive power filter design using genetic algorithm," Electr. Rev., vol. 5, pp. 294-301, 2013.

Ramaprabha, R., Mathur, B.L., Sharanya, M., 2009, "Solar array modeling and simulation of MPPT using neural network ", International Conference on Control, Automation, Communication and Energy Conservation, PP. 1-5, IEEE Published

Razak, J. A. and et al.: "Application of cross-flow turbine in off-grid Pico-hydro renewable energy systems", Proceeding of the American-Math 10 Conference on Applied Mathematics, pp. 519-526, 2010.

Razak, J. A. and et al.: "Application of cross-flow turbine in off-grid Pico-hydro renewable energy systems", Proceeding of the American-Math 10 Conference on Applied Mathematics, pp. 519-526, 2010.

Razak, J. A. and et al.: "Application of cross-flow turbine in off-grid Pico-hydro renewable energy systems", Proceeding of the American-Math 10 Conference on Applied Mathematics, pp. 519-526, 2010.

Renewable Energy System, Vol.9, Issue 4, pp. 1744-1751, November 1994

Republic of Togo Togo Energy Sector Policy Review Review of the Electricity Sub-Sector | Dharmendra Mahida - Academia.edu. 2017 [ONLINE] Available at: http://www.academia.edu/20743404/Republic_of_Togo_Togo_Energy_Sector_Policy_Review_Review_of_the_Electricity_Sub-Sector. [Accessed 18 February 2017].

Research degree writing, [online], available at http://www.ifm.eng.cam.ac.uk/phd/plan.html Accessed on 10/07/12

Research proposal guide, [online], available at http://www.law.ed.ac.uk/pg/files/researchproposalguide.pdf Accessed on 11/07/12

S. Armstrong, W.G. Hurley, 2004, "Self-Regulating Maximum Power Point Tracking for Solar Energy Systems ", NUI, Galway Faculty of Engineering Research Day.

S. Bal, and B. C. Babu, 'Comparative Study between P&O and Current Compensation Method for MPPT of PV Energy System', in Engineering and Systems (SCES), pp. 1-6, 2012 Students Conference on, 2012

S. Jain, and V. Agarwal, 'Comparison of the Performance of Maximum Power Point Tracking Schemes Applied to Single-Stage Grid-Connected Photovoltaic Systems', Electric Power Applications, IET, 1 (2007), pp. 753- 62.

S. Narkhede, Rajpritam, "Modelling of Photovoltaic Array" [Degree's Thesis], Rourkela National Institute of Technology, Department of Electrical Engineering, 2008.

S.P Mansoor, D.I. Jones, D.A. Bradley, F.C. Aris & G.R. Jones 'Stability of a Pump storage hydro-power station connected to a power system',

Safari and S. mekhilef, "Incremental Conductance MPPT Method for PV Systems," Seet Chin, P. Neelakantan, H. Pin Yoong, S. Siang Yang and K. Tze Kin Teo,

Shading on PV Array Characteristics," IEEE Transaction on Energy Conversion, vol. 23, no. 1, pp. 302-310, March 2008.

Shahraeini, M., et al., "Comparison between communication infrastructures of centralized and decentralized wide area measurement systems," IEEE Transactions on Smart Grid, vol. 2 (1), pp. 206-211, 2011.

Siano, P., et al., "Strategic placement of wind turbines in smart grids," International Journal of Emerging Electric Power Systems, vol. 13 (2), pp. 1-23, 2012.

softpedia. 2017. QBlade Download. [ONLINE] Available at: http://www.softpedia.com/get/Science-CAD/QBlade.shtml. [Accessed 18 February 2017]

Sonia Leva, Dario Zaninelli. Hybrid renewable energy-fuel cell system: Design and performance evaluation. Electric Power Systems Research 79 (2009) 316–324. Elsevier.

S. Khomfoi, Leon M. Tolbert “Multilevel power converters”, IEEE trans. Ind. Applicat.,vol. 31, p31-1 –P31-46

T. Esram and P. L. Chapman, “Comparison of Photovoltaic Array Maximum Power Point Tracking Techniques,” IEEE Transactions on Energy Conversion , vol. 22, no. 2, pp. 439-444, June 2007.

T. Esram, P.L. Chapman, "Comparison of Photovoltaic Array Maximum Power Point Tracking Techniques," IEEE Transactions on Energy Conversion, vol. 22, no. 2, (2007) pp. 439-449.

Thenkani, A., Senthil Kumar, N. , 2011, " Design of optimum Maximum Power Point Tracking algorithm for solar panel ", International Conference on Computer, Communication and Electrical Technology (ICCCET) , PP. 370-375, IEEE Publisher.

Thenkani, and N. Senthil Kumar, 'Design of Optimum Maximum Power Point Tracking Algorithm for Solar Panel', in Computer, Communication and Electrical Technology (ICCCET), 2011 International Conference on, 2011), pp. 370-75.

Third International Conference on Computational Intelligence, Communication Systems and Networks, pp. 72-77, 2011.

Thornley, V., et al., "User perception of demand side management," CIRED Seminar 2008: Smart Grids for Distribution, pp. 1-4, 2008.

Thornley, V., et al., "User perception of demand side management," CIRED Seminar 2008: Smart Grids for Distribution, pp. 1-4, 2008.

Tomoiag" and M. Chindri , “Reconfiguration of Distribution Networks with Dispersed Generation by Pareto Optimality and Evolution Strategies”, in Proc. 7st Balkan Power Conference – BPC 2008, Šibenik, Croatia, 10-12 September 2008, paper on CD ROM.

Trans. On Power System, Vol. 23, Issue 3, pp: 1125-1135, August 2008

V. T. Buyukdegirmenci, A. M. Bazzi, and P. T. Krein, 'A Comparative Study of an Exponential Adaptive Perturb and Observe Algorithm and Ripple Correlation Control for Real-Time Optimization', in Control and Modelling for Power Electronics (COMPEL), 2010 IEEE 12th Workshop on pp. 1-8. 2010

Vallee, F., et al., "System reliability assessment method for wind power integration," IEEE Transactions on Power Systems, vol. 23 (3), pp. 1288-1297, 2008.

Varaiya, P. P., et al., "Smart operation of smart grid: Risklimiting dispatch," Proceedings of the IEEE, vol. 99 (1), pp. 40-57, 2011.

Vineesh V, A. Immanuel Selvakumar, 'Design of Micro Hydel Power Plant', IJEAT, Vol. 2, issue 2, pp. 136-140, December 2012

Vojdani, A., "Smart integration," Power and Energy Magazine, IEEE, vol. 6 (6), pp. 71-79, 2008.

W. Xiao, F. Fongang Edwin, G. Spagnuolo and J. Jatskevich, "Efficient Approach for Modeling and Simulating Photovoltaic Power Systems," IEEE Journal of Photovoltaics, vol. 3, no. 1, pp. 500-508, January 2013.

Watts. M, 2010 Design considerations of the overshot water wheel; Princes Risborough, UK: Shire-Publications, Cambridge, UK. .

WEIDNER C.R., 2003, Overshoot water wheel design, Theory and test of an overshot water wheel, Bulletin of the Wisconsin University Issue No. 529, Engineering Series, Vol. 7, No. 2, 118-290.

Wenyuan, Z. D. Y. L. M., "Development Strategies of Smart Grid in China and Abroad," Proceedings of the Chinese Society of Electrical Engineering, vol. 33 (31), pp. I0001- I0028, 2013.

Working Group on prime Mover and Energy supply models for system Dynamics Performance Studies 'Hydraulic turbine and turbine control

Xiao Weidong, and W. G. Dunford, 'A Modified Adaptive Hill Climbing MPPT Method for Photovoltaic Power Systems', in Power Electronics Specialists Conference, 2004. PESC 04. 2004 IEEE 35th Annual, Vol.3, pp. 1957-63, 2004

Y. Cho and H. Cha, "Single-tuned passive harmonic filter design considering variances of tuning and quality factor," Journal of International Council on Electrical Engineering, vol. 1, pp. 7-13, 2011.

Y. Hong and W. Huang, "Interactive multi objective passive filter planning with fuzzy parameters in distribution systems using genetic algorithms," Power Delivery, IEEE Transactions On, vol. 18, pp. 1043-1050, 2003.

Y. Hsiao, "Design of filters for reducing harmonic distortion and correcting power factor in industrial distribution systems," Tamkang Journal of Science and Engineering, vol. 4, pp. 193-200, 2001.

Yaden, M.F., El Ouariachi, M., Mrabti, T., Kassmi, K.et.al. , 2011, "Design and realization of a photovoltaic system equipped with a digital MPPT control ", International Conference on Multimedia Computing and Systems, PP.1-6, IEEE Publisher, 2011.

Yan, Y., et al., "An efficient security protocol for advanced metering infrastructure in smart grid," Network, IEEE, vol. 27 (4), 2013.

Yun Tiam Tan, 2004, "Impact on The Power System with A Large Penetration of Photovoltaic Generation", Ph.D. dissertation, Manchester Institute University, 2004.

Zhang, P., et al., "Next-generation monitoring, analysis, and control for the future smart control center," IEEE Transactions on Smart Grid, vol. 1 (2), pp. 186-192, 2010.

Zhang, W. G. Hurley and W. Wolfle, “A New Approach to Achieve Maximum Power Point Tracking for PV System with a Variable Inductor,” *2nd IEEE International Symposium on Power Electronics for Distributed Generation Systems*, pp. 948-952, 2010.

APPENDIX (A) - SIMULINK MODELS

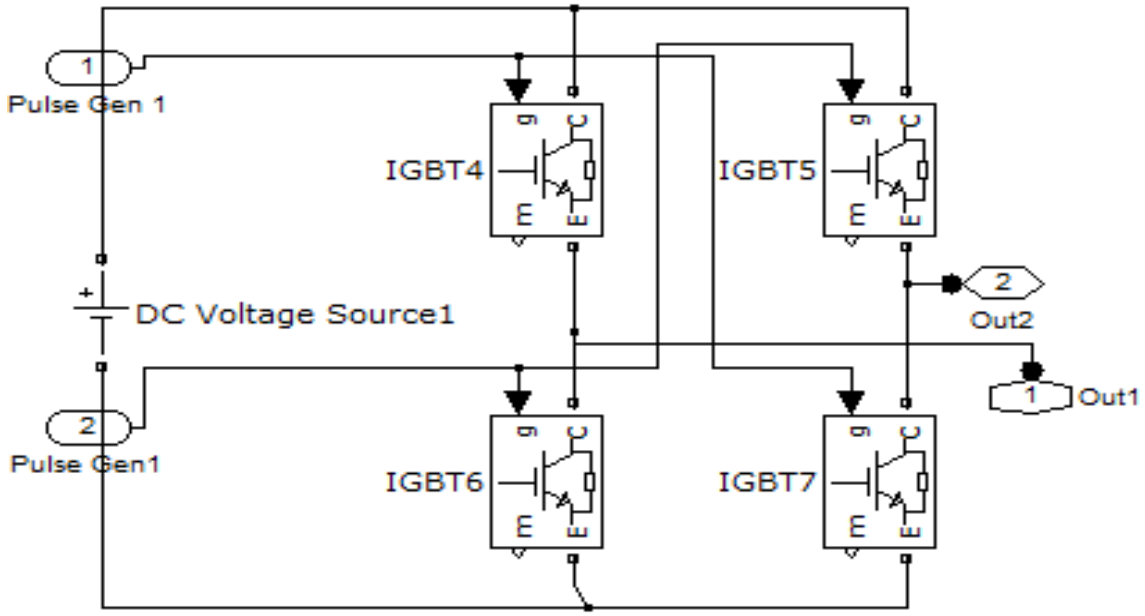

Figure A-1 Simulink block model for single H-Bridge circuit

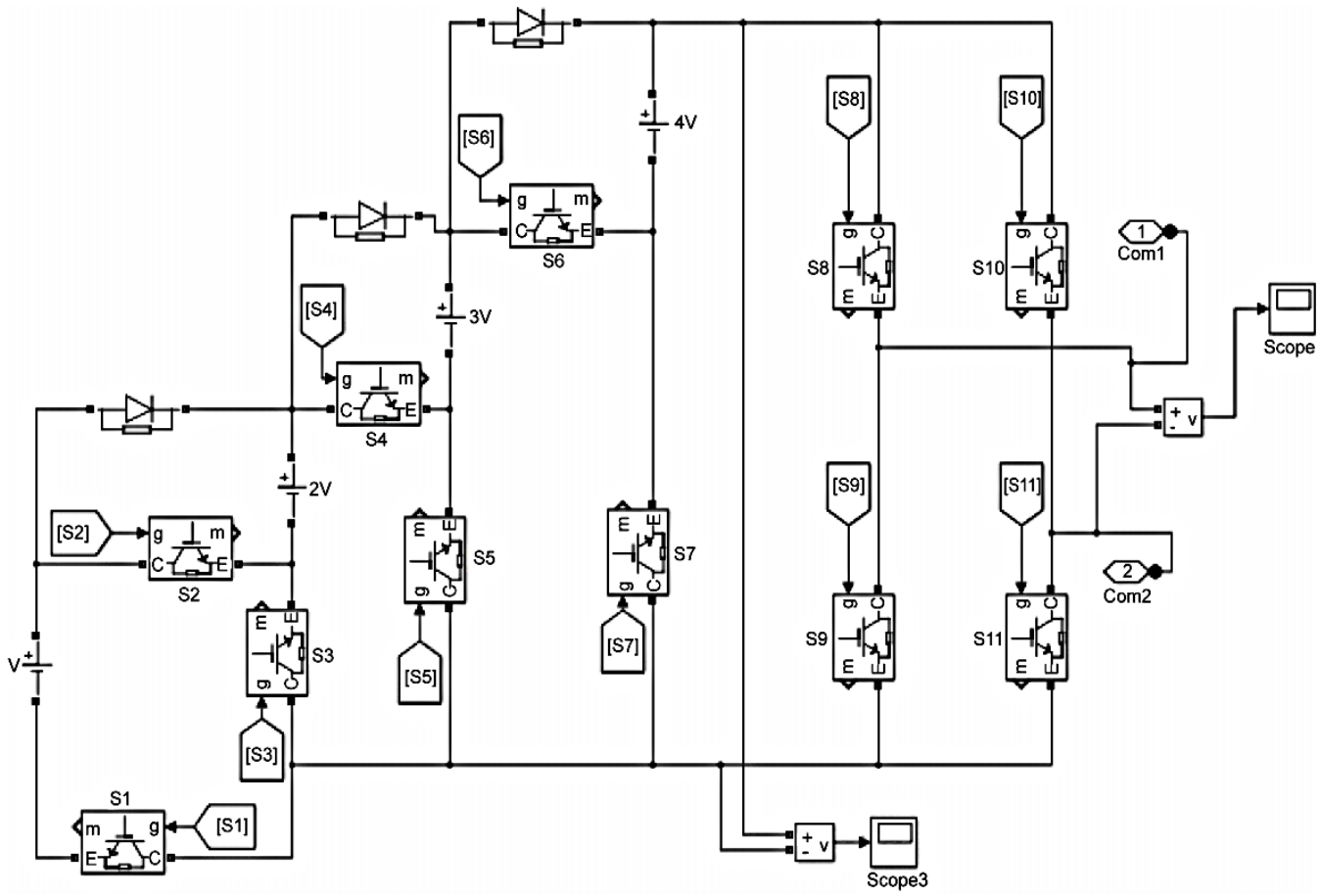

Figure A-2 Simulink model of proposed 21 level inverter

APPENDIX (B) - MATLAB SCRIPTS

```
**********************************************************************
% This MATLAB code is for solving the problem of SHE using Genetic
Algorithm
% (GA) method in Cascaded H-Bridge MLI (7-LEVEL given as example)
% THE SWITCHING ANGLES SHOULD BE Θ1 < θ2 < θ3< 90°
**********************************************************************
clc
clear all
opts = gaoptimset(@gamultiobj);
opts.Generations=30;
opts.StallGenLimit=50;
opts.PlotFcns={@gaplotbestf,@gaplotdistance };
lb=[0,0, 0];
ub=[90,90,90];
[Q,Fval,exitFlag,Output] = ga(@THD_Mingab7,3,[],[],[], ...
[],lb,ub,[],opts);
fprintf('\Switching_Angle_1 = ' ,X(1))
fprintf('\Switching_Angle_2 = ',X(2))
fprintf('\Switching_Angle_3 = ',X(3))
fprintf('Total Harmonic Distortion %THD =',THD)

function y = THD_Mingab7( x )
m=0.9;
H1 = cosd(x(1))+cosd(x(2))+cosd(x(3));
H= [1/5*(cosd(5*x(1))+cosd(5*x(2))+cosd(5*x(3)));
1/7*(cosd(7*x(1))+cosd(7*x(2))+cosd(7*x(3)));
1/11*(cosd(11*x(1))+cosd(11*x(2))+cosd(11*x(3)));
1/13*(cosd(13*x(1))+cosd(13*x(2))+cosd(13*x(3)));
1/17*(cosd(17*x(1))+cosd(17*x(2))+cosd(17*x(3)));
1/19*(cosd(19*x(1))+cosd(19*x(2))+cosd(19*x(3)));
1/23*(cosd(23*x(1))+cosd(23*x(2))+cosd(23*x(3)));
1/25*(cosd(25*x(1))+cosd(25*x(2))+cosd(25*x(3)));
1/29*(cosd(29*x(1))+cosd(29*x(2))+cosd(29*x(3)));
1/31*(cosd(31*x(1))+cosd(31*x(2))+cosd(31*x(3)));
1/35*(cosd(35*x(1))+cosd(35*x(2))+cosd(35*x(3)));
1/37*(cosd(37*x(1))+cosd(37*x(2))+cosd(37*x(3)));
1/41*(cosd(41*x(1))+cosd(41*x(2))+cosd(41*x(3)));
1/43*(cosd(43*x(1))+cosd(43*x(2))+cosd(43*x(3)));
1/47*(cosd(47*x(1))+cosd(47*x(2))+cosd(47*x(3)));
1/49*(cosd(49*x(1))+cosd(49*x(2))+cosd(49*x(3)))];
HH = H.^2;
HN = sum(HH);
THD = sqrt(HN)/H1*100;
'Total Harmonic Distortion %THD =', THD
'Fundamental', H1-3*m
'5th harmonic =', H(1,1)/H1*100
'7th harmonic =', H(2,1)/H1*100
y = 50*((H1-3*m)^4)+50*(H(1,1)^2+ H(2,1)^2)+THD/100 ;
end
```

```
**************************************************************************
% This MATLAB code is for the optimum design of passive power filter (PPF)
% using Genetic Algorithm (GA) method in Cascaded H-Bridge MLI (21-LEVEL)
% Two single tuned filter and one high pass filter
**************************************************************************
clc
clear all
opts = gaoptimset(@gamultiobj);
opts.Generations=10;
opts.StallGenLimit=50;
opts.PlotFcns={@gaplotbestf,@gaplotdistance };
lb=[300000,300000, 1000000];
ub=[1500000,1500000, 3000000];
[Q,Fval,exitFlag,Output] = ga(@Q_21_level_inverter,3,[],[],[], ...
[],lb,ub,[],opts);
fprintf('\nDesigned Parameter Q1= %f',Q(1))
fprintf('\nDesigned Parameter Q1= %f',Q(2))
fprintf('\nDesigned Parameter Q1= %f',Q(3))
fprintf('\nSum of designed parameters Q= %f',Q(1)+Q(2)+Q(3))
fprintf(' 1.6<%f<3.75',Q(1)+Q(2)+Q(3))
fprintf('\nTHD= %f \n',THD.THD)

function [Q ] = Q_21_level_inverter(Q)
assignin('base', 'Q1', Q(1));
assignin('base', 'Q2',Q(2));
assignin('base', 'Q3', Q(3));
sim('Seven_Level_CHB__Inverter_07')
pause(0.5);
assignin('base', 'Ploss', ploss);
f1=[(Q(1)+Q(2)+Q(3))*(1/100)]+[[(max(ploss.Data)/1000)*4380*0.11]*[(((1.05)
^15)-1)/(0.05*((1.05)^15))]];
assignin('base', 'VLL', VLL);
THD=power_fftscope(VLL);
THD.fundamental=50;
THD.maxFrequency=2500;
THD.startTime=0.01;
THD=power_fftscope(THD);
f2=THD.THD;
f3= 100-[(Q(1)+Q(2)+Q(3))/1000000];
assignin('base', 'THD', THD);
end
```

APPENDIX (C) LAB VALIDATION KEY COMPONENTS

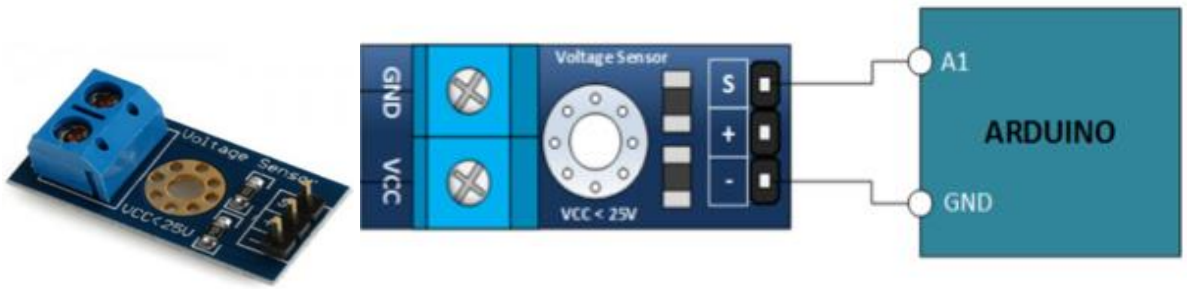

Figure C-1 Voltage sensor (RS components)

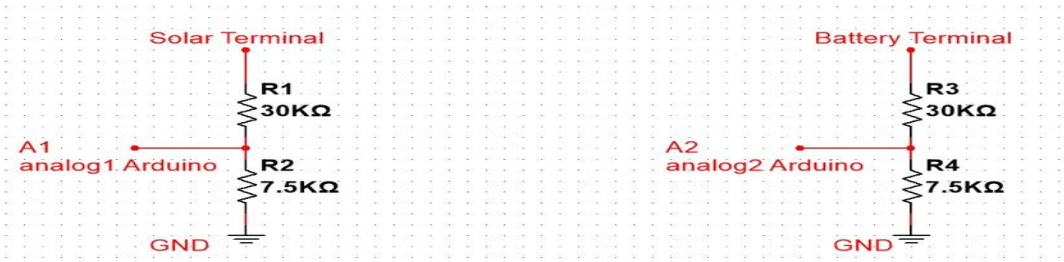

Figure C-2 Voltage Divider resistors and connection Setup

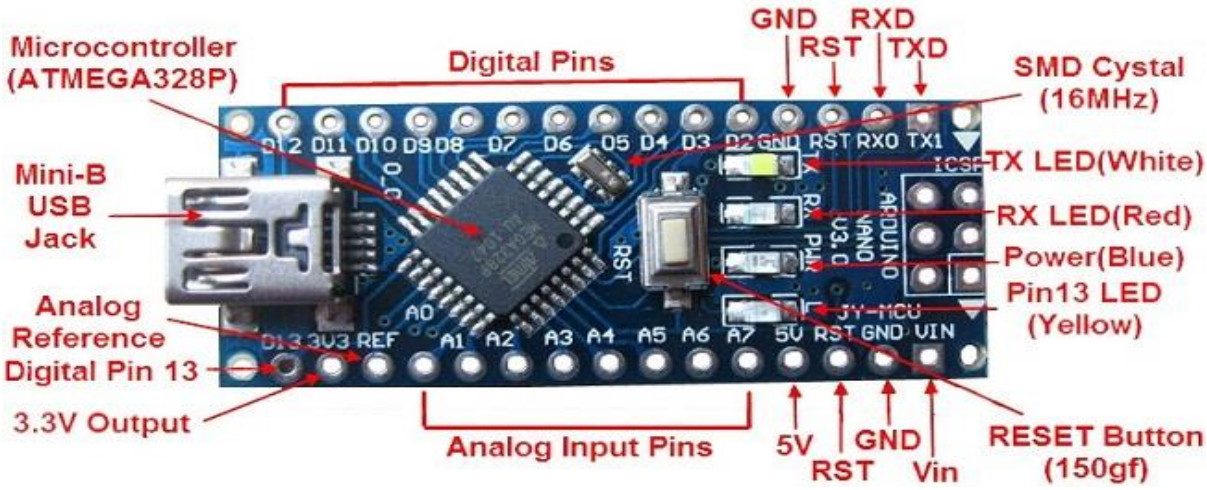

Figure C0-3 LM35 Temperature Sensor PIN Configurations

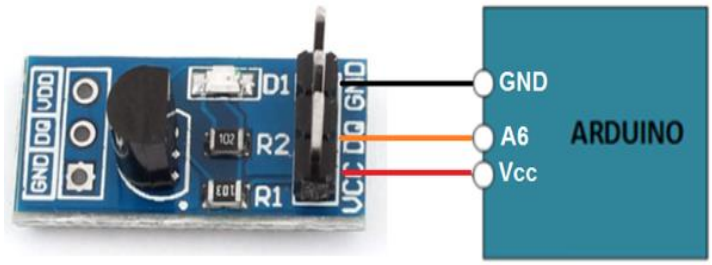

Figure C-4 Temperature Module Sensor Arduino Connection

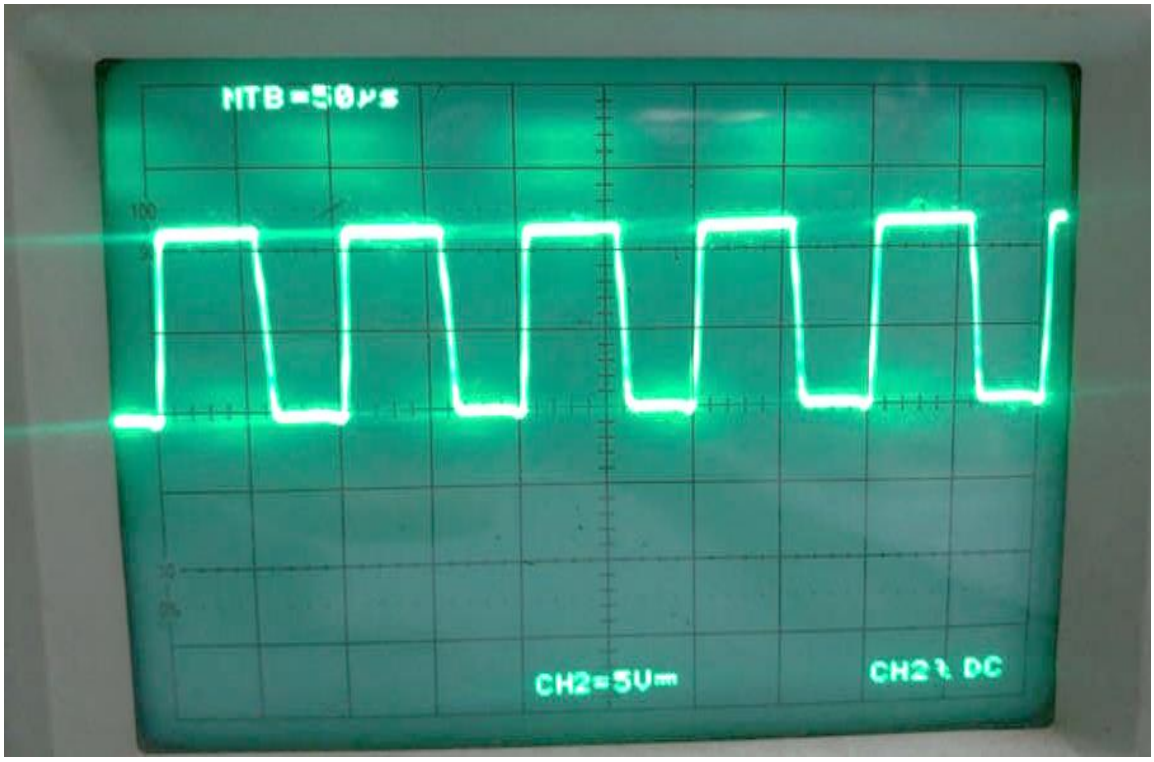

Figure C-5 Photo-coupler Signal Applied to MOSFET

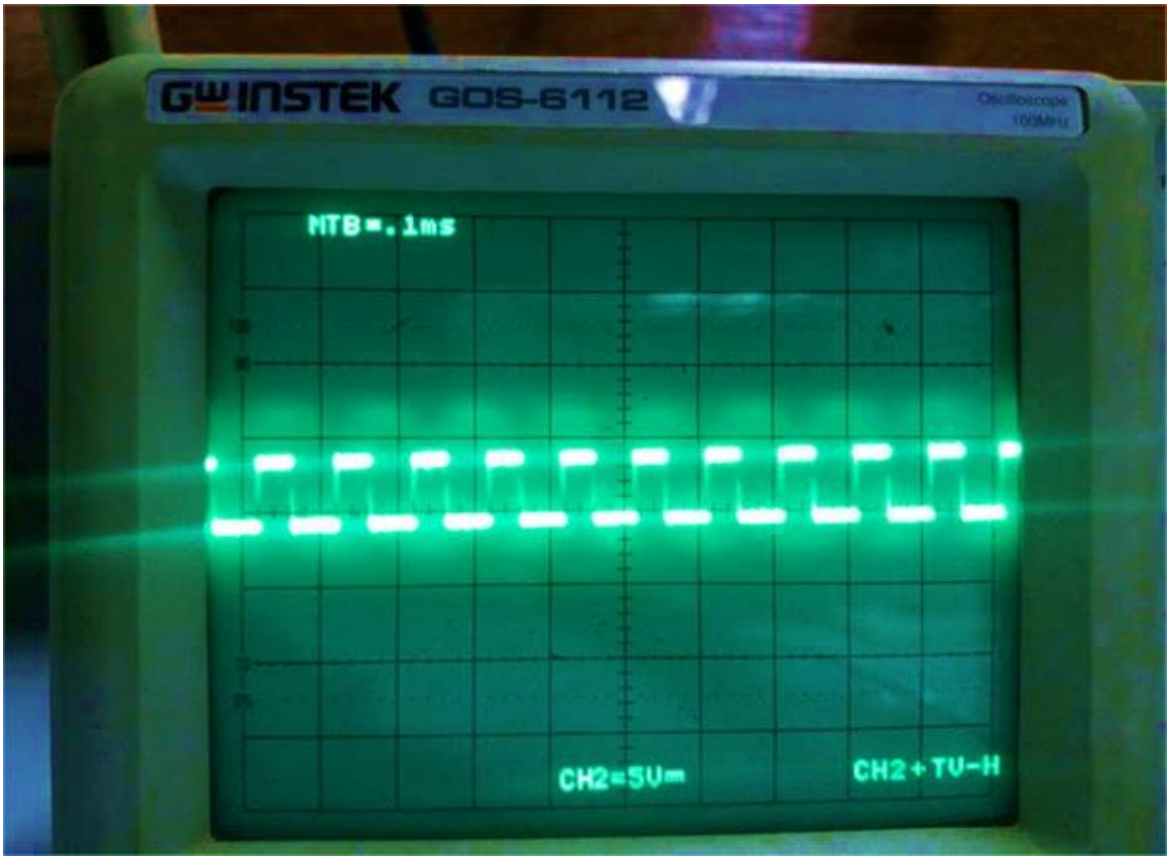

Figure C-6 Signal Oscilloscope Monitoring

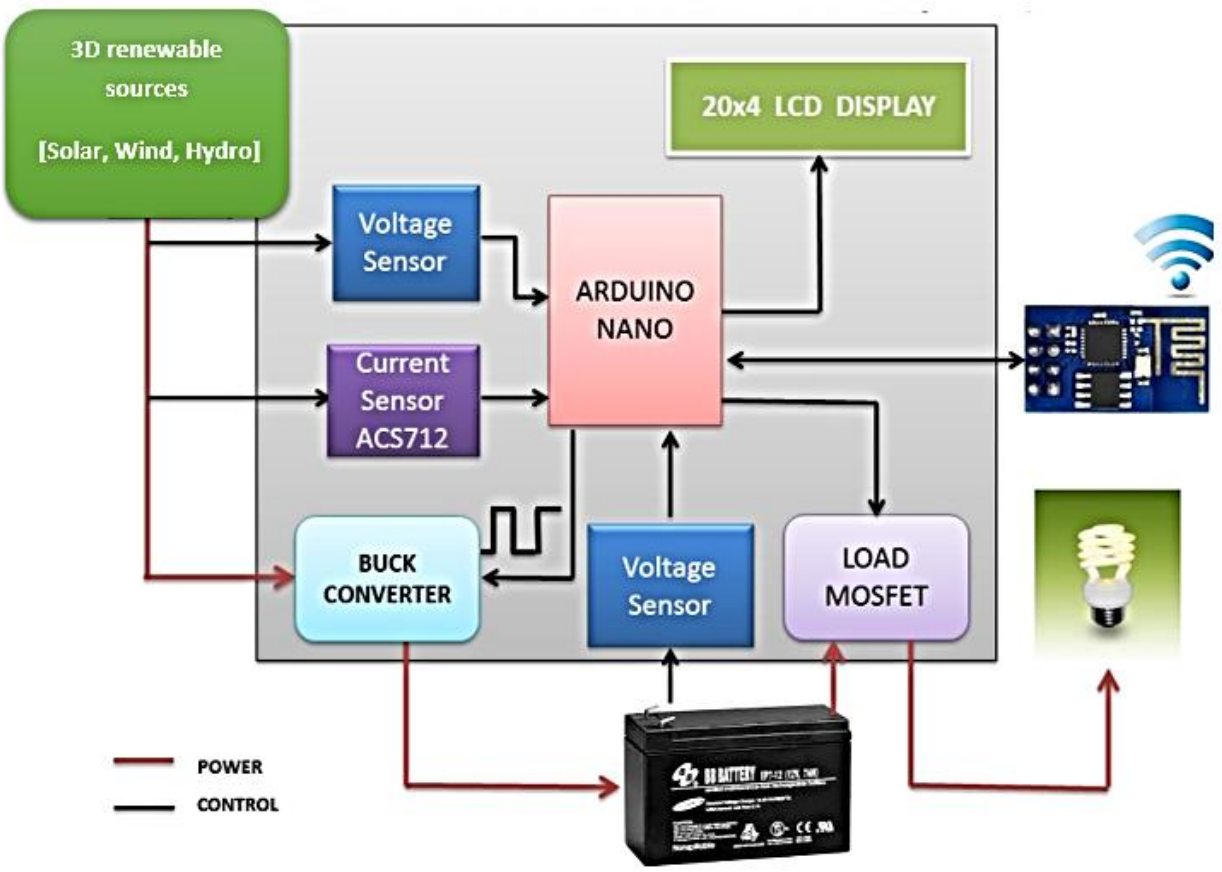

Figure C-7 3D sustainable renewable micro power station - Middle end unit

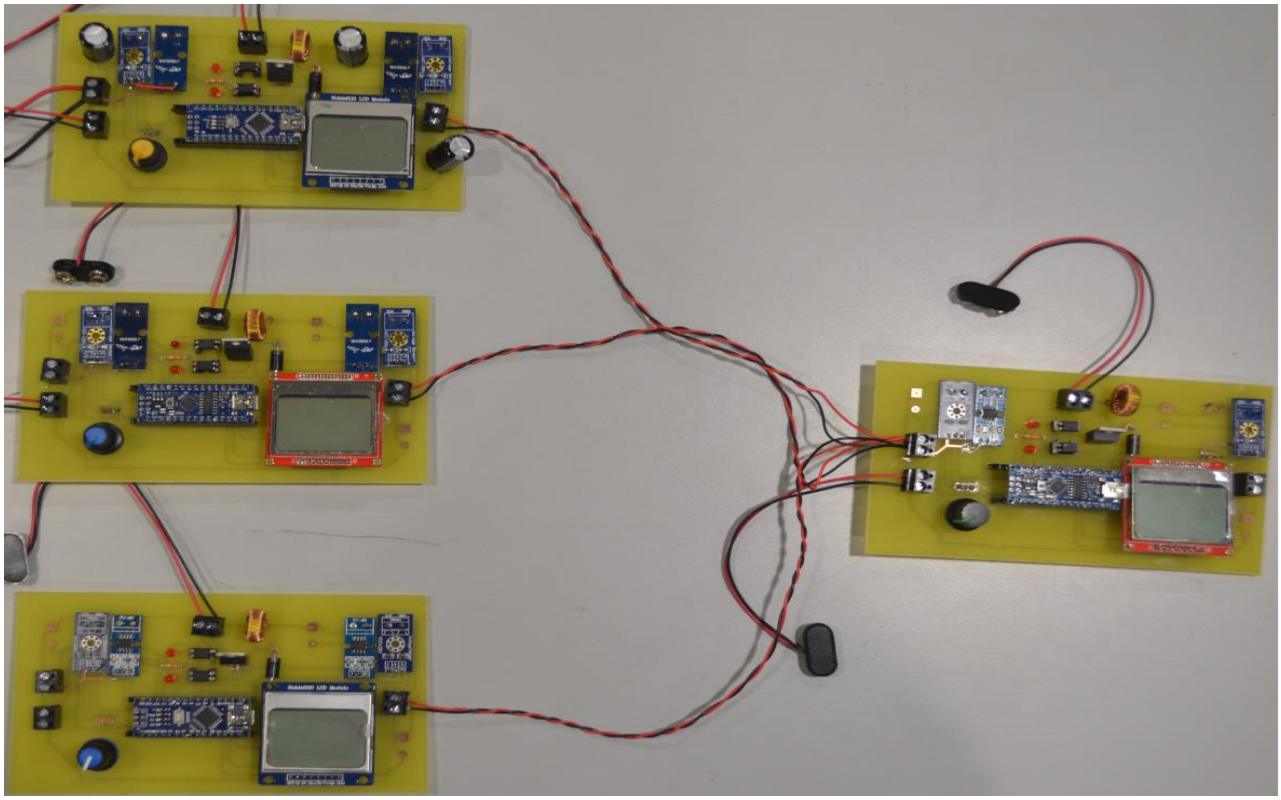

Figure C-8 3D renewable sources Practical system unit assembly (Middle end)

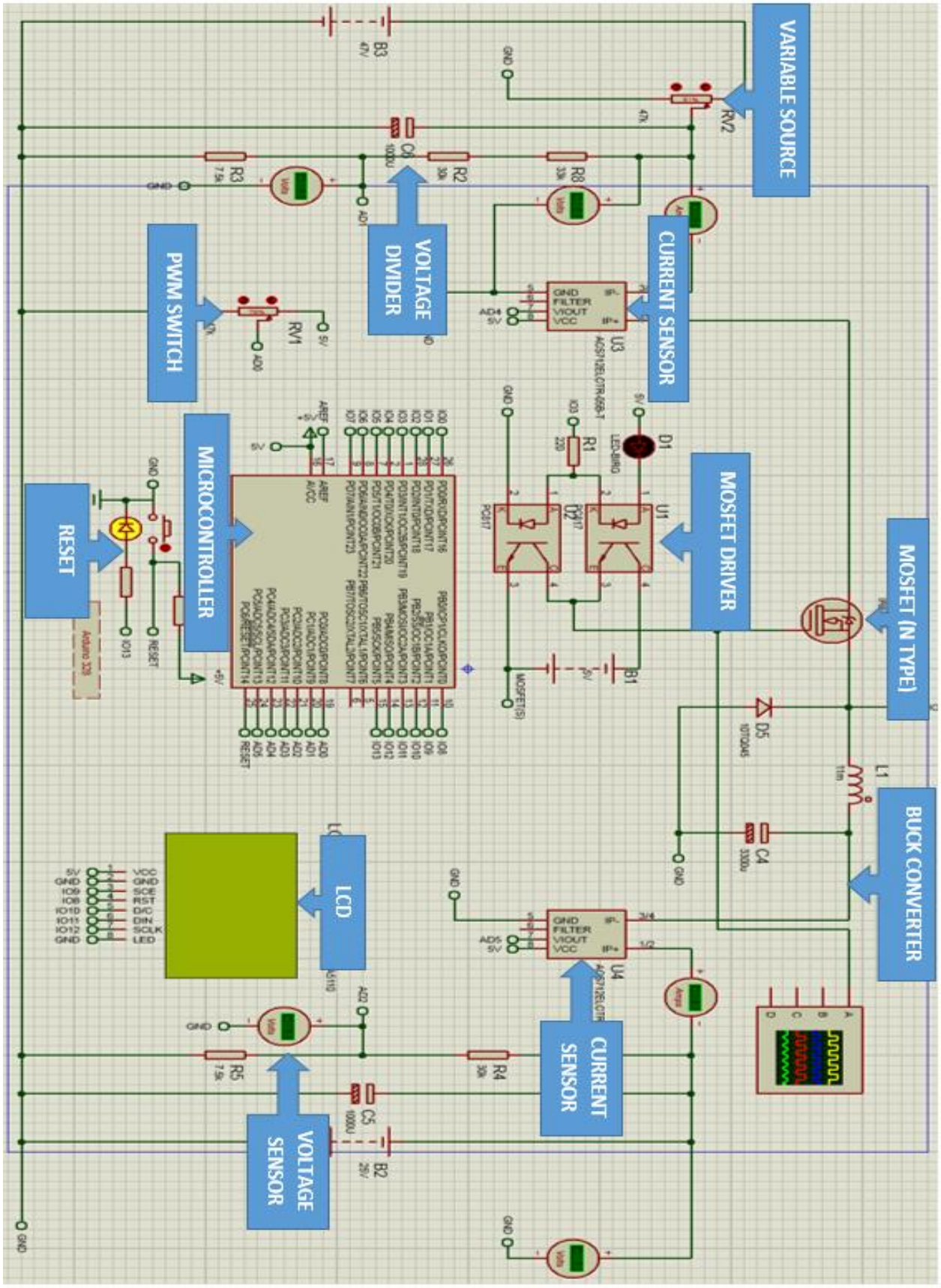

Figure C-9 Overall MPPT System Connection for Simulations showing each block diagram

APPENDIX (D) – SOLIDWORKS DESIGNS

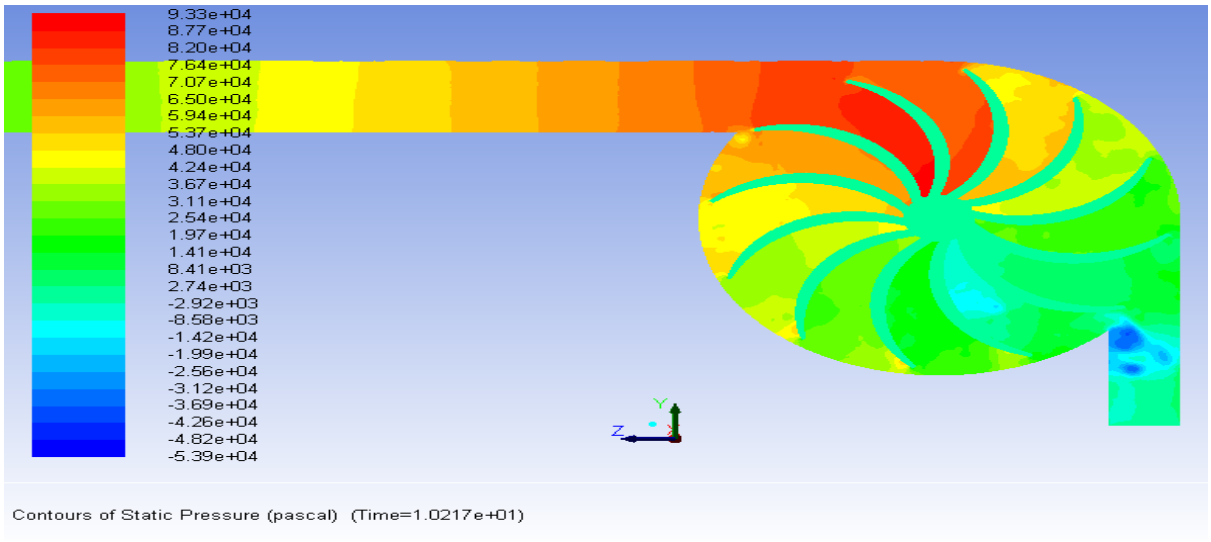

D1- Static simulation Overshot Wheel

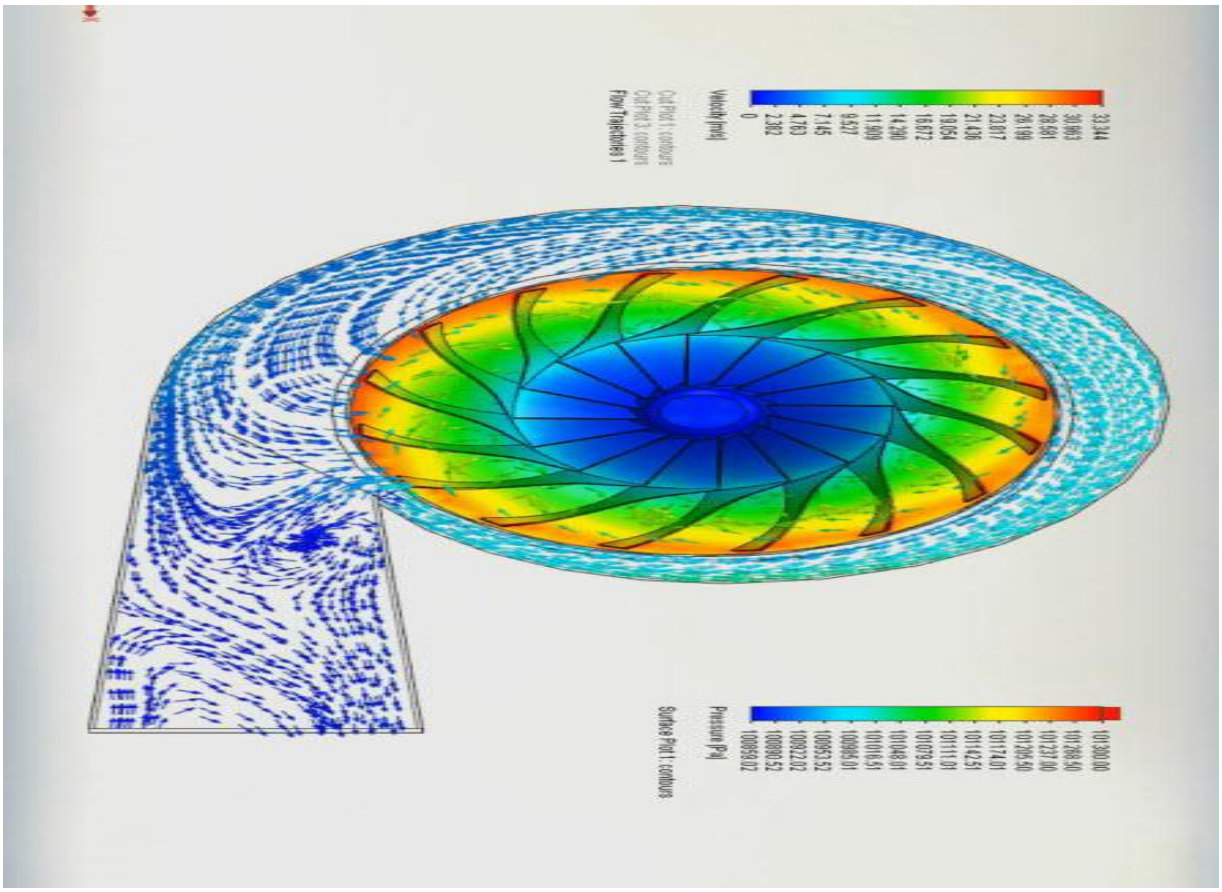

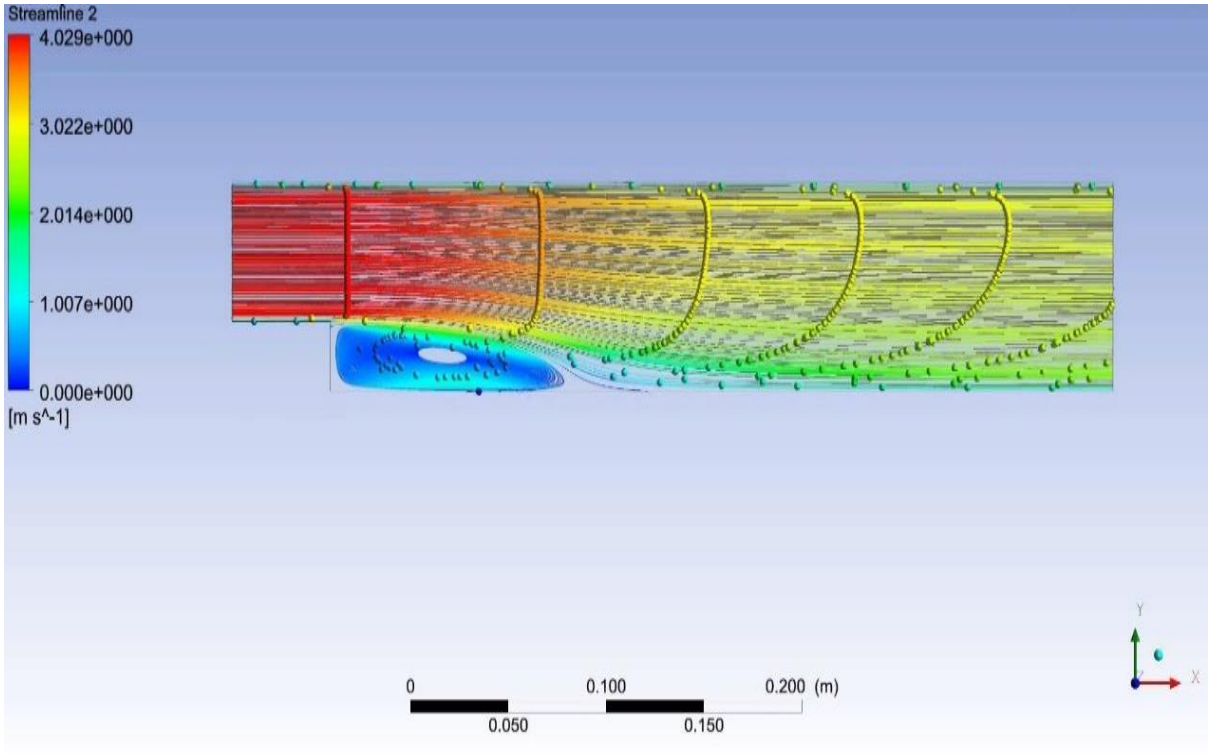

D2- Static simulation & (b) LES of Turbulence

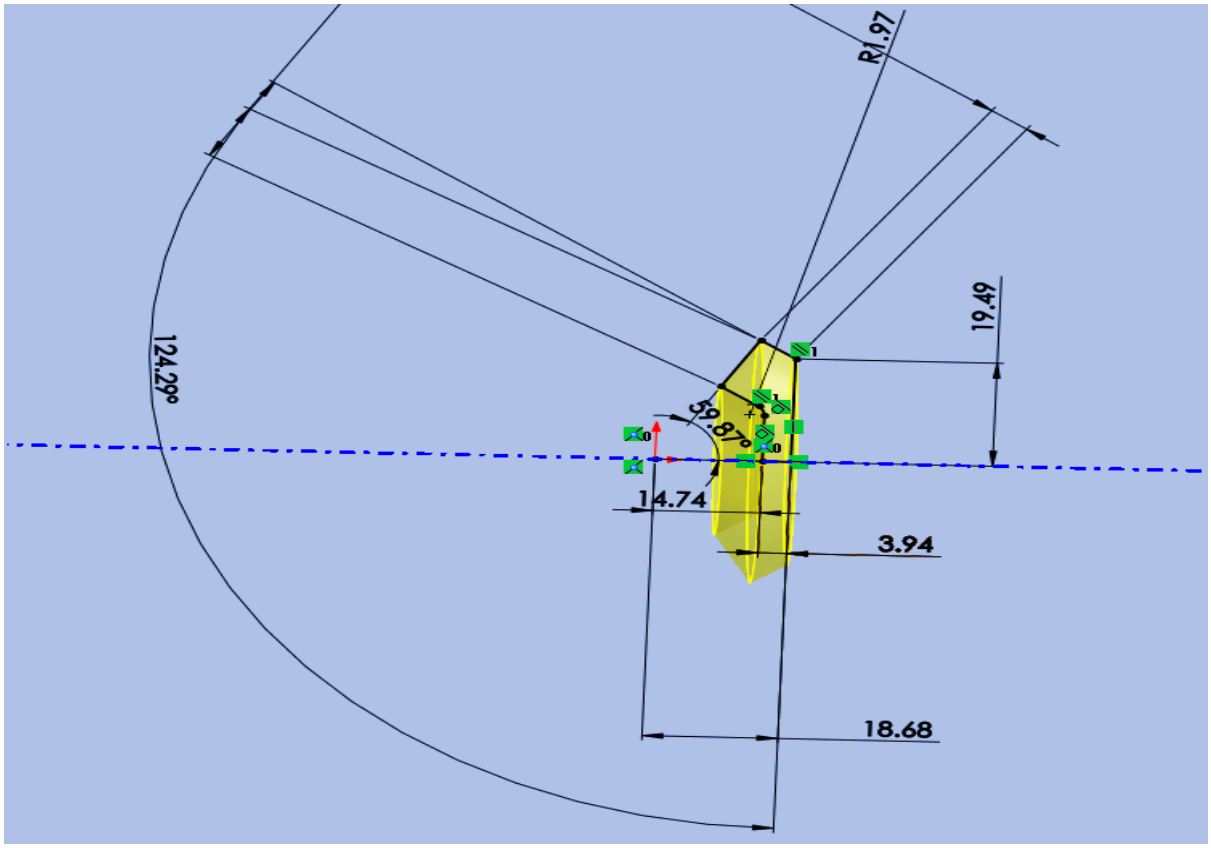

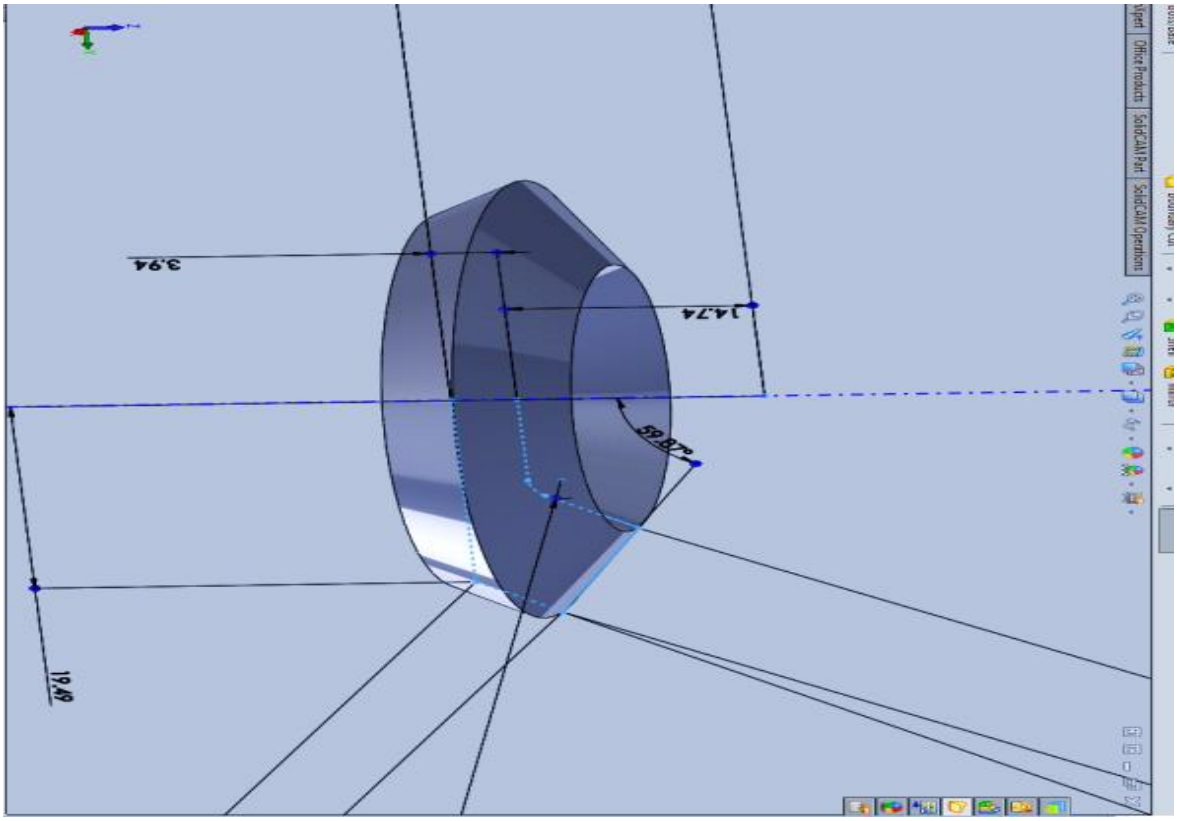

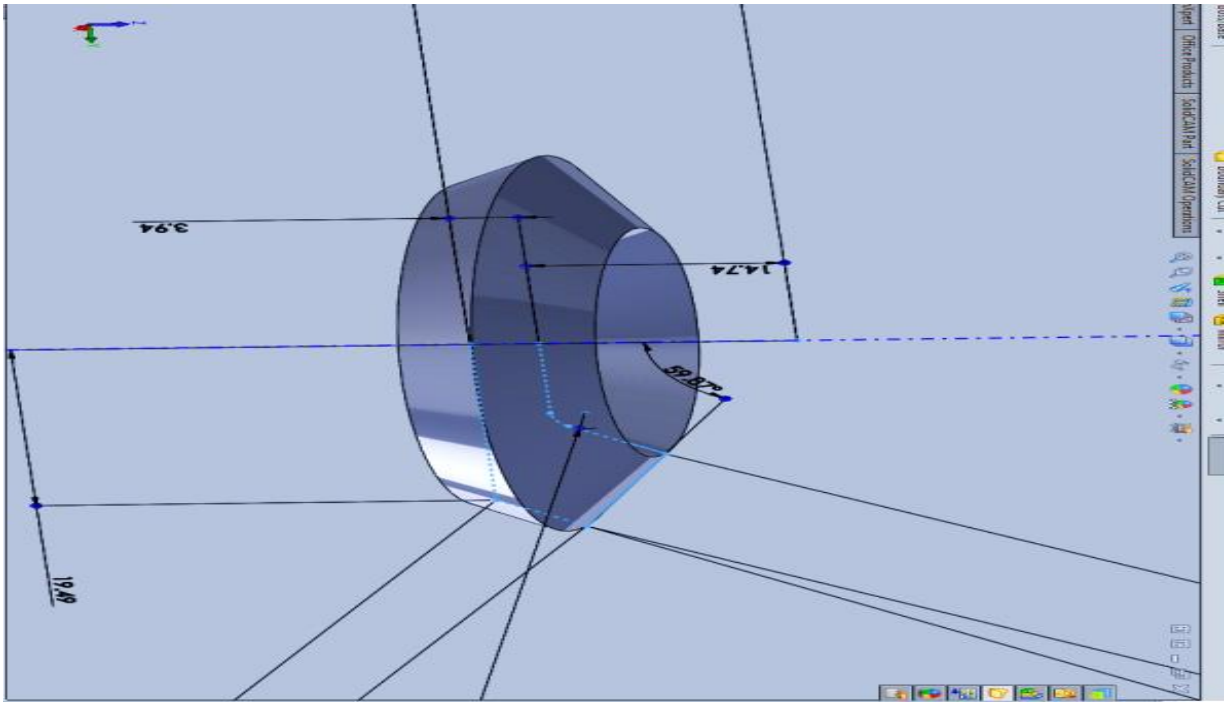

D3-Base formation

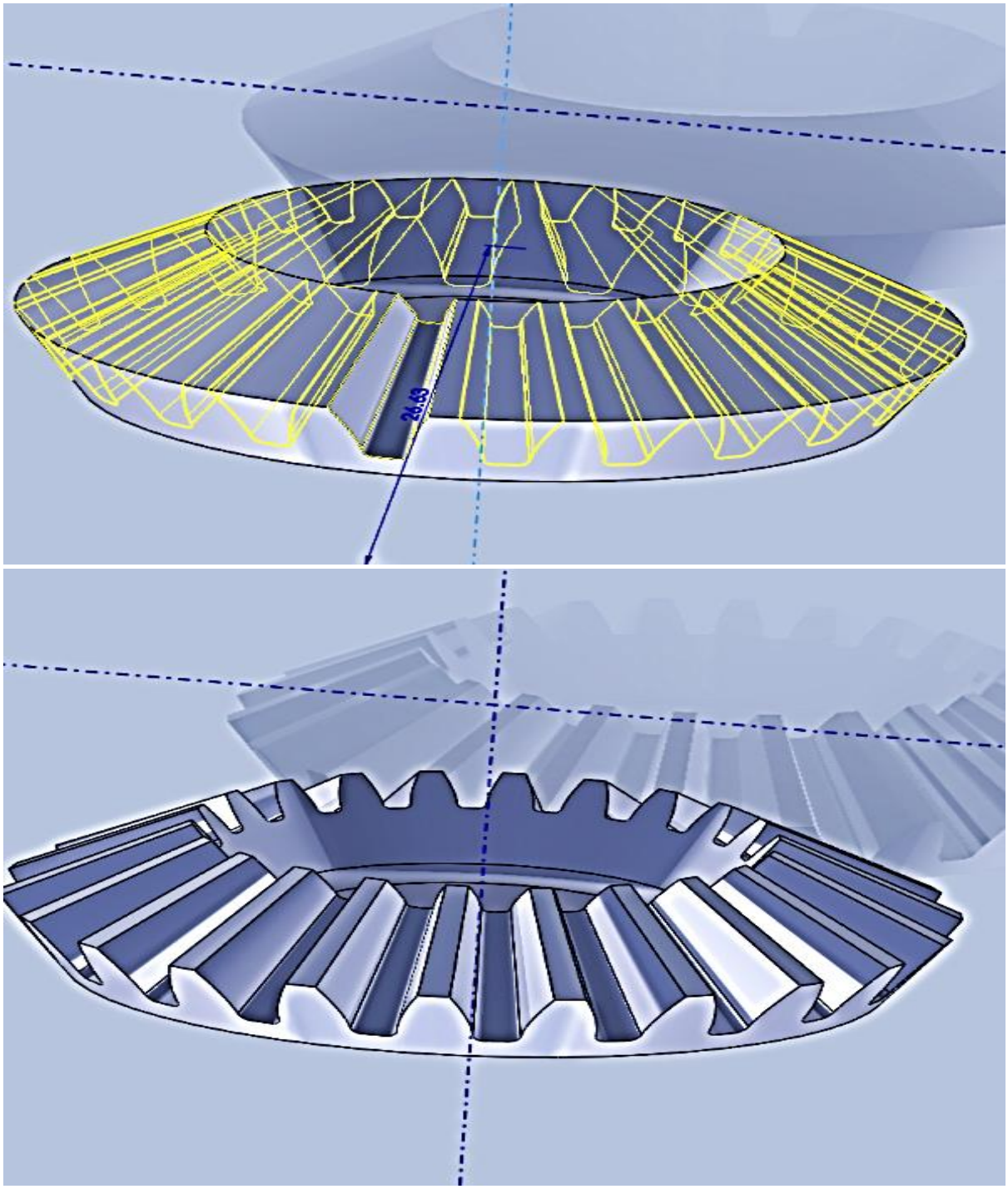

D4-Teeth formation

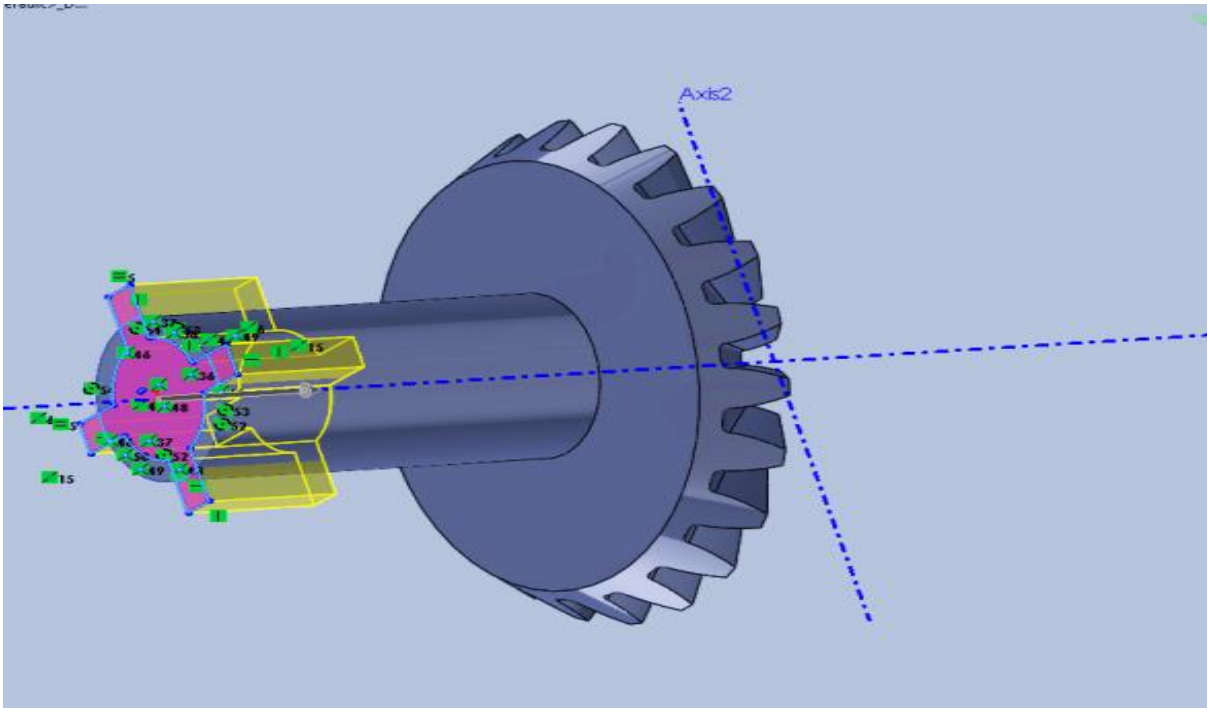

D5-Shaft extruded and Cut

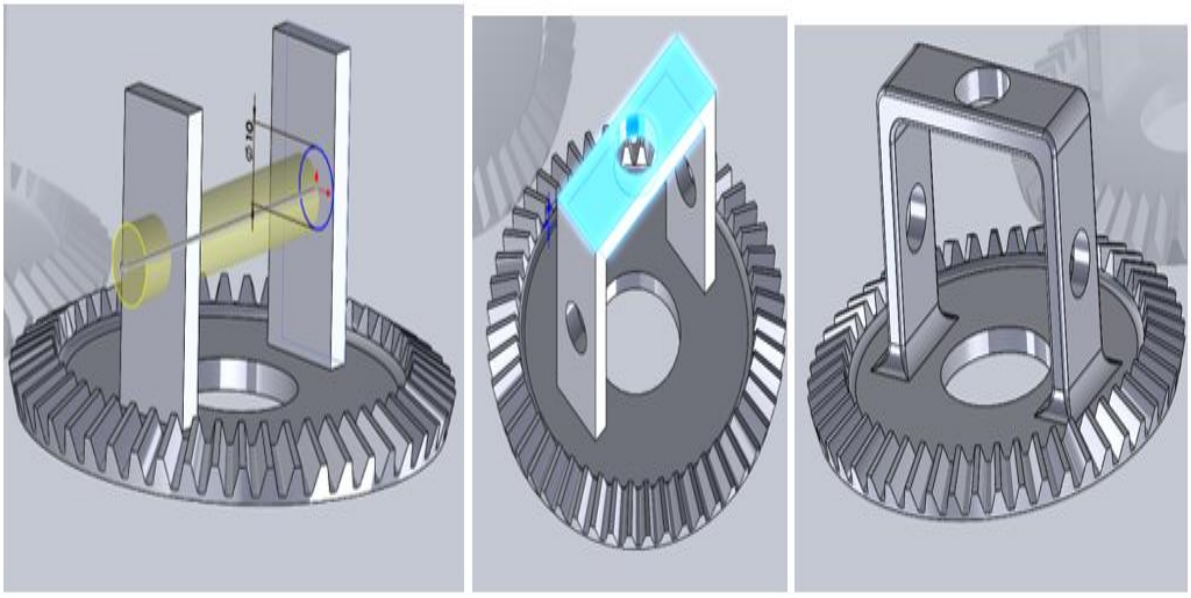

D6-Ring gear modelling

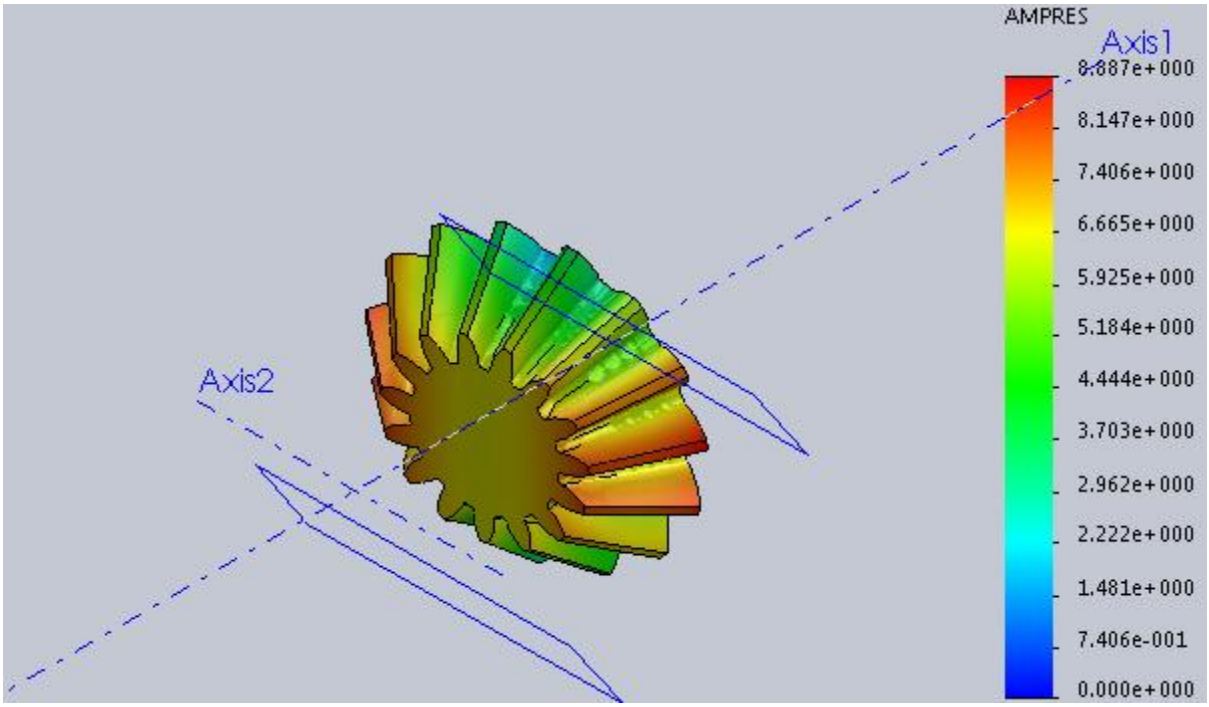

D7-Static Stress distribution and displacement

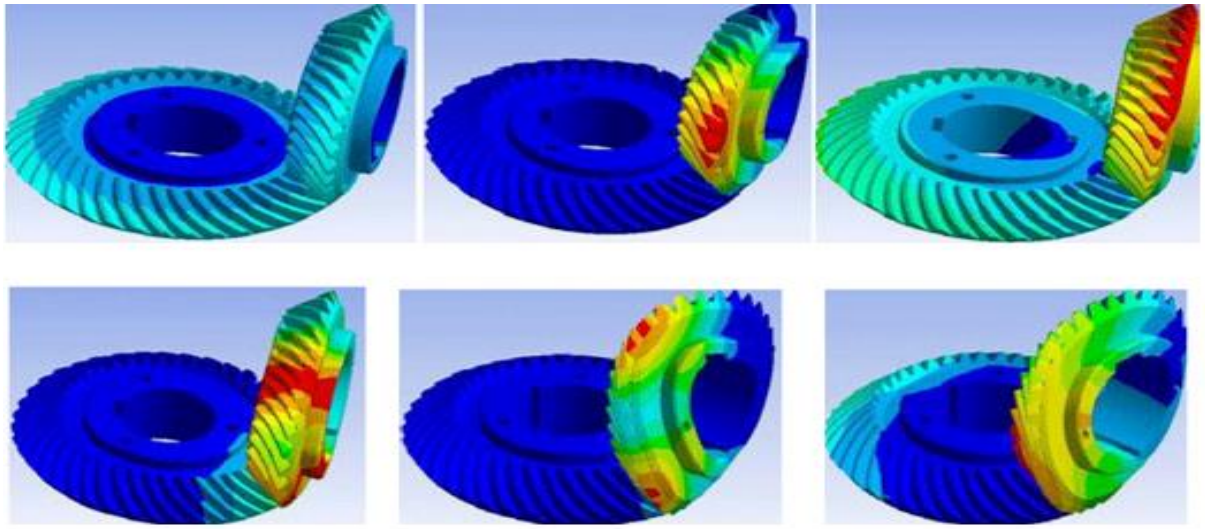

D8-Static Stress distribution

APPENDIX (E) - AUTHORS PUBLICATIONS

- M. Komlanvi & M. Shafik & M. Elvis Ashu "Evaluation of a 3D renewable Micro Power station for Smart grid application" ICMR2016, 06-08 of September 2016, Loughborough University, Loughborough, UK, 2016.
- M. Komlanvi & M. Shafik &, M. Elvis Ashu, (2015), '3D sustainable Renewable Micro-power station for smart grid Industrial Applications', International Journal of Robotics and Mechatronics, http://ojs.unsysdigital.com/index.php/ijrm, Issue 5, Vol. 1, 27th of December 2015.
- M. Komlanvi & M. Shafik & J. Garza Reyes, M. Elvis Ashu, K. Hunt, (2014), 'Micro-Hydro Generator using Eco-wheel system for Domestic and Industrial Building Applications', International Journal of Robotics and Mechatronics, http://ojs.unsysdigital.com/index.php/ijrm, Issue 1, Vol. 1, 15th of March 2014.
- M. Komlanvi & J. Banini, (2014) " Togo and Ghana energy crisis and the way forward, Power deficiency solution for Industrial Applications", Applied research conference in Africa (ARCA), Accra, Ghana, August 2014
- M. Komlanvi & M. Shafik & J. Garza Reyes, "Design and Development of 4D Sustainable Renewable Power Station Model for the republic of Togo Industrial Applications" ICMR2013, 16-20 of September 2013, Cranfield University, Cranfield, UK, 2013.
- M. Komlanvi & M. Shafik & J. Garza Reyes, M. Elvis Ashu," Computer simulation & modelling of a Micro-hydro power generator using Kaplan turbine for domestic & industrial building applications" International Conference in Sustainable design and Manufacturing, Cardiff, Wales, UK, 28-30 April 2014.